

Role of surface properties of titanium alloys on osteoblasts response

by

Subhash Sista

B.Tech

Submitted in fulfilment of the requirements for the degree of
Doctor of Philosophy

Deakin University

November, 2012



**DEAKIN UNIVERSITY
ACCESS TO THESIS - A**

I am the author of the thesis entitled **"Role of surface properties of titanium alloys on osteoblasts response"** submitted for the degree of Doctor of Philosophy

This thesis may be made available for consultation, loan and limited copying in accordance with the Copyright Act 1968.

'I certify that I am the student named below and that the information provided in the form is correct'

Full Name: SUBHASH SISTA

Signed:

Signature Redacted by Library

Date: March 13, 2013



**DEAKIN UNIVERSITY
CANDIDATE DECLARATION**

I certify that the thesis entitled **“Role of surface properties of titanium alloys on osteoblasts response”** submitted for the degree of Doctor of Philosophy is the result of my own work and that where reference is made to the work of others, due acknowledgment is given.

I also certify that any material in the thesis which has been accepted for a degree or diploma by any university or institution is identified in the text.

'I certify that I am the student named below and that the information provided in the form is correct'

Full Name: SUBHASH SISTA

Signed: Signature Redacted by Library

Date: November 8, 2012

CERTIFICATE

It is certified that the work incorporated in the thesis entitled “**Role of surface properties of titanium alloys on osteoblasts response**” submitted by **Mr. Subhash Sista** for a degree of Ph.D. was done at the Centre for Cellular and Molecular Biology, Hyderabad, India and at Deakin University, Waurn Ponds, Victoria, Australia, under the guidance of the undersigned Supervisors. It is also certified that the work in this thesis is original and was indeed carried out by **Mr. Subhash Sista** who is a registered candidate for a Ph.D. degree at Deakin University (Student ID-800381014).

Dated: November 8, 2012

Place: Geelong, (VIC), Australia
Hyderabad, (AP), India

Signature Redacted by Library

Professor, Peter Hodgson
Principal Supervisor

Signature Redacted by Library

Professor, Cuie Wen
Co-Supervisor

Signature Redacted by Library

Dr. Gopal Pande
Research Supervisor

Dr. GOPAL PANDE
Chief Scientist
CSIR-Centre for Cellular and Molecular Biology
Uppal Road, Hyderabad - 500 007 INDIA

List of Publications

Subhash Sista, Cuie Wen, Peter.D.Hodgson and Gopal Pande. The influence of surface energy of titanium-zirconium alloy on osteoblast cell functions *in vitro*. *Journal of biomedical materials research - Part A*. Volume 97 A. Issue 1, Pages 27-36, April 2011.

Subhash Sista, Cuie Wen, Peter.D.Hodgson and Gopal Pande. Expression of cell adhesion and differentiation related genes in MC3T3 osteoblast cells plated on titanium alloys: role of surface properties. *Material Science and Engineering C*. Volume 33. Issue 3, Pages 1573-1582, April 2013.

Subhash Sista, Alireza Nouri, Yuncang Li, Cuie Wen, Peter.D.Hodgson and Gopal Pande. Cell biological responses of osteoblasts on anodized nanotubular surface of a titanium-zirconium alloy. *Journal of biomedical materials research - Part A* (In press DOI: 10.1002/jbm.a.34638).

Awards

Travel grants from Department of Science (DST), Government of India, New Delhi, India and Deakin India Research Initiative (DIRI), Australia, to attend the 4th International conference on Tissue engineering organized by Aegean conferences in Chania, Crete, Greece (June 2011).

Received travel award of US \$670 for best oral presentation at the 4th international conference on Tissue engineering organized by Aegean conferences in Chania, Crete, Greece (June 2011).

Conferences

2nd DIRI Symposium "Frontiers in Science", November 2011, Delhi, India.

4th International conference on Tissue engineering organized by Aegean conferences in Chania, Crete, Greece (June 2011).

1st DIRI symposium "Trends in molecular and cellular application of Nano science" 2010, Hyderabad, India.

Acknowledgements

Undoubtedly, the two most important pages of this thesis. I express my heartfelt gratitude to the almighty and my family for supporting me right from the start till the end and to be with me in hard times and making me the person I am.

I would like to take this opportunity to thank Prof. Andrew Parrat, the former director of ITRI (Institute for Technology Research and Innovation, Deakin University, Australia) and Dr. Lalji Singh, the former director of CCMB (Centre for Cellular and Molecular Biology, Hyderabad, India) for initiating this program and making me a part of this. I thank them for providing me with the facilities to carry out research at CCMB and during my visit to Deakin University, Australia.

My heartfelt gratitude to the present director CCMB, Dr. Mohan Rao, for being a source of inspiration during my entire PhD and helping me grow both professionally and personally. My special thanks to Dr. Madhusudhana Rao, who helped me, start my research career making me a part of his lab and help me guide through the duration of the entire PhD program.

I am grateful to my supervisors Prof. Peter Hodgson and Prof. Cuie Wen at Deakin University and Dr. Gopal Pande at CCMB for helping me guide through my PhD, with all the intellectual discussions, without whom this wouldn't have been possible. I am grateful to Dr. Gopal Pande, for providing the necessary funds for all the consumables to carry out the research and for all the support needed during the course of my PhD.

Sincere thanks to my senior, Dr. Alireza Nouri, for providing a helping hand in the preparation of alloy samples involving laborious protocol for synthesising and processing them. Also, for sharing his knowledge and providing great inputs. Dr. Yuncang Li for helping me with some crucial experiments.

My past and present lab mates at CCMB, Dr. Ram Prasad, Dr. Rajeshwari, Abhilasha, Priya, Pavana, Renu, Sravanthi, Vibudha, Dolly, Mahalakshmi, for maintaining a friendly atmosphere in the lab and great support. Special thanks to Dr. Ram Prasad for his valuable time and inputs with regard to my project and helping me master the basic techniques in cell culture. Special thanks to my fellow Deakin student Wasnik

(Samiksha) for taking time in performing crucial experiments while I was away to Australia. Another special thanks to Priya (Past lab mate at CCMB and fellow Deakin student) in taking her precious time to help me with Real Time PCR experiments (Primer designing and standardization) as well as for her constant encouragement and support throughout the course of my PhD. Special thanks to all of them for accompanying with me for lunch and tea breaks. My senior colleagues in the lab Dr. Ushasri, Dr. Devarai Santhosh Kumar, Srinivas Gunda and Avinash Raj for their constant support, encouragement and fruitful discussions. Mr. Surendra mohan occupies a special place for being with me at hard times, sharing thoughts and our late night parties. Dr. Tripura for her patience in proofreading the thesis.

Special thanks to all my lab mates for bearing me as a person.

I thank the tissue culture staff at CCMB for their support and keeping the premises clean and sterile. Head of the instrumentation division, CCMB, Dr. Sekhar Ramachandran and the staff Mrs. Asha Ramesh, Mr. Chakravarthi, Mr. Fernandes, Mr. Shyam Kumar for their kind help and support with regard to the various facilities. Dr. Nandini Rangaraj for her help in imaging the cells using fluorescence microscope.

A special thanks to all my friends at Geelong for all the good times during my visit to Australia. My heartfelt gratitude to Mr. Mohan Setty, Mr. Rajesh Nanjappa, Mr. Bhanu Raj, Mr. Satish Venkatesan, Mr. Apoorva Gaonkar, Dr. Nishar Hameed, Nisa Salim, Dr. Sreekumar, Dr. Ganesh Mahidhara for making me feel at home. A special thanks to Mohan Setty for his constant support and encouragement.

All the technical and administrative staff at Deakin University, Geelong for their support.

All my friends in Hyderabad for being with me for all the fun times as well as hard times, encouraging me and associating with me.

Abbreviations

α -MEM	Alpha-Minimal essential medium
AFM	Atomic force microscope
ALP	Alkaline phosphatase
BMP	Bone morphogenetic protein
BSA	Bovine serum albumin
Bgn	Biglycan
BGLAP	Bone gamma-carboxyglutamate (gla) protein (Osteocalcin)
cDNA	complementary-Deoxyribonucleic acid
Cdh11	Cadherin 11
COL1	Type I collagen
COL3	Type III collagen
dNTP	deoxyribonucleotide triphosphate
DMP1	Dentin matrix protein
DMSO	Dimethyl sulfoxide
DTT	Dithiothreitol
DAPI	4',6-diamidino-2-phenylindole
ECM	Extracellular matrix
EDTA	Ethylenediaminetetraacetic acid
EtBr	Ethidium bromide
EGF	Epidermal growth factor
FGF	Fibroblast growth factor
FN	Fibronectin
FITC	Fluorescein isothiocyanate
FAK	Focal adhesion kinase
GAPDH	Glyceraldehyde 3-phosphate dehydrogenase

HF	Hydrofluoric acid
HNO ₃	Nitric acid
IGF	Insulin-derived growth factor
IgG	Immunoglobulin G
ITG	Integrin
IBSP	Bone sialoprotein
MAPK1	Mitogen activated protein kinase 1
MgCl ₂	Magnesium chloride
MTT	3-(4,5-Dimethylthiazol-2-yl)-2,5-diphenyltetrazolium bromide
MPa	Mega Pascal
MMP	Matrix metalloproteinase
MC3T3-E1	Mouse calvaria 3T3 cell line
NFκB	Nuclear factor kappa B
Nb	Niobium
OC	Osteocalcin
oligo-dT	Oligo deoxy-thymidine
PBS	Phosphate buffered saline
Pt	Platinum
pNPP	<i>p</i> -nitrophenyl phosphate
Pxn	Paxillin
Runx2	Runt-related transcription factor
Ra	Surface roughness
RNA	Ribonucleic acid
RT-PCR	Real time polymerase chain reaction
RT	Reverse transcriptase
RMS	Root means square
SDS	Sodium dodecyl sulphate

SiC	Silicon carbide
SEM	Scanning electron microscope
SPARC	Secreted protein acidic and rich in cysteine (Osteonectin)
SPP1	Secreted phosphoprotein 1 (Osteopontin)
TCP	Tissue culture polystyrene/Plastic
TBE	Tris boric acid
TiO ₂	Titanium oxide
TGF-β1	Transforming growth factor-β1
Ti	Titanium
TiZr	Titanium Zirconium
TiNb	Titanium Niobium
V	Volts
VTN/VN	Vitronectin
XPS	X-ray photoelectron spectroscopy
XRD	X-ray diffraction
Zr	Zirconium
nm	Nanometre
μm	Micrometer
mm	Millimetre
μl	Microlitre
mM	Millimolar
μg	Microgram

Abstract

The biocompatibility and bone forming ability of Zirconium (Zr) and Niobium (Nb) alloys of Titanium (Ti) were explored in this study. Zirconium and Niobium were used as alloying elements to Titanium with the aim of improving the mechanical properties for effective use as implant materials, for bone tissue engineering applications. Powder metallurgy was used for synthesizing the alloys by means of mechanical alloying from individual powders and green compacts made. The materials were then investigated for their bone forming ability and biocompatibility using bone forming cells namely, osteoblasts.

Understanding the interactions at the interface of a cell with the material surface is crucial for the design of ideal materials as implants for bone tissue engineering applications. Much of the cell-material interactions take place on the surface and it is the nature of the presenting surface which determines the reaction and behavior of cells. Properties of surfaces that are thought to play a pivotal role in determining the fate of the cells include surface roughness, surface composition, surface topography, surface chemistry and surface energy. Titanium-Zirconium (TiZr) and Titanium-Niobium (TiNb) alloys were tested for their biocompatibility and compared with the gold standard Titanium in their behavior towards osteoblast cells. The possible role of the surface properties at different stages of osteoblast cell- material interactions were sketched out. We observed a significant increase in the adhesion, proliferation and differentiation processes on TiZr alloy compared to Ti and TiNb at the cellular level. The surface characterization of the materials revealed interesting behavior. The surface energy of TiZr was higher compared to Ti and TiNb, whereas the surface roughness was in the sub-micron range with very little differences between the materials. We could attribute the observed cell responses to the differences in surface energy.

Furthermore, it was interesting to understand the possible mechanism for the observed behavior of cells towards the materials by looking at the profile patterns of the genes or candidate genes involved in the process of bone formation by osteoblast cells. Since, the materials used in the study were divided by the composition, making it even more exciting with regard to the cell behavior. This opened up the possibility for investigating the ideal role of substrate composition of similarly based materials on

osteoblast cell behavior. Since it was observed that the cellular level responses were dependent on surface energy (which, further accelerated cell adhesion on the material surfaces) we were interested in studying the responses at the molecular level. The expression of the genes involved in cell adhesion such as integrins and extracellular matrix related genes were observed to be higher on the TiZr alloy surface further strengthening our observation at the cellular level where, cell adhesion was higher on the TiZr alloy surface. Thus, we were able to establish the fact that, surface energy plays an upper hand in terms of accelerating the cell adhesion to materials surfaces where the surface roughness differences are minimal. However, the genes related to differentiation were higher on the TiNb surface compared to Ti and TiZr and therefore, the possible role of substrate composition on the differentiation process of osteoblast cells cannot be ruled out.

Surface modification of metallic materials explores the opportunity for the cells to interact with varied morphological features and surface chemistries. Surface modification strategies help in improving the osteoblast cell behavior directed towards a mature and a differentiated phenotype. One such process, anodization, involves electrochemical treatment, which produces different surface morphologies with varied features under standard experimental conditions. In this study, titanium-zirconium (TiZr) alloy was subjected to anodization at a constant voltage of 20V for 20 min to produce nanotubes on its surface with diameters ~30-50 nm. The response of osteoblast cells at the cellular and molecular level were observed on the nanotubular surface and the differences in the osteoblast cell behavior were investigated in comparison to the polished and acid etched substrates of the same alloy. We have observed a significant increase in the adhesion and proliferation of osteoblast cells on the anodized surface compared to acid etched and polished surfaces both at the cellular and molecular level. We could correlate the enhanced behavior of cells to nanoscale roughness, higher surface area and greater hydrophilicity of the anodized surface.

TABLE OF CONTENTS

List of Publications	v
Acknowledgements	vi
Abbreviations	viii
Abstract	xi
List of Figures	xviii
List of Tables	xxiv
1. Introduction	1
1.1 Scope of thesis	1
1.1.1 Materials as biomedical implants	1
1.1.2 Biological response to implant materials	3
1.2 Thesis objective	7
1.3 Outline of thesis	8
2. Literature review	9
2.1 Introduction	9
2.2 Biology of the bone	9
2.2.1 Types of bone cells	11
2.2.1.1 Osteoblasts	11
2.2.1.2 Osteoclasts	13
2.2.1.3 Osteocytes	15
2.2.2 Bone matrix	15
2.2.2.1 Organic	16
2.2.2.2 Inorganic	16
2.2.3 Bone homeostasis	17
2.3 Biomaterials for bone tissue engineering	18
2.3.1 Orthopedic biomaterials	18
2.3.2 Metals as orthopedic implants	19

2.3.2.1 Stainless steel	20
2.3.2.2 Cobalt-chromium	20
2.3.3 Titanium and titanium alloys	21
2.4 Surface modification of titanium and titanium alloys	24
2.4.1 Chemical methods	26
2.4.2 Wet-chemical	26
2.4.2.1 Acid treatment	26
2.4.2.2 Hydrogen peroxide treatment	28
2.4.2.3 Alkali treatment	28
2.4.3 Electrochemical methods	29
2.4.3.1 Anodization	29
2.5 Osteoblast cell-biomaterial interactions	38
2.5.1 Bone-implant interface	38
2.6 Osteoblast cell response to surface properties	40
2.6.1 Role of surface properties	40
2.6.1.1 Surface roughness and topography	41
2.6.1.2 Surface chemistry	42
3. Materials and experimental techniques	44
3.1 Sample preparation and processing	44
3.1.1 Raw materials	44
3.1.2 Powder handling, compaction, sintering and grinding	45
3.2 Surface characterization	46
3.2.1 Surface morphology	46
3.2.2 Surface chemical analysis	46
3.2.3 Surface roughness	47
3.2.4 Surface energy measurement	47
3.3 Cell culture	49
3.3.1 Cell line maintenance	49
3.3.2 MTT assay for cell viability and cell count estimation	49
3.3.3 Induction of cell differentiation	50
3.3.3.1 Alkaline phosphatase assay	50
3.3.3.2 Osteocalcin immunostaining	51
3.3.3.3 Alizarin red staining	52
3.4 Techniques for gene profiling	53

3.4.1 Total RNA isolation and purification	53
3.4.2 cDNA synthesis	54
3.4.3 Quantitative real time polymerase chain reaction (RT-PCR)	54
3.4.4 Agarose gel electrophoresis	55
4. The influence of surface energy of titanium-zirconium alloy on osteoblast cell functions <i>in vitro</i>	56
4.1 Introduction	56
4.2 Materials and methods	58
4.2.1 Surface characterizations	58
4.2.2 Cell culture and microscopy	58
4.2.2.1 Cell morphology	58
4.2.2.2 Cell adhesion assay	58
4.2.2.2.1 Vinculin and actin immunofluorescence	59
4.2.2.3 Cell viability	59
4.2.2.4 Cell proliferation assay	60
4.2.2.5 Cell differentiation assays	60
4.2.2.5.1 ALP activity	60
4.2.2.5.2 Osteocalcin immunostaining	60
4.2.2.5.3 ECM analysis	61
4.2.2.6 Matrix mineralization	61
4.3 Results	62
4.3.1 Surface characterization	62
4.3.2 Surface energy	64
4.3.3 Cell morphology	64
4.3.4 Cell adhesion and spreading	66
4.3.5 Cell viability	70
4.3.6 Cell proliferation	71
4.3.7 Cell differentiation	72
4.3.8 Matrix mineralization	77
4.4 Discussion	79
4.4.1 Cell adhesion and spreading	79
4.4.2 Cell proliferation and differentiation	80
4.5 Conclusions	83

5. Role of surface properties of titanium alloys on the expression of adhesion and differentiation related genes	85
5.1 Introduction	85
5.2 Materials and methods	88
5.2.1 Sample preparation and processing	88
5.2.2 Cell culture	88
5.2.3 Gene profiling	88
5.2.3.1 PCR array	88
5.2.3.1.1 RNA isolation	88
5.2.3.1.2 cDNA synthesis	89
5.2.3.1.3 Real time PCR	91
5.2.3.2 Real time PCR using gene specific primers	92
5.2.3.2.1 Cell adhesion specific gene expression studies	94
5.2.3.2.2 Induction of cell differentiation	95
5.2.3.2.3 Total RNA isolation and cDNA synthesis	95
5.2.3.2.4 Real time PCR	95
5.3 Results	96
5.3.1 PCR array	96
5.3.2 Gene profiling using gene specific primers	103
5.3.2.1 Expression of cell adhesion molecules and their cofactors	103
5.3.2.2 Expression of cell differentiation markers	111
5.4 Discussion	119
5.4.1 Role of integrins and ECM molecules	119
5.4.2 Cytoskeletal organization	120
5.4.3 Cell differentiation genes	120
5.4.4 Suitable properties of Ti versus Ti alloys for orthopedic applications	121
5.5 Conclusions	123
6. Cell biological responses of osteoblasts on anodized nanotubular surface of a titanium-zirconium (TiZr) alloy	125
6.1 Introduction	125
6.2 Materials and methods	128

6.2.1 Substrate preparation	128
6.2.2 Surface characterization	128
6.2.3 Cell culture	128
6.2.4 Cell adhesion, morphology and spreading	129
6.2.5 Cytoskeletal organization	129
6.2.6 Cell proliferation	129
6.2.7 Cell differentiation	129
6.2.7.1 Quantitative real time PCR	130
6.2.7.2 Osteocalcin immunostaining	132
6.2.7.3 Extracellular matrix analysis	132
6.2.8 Matrix mineralization	132
6.3 Results	133
6.3.1 Material surface characterization	133
6.3.2 Cell adhesion and spreading	136
6.3.2.1 Cell adhesion	137
6.3.2.2 Cell morphology and spreading	138
6.3.2.3 Cell adhesion related gene expression	141
6.3.3 Cell proliferation	147
6.3.4 Cell differentiation	148
6.3.4.1 Osteocalcin immunostaining	148
6.3.4.2 ECM analysis	150
6.3.4.3 Expression of differentiation related genes	152
6.3.5 Matrix mineralization	158
6.4 Discussion	159
6.4.1 Nanotubular surfaces and anodization	159
6.4.2 Cell adhesion and proliferation	159
6.4.3 Cell differentiation	161
6.5 Conclusions	163
7. Conclusions and Future directions	164
7.1 Conclusions	164
7.2 Future directions	167
Bibliography	168

List of Figures

Figure 2.1. The structure of long bones.	10
Figure 2.2. Organizational structure of the interface between endosteal and periosteal layers.	11
Figure 2.3. Lineage specificity of osteoblasts and osteoclasts involving various molecules.	14
Figure 2.4. Dual acid etching on Ti implant surface using HCl and H ₂ SO ₄ .	27
Figure 2.5. FE-SEM micrographs showing morphology of (a) Ti surface, anodized oxides surfaces prepared by anodization in (b) H ₂ SO ₄ , (c) H ₃ PO ₄ and (d) HF electrolytes.	31
Figure 2.6. Mineralization study for 7 days on the anodized surface H ₂ SO ₄ followed by heat treatment at (a) 400 °C, (b) 600 °C, anodized in H ₃ PO ₄ and heat treated at (c) 400 °C, (d) 600 °C for anodized HF surface.	31
Figure 2.7. Optical density measured after cell culture for 5, 11 and 16 days on the different anodized samples at a wavelength of 570 nm by spectrophotometer.	32
Figure 2.8. FE-SEM photographs of the surfaces of titanium metals untreated and subjected to anodic oxidation in H ₂ SO ₄ solution at 100, 150 and 180V.	33
Figure 2.9. FE-SEM photographs of the surfaces of titanium metals subjected to anodic oxidation in acetic acid solution at 100, 150 and 180V.	33
Figure 2.10. FE-SEM photographs of the surfaces of titanium metals subjected to anodic oxidation in H ₃ PO ₄ solution at 100, 150 and 180V.	33
Figure 2.11. FE-SEM photographs of the surfaces of titanium metals subjected to anodic oxidation in Na ₂ SO ₄ solution at 100, 150 and 180V.	33
Figure 2.12. FE-SEM photographs of the surfaces of titanium metals subjected to anodic oxidation in H ₂ SO ₄ solution at 100, 150 and 180V and then soaked in SBF for 1 or 7 d.	34

Figure 2.13. FE-SEM photographs of the surfaces of titanium metals subjected to anodic oxidation in Na₂SO₄ solution at 100, 150 and 180V and then soaked in SBF for 7 d. **34**

Figure 2.14. SEM photographs of (A) titanium metal without treatment and anodically oxidized titanium at (B) 90 V, (C) 155 V and (D) 180 V in 1 M H₂SO₄ for 1 min. **35**

Figure 2.15. TF-XRD patterns of (A) titanium metals without treatment and titanium metals anodically oxidized at (B) 90 V, (C) 155 V and (D) 180 V in 1 M H₂SO₄ for 1 min. **35**

Figure 2.16. FE-SEM top-view images of porous titanium oxide films anodized in 0.5 wt% HF solution for 20 min under different voltages: (a) 3V, (b) 5V, (c) 10V and (d) 20V. **37**

Figure 2.17. Representation of events at the bone-implant interface. (a) protein adsorption from blood and tissue fluids, (b) protein desorption, (c) surface changes and material release, (d) inflammatory and connective tissue cells approach the implant, (e) possible targeted release of matrix proteins and selected adsorption of proteins such as BSP and OPN, (f) formation of *lamina limitans* and adhesion of osteogenic cells, (g) bone deposition on both the exposed bone and implant surfaces, (h) remodelling of newly formed bone. **39**

Figure 4.1. SEM images of (a) Ti, (b) TiZr and (c) TiNb (scale bar represents 50 µm) and XPS survey spectra of (d) Ti, (e) TiZr and (f) TiNb, respectively. **63**

Figure 4.2. SEM images showing the morphology of MC3T3-E1 cells on (a) Ti, (b) TiZr and (c) TiNb, respectively after 48 h of cell seeding (scale bar represents 20 µm). [Inset shows filopodial extensions formed on the materials surface (scale bar represents 5 µm)]. **65**

Figure 4.3. The percentage of cells attached to the three materials Ti, TiZr and TiNb after 4 h of cell seeding. **66**

Figure 4.4a. (a) The immunostaining of cells on Ti, TiZr and TiNb after 8 h of seeding the cells. Panel 1 shows vinculin staining (the contact points of the cells to the surfaces is indicated by the arrows), panel 2 shows actin staining (the stress fibres are

clearly visible on the materials, indicating the spreading of the cells), panel 3 shows the merged image of vinculin and actin (the arrows indicate the co-localized regions), (scale bar represents 10 μm). **68**

Figure 4.4b. (b) The immunostaining of cells on Ti, TiZr and TiNb after 48 h of seeding the cells. Panel 1 shows vinculin staining (the contact points of the cells to the surfaces is indicated by the arrows), panel 2 shows actin staining (the stress fibres are clearly visible on the materials, indicating the spreading of the cells), panel 3 shows the merged image of vinculin and actin (the arrows indicate the co-localized regions), (scale bar represents 10 μm). **69**

Figure 4.5. The percent viable cells after 24 h of seeding the cells on Ti, TiZr and TiNb, respectively. **70**

Figure 4.6. The number of cells present at the end of each time period namely 1, 4 and 7 days on the three materials. **71**

Figure 4.7. ALP activity profile of cells on Ti, TiZr and TiNb at 1, 4 and 7 days. **72**

Figure 4.8. Immunostaining of osteocalcin protein at days 7, 15, 21 and 28 on Ti, TiZr and TiNb (scale bar represents 50 μm on all the individual images). **74**

Figure 4.9. (a) The extracellular matrix formation on the three material surfaces Ti, TiZr and TiNb after 2, 4 and 7 days of differentiation. (b) The extracellular matrix formation on the three material surfaces after 10, 15 and 21 days of differentiation. (scale bar represents 50 μm). Insets in each panel show the high magnification images of the ECM with cells. (scale bar represents 5 μm). **75**

Figure 4.10. Alizarin red staining on the three material surfaces Ti, TiZr and TiNb at 7, 15, 21 and 28 days after differentiation. **78**

Figure 5.1. Fold change of genes on Ti at 1 and 4 days after differentiation. **100**

Figure 5.2. Fold change of genes on TiZr at 1 and 4 days after differentiation. **101**

Figure 5.3. Fold change of genes on TiNb at 1 and 4 days after differentiation. **102**

Figure 5.4. The fold expression of integrins and extracellular matrix genes on the three materials Ti, TiZr and TiNb at 4 and 24 h after adhesion. **104**

Figure 5.5. The fold expression of focal adhesion and osteoblast specific genes on the three materials Ti, TiZr and TiNb at 4 and 24 h after adhesion. **106**

Figure 5.6. The fold expression of TGF- β 1, type III collagen, cadherin 11, MAPK1 and NF κ B genes on the three materials Ti, TiZr and TiNb at 4 and 24 h after adhesion. **108**

Figure 5.7. Real time PCR products of adhesion genes on the three materials Ti, TiZr and TiNb at 4 and 24 h time intervals. **110**

Figure 5.8. The fold expression of ALP, type I collagen, osteopontin, osteocalcin, osteonectin and bone sialoprotein genes on the three materials Ti, TiZr and TiNb at 1, 4, 10 and 15 days after differentiation. **112**

Figure 5.9. The fold expression of TGF- β 1, BMPs, Runx2 and SMADs genes on the materials Ti, TiZr and TiNb at 1, 4, 10 and 15 days after differentiation. **114**

Figure 5.10. The fold expression of DMP1, Biglycan, FGF-2, IGF-1 and MMP2 genes on the three materials Ti, TiZr and TiNb at 1, 4, 10 and 15 days after differentiation. **116**

Figure 5.11. Real time PCR products of differentiation genes on the three materials Ti, TiZr and TiNb after 1, 4, 10 and 15 days of differentiation. **118**

Figure 6.1. SEM image showing the morphology of cells on the three materials (A) polished, (B) acid etched (Inset shows high magnification image) and (C) anodized (Inset shows high magnification image with clear nanotubes of ~30-50 nm diameter). **134**

Figure 6.2. Surface topography image of the three material surfaces (A) polished, (B) acid etched and (C) anodized using AFM (scan area 1x1 μm^2). **135**

Figure 6.3. The percentage of cells attached to the three material surfaces after 4 h of cell seeding using MTT assay. **137**

Figure 6.4. SEM image showing cell morphology on the three material surfaces (A) polished, (B) acid etched and (C) anodized (scale bar represents 20 μm). Inset shows high magnification image of the numerous filopodial extensions (scale bar represents 2 μm). **139**

Figure 6.5. Actin immunostaining of cells on the three material surfaces (A) polished, (B) acid etched and (C) anodized (scale bar represents 10 μm). **140**

Figure 6.6A. The fold expression of integrins $\alpha 2$, $\alpha 5$, αV and $\beta 1$, osteopontin, osteocalcin, osteonectin and type I collagen genes on the three material surfaces after 4 and 24 h of adhesion. **142**

Figure 6.6B. The fold expression of TGF- $\beta 1$, FAK, vinculin, paxillin, fibronectin and vitronectin genes on the three material surfaces after 4 and 24 h of adhesion. **144**

Figure 6.7. Real time PCR products of adhesion genes on the materials at 4 and 24 h time intervals. **146**

Figure 6.8. The proliferation of cells on the three material surfaces after 24, 48 and 72 h of cell seeding using MTT assay. **147**

Figure 6.9. Immunostaining of osteocalcin protein at 2, 4, 7, 10, 15 and 21 days post induction on the three material surfaces. Intracellular and extracellular protein levels are stained green and the nucleus is stained blue using DAPI (scale bar represents 50 μm). **149**

Figure 6.10. (A) SEM images showing extracellular matrix formation on the three material surfaces after 2, 4 and 7 days of differentiation. (B) Extracellular matrix formation on the three material surfaces after 10, 15 and 21 days of differentiation. (scale bar represents 50 μm). Inset shows high resolution, high magnification image (scale bar represents 5 μm). **150**

Figure 6.11A. The fold expression of alkaline phosphatase, type I collagen, type III collagen, osteopontin, osteonectin, osteocalcin, bone sialoprotein and TGF- $\beta 1$ genes on the three material surfaces after 1, 4 and 10 days of differentiation. **153**

Figure 6.11B. The fold expression of BMP1, BMP4, Runx2, DMP1, Biglycan, IGF-1 and FGF-2 genes on the three material surfaces after 1, 4 and 10 days of differentiation. **156**

Figure 6.12. Real time PCR products of differentiation genes on the materials after 1, 4 and 10 days of differentiation. **157**

Figure 6.13. Alizarin red staining for calcium deposition on the materials after 7, 15, 21 and 28 days of differentiation on the materials. **158**

List of Tables

Table 2.1. Osteoblast specific secretary and extracellular products.	13
Table 2.2. Bone specific non-collagenous proteins.	16
Table 2.3. Properties to be satisfied by implant materials.	19
Table 2.4. Ti alloys developed for biomedical applications.	23
Table 3.1. Characteristics of the metal powders used.	44
Table 4.1. The roughness (Ra) values of the materials tested namely Ti, TiZr and TiNb.	62
Table 4.2. The water contact angles and the calculated surface energies of Ti, TiZr and TiNb.	64
Table 5.1. Table showing the forward and reverse primers of genes used for RT-PCR experiments.	92
Table 5.2. Genes not expressed on the materials Ti, TiZr and TiNb.	96
Table 5.3. Fold change expression of genes on the three material surfaces Ti, TiZr and TiNb after 1 and 4 days of differentiation.	97
Table 6.1. Forward and reverse primers of genes used for RT-PCR experiments.	130
Table 6.2. Surface roughness, surface area and water contact angles of the three TiZr alloy surfaces.	136

1. Introduction

1.1 Scope of thesis

1.1.1 Materials as biomedical implants

The use of ideal materials as orthopedic implants for bone tissue engineering applications is on the rise. The loss of bone due to trauma, degeneration or pathology is of major health concern with huge socioeconomic implications [1]. The major significant current discussion in orthopedics is the need for total joint arthroplasty especially knee and hip replacements also with increased problems related to bone related degenerative diseases such as osteoporosis and other musculoskeletal problems [2, 3]. An approximate 1 million hip replacements, 2.5 million knee replacements [3] and 1.5 million fractures related to osteoporosis [1, 4] are reported every year. Various classes of biomaterials including ceramics, polymers, metals and composites have been applied to treat these conditions with varying degrees of success [5]. A number of these materials have been used for bone repair depending on the site of implantation and injury. It should be stated that, these artificial biomaterials offer improved quality of life to millions each year.

However, the major concern with regard to present human needs is the availability of materials for hard tissue repair such as for load bearing applications as femoral and tibia replacements and total joint replacement. Materials for bone replacement and repair must possess certain properties to meet the requirements for implantation including good mechanical properties so as to be able to withstand the whole weight of the body and suitable biological properties for effective *in vivo* functioning. The choice of materials for such applications is currently limited to the use of metals [6]. Metals for their good mechanical properties such as excellent compressive and tensile strength limit the use of ceramics, polymers and composites for such load bearing applications

[7, 8]. Stainless steel, cobalt-chromium alloys, titanium and titanium alloys are certain classes of metals developed for use in bone tissue engineering and hard tissue repair [9].

Stainless steel (316L) and cobalt chromium alloys (Co-Ni-Cr-Mo, Co-Cr-Mo) were the first of the metals that were employed as artificial materials for applications in bone tissue engineering especially as balls and stems of artificial hip implants [2, 10]. The use of stainless steel, cobalt-chromium alloys for bone repair applications lost its prominence mainly due to the biocompatibility issues [11]. However, the toxicity of the elements Co (Cobalt), Cr (Chromium) and Ni (Nickel) present in stainless steel and Co-Cr alloys and their release in the highly corrosive environment of the human body limited their application [12, 13]. Additionally, functionality such as a low elastic modulus is required for metallic materials to be used in orthopedics, the before mentioned materials do not possess this quality. Titanium and Ti alloys thereof, due to their high strength to weight ratio, low density and more importantly due to their biocompatibility are gaining importance and are gradually replacing stainless steel and cobalt-chromium alloys for biomedical applications. Excellent resistance to corrosion, high strength-weight ratio, formability is among the properties in favor of titanium and titanium alloys [14].

In the last few decades research has been focused on developing new titanium alloys for applications in orthopedics, dental and healthcare goods [15, 16]. Ti-6Al-4V and NiTi are certain classes of titanium alloys that were developed for orthopedic applications [17-19]. The commercially available titanium alloys with the composition Ti-6Al-4V, has certain disadvantages with regard to the toxicity of aluminum and vanadium. This drawback provides opportunity for the development of new non-toxic materials [20-22]. Alloying elements such as Strontium (Sr), Silicon (Si), Molybdenum (Mo), Zr, Nb were selected for developing titanium alloys with suitable mechanical properties [6]. However, recent studies [23] suggest certain levels of toxicity with regard to the use of Sn, Si and Mo as alloying elements. Zr and Nb are two elements that have been shown to be biocompatible and therefore we have looked at developing toxic free alloys of titanium namely Titanium-zirconium (TiZr) and Titanium-niobium (TiNb) using the powder metallurgy method. We have further evaluated the biocompatibility and bone forming ability of these materials and tested their *in vitro* cytotoxicity and cellular behavior of osteoblasts when seeded on the materials, by investigating the adhesion, proliferation and differentiation processes.

1.1.2 Biological response to implant materials

Apart from the bulk mechanical properties, implant materials for bone tissue engineering applications should also possess certain biological properties, for their successful *in vivo* functioning. Biocompatibility is the prime requirement for an implant material [24]. Biocompatibility is the property of a material to be able to function in the physiological environment, without causing any inflammatory response to the host tissue upon implantation [25]. Furthermore, the ability of the implanted material to support the growth of cells and assist in the normal functioning of the host tissue is as well important. Osseointegration of implant material to the bone tissue is a requisite for the effective functioning of the implant in the long run. The biocompatibility of implant materials for orthopedic applications is often tested *in vitro* using primary cells and cell lines of mesenchymal origin. Sources of these include primary cells such as mesenchymal stem cells from mouse, rat, and human as well as established cell lines from these sources such as MC3T3 (Mouse calvaria), hFOB (Human fetal osteoblast), MG63 (Human osteocarcinoma), Saos (Human osteosarcoma). The performance of the implant materials *in vivo* is often judged by their *in vitro* performance which is evaluated using the above mentioned cell sources. Several studies in the literature are reported on the *in vitro* performance of several materials using the above cell sources [26-35].

The behavior of osteoblast cells on the material surfaces can be studied by examining the processes of adhesion, proliferation, maturation and differentiation of the cells in response to the material's surface properties. The surface of implant materials plays a pivotal role in directing the cell behavior, as the bulk of cell-material interactions occur at the surfaces upon implantation *in vivo* [36, 37]. Therefore, how a cell responds to different surface features it encounters holds equally important in determining the ideal surface features to be designed for successful bone response and integration. However, there are a number of factors which influence the successful functioning of the implanted materials. The physico-chemical properties of the material surfaces are amongst the most important. The success of the implant used is determined by the events that take place at the cell-material interface. Surface properties of the materials such as surface energy, surface roughness, surface topography and surface composition modulate the cellular properties by influencing the behavior of cells either directly or in an interdependent manner. Several studies have focused on the effect of surface properties on the response of osteoblast

cells [38-44]. For instance, early studies by researchers have evaluated the osteoblast cell behavior in response to surface roughness and reported on the increase in osteoblast adhesion and differentiation on rough surfaces compared to smooth surfaces [41, 45-47]. On rough surfaces, although the adhesion of cells is better, the proliferation ceases. In other words, the adhesion and proliferation are inversely related in terms of cell behavior on rough surfaces. However, the differentiation phenomenon is accelerated on rough surfaces in comparison to smooth surfaces. It should be noted that, no conclusive evidence exists with regard to roughness effects on osteoblast cell behavior as smooth surfaces in one study are termed rough in another study.

Later, the effects of surface topography on osteoblast cell responses were evaluated [38, 48-51]. It should be noted that, surface topography and surface roughness are interrelated and it is hard to isolate the effects of an individual property on observed osteoblast cell behavior. Surface energy and substrate composition effects on osteoblast cell behavior were also studied [40-42, 51-53]. Although several studies were reported on the surface properties influence on osteoblast cell behavior, still it was unclear as to which surface properties effects the cell behavior in terms of the different phases of cell- material interactions such as cell adhesion, cell proliferation and cell differentiation [27, 53, 54]. Therefore, we have focused on these aspects of cell-material interactions by looking at the behavior of MC3T3-E1 osteoblast cells on material surfaces namely TiZr, TiNb and Ti in terms of the surface properties at various stages of cell-material interactions. The surface roughness profiles of these three materials were in the sub-micron range apart from the different chemical compositions namely the presence of Zr and Nb as alloying elements to Ti. Furthermore, we have observed a significant difference in the surface energy of these three material surfaces and these differences were enough in modulating the cellular and molecular responses thereby resulting in enhanced cell behavior. We can interpret the possible role of surface energy in influencing various cellular processes, with the initial attachment of cells highly accelerated by the high energy surfaces. In our study, we have observed this behavior on TiZr surface which has a higher surface energy compared to Ti and TiNb.

It can therefore be concluded that the interaction of cells with the surface of the material, determines the fate of the implant inside the body. From various studies it was evident that, osteoblast cells respond differently to the material surface properties and are sensitive to the kind

of material surface encountered. The cellular response at each stage of cell-material interactions is determined by the signal transduction of proteins involved in the interactions [55-57]. It is the adsorbed proteins which modulate the signal transduction and thereby determine the fate of the cells with respect to the different cellular processes of morphology, adhesion and spreading. This further influences the processes thereof viz proliferation and differentiation in response to the surface properties of the materials [39, 58]. Adhesion of cells to the material surfaces plays a key role and dictates the further processes of proliferation and differentiation. Thus, it is not only important to understand the behavior of cells at the cellular level, but also the molecular mechanism behind the observed cellular response in order to evaluate the ideal conditions for improved overall biological response of implant materials. Therefore, we have focused on elucidating the possible candidate genes involved that play a significant role in the initial adhesion of cells to the material surfaces, thereby suggesting for possible signal transduction differences in the observed cell behavior on the three material surfaces at different stages of proliferation and differentiation.

Having looked at the varied behavior of osteoblast cells in response to alloys with different surface properties, it was interesting to observe the cell behavior on surfaces with different surface features altogether. Modification of surfaces is an effective strategy to improve on the bioactivity and biocompatibility of material surfaces without altering the bulk properties [59, 60]. Several physical, chemical and biological methods are available and have been employed for improving the bioactivity and enhancing the quality and quantity of interactions of implant materials at the bone-implant interface [61, 62]. Furthermore, nano-structured surfaces present a useful interface in understanding the biology of cells [63-72]. Several studies have shown the importance of nano-structured surfaces in improving the bioactivity and osteoconductivity of material surfaces [30, 73-76]. Different nano-structural surface features were generated using various surface modification techniques such as nanofibres, nanorods, nanogrooves, nanopits and nanotubes and their response to osteoblast cells was studied [71, 74, 77-84]. Anodization is a powerful technique with an ability to produce surfaces with improved oxide layer thickness and controlled nanoscale structures such as nanoparticles and nanotubes [63, 64, 81, 85-90]. The osteoblast cell behavior on these nano-structured surfaces [63, 64, 71, 72, 79, 81, 82, 87, 91, 92] are well documented. It should be noted that, in the natural environment of bone tissue, the organization of a cell is not only at a micrometric scale but it is also the nanometric scale features

which are encountered by the cells, especially in the bone, where, hydroxyapatite crystals interact with the nanofibrillar assembly of type I collagen fibrils [93]. Therefore, it becomes important to understand the contribution of nanoscale features on the events of osteoblast response. Studies in the past show the improved response of osteoblasts towards the modified surface compared to a polished surface both topographically and in terms of surface roughness differences [64, 94, 95]. Although the surface properties are interdependent and it is difficult to isolate the effect of one particular property in response to osteoblast cells, however, subtle differences in the surface properties could be well attributed to the observed cell behavior. Even though, the enhanced behavior of cells on nano-structured surfaces was shown, the molecular mechanism behind such observations is not very well understood. Therefore, we modified the surface of polished TiZr alloy using electrochemical treatment namely anodization under controlled conditions to create nanotubular surfaces. The cellular and molecular responses of these surfaces were tested and the response towards the modified surface gave insights into the behavior of osteoblast-cell material interactions towards developing better osteointegrated surfaces.

The observed differences in the differential expression of signaling molecules provide evidence for the observed behavior of cells on the materials. The selective choice of cells with regard to the material properties *in vitro* provides further opportunity for studies, thereby looking at the possible outcomes in the *in vivo* environment.

1.2 Thesis objective

The objective of this thesis was to evaluate the biocompatibility and bone forming ability of two titanium alloys namely Titanium-Zirconium (TiZr) and Titanium-Niobium (TiNb). This was achieved by looking at the following aspects:

- To investigate the adhesion, proliferation and differentiation of MC3T3 osteoblast cells on the surfaces of these alloys in comparison to titanium (Ti) both at the cellular and molecular level and in the process look at the effect of different surface properties on the osteoblast response.
- To further investigate and perform in depth analysis of the observed cell response by looking at the gene expression pattern of genes involved in osteogenesis on the three material surfaces at the stages of adhesion and differentiation.
- To evaluate the effect of surface modified TiZr alloy produced by anodization (nanotubular surface) on *in vitro* osteoblast cell response and evaluate the cellular and molecular responses to the surface properties.

1.3 Outline of thesis

Chapter two reviews the literature pertaining to the thesis with emphasis on the osteoblast cell-material interactions and the effects of various surface properties on cell behavior. Also reviewed are the basic structure of the bone and bone cells, titanium and titanium alloys currently available for orthopedic applications along with the surface modification techniques for improving the material surface properties for enhancing the bioactivity.

Chapter three lists the general experimental techniques and methodology used. However, methods specific to each chapter are discussed in detail in individual chapters.

Chapter four investigates the biocompatibility of TiZr and TiNb alloys in comparison to Ti and their ability to support bone cell growth and differentiation. The effect of various surface properties of Ti, TiZr and TiNb alloys on the overall osteoblast cell response is highlighted with particular focus on the effect of each surface property namely surface roughness, surface energy and surface composition at different stages of osteoblast cell behavior.

Chapter five gives insights on the role of several signaling molecules involved in the adhesion and differentiation of osteoblasts on the surfaces of Ti, TiZr and TiNb alloys.

Chapter six describes the effect of nanotubular surface of anodized TiZr in enhancing the osteoblast cell behavior, where the cellular and molecular responses were studied.

Chapter seven provides a summary of the findings from this study and discusses the directions for future research.

2. Literature review

2.1 Introduction

The success of materials for orthopedic applications, in the last few decades was quite encouraging and has offered scope for improvisations and further advancements in this field. The orthopedic materials currently in use are certainly proving positive in restoring the function especially in bone fracture fixation and total joint replacement, thereby improving the quality of life for millions every year. Before an efficient substitute for the bone tissue is synthesized, it is important to understand and learn about the intricacies involved in the organization of the bone tissue as a whole.

This review starts with a summary of the architecture of the bone tissue with a major focus on the cell types present in the bone and their functions. The various materials typically metals of titanium and titanium alloys, which were developed in an attempt to be used as implant materials for bone tissue engineering applications are discussed. The surfaces of these materials under investigation and their physico-chemical properties and their response to the cell biological processes are highlighted. Furthermore, the surface modification strategies for improving the cell-biomaterial interactions are reviewed.

2.2 Biology of the bone

Bone is a dense and complex connective tissue which has a highly organized structure, constituting a part of the endoskeleton of vertebrates. Bone tissue is structurally composed of two types of tissues namely, an outer shell of a hard and dense compact (cortical) bone and inner core comprising numerous open porous cellular structures, smooth or spongy cancellous (trabecular) bone. The compact and trabecular bone are part of the long bones. Figure 2.1 represents the structure of long bones [96].

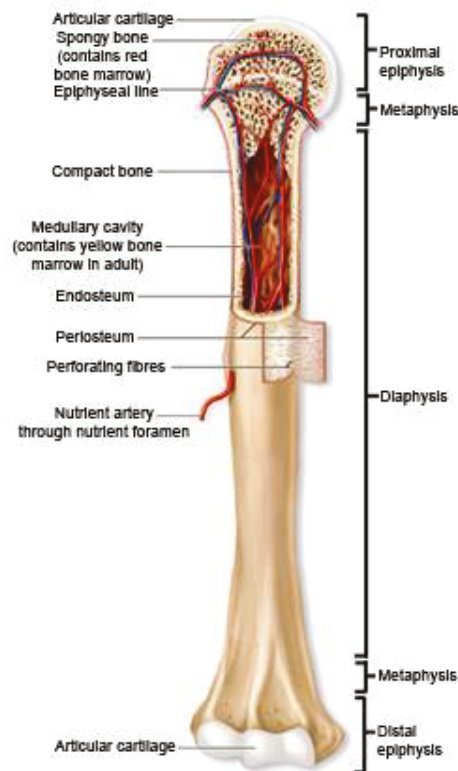


Figure 2.1. The structure of long bones [96].

Typically, long bones consist of upper and lower epiphysis and central diaphysis regions in between two metaphysic regions. The epiphysis and metaphysis consists of the trabecular bone surrounded by a thin layer of hard cortical bone. The diaphysis region is a cylindrical shaft consisting of outer cortical bone with inner bone marrow. The diaphysis is surrounded by the periosteum, which is a vascularized membranous tissue lining the compact or cortical bone tissue. This region of the cortical bone consists of an outer periosteum layer and an inner endosteal layer. It is between these two layers the whole process of bone remodeling occurs with the resorption of old bone tissue by the osteoclasts and new bone tissue formation by the osteoblasts. The various players involved in the osteogenesis process are depicted in Figure 2.2 [97]. The cortical bone contains a series of numerous concentric circular osteons, surrounded by interstitial lamellae, which in turn are connected by harvesian canals that house the blood capillaries, veins, nerves of the bone tissue.

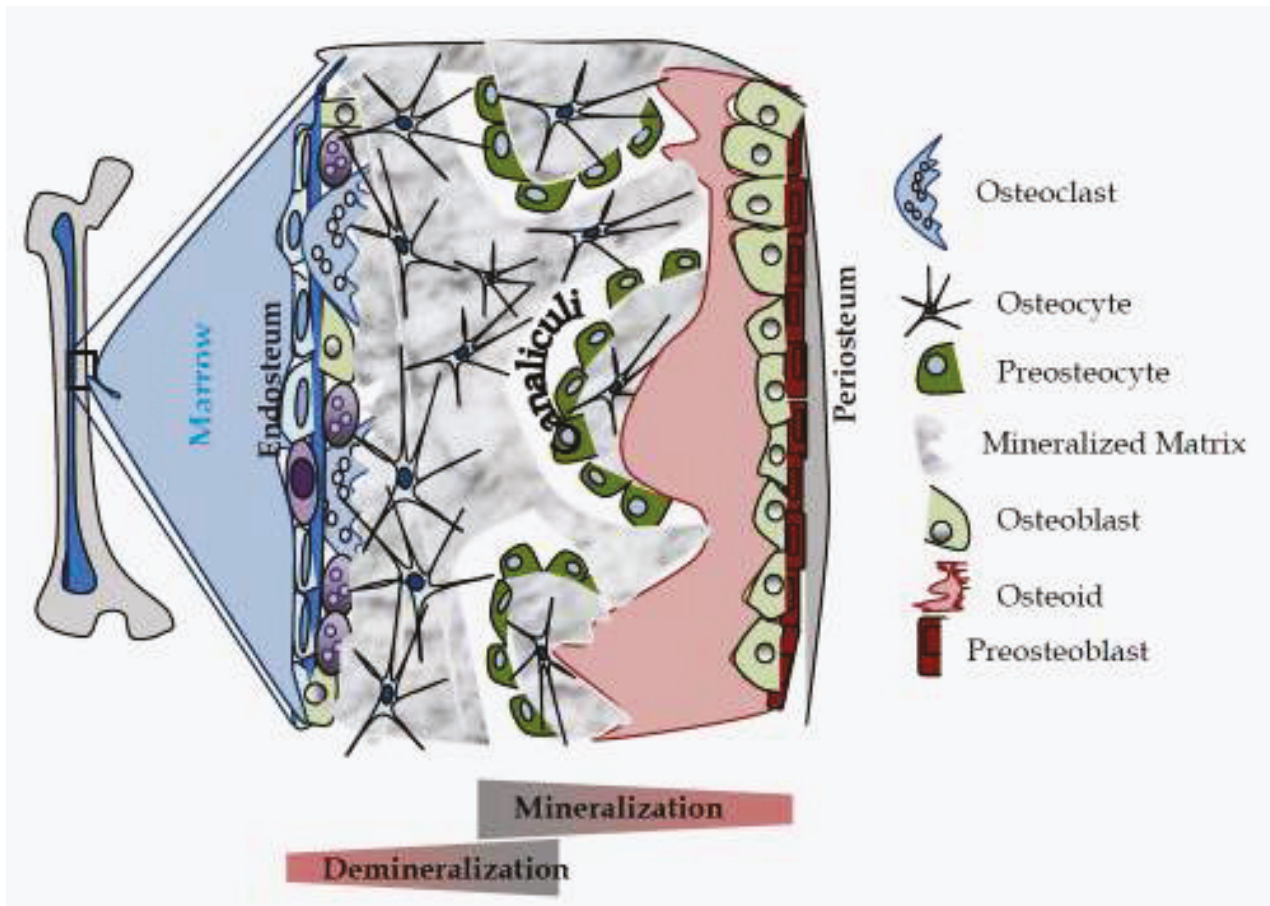


Figure 2.2. Organizational structure of the interface between endosteal and periosteal layers [97].

2.2.1 Types of bone cells

Bone is constituted by cells and a mineralized extracellular matrix (ECM) within which most of the cells are contained. Major type of cells which constitute bone tissue can be typically classified into three main types namely, osteoblasts, osteoclasts and osteocytes in addition to osteoprogenitor cells.

2.2.1.1 Osteoblasts

The most fundamental cell involved in the development, function, growth, repair and maintenance of the bone tissue is the osteoblast. In simple terms, the bone forming cells are

called osteoblasts. The osteoprogenitor (Stem) cells of the mesenchymal origin differentiate and give rise to mononuclear cells called osteoblasts. The major players responsible for the differentiation of osteoblasts include the transcription factors namely, core binding factor alpha-1 (cbfa-1)/runx-related transcription factor (RUNX2), osterix (SP-7) and msx2 (Homeobox protein) along with various other bone related proteins [98-103]. Bone morphogenetic proteins (BMPs), transforming growth factor- β 1 (TGF- β 1), insulin-derived growth factor (IGF), fibroblast growth factor (FGF), platelet-derived growth factor (PDGF) and interleukins (IL) are a certain family of growth factors which effect the differentiation into osteoblasts by the progenitor cells [98, 99, 101, 104-108].

Osteoblasts, with size of 15-30 μm in diameter are mononuclear cells with a large spherical nucleus, rich in rough endoplasmic reticulum and golgi apparatus along with actin, myosin and other active cytoskeletal proteins for maintaining the structural integrity and providing the motility and adhesion to surfaces [1, 98, 109]. Osteoblasts are secretory cells responsible for forming bone by generating, depositing and mineralizing the bone matrix. They are present in the periosteum region of the bone and typically function to form the tissue and minerals which give bone its strength. A major reservoir of osteoblast and osteoprogenitor cells however, is the endosteum surface whereas those required in appositional bone growth and fracture repair are supplied by the periosteal surfaces [110].

Osteoblast cells are solely responsible for the formation of organic, non-mineralized bone matrix termed osteoid by ejecting matrix vesicles. Matrix vesicles originate from the plasma membrane and are spheres (0.1 – 0.2 μm in diameter) containing alkaline phosphatase and pyrophosphatase which act to increase the phosphate concentrations and reduce the inhibitory effects of the process respectively, thereby facilitating mineralization of the osteoid. Figure 2.2 gives an illustration of the osteoid deposited by the osteoblasts. The osteoblasts deposit the extracellular matrix beneath the periosteum, entrapping the blood vessels by the formation of ridges and grooves which eventually fuse together with the deposited matrix thereby forming the osteon [98, 108]. Osteoblasts predominantly secrete the osteoid rich in type I collagen along with various other factors and glycoproteins [98, 99, 105, 109]. Table 2.1 shows the various factors and proteins produced by the osteoblasts [98]. Furthermore, they express certain genetic markers such as osterix, bone sialoprotein, macrophage colony stimulating factor (M-CSF) and more

importantly RANKL (Receptor activator of nuclear factor kappa B ligand) which activates osteoclastogenesis [98] to maintain bone homeostasis.

Table 2.1. Osteoblast specific secretory and extracellular products [98].

Collagen type I, type V (trace)
Osteocalcin
Osteonectin
Osteopontin
RANKL
Osteoprotegerin
Proteoglycans
Latent proteases
Growth factors, e.g. BMPs

2.2.1.2 Osteoclasts

Predominant cells which are involved in the resorption of the bone matrix are osteoclasts. They are multinucleated, polymorphic giant cells originating from the hematopoietic cells of the macrophage lineage [111-113]. Figure 2.3 illustrates the lineage specificity of osteoblasts and osteoclasts [1]. Osteoclasts are situated in depressions or resorption bays called Howship's lacunae where the process of bone resorption occurs. In more simple terms, the osteoclasts are involved in the demineralization of the bone matrix deposited by the osteoblasts. These cells bind to the bone surfaces via the integrins thereby forming a sealing zone creating a low pH environment and by secreting matrix metalloproteinases (MMPs). These cells express the acid hydrolases namely tartrate-resistant acid phosphatase (TRAP) and certain enzymes that help in destroying the organic matrix such as lysosomal (Cathepsin K) and non-lysosomal (Collagenases). Furthermore, in case of trauma to the bone, hematoma formation due to the breakage of vasculature allows for the recruitment of osteoprogenitor cells to the site of fracture from both the periosteal and endosteal regions [101, 105, 110]. Following this there is an intramembranous bone formation in the periosteum region where the fracture site is remodeled

by the osteoclasts to achieve an appropriate geometry and with the simultaneous angiogenesis in the region [105, 108]. The bone resorption and bone formation by the osteoclasts and osteoblasts respectively, is a finely coupled process which occurs in normal bone. The osteoclastic resorption is influenced and stimulated by various factors namely the cytokines from cells and blood circulating factors such as interleukin-1 (IL-1) and parathyroid hormone (PTH), 1,25 (OH)₂ vitamin D₃ (Calcitrol) respectively, whereas the process is inhibited by factors such as calcitonin and interleukin-10 (IL-10).

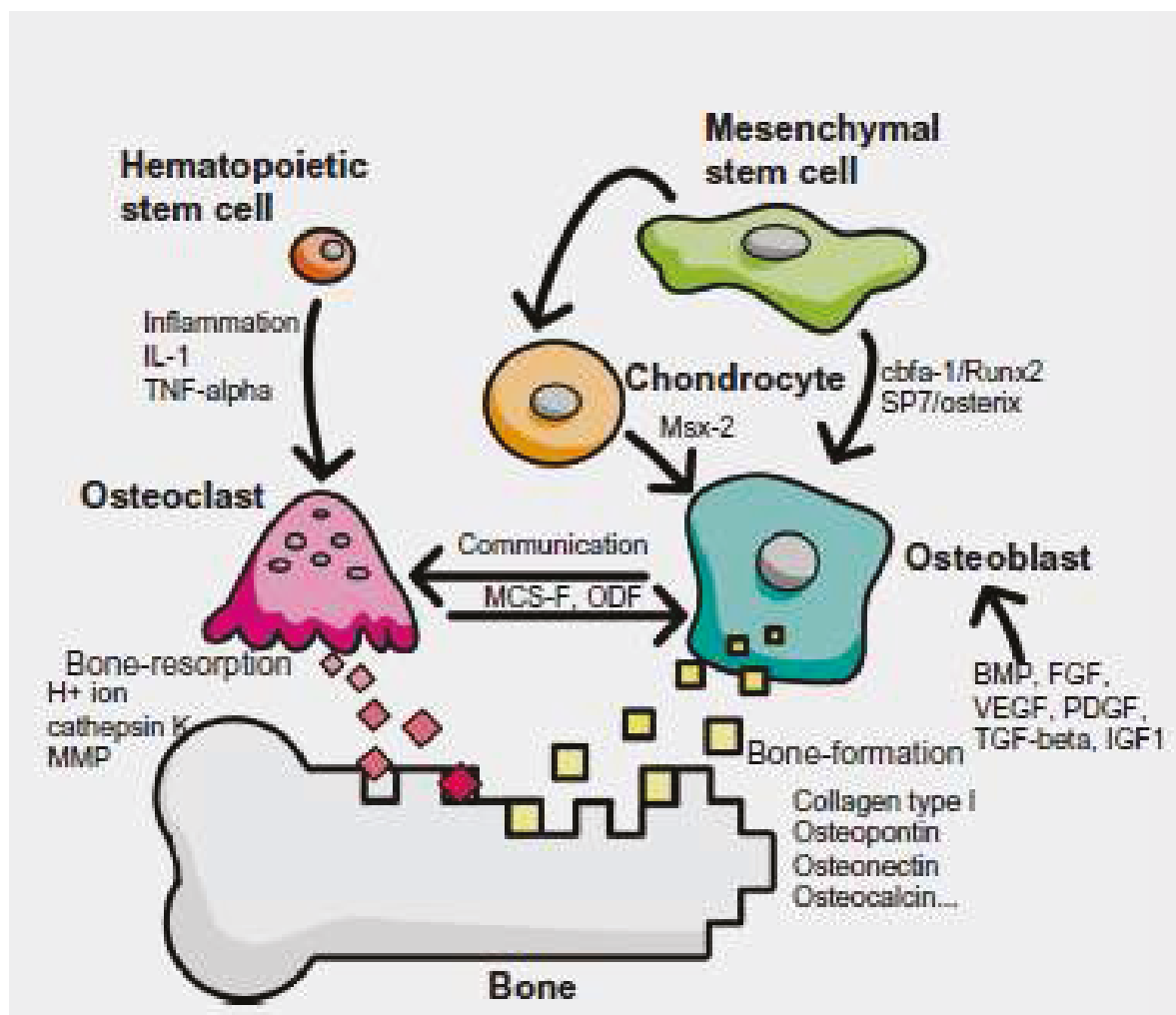


Figure 2.3. Lineage specificity of osteoblasts and osteoclasts involving various molecules [1].

2.2.1.3 Osteocytes

Osteocytes are cells which are present in the lacunae, trapped inside the osteoid or matrix of the bone tissue deposited by the osteoblasts. In other words, after the osteoblasts form and deposit the matrix, they get entrapped inside the matrix and mature into osteocytes. These osteocytes function to maintain bone as a living tissue. They are the most abundant and major cell type in the bone tissue comprising about 90% of cells in the mature skeleton and are important for controlling the extracellular calcium and phosphorous [114]. The major function of osteocytes is to communicate with other types of cells thereby functioning as sensors of the bone tissue. They have a high nucleus to cytoplasm ratio, multiple cytoplasmic projections called canaliculi and form an interconnected cellular network allowing for communication and transport thereby acting as sensors for mechanotransduction in the bone [99, 115-117]. Furthermore, these are the cells involved in the adaptation of the skeletal tissue and triggering the osteoblasts to form bone [115, 116].

The osteocytes and osteoblasts are connected through gap junctions which allows for a coordinated cellular activity, pivotal for their activity and survival [118, 119] whereas, the intercellular communication between the osteoblasts and osteoclasts occurs via calcium signaling and those between the osteoclasts occurs via specific receptors namely P2X and P2Y respectively [120-122]. Contrary to the osteoclasts activation, the osteocytes are inhibited by PTH and stimulated by calcitonin, thereby regulating the osteoclastogenesis process. The interconnections of osteocytes with osteoblasts are retained throughout their life span and when they die, they are phagocytosed and digested by the osteoclasts during bone resorption. Apart from the mechanotransduction role, the osteocytes are also involved in the mineral homeostasis and extracellular matrix mineralization [123]. These cells express DMP1 (Dentin matrix protein) which is crucial for their function, the absence of which leads to phosphate imbalance [124, 125].

2.2.2 Bone matrix

The ECM of the mineralized mature bone consists of organic and inorganic components which constitute to about 30% and 70% respectively. This matrix in the demineralized form is laid down by the osteoblast cells at the early stages of bone formation.

2.2.2.1 Organic

The organic matrix produced by the osteoblasts includes both collagenous and non-collagenous proteins together called, the osteoid. The major protein of the ECM of osteoblasts is the type I collagen that constitutes about 90% of the collagenous form with traces of type V collagen involved in fibrillogenesis. The non-collagenous proteins of the matrix include various proteoglycans, growth factors and cytokines which make up to 10% of the content. Major non-collagenous proteins of the bone matrix include osteocalcin, osteonectin, osteopontin and bone sialoprotein. The proteoglycans and growth factors include biglycan and decorin which interact with the growth factor TGF- β 1. Table 2.2 lists the major non-collagenous proteins of the bone matrix and their functions [98, 99].

Table 2.2. Bone specific non-collagenous proteins [98, 99].

Protein	Function
Osteocalcin	Required for mineralization, binding calcium and hydroxyapatite.
Osteonectin	A phosphorylated glycoprotein which binds to collagen and hydroxyapatite and initiator of crystallization of hydroxyapatite.
Osteopontin	Acidic protein with high affinity for calcium. Bind to integrins on osteoclasts and mediate cell adhesion to bone surfaces.
Bone sialoprotein	Bind to integrins on osteoclasts and mediate cell adhesion to bone surfaces.

2.2.2.2 Inorganic

The major inorganic components which make up the matrix include hydroxyapatite (HA) ($\text{Ca}_{10}(\text{PO}_4)_6(\text{OH})_2$) and calcium carbonate. Certain calcium phosphates, trace amounts of magnesium, fluoride, sodium and certain small amounts of calcium and phosphate hydroxides [126, 127]. The process wherein minerals being added to the bone matrix laid down by the osteoblasts is termed as mineralization. This mineralization can be both biologically induced as well as biologically controlled process. The biologically controlled mineralization is a more

dominant phenomenon with well defined and oriented crystals of uniform size, shape and distribution showing a balanced organization of salts with organic molecules [128]. Furthermore, mineralization in bone is mediated by matrix vehicles which when secreted out of the cells deposit the hydroxyapatite crystals in to the matrix and mineralize in conjunction with type I collagen [129, 130].

2.2.3 Bone homeostasis

Bone modeling and remodeling is often referred to as bone homeostasis (Bone turnover) wherein, the process of bone formation is by the osteoblasts and resorption of the formed bone matrix is by the osteoclasts, which is a continuous process that occurs throughout the life time of an individual [108, 131]. It is estimated that, 10% of adult bone skeleton undergoes bone turnover annually [98]. This process is finely coordinated by a balance between the osteoclasts and osteoblasts by RANKL-RANK-Osteoprotegerin (Opg) axis, whereby the bone modeling and remodeling is controlled [132, 133]. The RANKL-RANK-Opg axis is a signaling mechanism involved in bone. The osteoblasts express the ligand RANKL where as the osteoclasts express RANK. The binding of RANKL secreted by osteoblasts to RANK of osteoclasts, triggers the differentiation of osteoclast precursors to mature osteoclasts and the competitive inhibition of this process by the cytokine osteoprotegerin completes the pathway [132, 134, 135].

In other terms, bone modeling is a process wherein the osteoblasts secrete and deposit the organic bone matrix at the site of damage or repair rich in collagenous and non-collagenous proteins. This matrix is further mineralized by the addition of calcium and phosphate salts (hydroxyapatite crystals) with the help of matrix vehicles to type I collagen with further involvement of other non-collagenous proteins thereby completing the bone modeling phenomenon. On the other hand, bone remodeling involves the resorption / decalcification of this deposited mineralized matrix by the osteoclasts. Thus, the bone homeostasis is a finely tuned process involving the coordinated effort from the osteoblasts and osteoclasts. Furthermore, the bone modeling and remodeling is also directed by external factors of mechanical forces (Wolf's law and Hueter-Volkmann law) and electrical charges where the bone forms and remodels in relation to the mechanical cues and electrical charges it encounters in their environment [115, 116, 136].

2.3 Biomaterials for bone tissue engineering

Bone is a developing tissue, often prone to injuries as a result of trauma or due to ageing and disease. Therefore, it is a clinical challenge to regenerate large bone defects or replace the bone tissue as a whole. Data on bone therapy market indicates that an estimated 6.2 million fractures of bone are reported in the U.S. every year out of which 10% of the cases fail to heal properly [137]. Osteoporosis is a major disease estimated to effect around 10 million people which is expected to increase to 14 million by 2020 [138, 139]. The main cause of osteoporosis is a reduction in bone mass, which is due to a decrease in the number of osteoblast cells, responsible for forming bone and bone matrix, but not due to their ineffective functioning [140]. Recent statistics from the National Osteoporosis Society report an estimated £1.73 billion spent in the United States for treating hip fractures and massive amounts spent by the National Health Service for treating osteoporosis related fractures [1, 4]. Furthermore, it is estimated that, worldwide, 2.2 billion bone graft procedures are being performed annually to repair bone defects [141]. Therefore, it is increasingly important to find ideal substitutes and materials for restoring the normal functioning of the bone tissue resulting due to injury, disease or ageing.

The repair of bone defects is possible with autografts, allografts and with the use of synthetic/artificial materials [142-144]. But the issues of limited supply and donor site morbidity along with the expensive and adverse reaction of host-immune response of autografts and allografts respectively, render synthetic materials as the desirable option for treating such bone defects [142, 143, 145, 146].

2.3.1 Orthopedic biomaterials

The high success of using orthopedic biomaterials for the repair of bone defects in the past few decades, has offered for further developments in this field. These orthopedic biomaterials have shown great promise in improving the quality of life and restoring bone function for millions of people every year. Applications of these orthopedic biomaterials include craniofacial, dental, fracture fixation and in total joint arthroplasty. The major goal of materials in orthopedic use is to be able to restore the function and mobility of the tissue to be replaced or repaired. In order for materials to be used for orthopedic applications, they should be biocompatible, possess adequate

mechanical properties, offer corrosion and wear resistance and more importantly provide bioactive surfaces for bone bonding upon implantation. The materials used for orthopedic surgery include various ceramics, polymers, composites, natural materials and metals [5]. Each of these classes of materials has their advantages and disadvantages in their applications as implant materials. The major requirement and focus of synthetic materials is for their use in load bearing applications where the requirement is for long term performance. However, in this review major focus has been directed to the use of metal alloys as orthopedic implant materials for load bearing applications.

2.3.2 Metals as orthopedic implants

Metals as implant materials are currently the first choice for surgeons performing total joint arthroplasty such as hip and knee replacements. These load bearing implants must satisfy certain properties to be used for such applications, where the whole weight of the body is to be supported. Metallic biomaterials possess certain mechanical properties such as high strength, fracture toughness, hardness, formability and corrosion resistance, enabling them to be used vastly for the repair of bone defects and to be used for load bearing applications [7, 8]. Table 2.3 summarizes the various mechanical and non-mechanical properties required for metallic implants to be used as biomaterials and the consequences when not fulfilled [3].

Table 2.3. Properties to be satisfied by implant materials [3].

Significant requirements	Consequences of not fulfilling the requirements
Long fatigue life	Implant mechanical failure and revision surgery
Adequate strength	Implant failure, pain to patient and revision surgery
Modulus equivalent to that of bone	Stress shielding effect, loosening, failure, revision surgery
High wear resistance	Implant loosening, severe inflammatory response, destruction of the healthy bone producing wear debris which

	can go to blood
High corrosion resistance	Releasing non compatible metallic ions and allergic reactions
Biocompatibility	Body reaction and adverse effects in the organic system
Osseointegration	Fibrous tissue between the bone and the implant, poor integration of the bone and implant and finally implant loosening

The major classes of metals which are widely used in the biomedical field include stainless steel (316L), cobalt-chromium alloys (Co-Cr) and titanium and titanium alloys.

2.3.2.1 Stainless steel

The first metallic implant material to be used for orthopedic applications was stainless steel, which was successfully used as an alternative for joint prosthesis developed by Charnley in the late 1950's [147] where the total hip prosthesis consisted of a stem made up of stainless steel. The type of steel used in orthopedics especially for devices such as fracture plates, screws and hip nails, is austenitic stainless steel designated 316L [148]. This is composed of carbon, chromium, nickel, molybdenum with trace amounts of manganese, nitrogen, silicon and sulphur [2]. The corrosion resistance provided to this material is due to the presence of relatively higher amounts of Cr (17-20 wt%) which forms a coating of chromium oxide (Cr_2O_3) [2]. The stainless steel is an easily available metal with low production cost and possesses high strength compared to other metallic implants but its low corrosion and wear resistance together with a higher elastic modulus (200 GPa) limits its use as a medical device for load bearing applications [2].

2.3.2.2 Cobalt-chromium

The second class of metals which were employed in orthopedics includes the cobalt-chromium alloys (Co-Cr). There are two type of Co-Cr alloys that are widely used in the biomedical field especially in dentistry and involved as parts of orthopedic prosthesis (Stems) namely Co-Cr-Mo

and Co-Ni-Cr-Mo respectively. These Co-Cr alloys have a high strength and better corrosion and wear resistance compared to the stainless steel [2, 10, 149, 150]. However, the release of Ni, Co and Cr from these alloys in the corrosive environment of the human body have reduced their use in the biomedical field [12, 13]. Furthermore, it was reported that, the corrosion products of Co-Cr alloys are more toxic than those released by stainless steel [59]. These implants are strengthened by a relatively higher elastic modulus (220-230 GPa) which results in stress shielding of the adjacent bone when implanted. Biocompatibility is the prime and foremost requirement to be met for artificial materials to be used as biomaterials. Due to the biocompatibility issues with regard to stainless steel and Co-Cr alloys, the release of toxic Ni, Co, Cr, which forms an integral part of their composition, their use was limited in the biomedical field.

2.3.3 Titanium and titanium alloys

The third class of metals currently employed in the biomedical field consists of titanium and titanium alloys. The use of titanium and titanium alloys started in the 1940's, where they were routinely used for aeronautical applications. However, only after the phenomenon of osseointegration was proposed and coined by Branemark et al [151] in 1964, their use in the biomedical field was explored. As a result of this early work Ti and Ti alloys are used extensively as implant materials for a wide variety of applications such as stents, dental implants, bone plates, screws and especially in load bearing applications such as artificial hip joints and artificial knee joints. Ti and Ti alloys possess certain unique properties such as low density, high specific strength, excellent corrosion resistance and more importantly biocompatibility making it the preferred choice of metals for use as orthopedic implants over stainless steel and cobalt-chromium alloys [6, 14]. Furthermore, these materials possess moderate elastic moduli (110 GPa) which make them better suited for use in orthopedics, especially for hard tissue repair as load bearing implants, when compared to stainless steel and Co-Cr alloys [152]. The corrosion resistance of these materials is due to the presence of a thin layer of surface oxide (~5-29 nm) that is readily formed.

The most commonly used Ti-based implant biomaterials in orthopedics include commercially pure titanium (cp-Ti), Ti-6Al-4V alloy and NiTi shape memory alloys [14, 17, 153-155]. These

alloy materials possess excellent mechanical properties and offer good corrosion resistance making their use in orthopedic applications for hard tissue repair possible. However, in spite of their suitable mechanical properties, in the long run these materials are not suitable owing to their mild toxicity. Numerous studies reported the cytotoxicity of Al, V and Ni raising concerns over their use as implant materials [11, 12, 18, 19, 21, 22, 156-158]. Thus, continuous efforts were made to develop alloys with the use of toxic free elements. For instance, alloys with similar properties to Ti-6Al-4V but without the toxic V, Ti-6Al-7Nb [159] and Ti-5Al-2.5Fe [16] were developed. It is of utmost importance to develop materials which are biocompatible minimizing the effects of ion release resulting due to corrosion. Furthermore, these materials should be developed without compromising on the exceptional mechanical properties required for use in hard tissue repair such as for total joint arthroplasty. The alloying elements tend to improve the overall properties of materials compared to the unalloyed. Also, the selection of appropriate alloying elements also has an influence on the overall performance of the material and thus, the composition of a Ti alloy is of great importance for clinical success. Molybdenum (Mo), Tantalum (Ta), Silicon (Si), Tin (Sn), Niobium (Nb), Zirconium (Zr) were used as alloying elements to develop titanium alloys with better biocompatibilities and lower elastic modulus, to minimize the effect of stress shielding of the surrounding bone when used as implants, which is generally observed in materials with high elastic modulus [160]. Titanium alloys with various α , β and $(\alpha+\beta)$ structural phases: Ti-Zr-Nb [161], Ti-Zr-Nb-Ta-Pd [162, 163], Ti-Sn-Nb [164, 165], Ti-Nb-Ta-Zr (TNTZ) and Ti-Nb-Zr-Ta (TNZT) [15, 166, 167] Ti-Zr [168, 169], Ti-Nb [170] Ti-Ta [171] were developed for biomedical applications. Table 2.4 gives a list of Ti-based alloys developed for orthopedic applications [6, 16].

However, recent reports suggest that Mo and Si are cytotoxic and should be used diligently in permissible limits [23, 158]. In view of these, our lab has developed alloys of Ti with Zr, Nb and Sn for studying their mechanical compatibilities and biocompatibilities with living cells [164, 172-174]. Also, Nb, Ta and Zr seem to be the safest, non-toxic, biocompatible alloying elements to titanium for biomedical applications [16].

Table 2.4. Ti alloys developed for biomedical applications [6, 16].

Titanium and its alloys	ASTM standard	Type of alloy
CP-Ti	ASTM F 67	α
Ti-6Al-4V ELI	ASTM F 136	$\alpha+\beta$
Ti-6Al-4V	ASTM F 1472	$\alpha+\beta$
Ti-3Al-2.5V	ASTM F 2146	$\alpha+\beta$
Ti-6Al-7Nb	ASTM F 1295	$\alpha+\beta$
Ti-5Al-2.5Fe	-	$\alpha+\beta$
Ti-6Al-2Nb-1Ta	-	$\alpha+\beta$
Ti-5Al-3Mo-4Zr	-	$\alpha+\beta$
Ti-15Zr-4Nb-2Ta-0.2Pd	-	$\alpha+\beta$
Ti-15Sn-4Nb-2Ta-0.2Pd	-	$\alpha+\beta$
Ti-13Nb-13Zr	ASTM F 1713	β
Ti-12Mo-6Zr-2Fe	ASTM F 1813	β
Ti-15Mo	ASTM F 2066	β
Ti-15Mo-5Zr-3Al	-	β
Ti-12Mo-5Zr-5Sn	-	β
Ti-16Nb-10Hf	-	β
Ti-15Mo-2.8Nb-0.2Si	-	β
Ti-30Ta	-	β
Ti-45Nb	AMS 4982	β
Ti-35Zr-10Nb	-	β
Ti-35Nb-7Zr-5Ta	Task Force F-04.12.23	β
Ti-29Nb-13Ta-4.6Zr	-	β
Ti-8Fe-8Ta	-	β
Ti-8Fe-8Ta-4Zr	-	β

2.4 Surface modification of titanium and titanium alloys

Titanium and Ti alloys thereof offer certain unique properties for their use in the biomedical field especially in dental and orthopedics such as light weight, high strength and good biocompatibility. However, the corrosion resistance offered by these materials is limited especially in the highly corrosive environment of the human body when contact with the body fluids is encountered [12]. Furthermore, these materials show very poor wear resistance, which is a matter of concern with regard to the toxicity of the products released as a result of wear and shear. The body fluids contain a complex mixture of salts, trace metals, amino acids, proteins which produce various ions such as chloride, phosphate, bicarbonate, sodium, magnesium, potassium and calcium, which when in contact with the implant material can result in the wear and corrosion of the surface of implants [19]. The result of poor corrosion and wear resistance can have devastating effects mostly by reducing the performance of the implant thereby requiring a revised and painful surgery [18]. Therefore, it is highly essential for the implant materials to be able to function in a highly corrosive environment and provide resistance to corrosion.

Apart from the choice of material for bone tissue engineering, it is also important to have suitable surface properties and biological properties to be able to successfully function as implants for orthopedic applications. With regard to the use of titanium and titanium alloys in the biomedical field and especially for orthopedic and dental applications, it is extremely important for the implants to function in accordance with the host tissue upon implantation. In order to successfully achieve this function, the implants should be able to bond to the bone in quick succession at the site of implantation [10]. In other words, the implants should be able to osseointegrate into the surrounding bone tissue. Osseointegration is a process, wherein a stable and direct contact is made between the bone and the implant, without the growth of a fibrous tissue at the bone-implant interface [175]. Therefore, the interaction between the cells of the bone tissue and the implant materials is extremely important in determining the performance of the implant materials as well as in speeding up the osseointegration process [176]. The surface properties of the implant materials also play a pivotal role in influencing the osseointegration process because the interactions take place at the surface upon implantation [37]. It is extremely

important to strike a balance between the bulk properties and surface properties for effective performance as an implant material.

Titanium and Ti alloys possess a thin layer of naturally formed oxide on the surface which is responsible for providing the resistance to corrosion and rendering the biocompatibility of these materials. However, these are bioinert surfaces unable to develop anchorage directly to the bone tissue upon implantation which increases the recovery time for bone regeneration [177]. Moreover, when implanted in the living body, these Ti alloys are encapsulated by a fibrous connective tissue, which intervenes by reducing the stability of the implant and thereby resulting in the loosening of the implant [176]. In order for these materials to be able to support bone formation or become osteoconductive, it is important for these surfaces to be bioactive, thereby able to interact with the surrounding bone cells and tissue contributing to the osseointegration of implants to the bone tissue.

Synthetic hydroxyapatite (HA), $\text{Ca}_{10}(\text{PO}_4)_6(\text{OH})_2$, is considered to be a bioactive and biocompatible material that can bond to bone without the formation of fibrous tissue. Hydroxyapatite, when coated on the Ti implant surface enhanced the bioactivity of the materials. Kokubo et al [178] proposed that, any material to be able to bond to the bone requires the formation of bone like apatite on its surface. More importantly, apatite is the main component of bone crystal, which is also part of the inorganic content of the bone matrix. However, due to the issues relating to the bonding strength of the HA to the Ti alloys, various other methods for improving the bioactivity of the Ti alloys were explored.

Surface modification is an effective strategy in not only improving the corrosion resistance of materials but also rendering the surfaces bioactive [59]. The rationale of surface modification is to retain the bulk properties while modifying the surface properties to improve the biocompatibility and bioactivity to the material surfaces [60]. The surfaces of titanium and titanium alloys can be altered by means of various mechanical/physical, chemical, and biological methods for improving the quality and quantity of the bone-implant interface [61]. These methods include both directly involving the modification of the surfaces of the Ti alloys, where mechanical/physical methods are used; and the use of coatings on the surfaces using chemical and biological methods. In mechanical methods, the surface is modified utilizing the machining,

grinding and blasting techniques. The physical methods involve the utilization of thermal, kinetic and electrical energy, where thin films are deposited on the Ti alloy surfaces. Typically, these surface modifications involve alteration in the atoms, compounds or molecules on the surfaces chemically or physically or coating the surfaces with a different material [62]. This review will focus on the chemical methods of surface modification.

2.4.1 Chemical methods

The chemical methods for surface modification attract significant attention because of the unique features and the advantages they offer. The surface morphology can be easily controlled both at the nanometer and micrometer levels. More importantly, the chemical techniques can be manipulated more easily and a strong adhesion between bone and implant can be achieved using these techniques due to the chemical bonding. Chemical methods are generally cost effective without the requirement for special facilities. Chemical methods can be classified into wet-chemical, sol-gel processing, electrochemical processing and chemical vapor deposition (CVD). However, in this review, wet-chemical and electrochemical methods will be discussed in detail.

2.4.2 Wet-chemical

The wet-chemical treatments can modify the surface morphology and total composition via the rearrangement of the outer atoms of the surfaces of materials. The wet-chemical methods include three major treatments namely acid, hydrogen-peroxide and alkali treatments.

2.4.2.1 Acid treatment

Acid treatment involves the removal of the material from the existing surface to achieve various topographies. More often, acid treatment is used to remove contamination and oxide scales of Ti materials so as to produce clean and uniform scale finishes [179, 180]. Acids such as HCl (Hydrochloric acid), HNO₃ (Nitric acid), H₂SO₄ (Sulphuric acid) and HF (Hydrofluoric acid) have got the capability to react with the oxide on the surface of Ti and Ti alloy materials. In general, a predominant oxide layer of TiO₂ is formed on the surfaces of Ti and Ti alloys subjected to the acid treatments. However, the extent of acidic reaction is dependent on the concentration of the acid, specific composition of the mixture, the temperature and processing

time. Thus, the strongly etched part effects the extent of surface removed and thereby changes the surface topography.

Studies on the bioactivity of the acid etched titanium and titanium alloys were carried out [179-182]. Acid etching can be carried out using a single acid or dual acid etching or even after using a mechanical treatment such as blasting or turning. Dual acid etching with combinations (HCl/H₂SO₄ and HF/HNO₃) is usually applied on Ti [179, 180]. Figure 2.4 shows the surface of titanium after dual acid etching with HCl and H₂SO₄ [179]. For instance, acid etching is usually employed to decontaminate the surface of materials after mechanical processing or fabrication for improving the osseointegration. Takeuchi et al [180], after evaluating the decontamination efficiency of acids, suggested that HCl is an excellent decontaminant compared to Na₂S₂O₈ (Sodium persulphate) or H₂SO₄ for use in Ti surface modification process. Acid etching is usually applied alone as it can enhance the rapid osseointegration of implants [179, 183]. Several studies reported the better osteoconductive properties of the dual acid etched titanium implant surface for osteoblast adhesion and bone apposition [184-187]. *In vivo* studies on the performance of the acid etched surfaces were also carried out [179, 184, 186]. Studies by Cho et al [179], Cochran et al [188, 189], Trisi et al [186, 187] report the greater bone to implant contact of the acid etched surface compared to the machined surfaces.

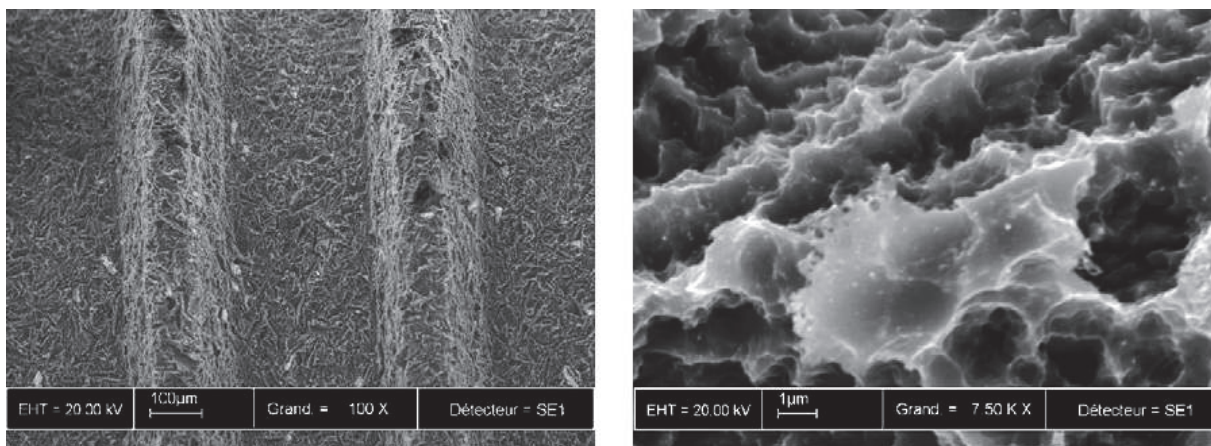


Figure 2.4. Dual acid etching on Ti implant surface using HCl and H₂SO₄ [179].

Acid etching can also be applied in combination with mechanical treatments of Ti materials such as smoothing, blasting etc along with other chemical treatments (alkali) for enhancing the bioactivity [39, 181, 183, 184, 190, 191].

2.4.2.2 Hydrogen peroxide treatment

Chemical surface modification of Ti implant surfaces with hydrogen peroxide (H_2O_2) results in Ti peroxy gels. The biocompatibility with improved bioactivity has been reported on the Ti hydrogel layer after reaction with H_2O_2 [192-194]. This process results in an increase in the thickness of the oxide layer linearly over time with exposure to H_2O_2 with roughening of the surface on the submicron scale [61, 195].

It should be mentioned that, the oxide layer consists of mainly TiO_2 and hydroxyl groups [61]. The titania gel formed on the surface after H_2O_2 treatment is amorphous which transforms into anatase phase on increasing the temperature to around 300 °C to rutile phase with further increase of temperature to 600 °C [196]. However, it should be noted that, increasing the temperature increases the rutile phase which decreases the bioactivity.

Several studies were reported on the detailed procedure of the acidic and hydrogen peroxide surface treatments for bioactivity [193, 195, 197, 198].

2.4.2.3 Alkali treatment

Surface modification using alkali treatment is a widely used method for improving the bioactivity of Ti and Ti alloys. This utilizes alkali (NaOH , KOH) solution for chemical treatment, where the Ti alloy materials are soaked into. The procedure was first introduced by Kim and Kokubo [199, 200], who treated Ti and Ti alloys in a concentrated solution of NaOH/KOH followed by subsequent heat treatment which resulted in the formation of a sodium titanate layer. This sodium titanate gel readily forms apatite (Calcium phosphate similar to bone apatite) after soaking in a super saturated solution, SBF (Simulated body fluid), which has the composition similar to human blood plasma. Briefly, the sodium titanate layer reacts with the Na^+ and H_3O^+ in the SBF to form Ti-OH groups which readily precipitates calcium forming apatite.

Several studies have been reported on the surface modification, characterization and bioactivity of Ti and Ti alloys using the alkali and heat treatment [201-204]. Furthermore, Kim et al have reported on the specific structural changes of the surface caused by the alkali treatment with different heating conditions, and the mechanism of apatite formation using SBF [199].

2.4.3 Electrochemical methods

Electrochemical processes usually involve the use of electrodes, an electric supply and an electrolyte. Various chemical reactions occur at the electrodes placed in an electrolyte solution when a voltage is applied. The cathode consists of inert materials such as platinum (Pt), gold (Au) or carbon (C) and the samples to be processed for treatment constitute the anode. The oxidation reaction occurs at the anode on the application of specific voltage when an electric current flows through the circuit. The electrochemical methods include three different treatments namely electro-erosion, electro polishing and anodic oxidation (anodization) [205]. The electrochemical treatments offer excellent advantages over the process control conditions as well as producing a wide range of surface properties with various finishing degrees. However, in this review, only the anodization is discussed.

2.4.3.1 Anodization

Electrochemical anodic oxidation or anodization is a novel and powerful technique used for surface modification of materials [206]. It is an excellent technique to improve the corrosion resistance and biocompatibility of Ti and Ti alloys [88, 207]. The process typically consists of an electrochemical cell with anode (sample) and cathode (inert metal) as electrodes. The electrodes are immersed in an electrolyte solution and a positive voltage is applied across the cell, resulting in the formation of a metal oxide layer at the anode surface with the diffusion of metal and oxygen ions to the anode. The oxide film formed on Ti and Ti alloys is usually TiO₂ although the exact composition and structure are still controversial. The thickness, topography, composition and structure of the oxide film formed by the anodization process is dependent upon various factors such as the electrolyte concentration and composition, temperature, the applied voltage and cathode to anode surface ratio [89]. An increase in the applied voltage increases the thickness of the oxide layer which offers the resistance to corrosion.

As previously mentioned, the nature of the oxide film formed using anodic oxidation is dependent on the nature of the electrolytes including the composition and concentration as well as the applied voltage or current density. All the Ti and Ti alloys possess a naturally formed oxide layer on their surfaces, which offer protection against corrosion but more importantly accounts for the biocompatibility of the materials to be used as implants in the biomedical field. Several studies by researchers reported on the bioactivity of the anodic oxide films formed using various combinations of electrolytes. The electrolytes commonly used include acids like H_2SO_4 , HNO_3 , H_3PO_4 (Phosphoric acid), HF and acetic acid. The anodic oxide films formed using these electrolytes show strong bone like apatite formation in SBF [208]. Moreover, the strength of adhesion of the apatite to these oxide films is better compared to the traditional HA coatings performed for rapid osseointegration.

Several studies show better bone tissue response on the anodized surfaces [209-211]. Jungner et al [212] in their study observed a better clinical success of the anodized materials compared to the turned titanium surfaces. Moreover, there is a greater mechanical interlocking and biochemical bonding observed on these anodized surfaces which results in better osseointegration of surfaces [210, 211, 213-215].

Several studies on the bioactivity of titanium and their ability for apatite formation in SBF was reported [76, 208]. Das et al [208] have evaluated the apatite formation as well as the cellular response in terms of osteogenesis on the surfaces of titanium electrochemically treated in three different electrolytes namely 1N H_3PO_4 , 1N HNO_3 , and 0.25N HF, respectively, at a constant voltage of 20V. TiO_2 non porous films with different microstructures were obtained using the three electrolytes. Figure 2.5 shows the morphology of the oxide films using the three electrolytes [208]. It was also observed that the native oxides were not better in their ability to induce apatite formation when soaked in SBF for 21 days, however, the apatite formation was visible on the surfaces at an early period of 7 days after soaking in SBF on heat treatment of the respective oxides at 400 °C but decreased at 600 °C due to the change of phase from anatase to rutile at high temperature which reduces the ability to induce apatite formation (Figure 2.6) [208]. The cell adhesion and proliferation was greater on the surface treated with H_3PO_4 and HF compared to the H_2SO_4 treated surface (Figure 2.7) [208].

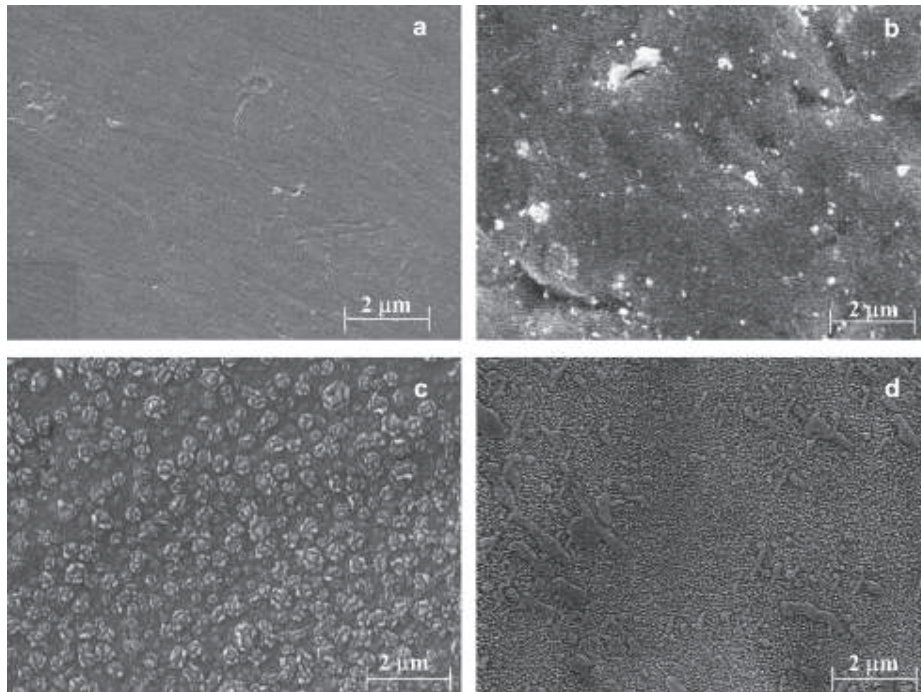


Figure 2.5. FE-SEM micrographs showing morphology of (a) Ti surface, anodized oxides surfaces prepared by anodization in (b) H_2SO_4 , (c) H_3PO_4 and (d) HF electrolytes [208].

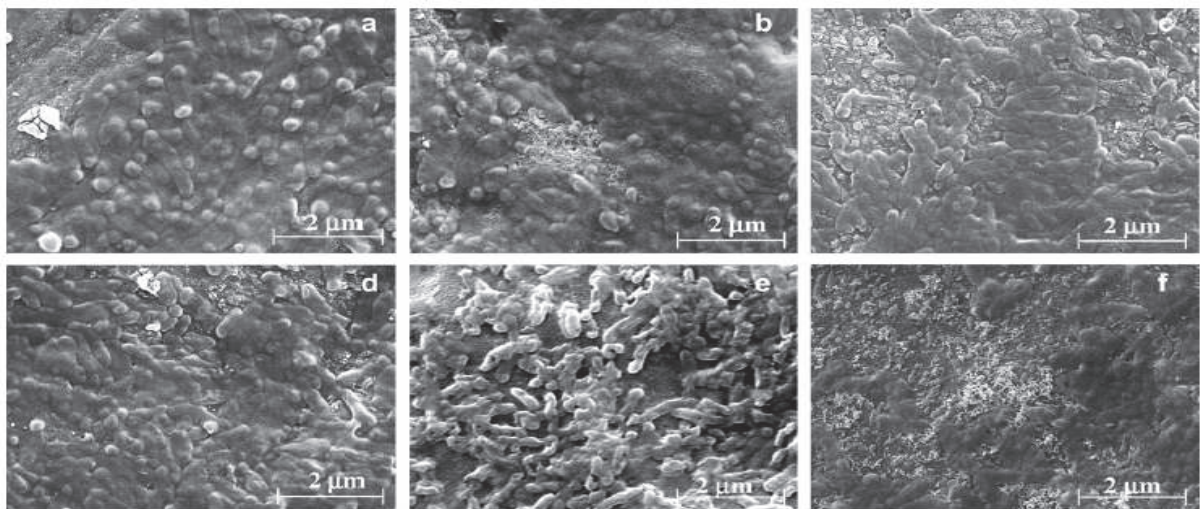


Figure 2.6. Mineralization study for 7 days on the anodized surface H_2SO_4 followed by heat treatment at (a) 400 °C, (b) 600 °C, anodized in H_3PO_4 and heat treated at (c) 400 °C, (d) 600 °C for anodized HF surface [208].

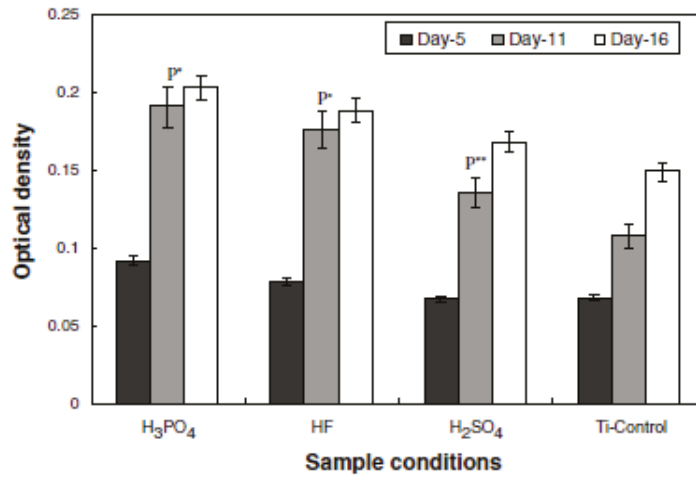


Figure 2.7. Optical density measured after culture for 5, 11 and 16 days at a wavelength of 570 nm by reader. There were significant differences in optical density after 11 days in the different anodized conditions samples. $p^* < 0.001$ for H₃PO₄, HF and $p^{**} < 0.01$ for H₂SO₄ compared with Ti control at 11 days of culture [208].

In another recent study, Cui et al [76] have evaluated the apatite forming ability of titanium in different electrolytes and studied the effect of the crystal structure of the anodic oxide films thus formed. The anodic oxidation was carried out using 2M solutions of H₂SO₄, H₃PO₄ and acetic acid and a 1M solution of Na₂SO₄ as electrolytes at constant time of 1 min with voltages of 100, 150 and 180 respectively. A uniform and porous layer consisting of anatase and rutile phases of titanium oxide was formed on the surfaces using Na₂SO₄ and H₂SO₄ respectively, where as amorphous films were obtained using H₃PO₄ and acetic acid electrolytes although the porosity increase was evident from 100V to 150V but not from 150V to 180V. Figures 2.8, 2.9, 2.10 and 2.11 show the morphologies of the oxide films formed on the three surfaces at different voltages [76]. The apatite formation was seen after 7 days of soaking in SBF on H₂SO₄ and Na₂SO₄ surfaces but the apatite formation was poor on the other two surfaces (acetic acid and H₃PO₄). A dense layer of apatite was formed at 150V and 180V but sparsely at 100V on the H₂SO₄ and Na₂SO₄ surfaces (Figure 2.12 and Figure 2.13) [76].

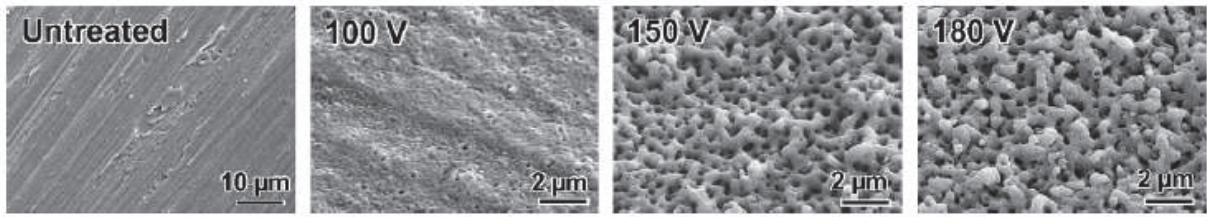


Figure 2.8. FE-SEM photographs of the surfaces of titanium metals untreated and subjected to anodic oxidation in H_2SO_4 solution at 100, 150 and 180V [76].

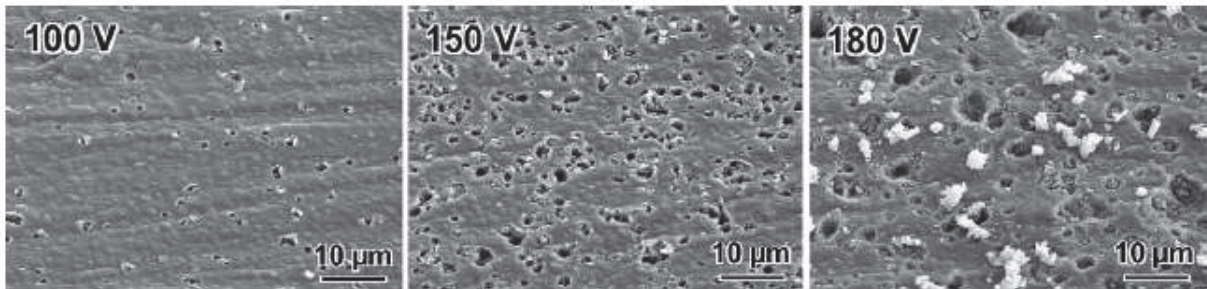


Figure 2.9. FE-SEM photographs of the surfaces of titanium metals subjected to anodic oxidation in acetic acid solution at 100, 150 and 180V [76].

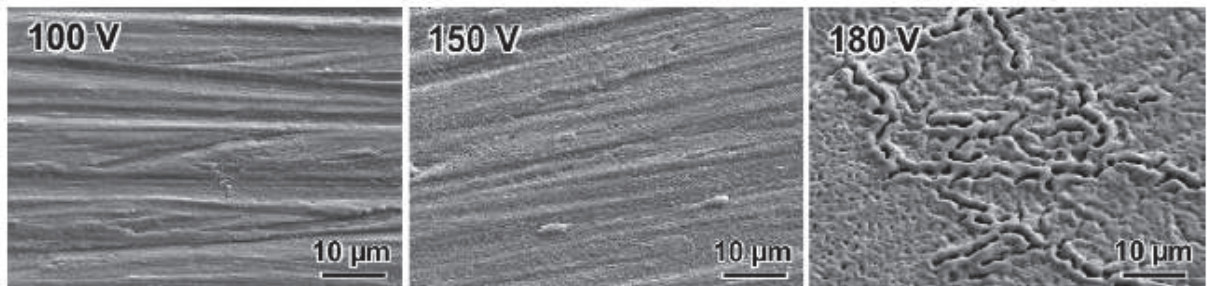


Figure 2.10. FE-SEM photographs of the surfaces of titanium metals subjected to anodic oxidation in H_3PO_4 solution at 100, 150 and 180V [76].

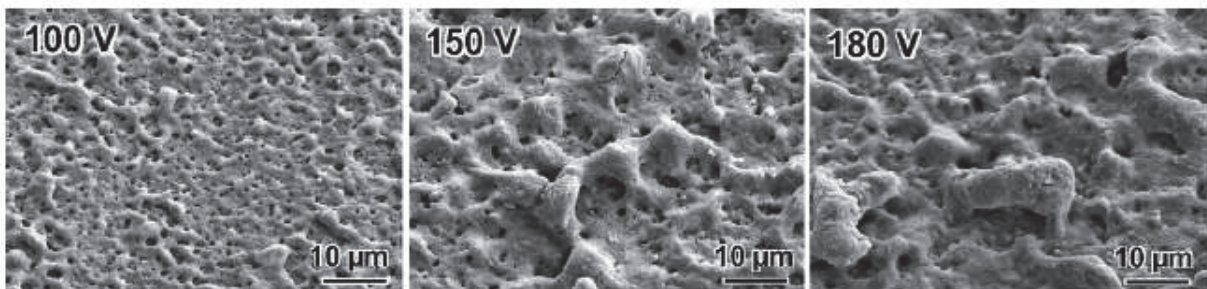


Figure 2.11. FE-SEM photographs of the surfaces of titanium metals subjected to anodic oxidation in Na_2SO_4 solution at 100, 150 and 180V [76].

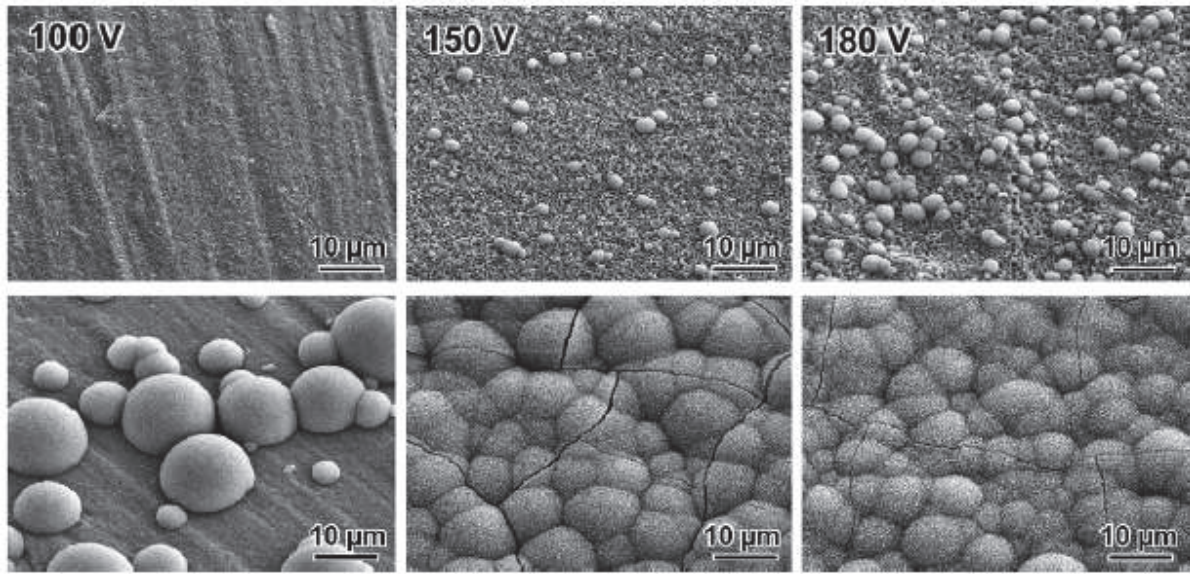


Figure 2.12. FE-SEM photographs of the surfaces of titanium metals subjected to anodic oxidation in H_2SO_4 solution at 100, 150 and 180V, and then soaked in SBF for 1 or 7 d [76].

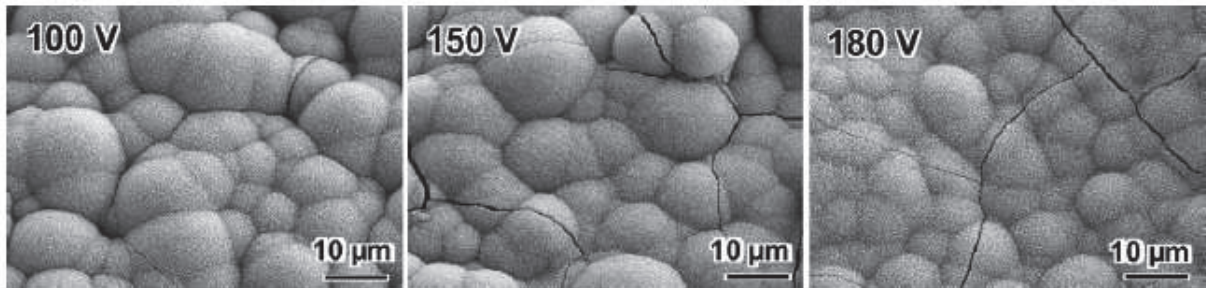


Figure 2.13. FE-SEM photographs of the surfaces of titanium metals subjected to anodic oxidation in Na_2SO_4 solution at 100, 150 and 180V, and then soaked in SBF for 7 d [76].

In a similar study by Yang et al [88] oxidations of titanium surfaces were carried out in H_2SO_4 at different voltages of 90V, 155V and 180V respectively. Figure 2.14 shows the morphology of the surfaces after treatments at different voltages [88].

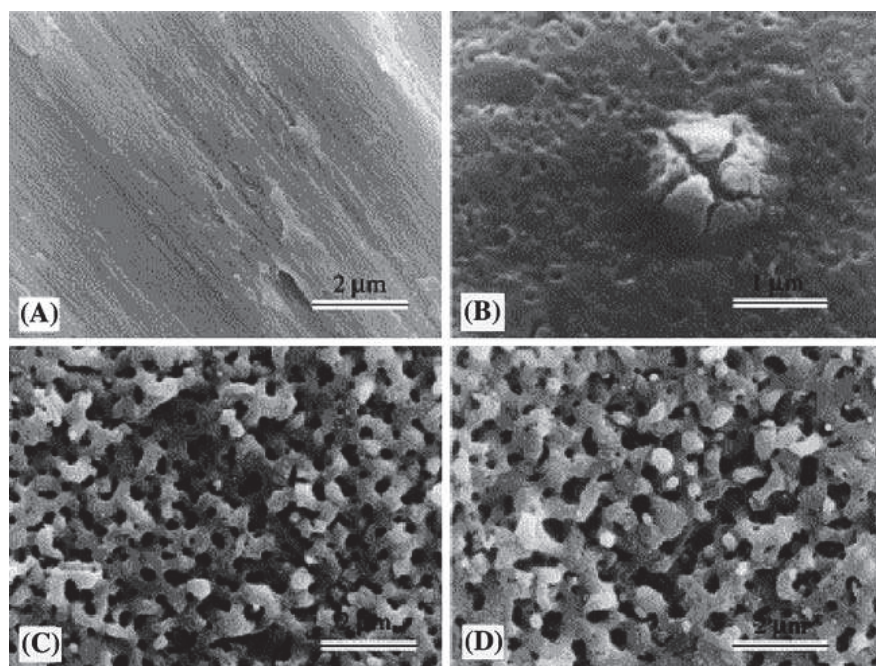


Figure 2.14. SEM photographs of (A) titanium metal without treatment and anodically oxidized titanium at (B) 90 V, (C) 155 V and (D) 180 V in 1 M H_2SO_4 for 1 min [88].

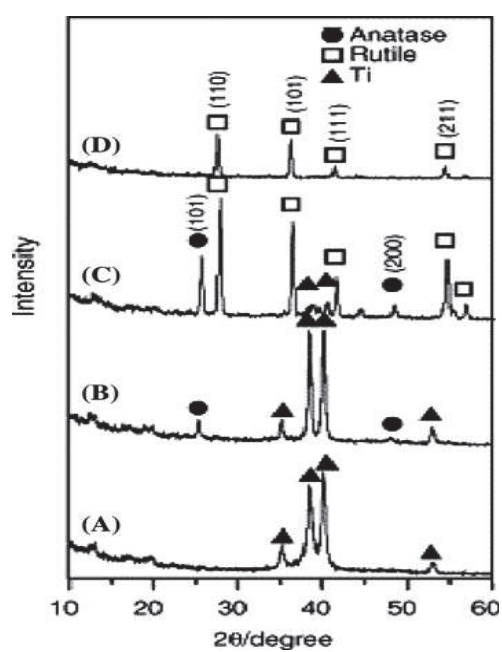


Figure 2.15. TF-XRD patterns of (A) titanium metals without treatment and titanium metals anodically oxidized at (B) 90 V, (C) 155 V and (D) 180 V in 1 M H_2SO_4 for 1 min [88].

The apatite formation was observed on the surfaces anodized at 155V and 180V but not at 90V after immersion in SBF for 3 days. This study also strengthened the hypothesis that a certain amount of titania of anatase and/or rutile is necessary for inducing bone like apatite formation on the surfaces. Figure 2.15 shows the different phase compositions of titanium after anodization [88].

Apart from the use of acid electrolytes for anodization, Ca and P containing electrolytes were also reported [216-218]. The films obtained using such electrolytes EDTA (Ethylenediamine tetraacetic acid)/calcium acetate [219], CaP/sodium fluoride [220], glycerophosphate/calcium acetate [221]) contain Ca and P in a concentration similar to that of Ti. A subsequent hydrothermal treatment results in the diffusion of Ca and P to TiO₂ surface and HA crystal precipitate [222]. Moreover, the bond strength of the Ca-P incorporated layer is higher than the HA coatings to the substrates [94]. Furthermore, this layer functions in improved biocompatibility and better osseointegration of implant materials.

The surfaces of implant materials play a crucial role in interactions with the bone tissue thereby determining the long term performance of the implants. Anodic oxidation is an excellent technique to obtain various surface features with great control over the processing conditions. As mentioned previously, the topography, structure and composition of the surface are greatly dependent upon the processing conditions such as the composition and concentration of the acid, the temperature and the applied voltage and can be modulated with control over the processing conditions. Both microporous and nanoporous surfaces can also be produced using anodization of titanium and titanium alloys [60]. Zhao et al [217], Wu et al [218] and Zhang et al [94] have used micro-arc oxidation of titanium alloys for producing microporous surfaces. They have also reported on the improved performance of the materials in terms of osteoblast cell response. Furthermore, different nanoscale structures with varied topographies can also be obtained using anodization of titanium and titanium alloys. Several studies reported the production of nanotubes and nanostructures on the titanium surfaces when employing anodization [90, 223, 224]. Gong et al [90] used HF as the electrolyte to produce nanoscale topographies on the surface of titanium films at different voltages for different time periods. A nanoporous surface with pore sizes of 15-40 nm was observed at lower voltage (3V) at 0.5wt% HF. At higher voltage of 5V and constant time of 20 min, particulate structures or nodules were formed. A further increased voltage

resulted in the formation of discrete, hollow, cylindrical nanotubes. Figure 2.16 shows the various surface structures formed at different voltages on titanium [90].

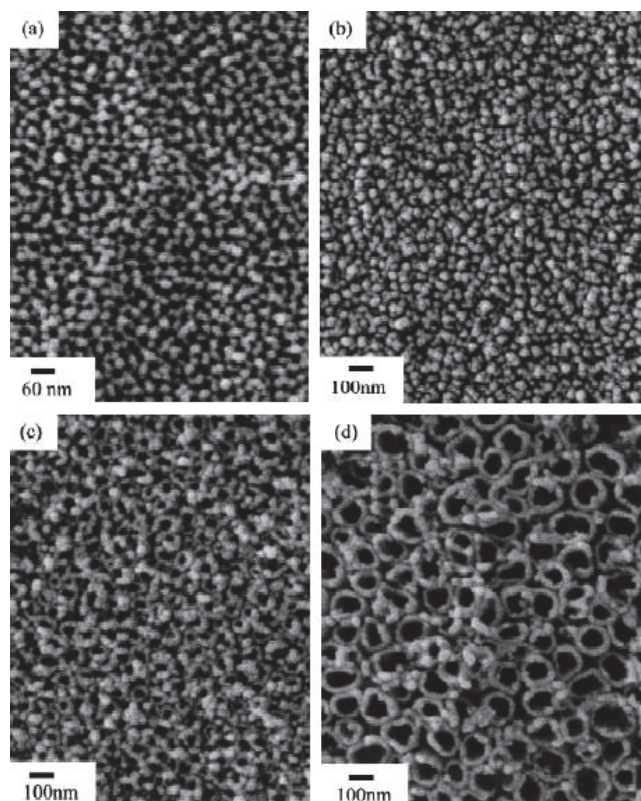


Figure 2.16. FE-SEM top-view images of porous titanium oxide films anodized in 0.5 wt% HF solution for 20 min under different voltages: (a) 3V, (b) 5V, (c) 10V and (d) 20V [90].

Zhao et al [223] have also reported the formation of nanotubes on titanium using HF at different electrolyte concentrations, voltages and time periods.

Osteoblast cell response to the surfaces of implants plays a crucial role in directing the fate of the cell as well as for enhanced performance. It is important for the surfaces to support the growth of cells for effective functioning of the implant. Nanotubes formed by anodization must be biocompatible as well as able to support the growth of cells for improved performance. A number of studies on the biocompatibility and bone bonding behavior of the titanium oxide nanotubes were carried out. More importantly, the effect of *in vitro* osteoblast cell response on the produced nanotubes was also reported [65, 69, 81-84, 90, 225, 226]. Bjursten et al [83] have also reported on the *in vivo* behavior of the nanotubes for bone formation.

Although these studies were reported on titanium metal, anodization on titanium alloys were not explored for nanotube formation and osteoblast cell response. Furthermore, although there are reports on the improved cell response on nanotube surfaces, the exact mechanism of cell behavior on these surfaces still remains unclear. We have evaluated the possibility of nanotube formation on the surface of a titanium-zirconium alloy and explored their osteogenesis ability with emphasis on the effects of surface properties at different stages of osteoblast cell-material interactions; the details form the basis for chapter 6.

2.5 Osteoblast cell-biomaterial interactions

The current goal in implantology research is the design of materials/ devices that can induce controlled, guided and rapid healing. With regard to orthopedics, the implant materials, in addition to accelerating the wound healing phenomenon should also result in the formation of an interfacial layer of bone matrix with adequate biomechanical properties. This is important in terms of the faster recuperation for the patient as well as a stable anchorage between the bone and the implant material. Successful integration of the implant to the bone tissue is determined by the events that take place at the tissue-implant interface, which ultimately has an effect on the performance of the implant [36, 176]. The interaction between the material and the host tissue is a dynamic complex process which involves implant related factors and patient (host) response. The various implant related factors which contribute to the performance include the surface properties of implant surface roughness, surface topography, surface composition and surface wettability [222, 227]. In order to achieve these goals, it is important to understand the events that take place at the interface of implant and bone.

2.5.1 Bone-implant interface

The performance of implant materials is determined by the nature of two components namely host response and material response [24]. The successful application of biomaterials as implants is largely determined by the balance between having ideal material properties and good response of the material in the host. Puleo et al [176] has published a thorough review on the various events which take place at the bone-implant interface as well as the various components involved

in the interface for achieving better osseointegration of implant materials. Figure 2.17 shows the various events which occur at the interface between bone and implant surface [176].

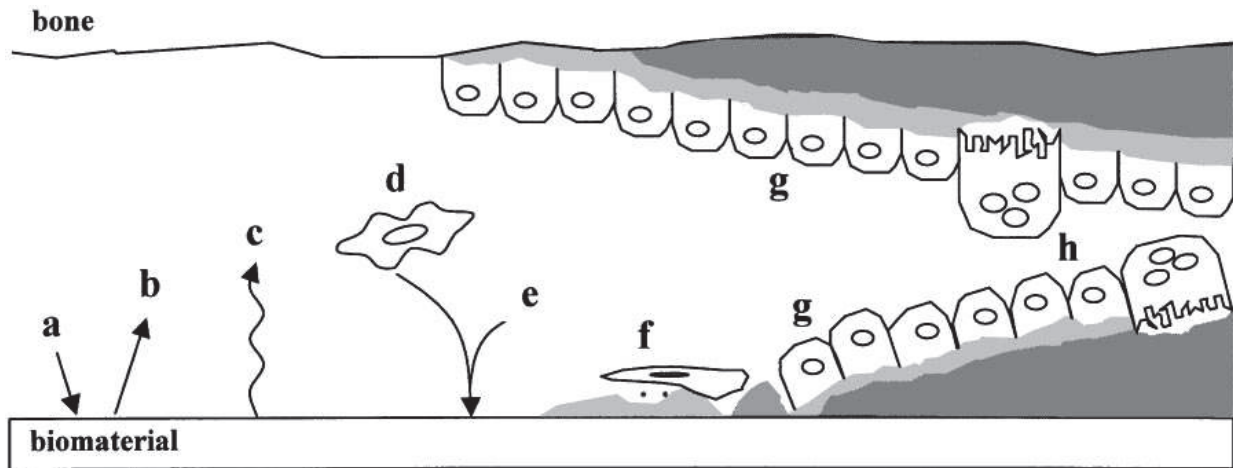


Figure 2.17. Representation of events at the bone-implant interface. (a) protein adsorption from blood and tissue fluids, (b) protein desorption, (c) surface changes and material release, (d) inflammatory and connective tissue cells approach the implant, (e) possible targeted release of matrix proteins and selected adsorption of proteins such as BSP and OPN, (f) formation of *lamina limitans* and adhesion of osteogenic cells, (g) bone deposition on both the exposed bone and implant surfaces, (h) remodeling of newly formed bone [176].

The initial event which occurs after implantation of materials involves protein adsorption. This protein adsorption usually involves the proteins from the blood and tissue fluids at the wound site as well as from the cellular activity [228, 229]. In other words, the interactions of cells are mediated by the adsorbed proteins from the physiological fluids *in vivo* and those in the culture medium *in vitro* such as fibronectin (FN), vitronectin (VN), fibrinogen (FG) as well as collagens and laminins [58]. Thus, the initial cell-material interactions is a complex multi-step process consisting of early events such as protein adsorption, cell attachment and spreading, followed by late events such as cell proliferation, differentiation and matrix mineralization. Also, these cell-material interactions are to a great extent driven by the nature of the surface property of the material and it is therefore extremely important to understand the response of osteoblast cells towards the material surfaces taking into view the surface properties of roughness, composition, chemistry, topography and surface energy. Therefore, this review focuses on the response of

materials to the bone cells taking into view the various surface properties and their influence on the cell biological behavior.

2.6 Osteoblast cell response to surface properties

The physico-chemical properties of a material surface play a crucial role in determining the behavior of osteoblast cells thereby influencing the performance as an implant. It is therefore extremely important to understand the response of osteoblast cells in terms of their adhesion, proliferation and differentiation processes towards the material surface properties in order to achieve faster osseointegration as well as for developing ideal materials for rapid bone healing. This section of the review discusses the events of osteoblast adhesion, proliferation and differentiation on titanium and titanium alloy material surfaces taking into view the contribution of the various surface characteristics towards the observed cell behavior.

2.6.1 Role of surface properties

The surface modifications performed on titanium and titanium-based alloys, such as physical and chemical methods (machining, polishing, turning, blasting and etching) alter the topographical features by formation of grooves, pits, pores (macro, micro and nano) which in turn effects the roughness of the surfaces both at the microscale and nanoscale. Furthermore, the roughness of the surfaces can be termed smooth and rough depending on the degree of roughness, which is described by the height descriptive parameters of Sa or Ra, which stand for the arithmetic mean deviation of a profile (Ra) or a surface (Sa). Apart from roughness and topography, surface chemistry, surface energy and the composite effect of these surface properties, plays a major role during the early and late events of protein adsorption, cell adhesion, cell proliferation and cell differentiation respectively [53]. It should be noted that, these surface characteristics are highly interrelated and it is extremely difficult to differentiate the response of cells amongst the effects of individual characteristics. Several studies tried to report on the response of osteoblast cells to the surface properties by exploiting each surface characteristic as well as synergistically thereby minimizing the effect of other properties [27, 51].

2.6.1.1 Surface roughness and topography

The biocompatibility of implant materials is to a large extent closely related to the adhesion of osteoblast cells onto their surfaces. The quality of adhesion and spreading of the cells will further influence the capacity of cells to proliferate and differentiate which ultimately leads to the establishment of an interlock between the implant surface and bone tissue. Osteoblast adhesion is mediated by transmembrane protein receptors called integrins which mediate the binding of the intracellular domain with the extracellular domain thereby transducing the signals for efficient cellular adhesion and processes thereof. The surface properties play a crucial role in determining the nature of osteoblast adhesion onto titanium and titanium alloys.

As described previously, the surface roughness and topography are interrelated properties and several studies aimed at observing the osteoblast cell response to these surface characteristics. Morphology of the cells is topography driven which results in varied shapes as spherical or elongated depending on the underlying material surface. On surfaces with a flat topography or plain surfaces, the cells usually appear spherical, fully spread with numerous filopodia, which are typical of adherent cells. On the other hand, on surfaces with grooves or pits, the cells usually become elongated, spindle shaped and orient themselves in the direction of the grooves, a phenomenon termed as contact guidance. The actin organization on these surfaces explains a lot in terms of the quality of cell adhesion. In cells with spherical morphology, the actin organization is seen all over the cell whereas in elongated cells, the actin is seen concentrated at the periphery of the cells, which denote a strong adhesion to surfaces. This kind of behavior is seen on smooth and rough surfaces with certain degrees of roughness profiles. In a study by Guehenne et al [230], a similar kind of morphology was seen on surfaces with varying degrees of roughness. A similar observation with regard to cell morphology was seen by Jayaraman et al [231]. This observation was also reported by many other researchers [45, 53, 232]. Thus, the cell morphology is a truly topography driven phenomenon.

The effects of various micro and nanoscale microtopography on osteoblast cell behavior were studied by many researchers [27, 41, 233-235]. Furthermore, the effect of surface topography on *in vivo* osteoblast cell response was excellently reviewed by Wennerberg and Albrektsson [236]. It was observed that, an improved osteoblast adhesion on the nanoscale topographical features which was believed to be due to enhanced interactions between the nanoscale surface features

and adhesion mediating molecules namely ECM proteins. A further increase in the proliferation of cells was seen on these surfaces. However, on the micro rough surfaces, the adhesion and proliferation of cells was reduced whereas the differentiation was increased. In a study by Rosa and Beloti [237], the cell behavior on titanium with varied degree of roughness was evaluated in terms of the adhesion, proliferation and differentiation. The study reported a decrease in adhesion and proliferation on the surfaces with increased roughness values and the differentiation increased with the onset of increased ALP activity and amount of total protein. Similar behavior was seen by Anselme et al [33] with regard to spreading of osteoblast cells on Ti surfaces with low roughness profiles compared to higher roughness profiles. Furthermore, several studies on the effect of roughness on osteoblast cell behavior in terms of their adhesion, proliferation and differentiation are known [27, 41, 46, 47, 182, 232, 238]. *Although studies on the effect of roughness on cell behavior exist, no comparisons could be made as smooth surfaces in one study were considered rough in another study. Therefore, it becomes extremely important to understand the biological responses of cells when comparing surface roughness within a similar range, which we have addressed in our study, where the surface roughnesses of the materials titanium-zirconium, titanium-niobium and pure titanium were in the submicron range.*

2.6.1.2 Surface chemistry

Apart from roughness and topography, surface chemistry of material surface has gained prominence and efforts were made to understand the specific role of surface chemical composition and surface energy on the osteoblast cell response [42, 53, 239-241]. Several studies have been reported on the effects of surface chemistry by using self assembled monolayers (SAM) and peptides on titanium surfaces and the response of osteoblast cells to such chemically modified surfaces [242, 243]. Surface hydrophilicity has been shown to be a prominent factor in enhancing early events of protein adsorption and osteoblast adhesion [239, 244, 245]. More importantly, surface energy has been thought to be playing a key role in influencing the cell behavior. Several studies have targeted on exploring its effect on the bioactivity and osteoblast cell response [44, 246-249]. *Although, these studies reported on the possible role of surface energy as a key factor in osteoblast cell response in terms of their cell behavior, no clear evidence yet exists as to the specific role at each stages of cell material interactions as well as the mechanisms for the enhanced behavior [247].*

Although there have been several studies reported on the behavior of osteoblast cells and more so on the effect of surface properties, no clear evidence yet exists with regard to their response. As such, studies on the influence of roughness and surface energy in specific on osteoblast cell behavior were reported, but their role in the cell response especially at the early and late events of adhesion, proliferation and differentiation is still unclear. Moreover, it is extremely important to understand the specific role of surface properties on osteoblast cell response for enhancing the performance of implant materials. Since there is no clear evidence with regard to their specific role we have explored the influence of surface characteristics on the cell behavior of osteoblast cells at different stages of cell-material interactions. This formed the basis of the objective of this study.

3. Materials and experimental techniques

This chapter describes the methodology and general details of experimental techniques pertaining to the thesis. In the first part, sources of raw materials used and processing of the alloy preparation are described. The surface characterization of the alloys such as morphology, topography and chemical analysis are detailed in the second part. The third part describes the *in vitro* cellular assays used in the study and the fourth part deals with the techniques for gene profiling.

3.1 Sample preparation and processing

For this study, we used three different materials namely Ti, TiZr and TiNb alloys in the form of circular discs with 15 mm diameter (Φ) and 2 mm thickness. The discs were prepared by powder metallurgy from the elemental powders by compaction, sintering and grinding. The various steps involved in this process are described in this part.

3.1.1 Raw materials

Commercially available elemental powders of Titanium (Ti), Zirconium (Zr) and Niobium (Nb) (Atlantic Equipment Engineers, USA) were used as starting materials. Table 3.1 shows the characteristics of the metal powders used in the study.

Table 3.1. Characteristics of the metal powders used.

Elements	Ti	Zr	Nb
Purity	99.7	99.5	99.8
Size (μm)	≤ 45 (-325 mesh)	≤ 150	≤ 45

3.1.2 Powder handling, compaction, sintering and grinding

Powder handling and mixing

The three metal powders Ti, Zr and Nb are sensitive to the oxygen in air and therefore, the handling was done in a stainless steel glove box chamber under high purity argon gas. The elemental powders were mixed together to obtain the targeted composition of Ti50Zr (Wt %) and Ti50Nb (Wt %) and mixing was achieved using ball milling. The mixing process was accomplished using ball milling process for 20-30 min at low rpm (50-100 rpm) using 2 steel balls of Φ 10 mm. The mixture was then processed for compaction, sintering and grinding.

Powder compaction

The powders were consolidated into green compacts using stainless steel mould by a uniaxial compaction method. The compaction of the powders was done using SUNEX 50 ton hydraulic shop press. The powder mixture was loaded into steel dies of cylindrical shape and 15 mm diameter and pressure was applied on the top of punch. The compaction was done by applying a pressure of 750 MPa.

Sintering

Solid bulk samples were prepared by thermal treatment of the green compacts at certain temperature under vacuum conditions. The prepared green compacts were treated in a G-Vac12 high vacuum furnace (Concepts and Methods Co., Inc. (CAMCO)). The compacts were kept in ceramic crucibles and were placed in the furnace and sintered at 1200°C for 2 h. The rate of heating/cooling was maintained at 10°C/min.

Grinding

The sintered samples were grinded by 240 grit silicon carbide paper (SiC) using a Struers Rotopol-1 Dual Disc Grinding Machine so as to maintain uniformity of the surface for all the samples.

The prepared samples were then characterized for the surfaces using various techniques as described in the second part.

3.2 Surface characterization

The surfaces of the materials were characterized for the morphology, topography, roughness, surface energy and chemical analysis using scanning electron microscope (SEM), atomic force microscope (AFM), profilometer, contact angle goniometer and X-ray photoelectron spectroscopy (XPS) respectively. The detailed procedures are described in this part.

3.2.1 Surface morphology

Scanning electron microscope

The samples were characterized for their surface morphology using SEM (3400N Hitachi, Japan). Plain samples after grinding were directly observed by placing the samples in the SEM chamber without sputter coating and those samples after seeding with cells after prescribed time periods were critical point dried and sputter coated with gold for conductivity. An accelerated voltage of 5 kV was applied for observing the surfaces of samples.

Cell morphology

The morphology of cells seeded on the three sample surfaces at varied time periods were processed in various steps before SEM observation. The samples were fixed in 2.5% glutaraldehyde in 0.1M sodium phosphate buffer pH 7.2 for 3 h. After fixing, the samples were washed with 0.1M phosphate buffer pH 7.2 for 5 min each 3 times. Next, the samples were dehydrated in a series of acetone washes starting with 30%, 50%, 70% and 90% for 10 min each. The samples were then critical point dried (CPD) with liquid CO₂ and sputter coated with gold to increase the conductivity for SEM observation. Different accelerating voltages were applied ranging from 5-15 kV for observing the morphology of cells at different magnifications.

3.2.2 Surface chemical analysis

X-ray photoelectron spectroscopy

The chemical analysis of the materials was studied using an X-ray photoelectron spectrometer with a dual anode (Mg and Al) apparatus using the Mg Ka anode (KRATOS AXIS 165, UK).

The X-ray gun was operated at a voltage of 15 kV and a current of 20 mA. The pressure in the analyzer chamber was about 10^{-8} Torr. Survey spectra were collected at pass energy of 80 eV.

3.2.3 Surface roughness

Profilometer

Average surface roughness (Ra) is defined as the arithmetic mean of the deviation of protrusions and depressions of the roughness profile from the average line. In this study, the surface roughness measurements were performed using a Taylor-Hobson profilometer (Talysurf 50, Leicester, UK) with a standard diamond 2 μm conisphere stylus. Taylor Hobson Ultra Software (V5.5.4.20) records the measured data for analysis. The average of three readings on three samples of each material type was measured and recorded.

3.2.4 Surface energy measurement

Contact angle goniometer

The contact angle is a quantitative measure of the wetting of a solid by a liquid. When a liquid does not completely spread on a substrate (usually a solid), a contact angle (θ) is formed, which is geometrically defined as the angle on the liquid side of the tangential line drawn through the three phase boundary where a liquid, gas and solid intersect, or two immiscible liquids and a solid intersect. The contact angle measurements were performed using a contact angle goniometer (Kruss, GmbH, Germany). A water drop of 10 μl was added and the average of three readings on three samples of each material type was used.

Surface energy determination

The surface energy was calculated based on the Owens-Wendt (OW) method [250]. In this approach the surface energy of a solid is related to its contact angle (θ):

$$(1 + \cos\theta)\gamma_L = 2(\sqrt{\gamma_L^d \gamma_S^d} + \sqrt{\gamma_S^p \gamma_L^p})$$

where γ_L is the liquid surface tension and γ_L^d , γ_L^p are its dispersive and polar components, respectively. γ_S^d and γ_S^p refer to the dispersive and polar components of the solid surface tension,

γ_s , which is the sum of its dispersive and polar components respectively ($\gamma_s = \gamma_s^d + \gamma_s^p$). The dispersive component refers to the van der Waals and other non-site specific interactions between the solid surface and the applied liquid. The hydrogen bonding, dipole-dipole interactions and other site-specific interactions are related to the polar component γ_s^p . The adhesion processes on the solid surfaces are strongly effected by these two components. The liquids used were ultrapure water and glycerol, where the surface tension, dispersive component and polar components are known [251]. A drop of 10 μl of each liquid was added and the contact angles measured. A total of three measurements on each sample type in triplicate were performed. The surface tension, dispersive component and polar component for water are γ , 72.8 mJ/m^2 , γ^d , 21.8 mJ/m^2 and γ^p , 51.0 mJ/m^2 , respectively; for glycerol these parameters are γ , 48.0 mJ/m^2 , γ^d , 29.0 mJ/m^2 and γ^p , 19.0 mJ/m^2 , respectively.

3.3 Cell culture

The procedures and assays related to cell culture are described in this part.

3.3.1 Cell line maintenance

In this study, mouse osteoblast cell line (MC3T3-E1) subclone 4 from ATCC (American Type Culture Cultivation, USA) was used for all experiments. The cells were maintained in α -MEM (Invitrogen, Gibco, USA) supplemented with 10% fetal calf serum, 100 U mL^{-1} penicillin and 100 μgml^{-1} streptomycin at 37 °C in a humidified atmosphere of 95% air and 5% CO₂. The cells were used within 5 passages after revival from frozen condition where they were maintained in the original condition.

3.3.2 MTT assay for cell viability and cell count estimation

The activity of cellular enzymes in cells can be quantitatively estimated using MTT assay. MTT ((3-(4,5-Dimethylthiazol-2-yl)-2,5-diphenyltetrazolium bromide)) is a tetrazolium dye which is reduced to insoluble purple formazan crystals by the NAD(P)H-dependent cellular oxidoreductase enzymes present in the mitochondria of live cells. The insoluble crystals are then dissolved in a solubilization reagent (usually dimethyl sulfoxide (DMSO), acidified isopropanol or SDS (sodium dodecyl sulphate) in diluted hydrochloric acid)) and the absorbance measured in a spectrophotometer between 500-600 nm wavelength. Thus, this is a colorimetric assay which can be used to estimate the number of live cells present in a culture. The dead cells don't take the dye and is a litmus test which directly reflects only the live cells present. The following procedure was adopted in this study. 50 μl of a 2 mg/ml MTT reagent (Sigma, USA) mixed in 200 μl of plain α -MEM (Invitrogen, Gibco, USA) was added to the cells at specific time points during the culture and incubated for 4 h at 37 °C. After which, acidified isopropanol (150 μl) was added to dissolve the formed formazan crystals and the absorbance was measured at 570 nm in a plate reader. A standard curve was generated using known cell numbers plotted against the absorbance values. The viable cell numbers were extrapolated from the absorbance values for calculating the adhesion and proliferation of cells on the material surfaces.

3.3.3 Induction of cell differentiation

Osteoblast cells were maintained in culture as described above (section 3.3.1). After culturing for prescribed time periods, the growth medium (α -MEM) was supplemented with 50 μ g/ml ascorbic acid (Sigma-aldrich Inc, USA) and 10 mM β -glycerophosphate (EMD Biosciences, CA) to induce osteoblast differentiation. The onset and extent of differentiation on the material surfaces was estimated by performing the following assays.

Assays for estimating in vitro cell differentiation

3.3.3.1 Alkaline phosphatase assay

Alkaline phosphatase (ALP) is an enzyme which catalyzes the hydrolysis of phosphate esters into organic radical and inorganic phosphate in an alkaline environment. This enzyme is predominantly found in the liver and bones. During the process of differentiation of osteoblast cells, the alkaline phosphatase is found in elevated levels and increases with function of time. In other words, in osteoblast culture, an increase in the specific activity of this enzyme is seen with increase in the time of differentiation. The following procedure was adopted for measuring the intracellular activity of alkaline phosphatase in the cells cultured on material surfaces at specific time points. The cell lysates from each of the materials at different time points were isolated in triplicates in a 100 μ l of lysis buffer consisting of 10 mM Tris-HCl pH 7.4, 100 mM $MgCl_2$ and 0.1% Triton-X-100. The prepared lysates were processed for ALP activity and the remaining solution was stored at -70 °C for future use. Following this, the mixture was sonicated and the supernatant was subjected to ALP activity measurements using a QuantiChrom™ Alkaline phosphatase assay kit (Bioassay systems, CA, USA) according to the manufacturer instructions. In this method, the ALP enzyme present in the cells hydrolyzes the *p*-nitrophenyl phosphate substrate into a yellow colored product *p*-nitrophenyl phosphite and inorganic phosphate. The absorbance of the colored product was measured at 405 nm in a spectrophotometer. The activity was measured till time ($t=20$ min) for each sample and the activity was calculated as follows:

$$\text{ALP Activity (IU/L = } (\mu\text{mol/L.min))} = \frac{(\text{O.D sample}_t - \text{O.D sample}_0) * \text{reaction vol} * 35.3}{(\text{O.D calibrator} - \text{O.D water}) * \text{sample vol} * t}$$

The activity was normalized to the total protein content in the samples at the tested time points, which was estimated by Lowry's protein estimation [252]. The representative ALP values for each sample were calculated as the average of triplicate samples from three separate experiments.

The following protocol was used:

The stock solution consisted of assay buffer (50ml, pH10.5), magnesium acetate (1.5 ml, 0.2 M), pNPP liquid substrate (600 μ l, 1 M) and calibrator (10 ml, tartrazine). The working solution was prepared by mixing 200 μ l assay buffer, 5 μ l magnesium acetate and 2 μ l pNPP substrate for each 96 well assay.

1. 200 μ l distilled water (H_2O) and 200 μ l Calibrator were transferred into separate wells of a clear bottom 96-well plate.
2. 50 μ l of prepared ALP lysate from each sample at specific time points was added to individual wells in triplicates.
3. 150 μ l of freshly prepared working solution was added to sample wells and the final reaction volume in the sample wells was 200 μ l.
4. The plate was tapped briefly to mix and air bubbles removed.
5. Next, the absorbance was read at 405 nm in a spectrophotometer with OD_{405nm} ($t = 0$), and again after 20 min ($t = 20$ min).
5. The activity of the sample was calculated using the equation as described above.

The amount of total protein present in the 50 μ l sample used for ALP assay was estimated using Lowry estimation. The specific activity of the sample was normalized to the total protein present in the sample and the graphs plotted.

3.3.3.2 *Osteocalcin immunostaining*

The following procedure was adopted for staining osteocalcin (OC) protein in the cells on the material surfaces. Cells at different culture periods on the materials were fixed in 4%

paraformaldehyde for 10 min at room temperature. Permeabilization was done with 0.5% Triton-X-100 for 10 min. Blocking was done with 1% BSA (Bovine Serum Albumin, Sigma, USA) for 30 min and goat anti-mouse OC at 1:200 (AbD Serotec, USA) was added for 1 h at room temperature followed by a 1 h incubation with rabbit anti-goat FITC (Fluorescein isothiocyanate) at 1:200 (GeneI, Bangalore, India) in the dark at room temperature. Images were captured using a 20X objective in an Axioplan 2 imaging system (Zeiss, Germany).

3.3.3.3 Alizarin red staining

Osteoblast cells during the process of differentiation secrete matrix rich in extracellular proteins which finally mineralize forming calcium deposits. Alizarin red is a dye which stains extracellular calcium. Cells after prescribed time periods were washed with PBS (Phosphate buffered saline) and fixed in 4% formaldehyde for 10 min at room temperature. One ml of alizarin red stain was added to each material surface and was kept at room temperature for 30 min with shaking. The stain was removed and washed 3 times with distilled water for 5 min each and was photographed using a digital camera. The calcium deposits stain red which can be visualized on the materials with increase as a function of time.

3.4 Techniques for gene profiling

The protocol pertaining to RNA isolation, purification, cDNA synthesis and RT-PCR will be described in this part.

3.4.1 Total RNA isolation and purification

The total RNA from the cells after specific time periods was isolated using the Qiagen RNA Plus kit (QIAGEN, USA).

The following protocol was used:

1. Cells were trypsinized and collected as a cell pellet.
2. The pellet was loosened by tapping the tube at the bottom.
3. Buffer RLT (Cell lysis buffer) was added (600 µl) to the loosened cell pellet and was vortexed to ensure that no cell clumps were present.
4. The lysate was then homogenized by passing through a 20 gauge needle for at least 10 times till the suspension was homogenous.
5. An equal volume of 70% ethanol (600 µl) was added to the lysate and mixed well by pipetting.
6. The sample was then transferred to an RNeasy spin column and centrifuged at 12,000 rpm for 15 s.
7. The flow-through was discarded and to the top of the spin column, 700 µl buffer RW1 (Wash buffer) was added and centrifuged at 12,000 rpm for 15 s.
8. Next, 500 µl buffer RPE (Containing ethanol) was added to the column and centrifuged at 12,000 rpm for 15 s.
9. The same buffer RPE was added again and centrifuged for 2 min at 12,000 rpm.

10. The flow-through was discarded and the spin column was again centrifuged for additional 1 min to remove residual ethanol.

11. RNase-free water was added to the column and the RNA was then eluted by centrifugation at 12,000 rpm for 1 min.

12. The isolated RNA was stored at -30 °C for future use.

The isolated RNA was quantified using a nanodrop spectrophotometer (Thermo Scientific, USA). The quantified RNA was treated with DNase1 (Ambion[®]) to remove any residual genomic DNA contamination and was checked on a 0.8% agarose gel for its purity. The DNase treated RNA was used for cDNA synthesis.

3.4.2 cDNA synthesis

cDNA synthesis was performed using the protocol with superscript III reverse transcriptase (RT) enzyme (Invitrogen life sciences, USA). 2 µg of RNA (DNase treated and purified) with 10 mM deoxyribonucleotide triphosphate mix (dNTP) and 50 µM oligo-dT (Oligo deoxy-thymidine) were taken in an Eppendorf[®] tube for first strand synthesis at 65 °C for 5 min after which it was immediately placed on ice for at least 2 min. A master mix consisting of 5X reaction buffer, 0.1M DTT (Dithiothreitol), RNase inhibitor and superscript III reverse transcriptase was prepared and added to the first strand synthesized mixture by incubating at 50 °C for 1 h followed by inactivation of RT at 70 °C for 15 min. The prepared cDNA was used for real time PCR experiments.

3.4.3 Quantitative real time polymerase chain reaction (RT-PCR)

A 10 µl reaction mixture, each consisting of triplicate samples of cDNA, specific primer mix and Power SYBR green Master mix (ABI systems, USA) was setup in each well of a 384-well reaction plate (ABI Systems, USA). Forward and reverse primers specific for genes were designed using pubmed nucleotide design software (Primer-BLAST) for all the genes. cDNA for GAPDH was used as endogenous control for calculating fold differences in RNA levels of cells on materials vs TCP by $2^{-\Delta\Delta CT}$ method. Two sets of primers were prepared- one for cell adhesion related genes and one for osteogenesis related genes. The plate was sealed using optical adhesive

cover (ABI systems, USA) and was placed in Applied Biosystems 7900HT Fast real time PCR system (Applied Biosystems, USA) machine. The cycle conditions were set up as detailed: 50 °C for 2 min initial heating, 95 °C for 1 min, 40 cycles of 95 °C for 30 s followed by 60 °C for 30 s with 72 °C elongation for 30 s each. A dissociation curve analysis was done at the end of every reaction to check for the specificity of the final product formed.

3.4.4 Agarose gel electrophoresis

Agarose gel electrophoresis is a procedure which is used for checking the purity of DNA or RNA isolated by respective procedures. In this study, the purity of RNA after isolation and after DNase treatment was checked using 0.8% agarose gel electrophoresis. The procedure followed is described as follows. 0.8% agarose gel was prepared in TBE buffer (Tris boric acid). Ethidium bromide (EtBr) was added just before solidification of the gel which was prepared after boiling the solution for ~ 10 min. The resultant solution was poured into a casting tray with multi well comb and allowed to solidify at room temperature. After which, the samples were loaded into each well mixed with a 6X loading dye consisting of bromophenol blue, xylene cyanol and β -mercaptoethanol; and was run at a constant voltage of 100V for 1 h. EtBr is a chelating agent which chelates between the bases present in the double stranded helix of DNA and RNA. The RNA was visible as bands after exposing the gel to a UV lamp and the images were capture using software.

Similar procedure was used for checking the specificity of the final product formed after RT-PCR where a 2% agarose gel was prepared.

4. The influence of surface energy of titanium-zirconium alloy on osteoblast cell functions *in vitro*

4.1 Introduction

An ideal biomaterial for orthopedic application should not only possess the bulk mechanical properties required to replace the damaged tissue, but also possess the biological properties required for rapid wound healing. An understanding of the cellular response to the material gives insights into the selection of the most appropriate material for this application. Interactions at the cell-material interface play an important role in determining the success of the implant by influencing the processes of cell adhesion, proliferation and differentiation on the material surface [36, 38-40]. The surface properties of a material such as its composition, roughness, topography and surface energy play a significant role in determining these biological effects, either independently or in an interdependent manner [41-44, 47, 48, 253].

Titanium and Ti based alloys due to their superior biocompatibility, good corrosion resistance and excellent mechanical properties such as high strength-to-weight ratio etc, have long been recognized for their use in the biomedical field and, in particular, for orthopedic and dental implant applications [17, 18, 153, 254]. These titanium based implants possess a passive oxide layer on their surface that offers resistance to corrosion and favors osseointegration into the surrounding bone tissue [19, 25, 255]. Commercially pure Ti, and TiNi, Ti-6Al-4V, Ti-6Al-7Nb are among the materials currently being used for this purpose [17-19]. However, it has been reported that the gradual release of aluminium and vanadium ions from the surface of Ti-6Al-4V alloy into the surrounding fluid causes local adverse tissue reactions and immunological responses [20, 21]. Further, Okazaki et al have shown the toxicity of vanadium and hypersensitivity of nickel [13]. Hence there has been a continuing interest in exploring new formulations of Ti alloys that do not have these detrimental effects and are not toxic. A number

of toxicity free Ti alloys, with beta phase stabilizing elements such as tantalum (Ta), molybdenum (Mo) and niobium (Nb), or neutral strengthening elements such as zirconium (Zr), have been reported [168, 171, 172, 256, 257].

Materials for biomedical applications should not only satisfy the bulk mechanical properties but also possess superior biological properties. Alloys with superior mechanical properties better than Ti with elastic modulus close to that of natural bone were reported [6, 14, 160]. In order to achieve better bone osseointegration upon implantation, apart from the bulk mechanical properties, the response of osteoblast cells towards the implanted material decides the functional longevity of the implant. TiZr and TiNb alloys, are of considerable value for use as biomaterials for it has been reported that Zr and Nb based alloys show good mechanical properties such as, high fracture toughness, low modulus of elasticity, excellent corrosion resistance [258] and have low toxicity and excellent biocompatibility [15, 257, 259]. Furthermore, the mechanical properties of TiZr [169] and TiNb [170] alloys were reported to be better than Ti. The bioactive nature for *in vitro* apatite formation on these two alloys has been shown independently [248, 260]. However, the biocompatibility of these two alloys and the behavior of osteoblast cells in response to these materials are not clearly understood.

In this background, we have examined the behavior of osteoblasts on pure Ti and its two alloys namely, TiZr and TiNb. This study was focused on measuring the surface energy and roughness of these materials and the adhesion, proliferation and differentiation of mouse calvarial osteoblasts (MC3T3-E1) on these different materials was compared. Results indicate that the TiZr alloy, with the highest surface energy, is superior to pure Ti or TiNb alloy with respect to the biological properties of these materials, which further emphasize the role of surface energy of the substrates in regulating osteoblast cell behavior.

4.2 Materials and methods

The experimental procedures pertaining to this chapter are described in detail.

The three materials namely Ti, TiZr and TiNb were processed as described in the material and experimental techniques (section 3.1 of chapter 3) and used in this study. All the samples were washed in a series of distilled water, acetone, ethanol and distilled water for 10 min each in an ultrasonic bath and air dried. The samples were then sterilized in an autoclave at 121 °C for 15 min and used for surface characterizations and cell culture experiments.

4.2.1 Surface characterization

The surfaces were characterized for morphology, roughness, chemical analysis and surface energy (procedures as described in Section 3.2 of chapter 3).

4.2.2 Cell culture and microscopy

Cells were maintained, cultured and used as described in the materials and experimental techniques chapter (section 3.3 of chapter 3).

4.2.2.1 Cell morphology

Cells at a density of 2.5×10^3 were seeded on the three material surfaces namely Ti, TiZr and TiNb and were cultured for 48 h in a humidified atmosphere of 95% air and 5% CO₂ at 37 °C. After the time period, the medium was removed and the materials were washed thrice with PBS. The samples were then processed for SEM (as described in Section 3.2.1 of chapter 3) and the morphology of the cells on the three materials were observed at lower and higher magnifications to examine the details.

4.2.2.2 Cell adhesion assay

Cells, at a density of 5×10^3 suspended in 80 µl of α -MEM were seeded on the three material surfaces placed in each well of a 24 well plate (TPP, Switzerland) ensuring that no medium overflows the disks. The same number of cells in the same volume of complete α -MEM medium was plated in triplicate cultures, on bare plastic surface of 24 well plate, these cells were used as

controls for the adhesion assay. Cells were incubated for 30 min at 37 °C in a humidified atmosphere of 95% air and 5% CO₂. After which additional 2 ml medium was added to each well and incubated for 3 h. Next, the supernatant medium was removed carefully without disturbing the adherent cells and the discs were washed twice with PBS to remove the non-adherent cells. The discs were transferred to individual well of a fresh culture plate and MTT assay was performed to estimate the viable adherent cell number on each surface. The percentage of adherent cells on each material surface was calculated based on a standard curve plotted with known cell numbers on tissue culture plastic (TCP).

4.2.2.2.1 Vinculin and actin immunofluorescence

The adhesion and spreading on the material surfaces was also evaluated by immunostaining the cells for focal adhesion protein vinculin and cytoskeletal protein actin after 8 h and 48 h of cell seeding. Cells at a density of 2.5×10^3 were seeded on the three material surfaces and were cultured under standard culture conditions. After 8 and 48 h of culturing, the medium was removed and washed thrice with PBS. The cells were fixed in 4 % paraformaldehyde for 30 min after which the cells were permeabilized for 5 min in 0.25% Triton-X-100 (Sigma Chemical Co, Inc, USA). Blocking was done with 5% BSA (Bovine Serum Albumin, Sigma, USA). Mouse monoclonal anti-vinculin antibody at 1:100 (Upstate Cell Signaling Solutions, NY) was added for 1 h followed by FITC labeled goat anti-mouse IgG at 1:200 (Sigma Inc, USA) in dark for 1 h. Rhodamine phalloidin at 1:200 (Invitrogen, USA) was added and allowed to incubate in dark for 1 h to stain actin. The materials were mounted with vectashield mounting medium (Vector laboratories Inc, CA) containing anti-fade and imaged using a multi-photon confocal laser-scanning microscope (Zeiss, Germany).

4.2.2.3 Cell viability

The percent viable cell number after 24 h of seeding the cells on the materials was calculated using MTT assay. Briefly, 2.5×10^3 cells were plated per disc and incubated at 37 °C in a humidified atmosphere of 95% air and 5% CO₂ for 24 h after which the viable cell number was estimated by MTT assay. The cell viability values have been represented as the average of percent surviving cells (form the total plated cells) on each material in three separate experiments. Each experiment was performed with each sample used in triplicates.

4.2.2.4 Cell proliferation assay

Cells were seeded (in triplicate cultures) at a density of 2.5×10^3 per disc and cultured for different time periods of 1, 4 and 7 days. At the end of the specified time periods, viable cell counts for each culture were done by MTT assay as described in section 3.3.2 of chapter 3. The values were represented as the average of triplicate samples of each material from three separate experiments.

4.2.2.5 Cell differentiation assays

Cells were plated on each material surface and plastic surface at a density of 2.5×10^3 per disc/well in triplicate and cultured till the cells reached confluence (after 3 days as seen using SEM). Next, 10 mM β -glycerophosphate (EMD Biosciences, CA) and 50 μ g/ml ascorbic acid (Sigma-Aldrich Inc, USA) were added to the medium in all cultures to induce differentiation and were cultured for 1, 2, 4, 7, 10, 15, 21 and 28 days respectively post induction.

Cell differentiation on all surfaces was assessed using ALP activity, osteocalcin immunostaining and quantitative ECM formation. The mineralization of ECM was evaluated using alizarin red staining for calcium. The methodology for these assays has been described in detail in chapter 3 (sections 3.3.3.1, 3.3.3.2 and 3.2.1 respectively).

4.2.2.5.1 ALP activity

After the cells were induced for differentiation on the three materials Ti, TiZr and TiNb, ALP activity was performed on the cell lysates isolated from the cultures after 1, 4, and 7 days using the procedure described in section 3.3.3.1 of chapter 3.

4.2.2.5.2 Osteocalcin immunostaining

The levels of intracellular and extracellular osteocalcin protein were assessed after culturing for 7, 15, 21 and 28 days post induction. The procedure described in section 3.3.3.2 of chapter 3 was followed.

4.2.2.5.3 ECM analysis

The extracellular matrix formation after differentiation on the material surfaces was evaluated after 2, 4, 7, 10, 15 and 21 days using SEM. The procedure described in section 3.2.1 of chapter 3 was followed.

4.2.2.6 Matrix mineralization

Alizarin red staining was done on the materials after 7, 15, 21 and 28 days following differentiation for staining calcium nodules to evaluate the mineralization of the extracellular matrix. The detailed protocol was followed as described in section 3.3.3.3 of chapter 3.

4.3 Results

4.3.1 Surface characterization

The physico-chemical analysis of the material surfaces was performed by determining the following properties: a) surface roughness, b) surface morphology and c) chemical composition. The average roughness (Ra) values of the materials calculated were 0.20 ± 0.02 , 0.17 ± 0.02 and 0.46 ± 0.03 for Ti, TiZr and TiNb respectively as shown in table 4.1. As per these results the roughness range of the surfaces was as follows $\text{TiNb} > \text{Ti} > \text{TiZr}$, indicating that TiZr surface was the smoothest of the three materials based on the Ra values.

Table 4.1. The roughness (Ra) values of the materials tested namely Ti, TiZr and TiNb.

Tested Material	Average Ra (μm)
Ti	0.20 ± 0.02
TiZr	0.17 ± 0.02
TiNb	0.46 ± 0.03

The surface morphology of materials was observed by SEM images and is shown in Fig. 4.1(a-c). The parallel grooves all over the material surfaces generated by the grinding of the surfaces with the SiC paper could be visualized in the SEM images. Although, the TiZr surface was smoothest as per the profilometer readings given above, no significant morphological differences could be observed between the materials at the SEM level.

The XPS survey spectra, shown in Fig. 4.1(d-f), indicate the chemical composition of the three materials. The Presence of Zr and Nb was seen specifically in the spectra of TiZr and TiNb respectively (Fig. 4.1e & 4.1f). All three materials showed characteristic peaks for O1s, C1s and N1s, indicating only minor hydrocarbon contamination.

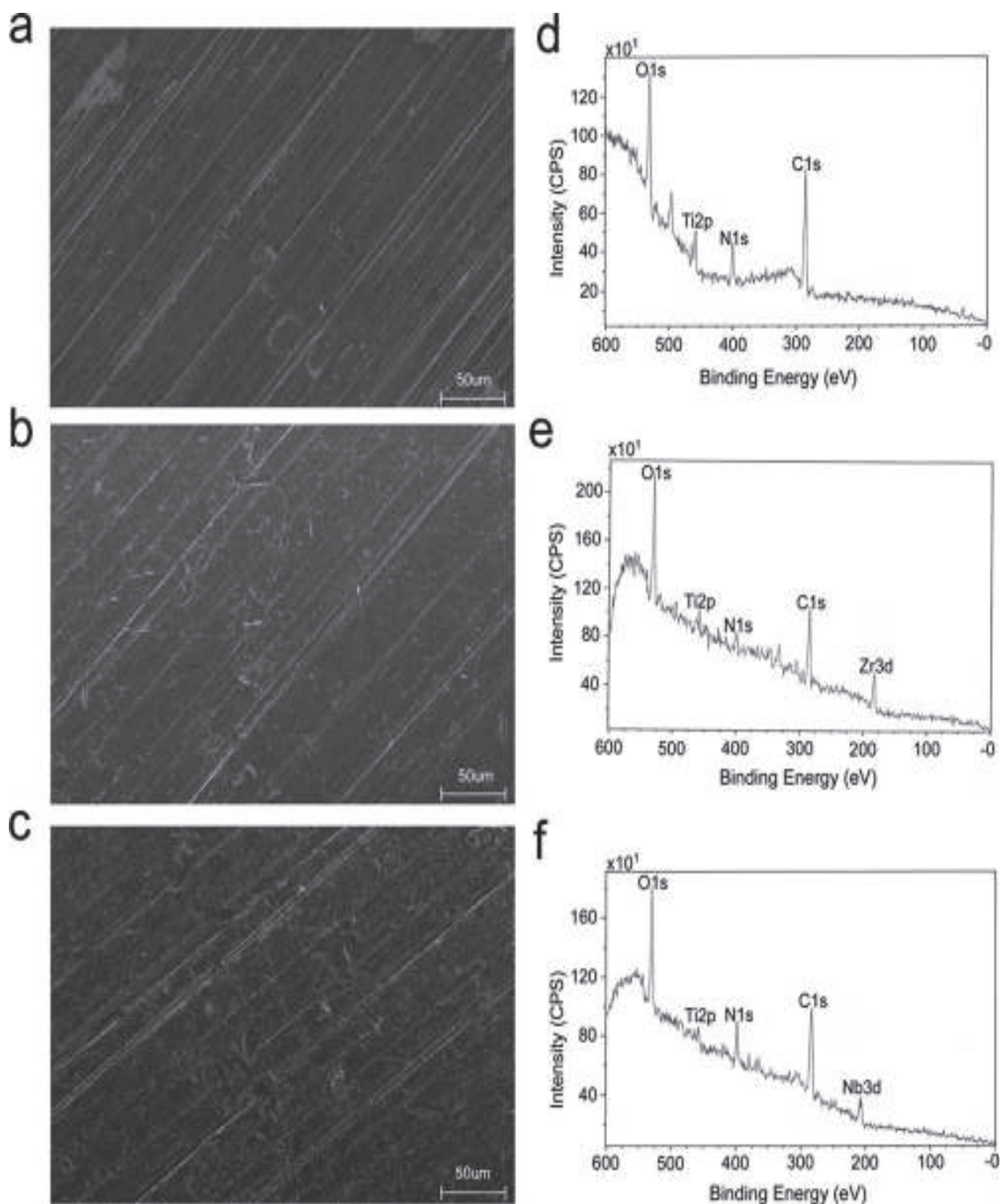


Figure 4.1. SEM images of (a) Ti, (b) TiZr and (c) TiNb (scale bar represents 50 μm) and XPS survey spectra of (d) Ti, (e) TiZr and (f) TiNb, respectively.

4.3.2 Surface energy

The surface energy of each substrate was calculated from the contact angles of water and glycerol respectively using the Owen-Wendt (OW) method (Table 4.2). All materials showed contact angles in the range of $63^{\circ} - 70^{\circ}$; the contact angle of TiNb was less than Ti, which in turn was less than TiZr. Based on these data the calculated surface energy of the materials was in the order $\text{TiZr} > \text{Ti} > \text{TiNb}$.

Table 4.2. The water contact angles and the calculated surface energies of Ti, TiZr and TiNb.

Material	Contact angle (θ)	γ_s^d (mJ/m ²)	γ_s^p (mJ/m ²)	$\gamma_s = \gamma_s^d + \gamma_s^p$ (mJ/m ²)
Ti	68.31 ± 3.83	11.97	22.28	34.25
TiZr	63.85 ± 3.16	11.42	26.32	37.74
TiNb	70.01 ± 3.83	8.01	24.8	32.81

4.3.3 Cell morphology

The morphology of MC3T3 cells on the materials was observed by SEM after 2 days of seeding. Fig. 4.2(a-c) shows the SEM images of the cells on Ti, TiZr and TiNb. On all the surfaces, cells were fully spread with well formed cytoplasmic extensions and filopodia. The cells were oriented longitudinally along the parallel grooves of the surface and were spindle shaped, indicating that after adhering to the surface, they were similarly contact guided on all the three surfaces in spite of differences in the surface roughness of the materials.

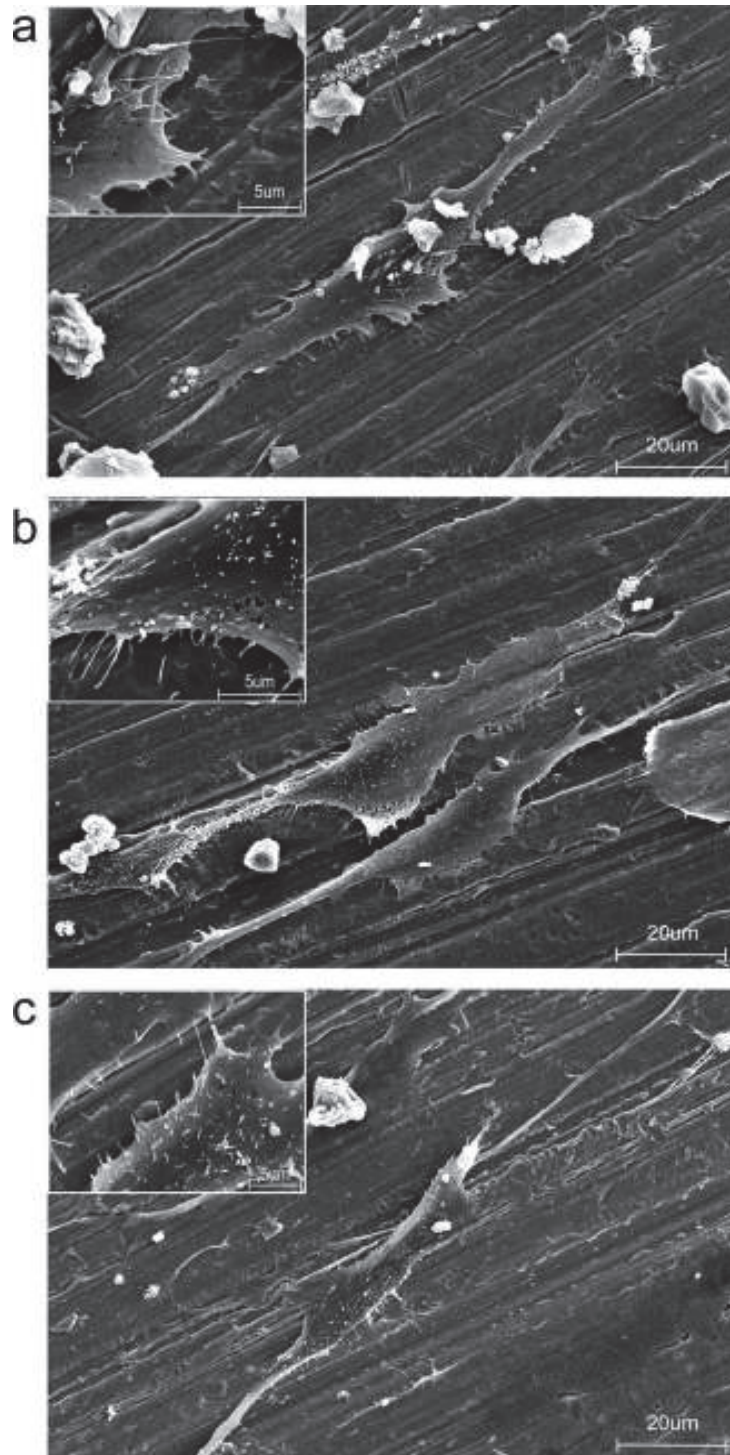


Figure 4.2. SEM images showing the morphology of MC3T3-E1 cells on (a) Ti, (b) TiZr and (c) TiNb, respectively after 48 h of cell seeding (scale bar represents 20 μm). [Inset shows filopodial extensions formed on the materials surface (scale bar represents 5 μm)].

4.3.4 Cell adhesion and spreading

Fig. 4.3 shows the percentage of cells attached on all the materials after 4 h of plating, as described in materials and methods section. A significant difference was observed in the number of cells attached to the materials. The percentage of cells attached to TiZr was higher than Ti and TiNb ($p < 0.05$).

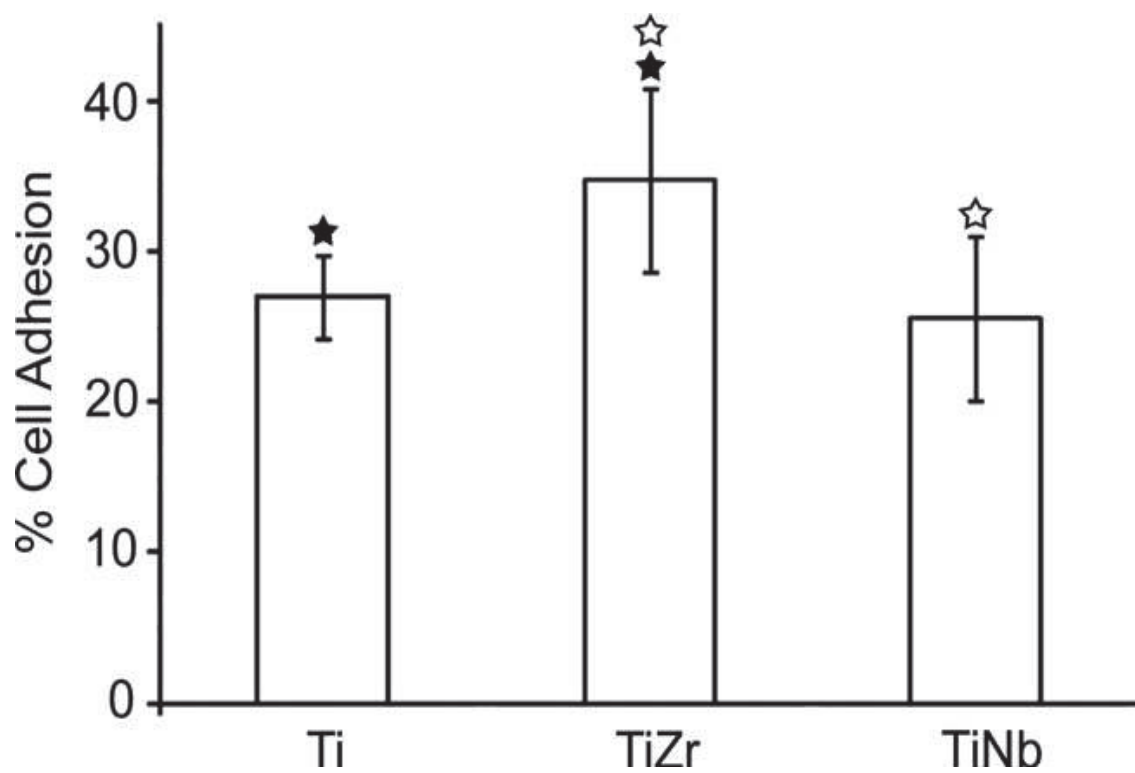


Figure 4.3. The percentage of cells attached to the three materials Ti, TiZr and TiNb after 4 h of cell seeding. ☆ ★ represents $p < 0.05$ between groups.

The spreading of the attached cells on the materials was determined by visualizing the formation of focal contacts by vinculin immunofluorescence and fluorescent phalloidin binding to actin stress fibers, as described in materials and methods section. Fig. 4.4a and 4.4b show the images of actin (red fluorescence) and vinculin (green fluorescence) staining of cells on all the three materials, as indicated in the respective panels. Actin stress fibers and vinculin localization could be seen in the cells on all three materials at both the time points tested. These data indicate that, although TiZr bound more cells than Ti or TiNb, the spreading of cells was similar within 8 h of attachment on all surfaces. The focal contacts were evenly distributed on all the membrane surfaces on the materials that were in contact with the substratum surface. We could also notice that the cells and the actin fibers were oriented along the direction of the parallel grooves generated by the grinding process.

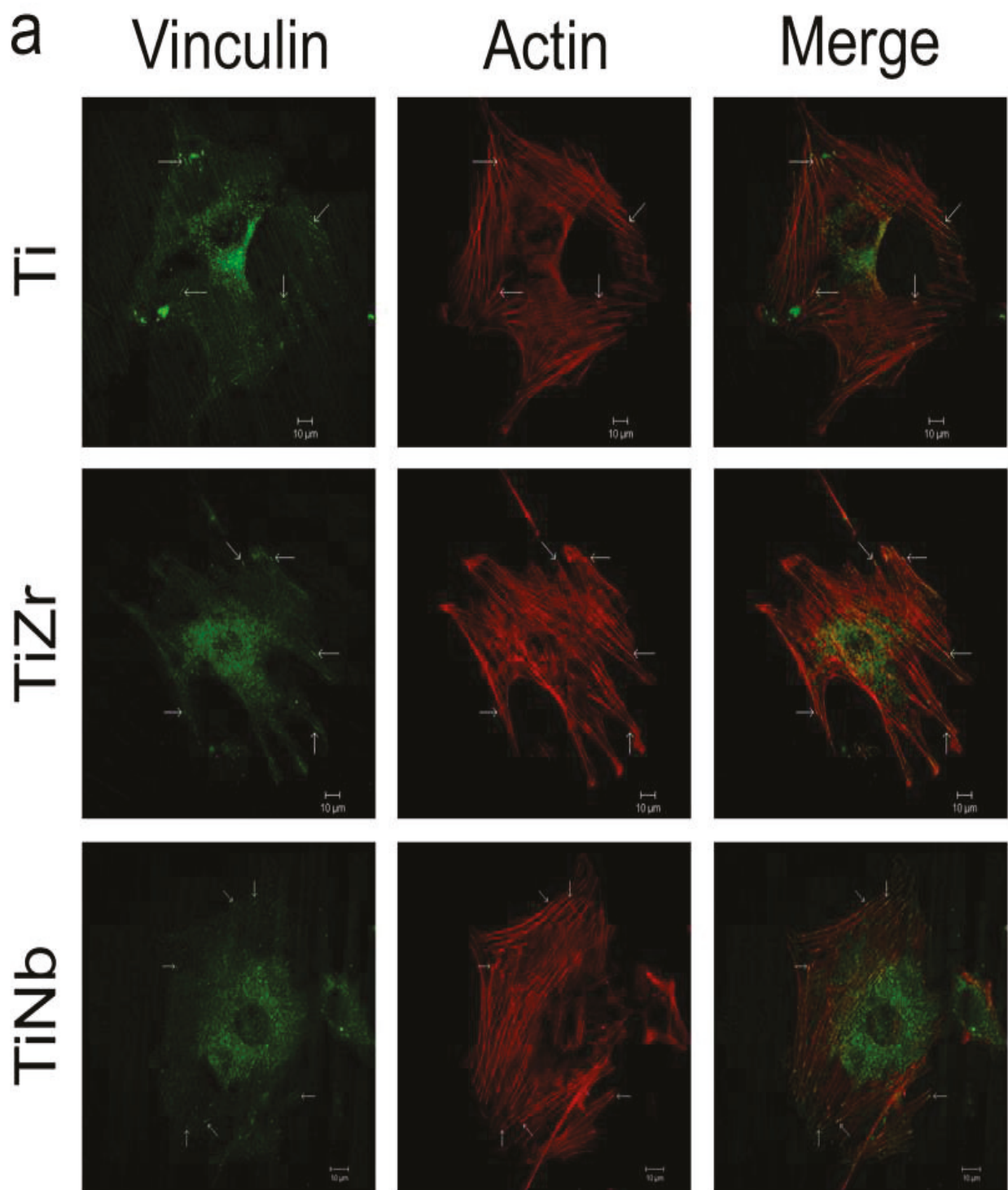


Figure 4.4. (a) The immunostaining of cells on Ti, TiZr and TiNb after 8 h of seeding the cells. Panel 1 shows vinculin staining (the contact points of the cells to the surfaces is indicated by the arrows), panel 2 shows actin staining (the stress fibers are clearly visible on the materials, indicating the spreading of the cells), panel 3 shows the merged image of vinculin and actin (the arrows indicate the co-localized regions), (scale bar represents 10 μm).

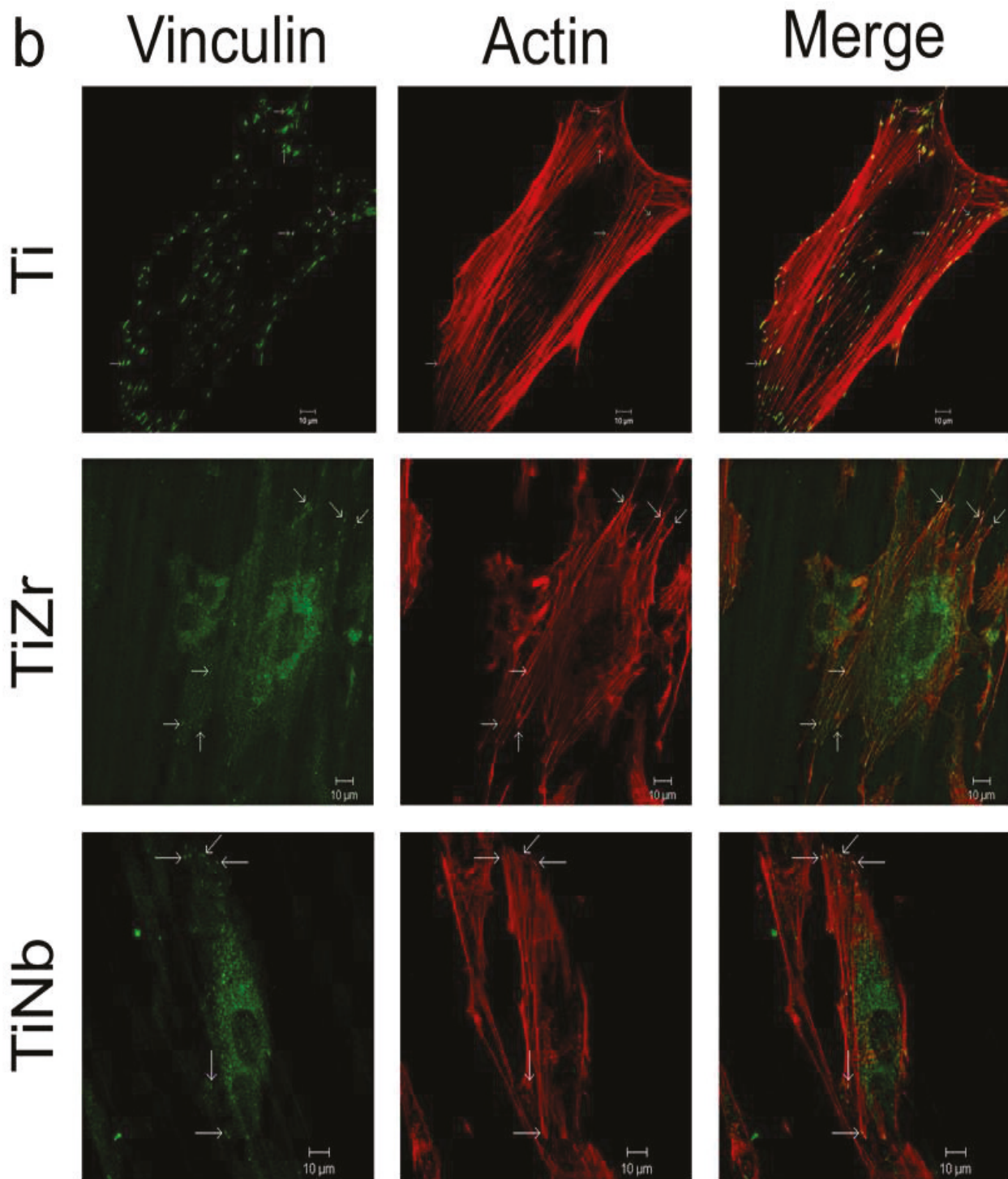


Figure 4.4. (b) The immunostaining of cells on Ti, TiZr and TiNb after 48 h of seeding the cells. Panel 1 shows vinculin staining (the contact points of the cells to the surfaces is indicated by the arrows), panel 2 shows actin staining (the stress fibers are clearly visible on the materials, indicating the spreading of the cells), panel 3 shows the merged image of vinculin and actin (the arrows indicate the co-localized regions), (scale bar represents 10 μm).

4.3.5 Cell viability

The viable cell percentage, after 24 h of plating, on the materials is shown in Fig. 4.5. These data indicate that after 24 h, 50-70% of cells could survive on these materials although the cell number was highest on TiZr when compared to either Ti or TiNb.

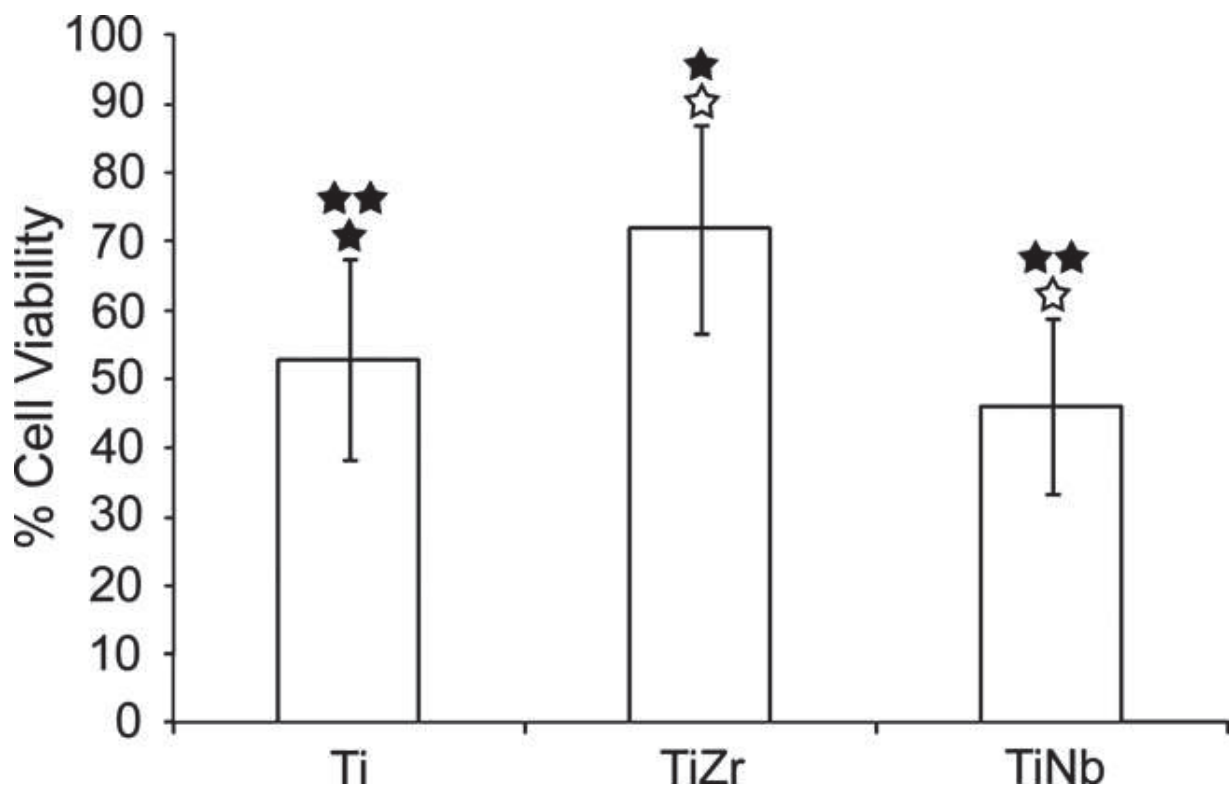


Figure 4.5. The percent viable cells after 24 h of seeding the cells on Ti, TiZr and TiNb, respectively. ★ ☆ ★★ represents $p < 0.05$ between groups.

4.3.6 Cell proliferation

The viable cell number of MC3T3 cells on the materials was calculated at three time points (days 1, 4 and 7) after plating 2.5×10^3 cells on each material and these data are shown in Fig. 4.6. At the end of day 1, as also reflected in the viability data (Fig. 4.5), the viable cell number on all the materials was lesser than that was plated on them. However after 4 days the cell number increased due to proliferation and this increase was significantly higher on TiZr than on Ti or on TiNb ($p < 0.05$). After 7 days, MC3T3 cell proliferation picked up on both TiZr and Ti and the cell number was significantly higher than on TiNb.

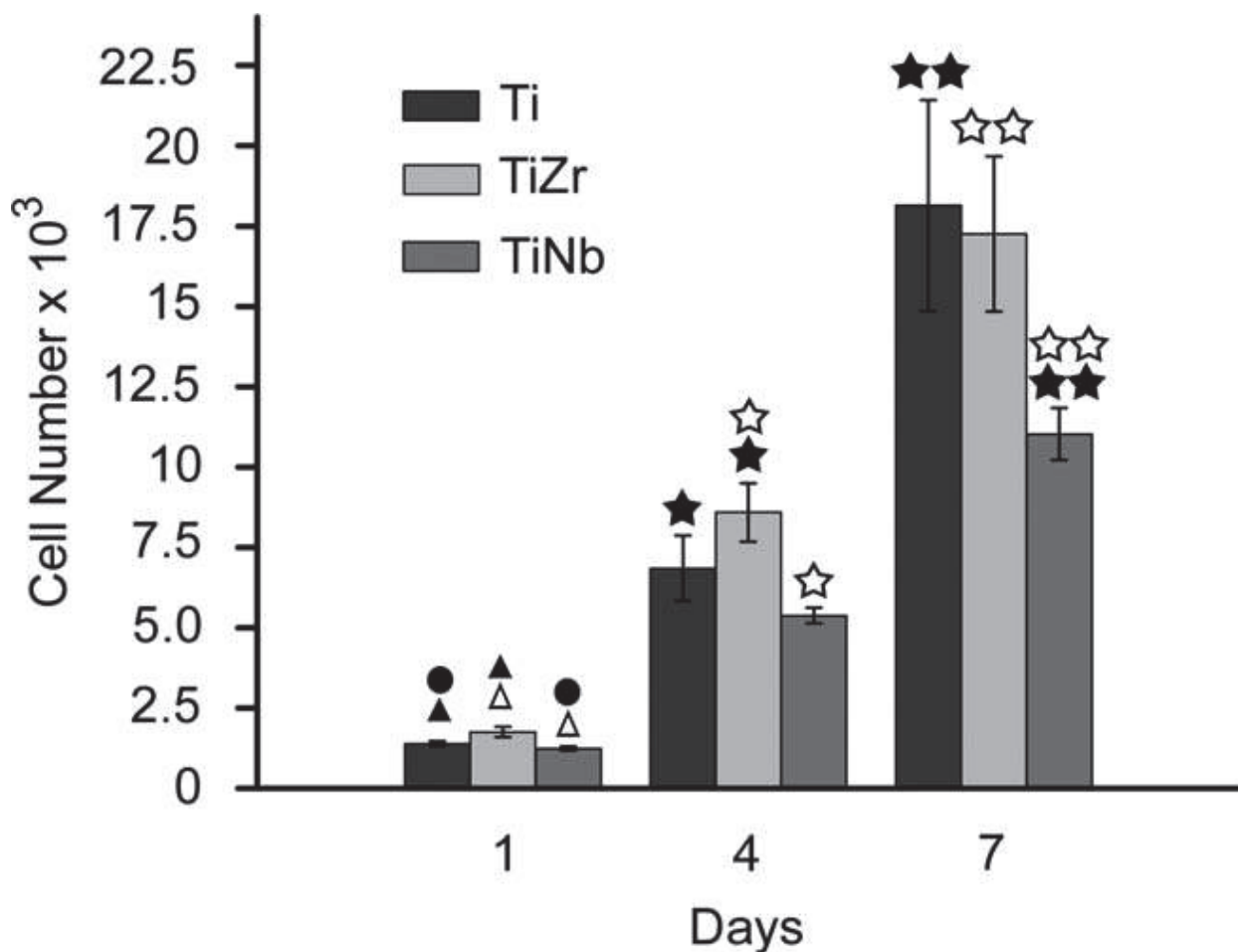


Figure 4.6. The number of cells present at the end of each time period namely 1, 4, and 7 days on the three materials. ★ ☆ ★★ ☆☆ △ ▲ ● represents $p < 0.05$ between groups at various time points.

4.3.7 Cell differentiation

The differentiation of osteoblasts on the material surfaces was assessed by the activity of ALP and the presence of OC in the cells as described in materials and methods section as well as ECM detection using SEM. Fig. 4.7 shows the cellular ALP activity on the three materials at different stages of differentiation. ALP activity increased as a function of time on all the surfaces and the activity on TiZr was higher when compared to Ti or TiNb on all the tested time points, however significant differences were noticed only on day 7.

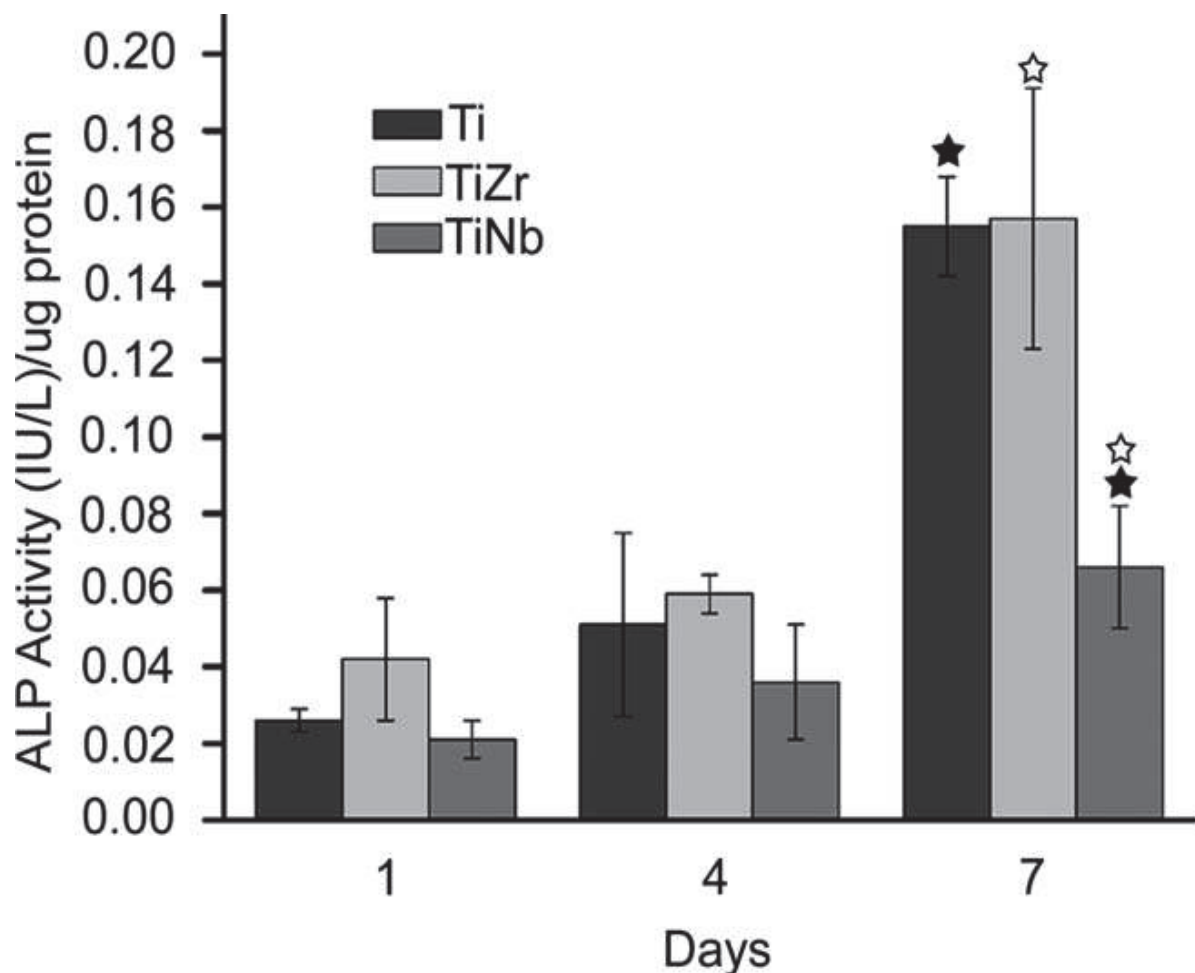


Figure 4.7. ALP activity profile of cells on Ti, TiZr and TiNb at 1, 4 and 7 days. ☆★ represents $p < 0.05$ between groups (the activity was normalized to the protein content in each sample on each material at the tested time points).

Fig. 4.8 shows the expression of OC at different times after inducing differentiation. OC levels increased on all the three materials, however, higher amounts of OC deposition in the matrix were seen on Ti and TiZr at day 15 and this process further increased at day 21. The level of OC expression in the matrix on TiNb was lesser than that on Ti or TiZr on days 15 and 21 with most of the OC fluorescence being restricted to the nucleus of the cells. Similar results were seen even at day 28.

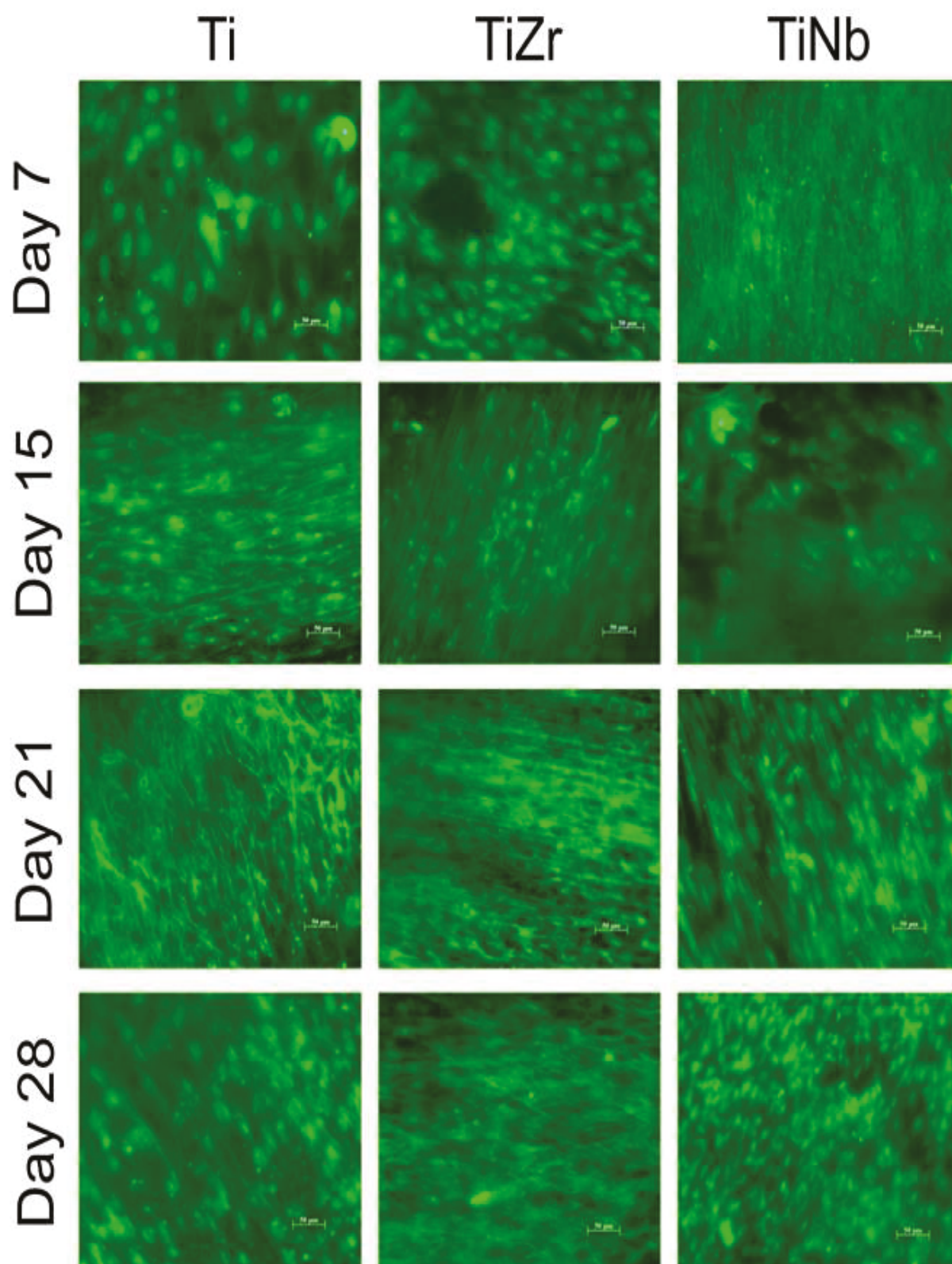
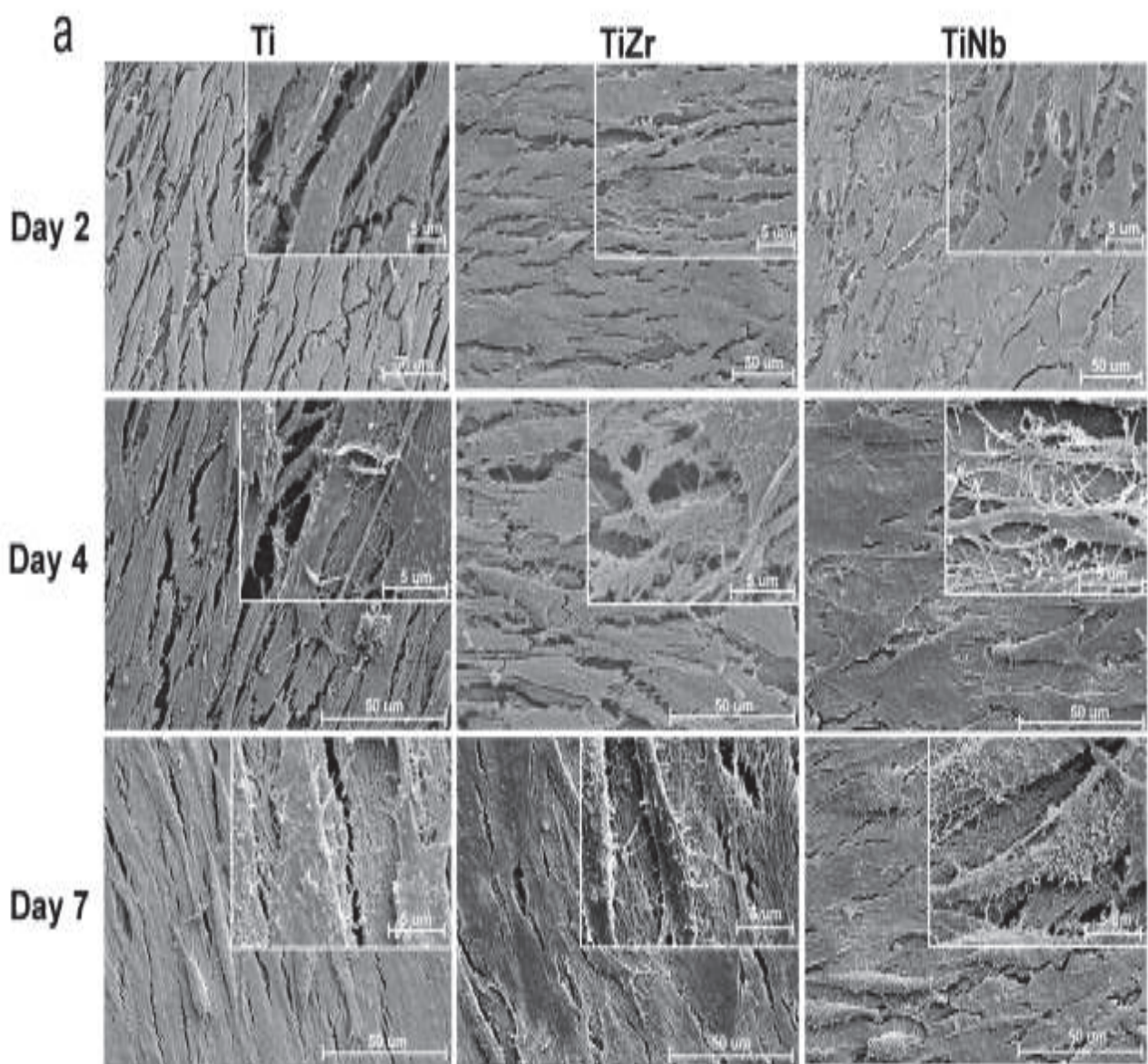


Figure 4.8. Immunostaining of osteocalcin protein at days 7, 15, 21 and 28 on Ti, TiZr and TiNb (scale bar represents 50 μm on all the individual images).

ECM analysis

The extent of extracellular matrix formation on the surfaces of materials was assessed at different time periods after differentiation namely 2, 4, 7, 10, 15 and 21 days by observing the surfaces in an SEM as shown in Fig. 4.9a and 4.9b. ECM formation on the three surfaces was seen early after 4 days of differentiation. With an increase in time, the thickness of the ECM increased till 21 days on all the three material surfaces. An increase in the cell number was also seen at lower magnifications and the quantity of formed ECM at higher magnifications.



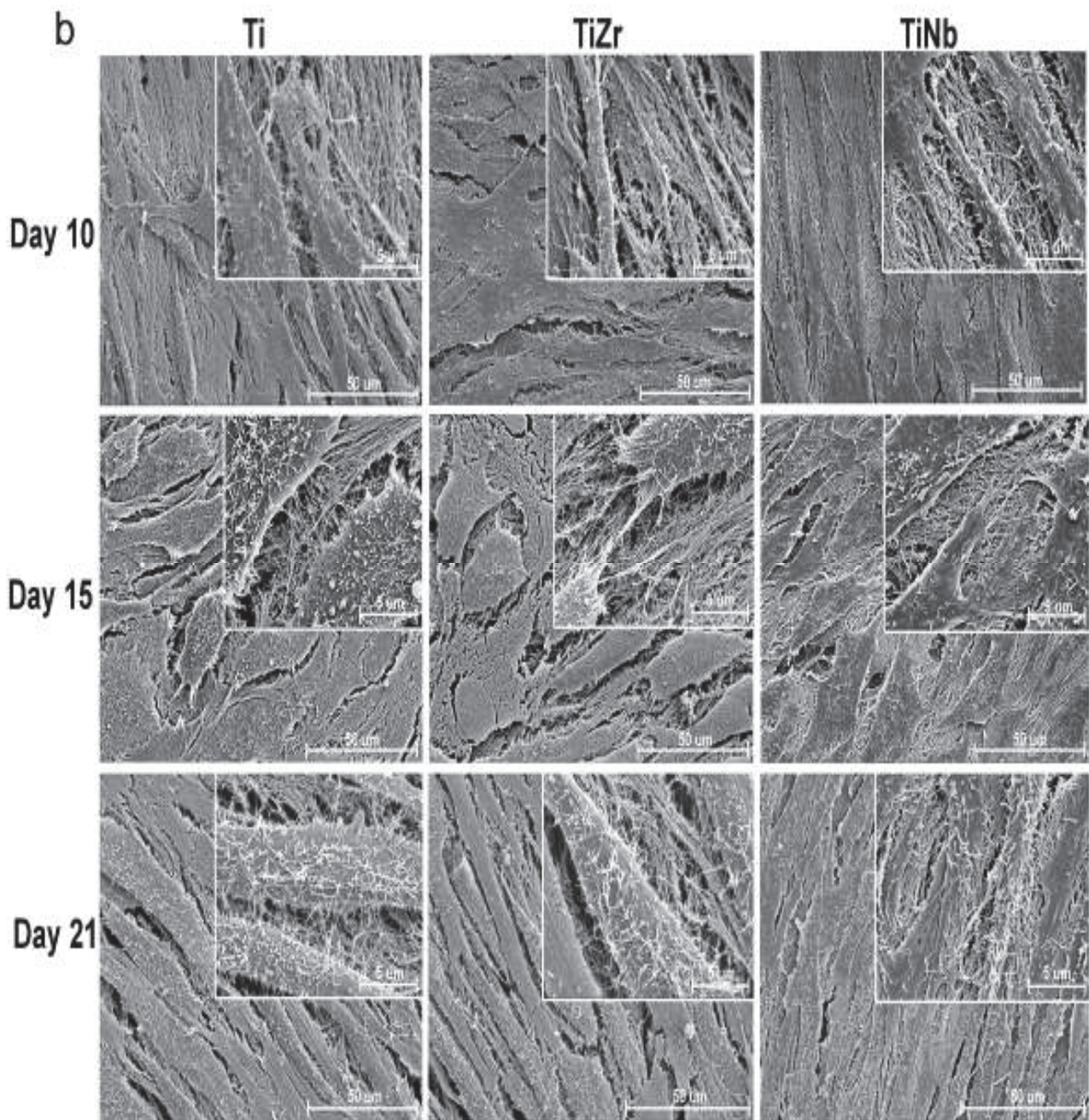


Figure 4.9. (a) The extracellular matrix formation on the three material surfaces Ti, TiZr and TiNb after 2, 4 and 7 days of differentiation. (b) The extracellular matrix formation on the three material surfaces after 10, 15 and 21 days of differentiation. (scale bar represents 50 μm). Insets in each panel show the high magnification images of the ECM with cells. (scale bar represents 5 μm).

4.3.8 Matrix mineralization

Fig. 4.10 shows the alizarin red staining for matrix mineralization on the materials. As the days progressed, the intensity of the red color increased with time, indicating the deposition of calcium as stained with alizarin red dye. Qualitative analysis indicates that, the intensity increased on the materials, but this increase was found to be more on Ti and TiZr but to a lesser extent on TiNb. The data further shows that the cells differentiated on all the three materials becoming mature osteoblasts and the materials supported the differentiation of osteoblasts.

The combined analysis of ALP activity and OC staining showed that, MC3T3 osteoblast cells differentiated on all the three materials but the process was better on TiZr and Ti compared to TiNb.

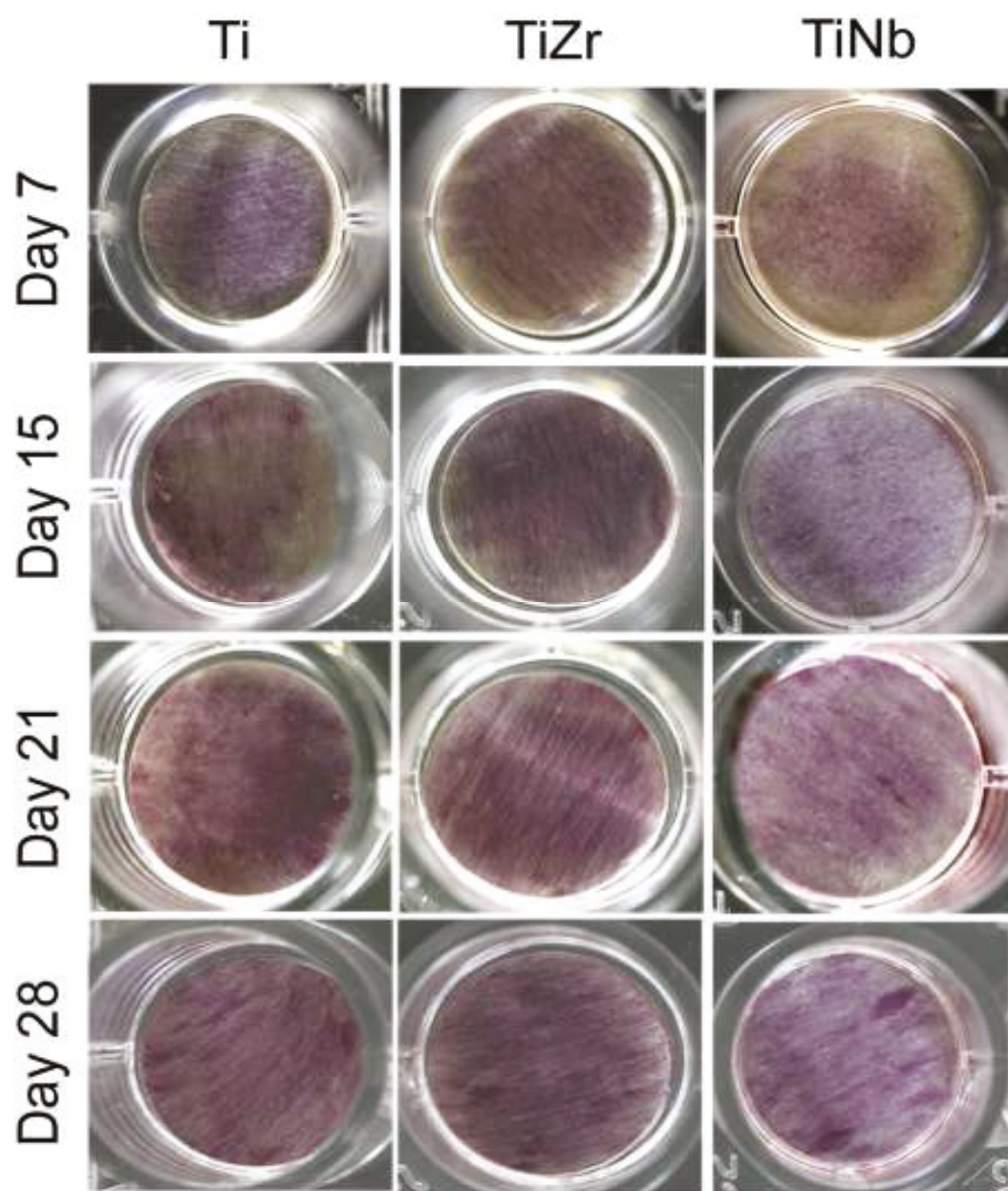


Figure 4.10. Alizarin red staining on the three material surfaces Ti, TiZr and TiNb at 7, 15, 21 and 28 days after differentiation.

4.4 Discussion

The surface of an implant plays an important role in its interaction with the surrounding tissues *in vivo* and in determining its functional longevity. The molecular mechanisms of the *in vivo* cellular responses to the implant materials are studied by *in vitro* assays using cell lines plated on the implant material. Based upon such *in vitro* assays it has been repeatedly shown that their surface properties such as material composition, micro-topography, roughness and surface energy, play a significant role in determining the adhesion and spreading of bone precursor cells, and also assist in their subsequent proliferation and differentiation [39, 231, 261-263]. In the present study we took a similar approach to compare the cell modulating properties of two Ti based alloys- TiZr and TiNb. Our analysis has revealed some interesting though subtle variations in the biological behavior of these two materials, whose surface properties could be responsible for the observed variation.

4.4.1 Cell adhesion and spreading

In this study, we have focused on the effect of surface roughness and surface energy on the initial events of cell-material interaction i.e. cell adhesion and cytoskeletal organization after the adherent cells are well spread on the three different materials. Using immunostaining for vinculin and fluorescent phalloidin for actin fibers we observed that focal contacts were well formed and the cells were well spread with stress fibers oriented in a parallel direction to the axis of the cells on the three material surfaces (Fig 4.4a and 4.4b). These observations regarding cytoskeletal organization were similar to those reported by Eisenbarth et al [232] and Anselme et al [45] on ground titanium surfaces and Ti-6Al-4V alloy, respectively which had similar roughness levels as the materials used in our study. Further, in our case the cytoskeletal organization did not change with the degree of roughness of the surface.

The morphology of the adherent cells, as observed by SEM, also showed no difference on the three material surfaces (Fig. 4.2). The observations were similar to those seen by Jayaraman et al [231]. We did observe significant differences with regard to the initial attachment of cells where a higher percentage of cells attached to TiZr when compared to either Ti or TiNb (Fig. 4.3). In the context of the different roughness of the three surfaces, our results differ from that reported

by Castellani et al [264] who did not observe any relationship between cell adhesion and the surface roughness, although the roughness values were comparable to ours. Based on our results and the earlier reports, [45, 264] the role of minor differences in surface roughness ($R_a < 0.50 \mu\text{m}$) of the materials, in directly regulating the adherent cell percentage and cytoskeletal organization remains debatable.

The role of surface energy in regulating the adhesion of cells to materials has been studied by several groups [55, 56]. A study by Hallab et al [44] has shown that the surface energy of the material is more important than the roughness in regulating the adhesion of cells to the metal substrates. Furthermore, studies on the role of hydrophilicity and surface energy in regulating osteoblast cell adhesion seem contradictory [249, 262]. In our study, we observed that TiZr with high surface energy supported better adhesion of osteoblast cells when compared to Ti or TiNb (compare Table 4.2 and Fig. 4.3). Our data supports Hallab et al [44] observations and therefore surface energy could be a major parameter in regulating the adhesion and spreading of cells on the materials.

4.4.2 Cell proliferation and differentiation

The processes of cell proliferation and differentiation are determined by cell adhesion, the nature of which is influenced by the surface properties of roughness, composition and topography of the materials. A number of studies have shown that the proliferation of cells decreases with an increase in the roughness and the changes in the topography and the differentiation of cells increases with increase in the roughness [39, 46, 48]. We have noticed significant differences with regard to proliferation and differentiation of cells on the two alloys tested in our study. A time dependent significant difference in cell proliferation was seen between TiZr and TiNb surfaces [Fig 4.6], although the difference between Ti and TiZr surfaces was insignificant. Unlike the study by Castellani et al [264] who did not observe any difference in cell proliferation on surfaces with different roughness, we have observed the maximum cell proliferation on the material (TiZr) which has the lowest surface roughness. These results are in agreement with earlier studies on the effect of surface roughness on cell proliferation [46]. If examined together with the data on cell adhesion, the proliferative behavior of cells on TiZr could be due to a synergistic effect of surface energy and surface roughness.

The differentiation of osteoblasts is a surface sensitive phenomenon, which is influenced by the topography, roughness and the composition of the materials surface. An early indicator of osteoblast differentiation is the time dependent increase in the activity of ALP post induction [265, 266]. We have also observed an increase in the ALP activity as a function of time on all the surfaces (Fig. 4.7). Regarding the association of the ALP activity with the surface roughness no conclusive remarks can be made because the differences in the surface roughness of our substrates were only minor. In an earlier report [267] no differences in ALP activity could be seen in cells that were similarly induced on surfaces with large differences in surface roughness.

In addition to ALP activity the expression of the bone matrix protein OC in the ECM is important for complete osteoblast differentiation. We observed a significant increase in OC expression, after a period of 21 days post induction, on Ti and TiZr in comparison to TiNb (Fig. 4.8). Our results support the study in which similar results were seen using OC expression on pure Zr and Ti substrates [268]. Furthermore, the ECM formation on the surfaces was clearly seen with early detection after 4 days of differentiation (Fig. 4.9a and 4.9b). An increase in the density of the matrix was seen with increase in the time periods (Insets showing high magnification images of cells with ECM).

It is important for bone cells to be differentiated and mineralized for effective bone apposition. The completion of differentiation is followed by mineralization of the matrix with the deposition of calcium. We have observed the differentiation of osteoblasts with the formation of mineralized bone matrices on the three materials (Fig. 4.10). Alizarin red S is a dye that binds to calcium and is stained red. The alizarin red staining indicated the deposition of calcium and the matrix mineralization on Ti, TiZr and TiNb materials, although the levels were less on TiNb when compared to Ti and TiZr (Qualitative analysis). During the mineralization process, ALP being the early marker for bone differentiation reaches its maximum levels while, the late marker for differentiation, osteocalcin expression increases as the mineral gets deposited. Our observations are similar to the observed changes in the ALP activity (Fig. 4.7) and osteocalcin levels (Fig. 4.8).

Taking the proliferation and differentiation results together, we can say that MC3T3 cells reach a peak of proliferation around day 7 on all the substrates and the differentiation process is induced

as reflected by ALP activity. TiZr alloy is better when compared to TiNb at the time points tested.

Substrate composition has been reported to influence osteoblast cell behavior in studies that have used similar or dissimilar group of materials [40-42, 47, 253]. Some of these studies have focused on the exclusive role of the substrate composition and some others have studied it in association with other properties of the materials. Since we have noticed significant differences in the osteoinducing properties of the three surfaces and we have not seen a significant association of surface roughness with it, we believe that in our materials the difference in the chemical composition of the two Ti alloys plays a role in the osteoinducing ability of the substrate, where the TiZr alloy scores better than TiNb.

In summary our *in vitro* results indicate that TiZr has a better biological profile than Ti or TiNb based on the initial attachment of MC3T3-E1 osteoblast cells on these materials. The influence of subtle differences in the surface properties such as roughness, surface energy and substrate composition can modulate these characteristics. This offers the potential for further improvement in their biological performance of materials by introducing surface modifications with physical and chemical means. The preference of Ti based alloys over pure Ti in designing better implant materials suggests that TiZr would perform better than TiNb. These studies are further enhanced by other reports on TiZr where its mechanical properties and bioactivity have been demonstrated [168, 260, 269].

4.5 Conclusions

In this chapter, we have attempted to study the biocompatibility and ability of materials to support osteoblast cell growth on three materials namely titanium and its two alloys TiZr and TiNb. The following conclusions can be drawn from this study.

- The two alloys of titanium namely TiZr and TiNb were biocompatible as evident by the viability of osteoblast cells present on the materials after seeding for 24 h.
- The surface roughness of the three materials were in the sub-micron range with subtle differences in the roughness values
- Notable differences in the water contact angles and calculated surface energies were seen on the three material surfaces with the TiZr surface being more hydrophilic and a higher surface energy.
- The cell adhesion using MTT assay showed a higher percentage of cells attached on TiZr surface compared to Ti and TiNb surfaces, although immunostaining of focal adhesion protein vinculin did not show any notable differences on the three material surfaces. Also, the spreading of the cells as seen using actin immunofluorescence also showed no notable differences where the attachment and spreading was seen on all the three surfaces.
- The morphology of cells also did not show any marked differences between the three material surfaces and it is a topography driven phenomenon where, the topography was similar on the three surfaces.
- Cell proliferation was higher on the TiZr surface compared to Ti and TiNb after 1 and 4 days of cell seeding with significant differences. No significant difference was seen on Ti and TiZr on the 7 days but was consistently higher compared to TiNb surface. This result was consistent with the adhesion results using MTT, where the cell number was higher on the TiZr surface after plating equal number of cells on the materials.

- The differentiation of cells was seen on all the three material surfaces but marked differences were seen with regard to ALP activity profiles. The activity was seen on the three material surfaces as a function of time, however, the process was accelerated on the TiZr surface compared to Ti and TiNb.
- The surface energy is a dominant property of a surface where, the adhesion of cells was higher on a higher energy surface (TiZr) compared to surface roughness where the materials differed in subtle changes in the roughness values.
- The same reasoning can be given with regard to cell proliferation where the number of cells was higher on a higher energy surface namely TiZr.

Having looked at the response of osteoblast cells on the three material surfaces at the cellular level, it was interesting to understand whether the same behavior of cells was noticed on the materials at the molecular level. This could be achieved by looking at the gene expression patterns of candidate genes involved in osteogenesis by observing the gene profiles at different stages of cell-material interactions namely at cell adhesion and differentiation processes. This forms the crux of chapter 5.

5. Role of surface properties of titanium alloys on the expression of adhesion and differentiation related genes

5.1 Introduction

The biocompatibility of two titanium alloys, TiZr and TiNb in terms of their ability to support the growth and differentiation of osteoblast cells was studied in detail as described in the previous chapter. The effect of surface properties namely surface energy on the cell behavior was very interesting. Several reports suggest that the surface roughness effects the adhesion of cells [41, 43, 46] however, in our study with Ti, TiNb and TiZr though the surface roughness differences were minimal and in the submicron range we found that the adhesion of cells was better on the TiZr surface compared to pure Ti and TiNb. This can be attributed to the higher surface energy of TiZr, indicating that a material with higher surface energy helps in accelerating the attachment of cells on material surfaces and holds an edge over surface roughness. Interestingly, the extent of adhesion as observed by immunostaining of focal adhesion protein vinculin did not show any significant differences between the three materials. Therefore, we were interested to look into the molecular level responses in cells with regard to the surface properties encountered by osteoblast cells. We have also seen that the cells not only adhered well but even the cell proliferation was higher on TiZr surface with a similar behavior on Ti but higher compared to TiNb. Similar observations with regard to cell differentiation were also made where the differentiation process was better on Ti and TiZr compared to TiNb. This prompted us to understand the differences in the cell responses at the molecular level during the stages of cell adhesion and differentiation. So, we continued our study further by looking the gene expression patterns upon seeding the cells on the three materials and investigating the fold change

differences of candidate genes at the stages of adhesion and differentiation on the material surfaces after various time periods of culturing.

The surface properties of a material determine the physiological response of cells that come in its contact [37]. In other words, the physico-chemical and morphological features at the surface of an implant material can significantly influence the outcomes of the molecular events that take place at the cell-material interface and also intracellularly [39, 41, 43, 46, 47, 249, 267, 270]. In the case of orthopedic implant materials their surface properties namely roughness, topography, chemistry and energy can influence the initial cellular response of osteoblasts which ultimately effects the quality and stability of the newly formed bone tissue around the implant and thus determine the long term performance of the implant [38, 42, 48, 271-273].

The first phase of the cell-material interactions includes formation of the initial cell contact and subsequent adhesion and spreading of osteoblast cells on the material surface [274, 275]. The nature of these initial interactions and the cellular response significantly determines the subsequent proliferation and differentiation of the cells. The qualitative and quantitative features of the initial contact and cell adhesion to the material surface are also influenced by the proteins adsorbed onto the surface from the biological milieu [37, 55, 56] which in turn can be directed by the nature of surface properties [276-279]. Anselme et al. [177] while reviewing these features have described the role of short-term events of ionic forces such as van der Waal forces and the long term role of ECM proteins and cytoskeletal proteins within the cells that promote the action of the transcription factors and specific gene expression in the cells.

Although it has not been clearly demonstrated, but is likely that osteoblast interactions with the material surface are mediated by transmembrane adhesion protein receptors namely integrins. These receptors are signaling proteins that are known to mediate the anchorage of cells to specific components of the ECM and signals generated by them are known to regulate cell proliferation and differentiation [280, 281]. Integrins work in collaboration with cytoskeletal molecules such as focal adhesion kinase (FAK), vinculin, paxillin and actin which are all part of the focal adhesion complex [281-283]. Vinculin acts as a linking molecule and it helps in generating a very large molecular assembly of docking and signaling molecules that assist in the functional and structural stability of the focal adhesion complex [282-287].

Several studies have shown that integrins along with FAK, MAPK1 (Mitogen activated protein kinase 1) and osteopontin play a significant role in osteoblast adhesion and differentiation [288-298]. The involvement of these molecules in osteoblast differentiation on different material surfaces has been shown but the process is not clear [268, 299-301].

In the previous chapter, we compared the *in vitro* adhesion of MC3T3 osteoblast cells to two titanium alloys namely titanium-zirconium (TiZr) and titanium-niobium (TiNb) [302] and demonstrated that the surface energy and substrate composition of titanium alloys could significantly determine the quantity and strength of osteoblast cell adhesion to titanium alloys. In the present chapter we have provided further evidence in that direction by comparing the gene expression profiles of candidate genes involved in cell adhesion and osteoblast differentiation on Ti and its two alloys TiZr and TiNb. Our results show that genes related to cell adhesion are maximally expressed in cells plated on TiZr and genes related to osteogenic differentiation are better expressed on the surfaces of both the alloys, in comparison to titanium. Our results provide a good experimental system to study how integrin based cell signaling systems can be regulated by the properties of material surfaces.

5.2 Materials and methods

The methodology pertaining to this chapter is described.

5.2.1 Sample preparation and processing

The three material groups namely Ti, TiZr and TiNb samples were prepared, processed and used as described in section 3.1 of chapter 3. All the materials were sterilized in an autoclave at 121 °C for 15 min and used for cell culture experiments.

5.2.2 Cell culture

Cells were maintained, cultured and used as described in the materials and methods chapter (section 3.3.1 of chapter 3).

5.2.3 Gene profiling

5.2.3.1 PCR array

The effect of surface property differences on osteoblast gene expression was evaluated on the three material surfaces using a PCR array (SA Biosciences, Cat# PAMM-026). The Mouse Osteogenesis RT² Profiler™ PCR Array profiles the expression of 84 genes related to osteogenic differentiation. This array contains genes functioning in the development of the skeletal system as well as bone mineral metabolism. Growth factors and genes mediating osteogenesis and related cell growth, proliferation, and differentiation processes are included. Also represented are the extracellular matrix molecules and cell adhesion molecules involved in bone development.

5.2.3.1.1 RNA isolation

Cells at a density of 2.5×10^3 were seeded on the three material surfaces namely Ti, TiZr and TiNb with the tissue culture polystyrene (TCP) surface serving as the control. Culturing of the cells on the materials was done at standard conditions by incubating at 37 °C. After the cells reached confluence (as seen on TCP), the growth medium was supplemented with ascorbic acid and β -glycerophosphate for inducing differentiation. After 1 and 4 days of induction, RNA was isolated and purified from the three material surfaces along with TCP as per the manufacturer

instructions (Qiagen RNA Plus kit, USA) (protocol described in section 3.4.1 of chapter 3). The RNA was quantitated using a nano-drop spectrophotometer (Thermo fisher Scientific Ltd, USA) and subjected to DNase (Ambion[®]) treatment. The treated RNA was then used for cDNA synthesis using RT² First-Strand cDNA synthesis kit (SA Biosciences). The procedure for DNase treatment is described below.

1. 2.5 µg of RNA isolated from the samples at various time points was taken in an Eppendorf[®] tube.
2. 1 µl of 10X buffer was added along with 0.3 µl of DNase1 to the RNA mixture.
3. The reaction volume was made upto 10 µl with RNase free water and incubated at 37 °C for 30 min.
4. To this reaction mixture EDTA at 5 mM concentration was added to inactivate the DNase by incubating at 75 °C for 10 min.
5. The purity of the isolated RNA was checked using a 0.8% agarose gel and the sample was stored at -70 °C and was processed for cDNA synthesis.

5.2.3.1.2 cDNA synthesis

The DNase treated RNA was processed for cDNA synthesis using RT² First-Strand cDNA synthesis kit. The procedure is described below.

1. The contents of the kit were briefly spun down in a table top centrifuge.
2. Genomic DNA elimination mixture was prepared
 - a. For each RNA sample

Component	Amount
RNA	2 µg
Buffer GE	2 µl

RNase free water	Variable
Total volume	10 µl

3. The contents were mixed briefly by pipetting followed by centrifugation.
4. Incubation was done at 42 °C for 5 min.
5. The tube was then place on ice for at least 1 min.
6. RT cocktail (Reverse Transcription mix) was then prepared as below.

Component	Volume for 1 reaction (µl)	Volume for 2 reactions (µl)	Volume for 4 reactions (µl)
5x Buffer BC3	4	8	16
Control P2	1	2	4
RE3 Reverse Transcriptase Mix	2	4	8
RNase free water	3	6	12
Total volume	10	20	40

7. First strand cDNA synthesis reaction was set up by adding 10 µl of RT cocktail to 10 µl of genomic DNA elimination mixture.
8. This mixture was incubated at 42 °C for exactly 15 min and the reaction was stopped immediately by heating at 95 °C for 5 min.
9. To this cDNA reaction mixture 91 µl of water was added and stored at -20 °C for further processing with real time PCR.

5.2.3.1.3 Real time PCR

Following the cDNA synthesis of the four samples (Ti, TiZr, TiNb and TCP) at two time points (1 day and 4 days), the samples were loaded in to a PCR array plate (96 well format) as per the protocol of the manufacturer and RT-PCR was done in an ABI 7500 Standard machine (Applied Biosystems, USA). The protocol is described below.

1. RT² SYBR Green Master Mix vial was thawed on ice and briefly centrifuged (10-15s) to bring the contents to the bottom of the tube.
2. PCR component mix was prepared as below

Component	Amount (μl)
2x RT2 SYBR Green Mastermix	1350
cDNA synthesis reaction	102
RNase-free water	1248
Total volume	2700

3. Next, 25 μl of PCR component mix was added to each well of the RT² Profiler PCR Array and was sealed using a optical adhesive film.
4. The plate was then centrifuged at 1000g for 1 min at room temperature to remove bubbles.
5. The plate was placed on ice and the PCR cycling program was set up with the following cycling conditions.

Cycle	Duration	Temperature	Comments
1	10 min	95 °C	HotStart DNA Taq Polymerase is activated by this heating step.
40	15s 1 min	95 °C 60 °C	Perform fluorescence data collection.

6. The plate was then placed in the ABI 7500 Standard machine and the program was run.
7. The PCR specificity was verified by running a default melting curve program (95 °C, 1 min; 65 °C, 2min (optics off); 65 °C to 95 °C at 2 °C/min (optics on)).

The fold change values at each time point of the three materials (Ti, TiZr and TiNb) were calculated after feeding the C_T values in software RT² profiler PCR Array Data Analysis version 3.5 (SA Biosciences) and the graphs plotted against control (TCP). The data of only one PCR plate was used for analysis.

5.2.3.2 Real time PCR using gene specific primers

The gene profiling on the three material surfaces using PCR array at the two time points gave us clues about the possible genes being expressed on the materials and their respective fold change differences compared to control (TCP). The expression profiles of some of genes from the real time PCR data were validated using the RNA isolated at 4 and 24 h of adhesion as well as 1, 4, 10 and 15 days post induction for differentiation. The primer sequences for the genes used are given in table 5.1.

Table 5.1. Table showing the forward and reverse primers of genes used for RT-PCR experiments.

Gene	Primers (5'-3')		Product length (bp)
GAPDH	Fwd	AGCGAGACCCCACTAACATCA	118
Integrin $\alpha 2$	Rev	CTTTTGGCTCCACCCTTCAAGT	119
	Fwd	AAGTGCCCTGTGGACCTACCCA	
Integrin $\alpha 5$	Rev	TGGTGAGGGTCAATCCCAGGCT	111
	Fwd	ACCACCTGCAGAAACGAGAGGC	
Integrin αV	Rev	TGGCCCAAACCTCACAGCGCA	121
	Fwd	TCCCACCGCAGGCTGACTTCAT	
Integrin $\beta 1$	Rev	TCGGGTTTCCAAGGTCGCACAC	122
	Fwd	TTCAGACTCCGCATTGGCT	
Fibronectin	Rev	AATGGGCTGGTGCAGTTTTG	119
	Fwd	TGCAGTGGCTGAAGTCGCAAGG	

Vitronectin	Rev Fwd	GGGCTCCCCGTTTGAATTGCCA TGTTGATGCAGCGTTCGCCCT	114
FAK	Rev Fwd	TCCTGGCTGGGTTGCTGCTGAA AGCACCTGGCCACCTAAGCAAC	125
Vinculin	Rev Fwd	CATTGGACCGGTCAAGGTGGCA TCAAGCTGTTGGCAGTAGCCGC	120
Paxillin	Rev Fwd	TCTCTGCTGTGGCTCCAAGCCT AGGGCCTGGAACAGAGAGTGGA	129
Osteocalcin	Rev Fwd	AGCTGCTCCCAGTTTTCCCCTG AGCAGGAGGGCAATAAGGTAGT	118
Osteonectin	Rev Fwd	TCGTCACAAGCAGGGTTAAGC ATGTCCTGGTCACCTTGTACGA	103
Osteopontin	Rev Fwd	TCCAGGCGCTTCTCATTCTCAT TGATTCTGGCAGCTCAGAGGA	110
Type I collagen	Rev Fwd	CATTCTGTGGCGCAAGGAGATT CTCCTGACGCATGGCCAAGAA	100
TGF- β 1	Rev Fwd	TCAAGCATACCTCGGGTTTCCA ACCCGCGTGCTAATGGTGGA	111
Type III collagen	Rev Fwd	GGGCACTGCTTCCCGAATGTCT CCCTGGCTCAAATGGCTCACCA	113
Cadherin 11	Rev Fwd	CCTTTCCACCAGGACTGCCGTT GGCCCAAACAGGTATCATCA	126
MAPK1	Rev Fwd	TTGGTTGTCCCTGAGAGTCC ATCCGGGCACCAACCATTGAGC	108
NFkB	Rev Fwd	GTGGTCATTGCTGAGGTGCTGTGT AACCCATCGCCTTGGCATCCAC	120
Alkaline phosphatase	Rev Fwd	AGTCGAAAAGGGCGTTGGCGT ACCCGGCTGGAGATGGACAAAT	113
Bone sialoprotein	Rev Fwd	TTCACGCCACACAAGTAGGCA ACCGGCCACGCTACTTTCTTTA	113

BMP1	Rev	GGAACATATCGCCGTCTCCATTT	
	Fwd	AGCCGCCTGTGCTGGTATGA	106
BMP4	Rev	AGACGATGGGCTCGGGGAGTTT	
	Fwd	ATCCTGGTAACCGAATGCTG	89
Runx2	Rev	CCGGTCTCAGGTATCAAAGTAGC	
	Fwd	ATCACTGACGTGCCCAGGCGTA	114
SMAD1	Rev	AGGGCCCAGTTCTGAAGCACCT	
	Fwd	ACAGCAGCTACCCCAACTCTCCT	133
SMAD2	Rev	GGGTCTTCAGGAGGCAGGTAAGCA	
	Fwd	AGATACGGCTGGCACCCCTGCAA	102
SMAD4	Rev	ACAGACTGAGCCAGAAGAGCAGCA	
	Fwd	AGCCAGGACAGCAGCAGAATGGA	128
DMP1	Rev	ATGGCCGTTTTGGTGGTGAGGC	
	Fwd	AGGACGGGTGATTTGGCTGGGT	113
Biglycan	Rev	TCACTGCTGTCCGTGTGGTCACT	
	Fwd	AACCGTATCCGCAAAGTGCCCAA	119
FGF-2	Rev	AGGCCATCAAAGGCTCCTGGTTCA	
	Fwd	TTCTTCCTGCGCATCCATCCCG	128
IGF-1	Rev	CGGTTGGCACACACTCCCTTGA	
	Fwd	GTGTGTGGACCGAGGGGCTTTT	109
MMP2	Rev	CACAGCTCCGGAAGCAAACTCA	
	Fwd	GCTGCACCATCGCCCATCATCA	115
	Rev	GGTTGCAACTCTCCTTGGGGCA	

5.2.3.2.1 Cell adhesion specific gene expression studies

Cells at a density of 1.5×10^4 suspended in 100 μ l complete medium were plated on 15 discs of each material Ti, TiZr, TiNb and tissue culture plastic (TCP) and allowed to attach for 45 min after which complete medium was added very gently to each culture without disturbing the cells. The cells were incubated in standard conditions and RNA from each culture was prepared at 4 and 24 h after initial plating using Qiagen RNA Plus kit (QIAGEN, USA) as per the

manufacturer instructions and cDNA from the RNA was made as described in the section 3.4.2 of the materials and experimental techniques (chapter 3).

5.2.3.2.2 Induction of cell differentiation

Cells were plated on 10 discs of each material and TCP at the same density as described above. For each culture the cells were allowed to reach confluence (as seen on TCP) which was generally after 4 days of initial plating. After this, cells were induced for differentiation as described in the section 3.3.3 of chapter 3. Total RNA from 10 discs was isolated at 1, 4, 10 and 15 days after adding osteogenesis inducing medium by using Qiagen RNA Plus kit (QIAGEN, USA) as per the manufacturer instructions and cDNA from the RNA was made as described in section 3.4.2 of chapter 3.

5.2.3.2.3 Total RNA isolation and cDNA synthesis

The total RNA from the cells on each material (Ti, TiZr and TiNb) from all the discs at each time point was pooled namely 4 and 24 h after adhesion (15 discs) and 1, 4, 10 and 15 days after differentiation (10 discs) using the Qiagen RNA Plus kit (QIAGEN, USA). RNA from two separate experiments was isolated for preparing cDNA following the protocol described in section 3.4.1 of chapter 3. cDNA synthesis was done for both RNA preparations as following the protocol described in section 3.4.2 of chapter and used for real time PCR experiments.

5.2.3.2.4 Real time PCR

After isolation, purification and quantification of RNA from the samples after various culturing days, the cDNA was made and the gene expression was evaluated using real-time PCR approach and the protocol was followed as described in section 3.4.3 of chapter 3. The recorded C_T values from triplicate samples in two separate experiments were then used for calculating the fold change values of each gene of each material with respect to control (TCP). The fold change values were calculated using the $2^{-\Delta\Delta CT}$ method and plotted. The entire quantitative real time PCR was done for both RNA preparations for calculating the statistical significance of data. The specificity of the reaction was also checked for each gene by running the PCR products in a 2% agarose gel.

5.3 Results

5.3.1 PCR array

As described in the materials and methods section, real time PCR was performed at two time points namely after 1 and 4 days post induction for differentiation on the three material surfaces Ti, TiZr and TiNb along with TCP serving as control. This was achieved using a PCR array with standard set of genes involved in osteogenesis. The results are described below:

All the genes involved in osteogenesis were divided into different subsets belonging to various categories as genes involved in *skeletal development*, *bone mineral metabolism*, *cell growth and differentiation*, *extracellular matrix proteins*, *cell adhesion* and *transcription factors and regulators*. Most of the subsets included genes involved in the process of differentiation and therefore, we studied the expression pattern of genes after 1 and 4 days post induction for differentiation, on each of the three materials namely Ti, TiZr and TiNb along with TCP. Notably, out of all the 84 genes present in the array, certain genes were not expressed on all the three materials with most of them being related to the hematopoietic lineage and fibroblast cell specific. The genes not expressed on the three material surfaces are given in table 5.2 after both time intervals.

Table 5.2. Genes not expressed on the materials Ti, TiZr and TiNb.

Genes not expressed		
Enam	Mmp8	Bmp6
Tuft1	Fgf1	Tnf
Bmpr1b	Bmp2	Mmp10
Sost	Bmp3	Cd36
Bmp5	Csf2	Csf3
Icam1	Gdf10	

The fold change expression of the genes on the three material surfaces Ti, TiZr and TiNb after 1 and 4 days of differentiation with respect to control (TCP) are given in table 5.3.

Table 5.3. Fold change expression of genes on the three material surfaces Ti, TiZr and TiNb after 1 and 4 days of differentiation.

Genes	Fold Change					
	1D	4D	1D	4D	1D	4D
	Ti		TiZr		TiNb	
Ahsg	0.301867	0.578414	0.16765	0.591379	0.529681	1.822081
Alpl	0.928968	1.558116	1.334294	1.445754	1.163437	1.797901
Ambn	0.426636	1.739513	0.759868	1.716898	1.168407	3.33633
Anxa5	0.759265	0.714594	0.686136	0.942254	0.895911	0.753713
Bgn	1.433764	1.269413	1.259194	1.257366	1.475146	1.165919
Bmp1	0.87313	0.765429	0.760291	1.165497	0.997977	0.946879
Bmp4	0.682133	0.879161	0.573845	1.240148	1.050783	1.025893
Bmpr1a	0.88021	0.968871	0.664683	1.150631	1.046399	0.856514
Cdh11	0.727235	0.868419	0.564722	1.063509	0.787008	0.77054
Col10a1	0.4959	0.8781	0.6085	0.4438	1.5766	0.8452
Col11a1	0.652647	0.706187	0.612674	1.187459	1.001548	0.801314
Col12a1	0.923629	1.037675	0.853411	1.156683	1.032001	0.679899
Col14a1	0.628354	1.929888	0.317279	1.642432	0.635302	4.322763
Col1a1	1.249369	2.053894	1.317374	1.75521	1.375548	2.105959
Col1a2	0.813753	1.132931	0.764685	1.587835	1.058787	1.372748
Col2a1	3.256985	5.378935	2.696096	11.28844	5.227751	9.696114
Col3a1	0.859274	0.899192	0.754261	1.133741	1.027699	0.649182
Col4a1	1.737439	1.178282	1.849387	1.032251	1.865207	0.525434
Col4a2	1.40033	1.154884	1.1248	1.068308	1.446161	0.5767
Col5a1	1.151089	1.44918	1.400295	1.391651	1.232515	1.140996
Col6a1	0.900712	1.148436	0.84691	1.30453	1.175379	0.824141
Col6a2	1.065807	1.770276	1.308155	1.422615	1.447127	1.043506
Col7a1	1.024765	0.713019	0.942709	1.003224	1.112336	0.886114
Comp	1.099392	1.27118	1.022115	1.788726	1.81537	1.503024
Ctsk	1.193122	0.604812	0.927604	0.811653	1.399113	0.665655
Dmp1	3.835115	2.111045	2.092591	1.953556	1.715201	2.104978
Egf	0.616648	0.857945	0.768919	1.555118	1.028318	1.293759
Fgf2	0.938845	1.50364	1.371907	1.251346	1.491458	0.706776
Fgf3	0.343858	0.4924	0.276797	0.6203	0.673105	1.0676
Fgfr1	0.887948	0.819274	0.809999	1.063622	0.964226	0.846462
Fgfr2	1.035471	0.849112	0.844235	1.069488	1.508891	0.746728
Flt1	0.593726	0.754664	0.54003	0.71416	0.649303	0.456818

Fn1	1.639042	1.083624	1.419742	0.791493	1.190332	0.779975
Igf1	0.717556	1.490468	0.807047	1.601854	1.3882	0.77714
Igf1r	0.870035	0.86205	0.917899	0.997913	1.073369	0.700735
Itga2	0.865458	1.169991	1.999165	1.438268	2.82273	0.815001
Itga2b	0.781593	0.752521	0.666418	0.757474	0.845006	0.484779
Itga3	1.528831	1.178154	1.072749	1.071111	1.22034	0.991399
Itgam	0.372385	0.418959	0.184363	0.654962	0.462472	1.450447
Itgav	1.128283	0.886222	0.854414	1.019487	1.073634	0.857527
Itgb1	1.053579	1.018936	0.887054	1.133726	1.164368	0.871507
Mmp2	1.066712	1.080558	0.964264	1.350596	1.363149	0.979593
Mmp9	3.591872	2.303398	3.531969	2.10461	6.776409	2.073408
Msx1	1.431885	0.7616	0.605343	0.770264	0.838757	0.561903
Nfkb1	0.788577	0.732103	0.774421	1.041855	1.013748	0.741764
Pdgfa	1.069806	0.540931	1.130946	0.636998	1.260226	0.563042
Phex	1.379892	4.571595	1.538602	5.122384	3.216296	5.080346
Runx2	1.03138	1.326111	1.357961	1.08672	1.520494	0.915709
Scarb1	1.43494	1.056035	1.014365	1.155688	1.165389	1.426129
Serpinh1	0.578466	1.165941	0.903214	1.100949	0.970962	0.988399
Smad1	0.820742	0.74156	0.856457	0.989263	1.139299	0.755726
Smad2	0.707809	0.746542	0.743215	0.970309	0.972127	0.773414
Smad3	0.987164	0.884688	0.865313	1.03988	1.10234	0.849987
Smad4	0.788236	1.161356	1.080928	1.043352	1.0904	0.827602
Sox9	0.963791	1.66287	1.939918	1.613619	1.912942	1.307114
Tfip11	0.798456	0.774462	0.698545	1.063256	0.980821	0.789364
Tgfb1	1.059231	1.64712	1.811824	1.556152	1.648737	1.227453
Tgfb2	0.586102	0.632828	0.678776	0.639921	0.641727	0.432709
Tgfb3	0.747698	1.369832	1.075804	1.283106	0.914697	1.046149
Tgfbr1	1.056268	0.785554	0.805423	0.856288	0.968394	0.757713
Tgfbr2	0.485766	1.563825	0.844878	1.195543	0.896341	1.005927
Tgfbr3	0.705815	1.791229	1.103409	0.996169	1.052458	0.854896
Twist1	0.562571	0.792834	0.487402	0.809575	0.592884	0.00013
Vcam1	0.840939	0.761501	0.635909	1.02988	1.119474	0.67525
Vdr	0.938506	1.384204	0.856741	1.824709	1.537467	1.583675
Vegfa	1.313706	0.679361	0.903758	0.762907	0.945753	0.638622
Vegfb	0.805747	1.139487	0.894027	0.958637	0.836904	0.715841

We could clearly see that, most genes were highly expressed on the TiNb surface after 1 day of differentiation compared to Ti and TiZr, whereas, their expression was reduced at day 4 and elevated levels were seen on TiZr surfaces compared to Ti and TiNb. This was the trend observed with almost all of the genes.

Furthermore, the BMP pathway and TGF- β pathway play a crucial role in regulating the osteogenesis of cells. The genes belonging to these pathways and their regulators namely BMP4, TGF- β 1 and SMAD proteins were found to have followed the trend described above, with greater expression on TiNb surface at 1 day and elevated levels on TiZr after 4 day time periods. This mixed behavior on these surfaces of the genes prompted us to verify their expression using gene specific primers.

The expression of genes on Ti, TiZr and TiNb are shown in figure 5.1, figure 5.2 and figure 5.3 respectively. Among the genes expressed, based on the general functions of all the genes, we have selected certain genes from each subset and studied their expression pattern on the materials at different time periods namely after 4 and 24 h of adhesion and 1, 4, 10 and 15 days after differentiation and have analyzed their details with respect to the effect of different surface properties namely surface energy and substrate composition differences of the materials.

5.3.2 Gene profiling using gene specific primers

The gene expression pattern using PCR array on the three material surfaces, gave us clues regarding the function of the genes involved in differentiation of osteoblast cells. We therefore, chose certain genes from each subset along with certain genes not included in the array namely osteocalcin, osteonectin, osteopontin and bone sialoprotein; and looked for their expression on the three material surfaces mainly at adhesion and differentiation stages of the cell-material interactions. Also the expression of certain genes involved at early time points of interaction with material surfaces namely genes involved in osteoblast cell adhesion such as integrins, focal adhesion proteins and extracellular matrix proteins were looked at 4 and 24 h of seeding the cells on the three material surfaces. The results of the gene profiles are described below:

Based upon the RNA expression patterns and their relative quantities as determined by the methods described above we have classified the gene expression patterns into several categories. The significant features of gene activity in each category are described below:

5.3.2.1 Expression of cell adhesion molecules and their cofactors

Integrins and its associated molecules play one of the most important roles in the interaction of cells with any substratum. We examined the expression of four integrin genes and some of their signaling partners at the indicated time points, in order to analyze their role in adhesion of osteoblasts to Ti, TiZr and TiNb alloys. The results of this analysis are summarized below:

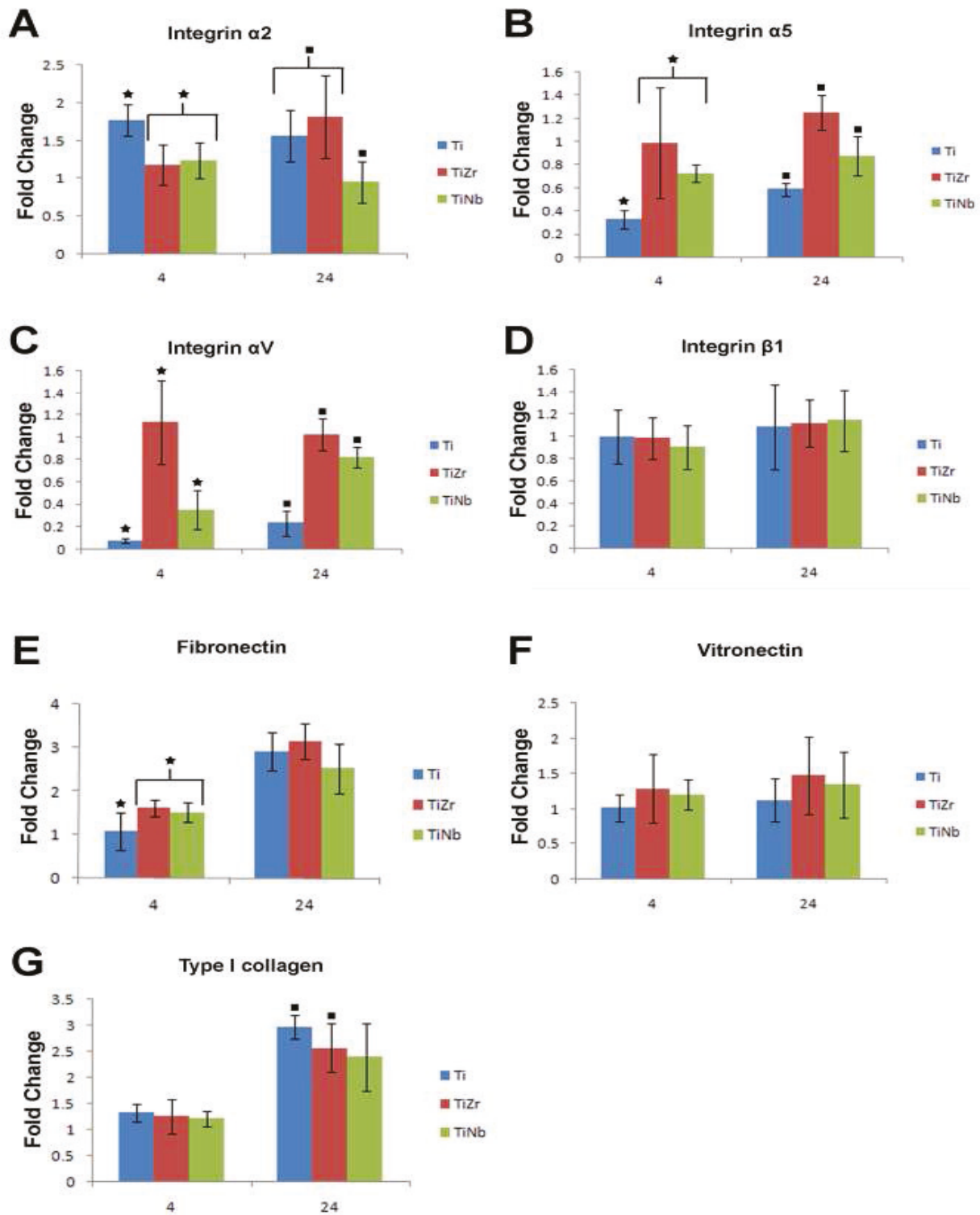


Figure 5.4. The fold expression of integrins and extracellular matrix genes on the three materials Ti, TiZr and TiNb at 4 and 24 h after adhesion. ★ ■ represents $p < 0.05$ between groups at 4 and 24 h respectively.

Integrins

We estimated the expression of integrin $\alpha 2$ (collagen specific), $\alpha 5$ (fibronectin specific), αV (vitronectin specific) and $\beta 1$ genes on Ti, TiZr and TiNb with reference to their levels on TCP at 4 and 24 h after seeding the cells (Fig. 5.4(A-D)). The expression of the integrin $\alpha 5$ and αV was higher on TiZr surface when compared to Ti and TiNb at both the time points (Fig. 5.4B and C). A gradual increase in the expression was seen on the three surfaces from 4 h to 24 h. However, the expression of integrin $\alpha 2$ was higher on Ti at the 4 h time point compared to the two alloys. At 24 h, expression of $\alpha 2$ on TiZr increased to Ti levels but that on TiNb lagged behind (Fig. 5.4A). No significant differences were seen in the expression pattern of integrin $\beta 1$ at 4 and 24 h time points on the three material surfaces (Fig. 5.4D).

Extracellular matrix (ECM) components

Osteoblasts and osteocytes secrete number of ECM proteins in their *in vivo* milieu. Fig. 5.4E and F show the expression of fibronectin and vitronectin on the materials at the two time intervals. Although fibronectin expression was higher on the TiZr and TiNb alloys when compared to Ti at 4 h time point, the difference in the expression between the materials at 24 h was not significant (Fig. 5.4E). On the contrary, no differences in the expression of type I collagen was seen on the material surfaces at 4 h time point but at 24 h a higher expression of type I collagen was seen on Ti compared to TiZr and TiNb (Fig. 5.4G). No significant difference was seen in the expression of vitronectin over the two time points on the three material surfaces (Fig. 5.4F).

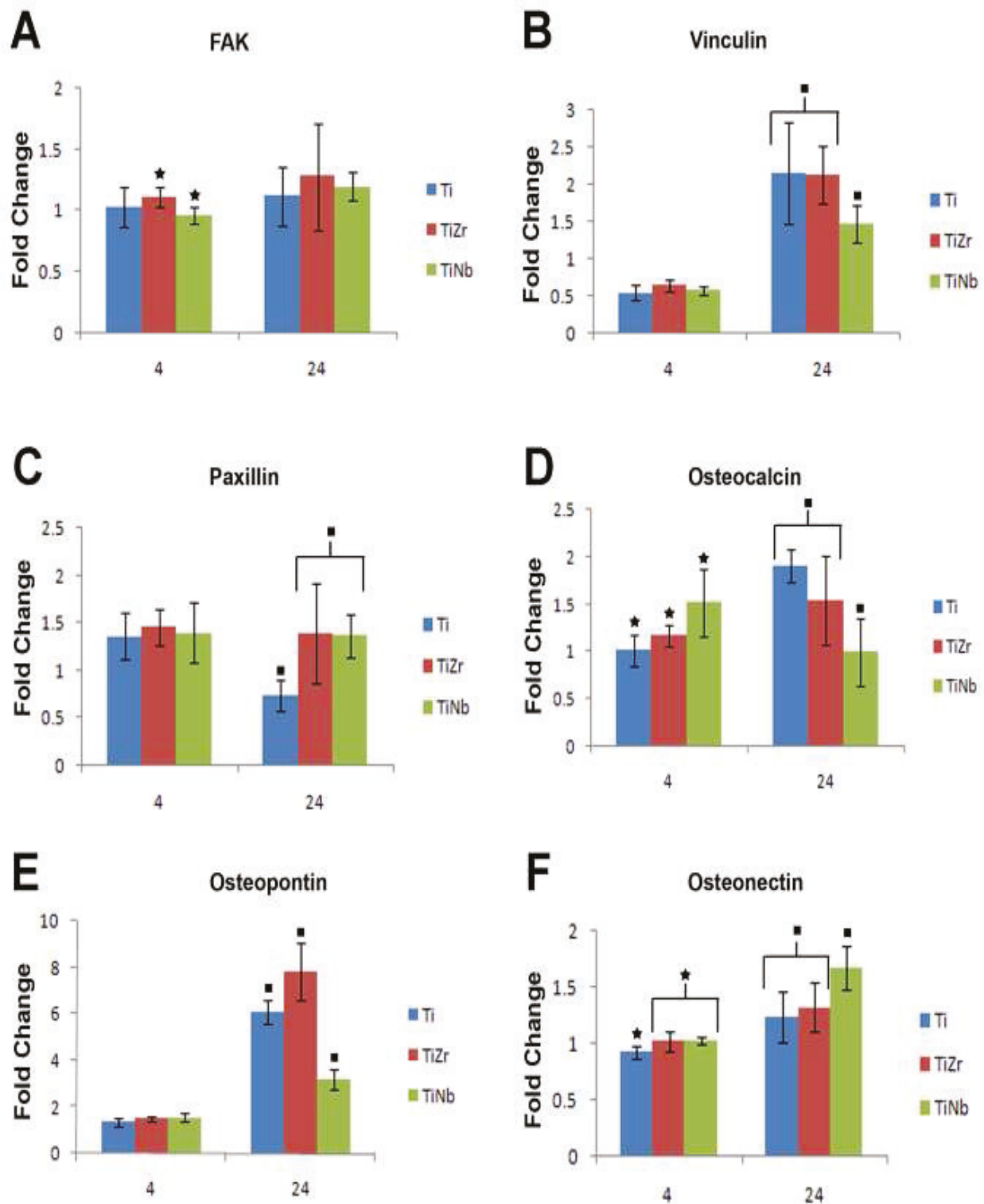


Figure 5.5. The fold expression of focal adhesion and osteoblast specific genes on the three materials Ti, TiZr and TiNb at 4 and 24 h after adhesion. ★ ■ represents $p < 0.05$ between groups at 4 and 24 h respectively.

Focal adhesion markers:

The expression of focal adhesion markers namely FAK, vinculin and paxillin were tested on the materials and are shown in Fig. 5.5 (A-C). At 4 h FAK expression was higher on TiZr and Ti compared to TiNb. However, at 24 h no differences were seen on the materials (Fig. 5.5A). Although, no differences in the expression of vinculin and paxillin were seen at the 4 h time point on the three material surfaces, at 24 h, the expression of vinculin was higher on Ti and TiZr compared to TiNb (Fig. 5.5B) while, the expression of paxillin was higher on TiZr and TiNb compared to Ti at 24 h time point (Fig. 5.5C).

Osteoblast specific markers:

The expression of osteocalcin, osteopontin and osteonectin are shown in Fig. 5.5 (D-F). Although osteocalcin expression was higher on TiNb compared to TiZr and Ti at 4 h time point, at 24 h its expression was reduced on TiNb and was higher on TiZr and Ti surfaces (Fig. 5.5D). Osteonectin expression was higher on the alloys at 4 h time point compared to Ti and at 24 h the expression was seen higher on TiNb compared to Ti and TiZr (Fig. 5.5F). No differences in the expression of osteopontin was seen on the material surfaces at 4 h time point and at 24 h, a higher expression of osteopontin was seen on TiZr compared to Ti and TiNb (Fig. 5.5E).

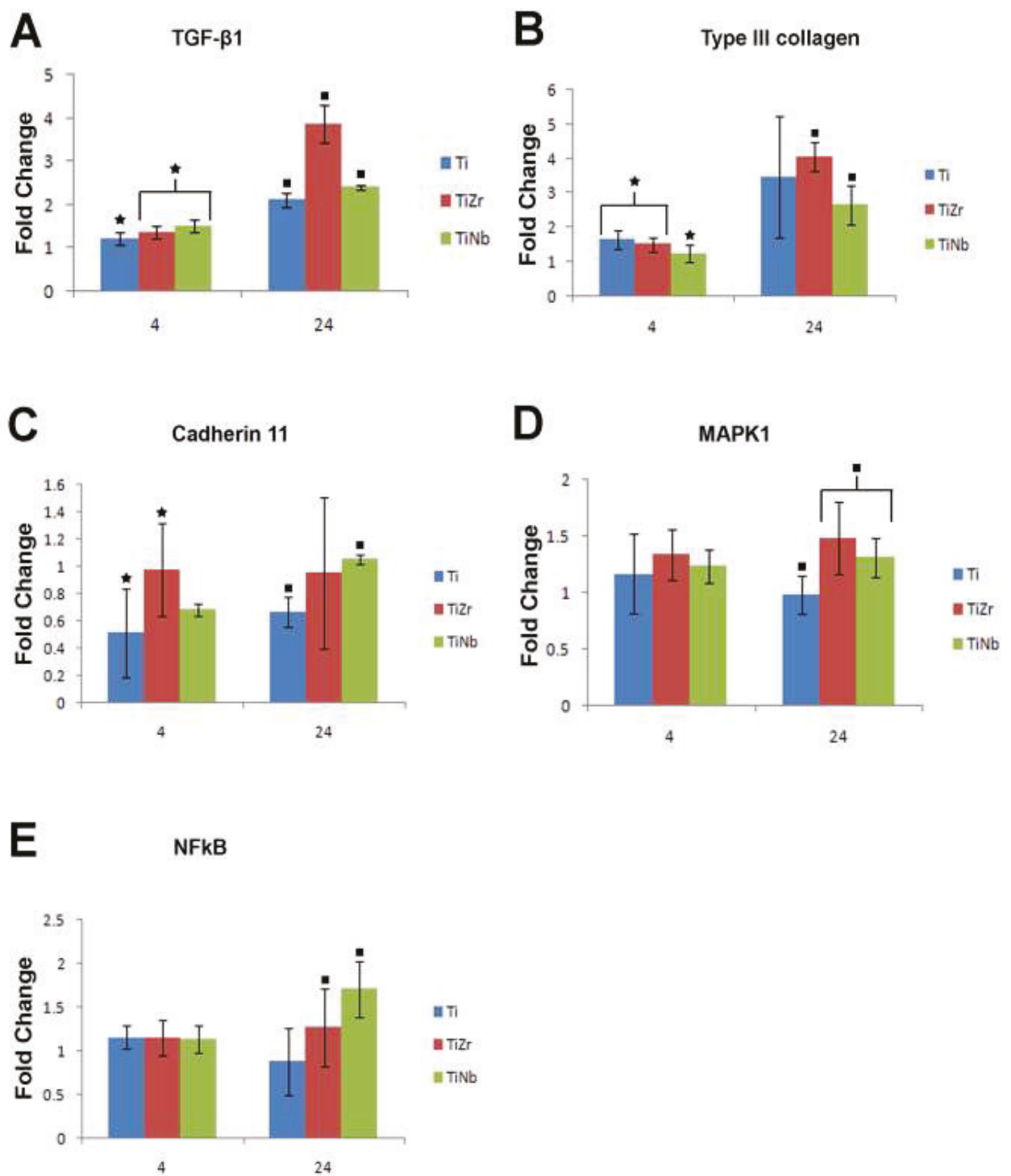


Figure 5.6. The fold expression of TGF- β 1, type III collagen, cadherin 11, MAPK1 and NF κ B genes on the three materials Ti, TiZr and TiNb at 4 and 24 h after adhesion. ★ ■ represents $p < 0.05$ between groups at 4 and 24 h respectively.

Transforming growth factor (TGF- β 1), Type III collagen, Cadherin 11:

Fig. 5.6A shows the expression of TGF- β 1 on the three material surfaces. The levels were higher on the alloys at 4 h interval however, at 24 h the expression was maximum on TiZr compared to Ti and TiNb. Type III collagen expression was higher on Ti and TiZr at 4 h time point, whereas, the expression was higher on TiZr at 24 h compared to Ti and TiNb (Fig. 5.6B). The expression of cadherin 11 was higher on TiZr at 4 h time point and higher on TiNb at 24 h time point (Fig. 5.6C).

Mitogen activated protein kinase (MAPK1) and nuclear factor kappa B (NFkB):

The expression of MAPK1 and NFkB are shown in Fig. 5.6D and Fig. 5.6E respectively. The expression levels of MAPK1 and NFkB were not different at 4 h time point, however, differences were seen at the 24 h time point with MAPK1 expression higher on TiZr compared to Ti and TiNb (Fig. 5.6D) and NFkB expression higher on TiNb compared to Ti and TiZr respectively (Fig. 5.6E).

Agarose gel electrophoresis

The specificity of the PCR reaction was tested by running the PCR products in a 2% agarose gel electrophoresis. We could clearly see the presence of only one band upon ethidium bromide staining of the gel after loading the products. We observed a single product (band) for all the adhesion genes of all the three material samples at both the time points. The PCR products of all the genes for the three samples at 4 and 24 h are shown in Fig. 5.7.

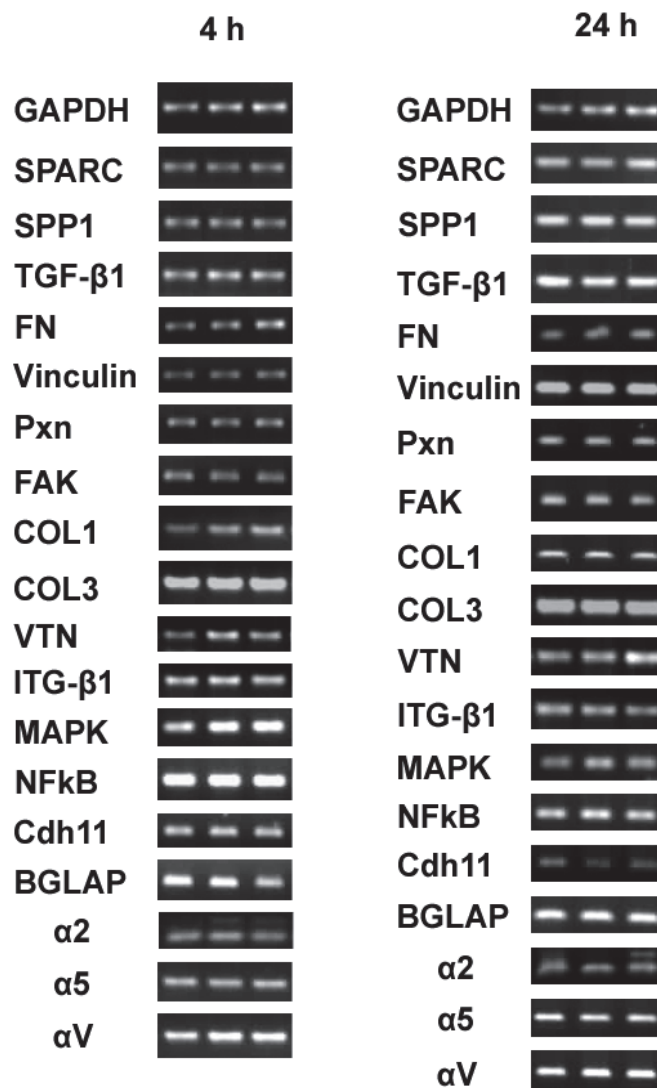


Figure 5.7. Real time PCR products of adhesion genes on the three materials Ti, TiZr and TiNb at 4h and 24 h time intervals.

5.3.2.2 Expression of cell differentiation (osteogenesis specific) markers:

In addition to the adhesion related markers, that are expressed during the initial phase of attachment to the substrates, we examined the expression pattern of genes involved in osteogenesis on the three material surfaces and TCP at four time points namely 1, 4, 10 and 15 days after induction for osteogenesis. The results of this analysis are described below:

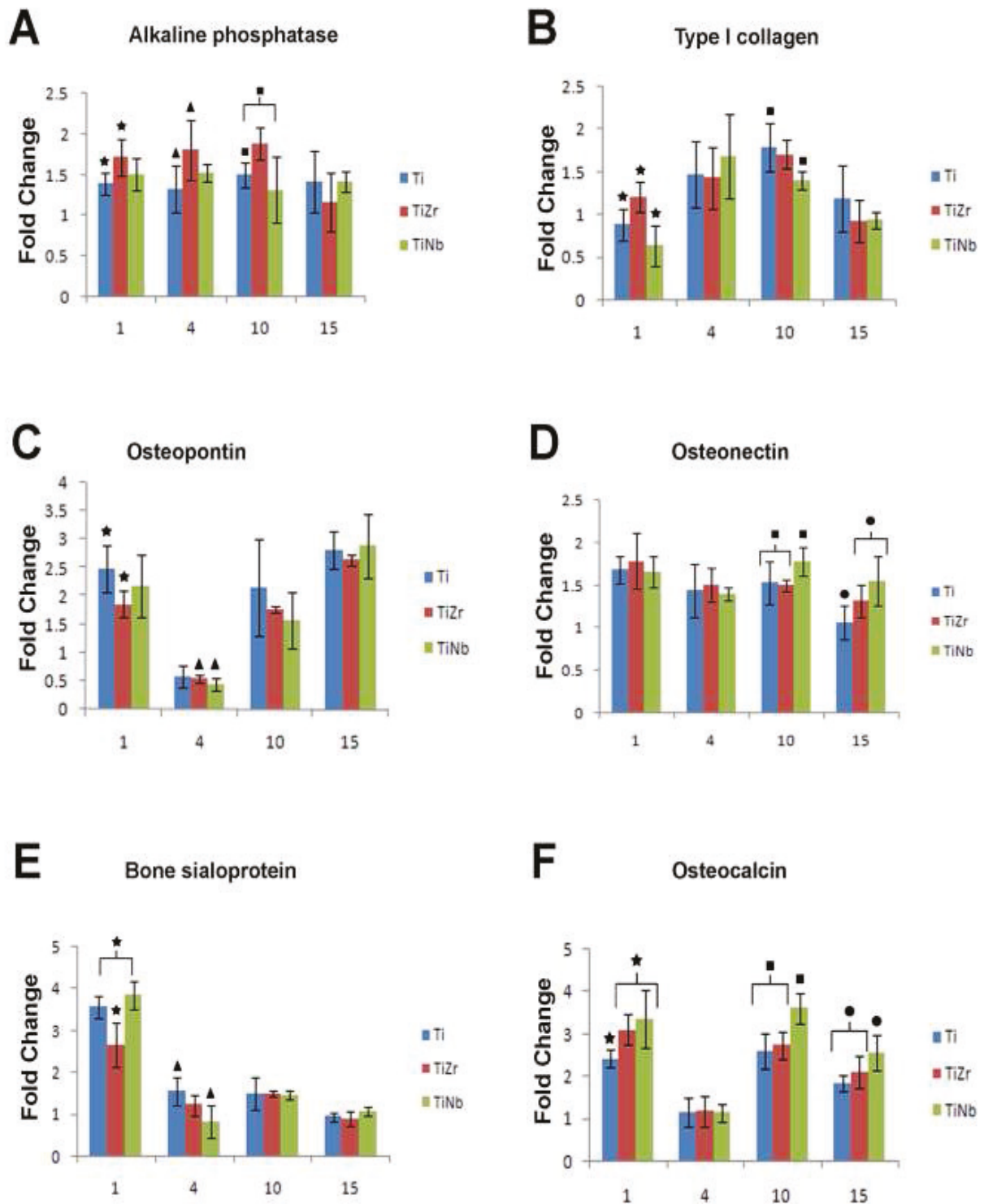


Figure 5.8. The fold expression of ALP, type I collagen, osteopontin, osteocalcin, osteonectin and bone sialoprotein genes on the three materials Ti, TiZr and TiNb at 1, 4, 10 and 15 days after differentiation. ★▲■● represents $p < 0.05$ between groups at 1, 4, 10 and 15 day time points respectively.

Alkaline phosphatase (ALP), Type I collagen:

Fig. 5.8A and 5.8B shows the expression of ALP and type I collagen on the materials at the tested time points. The expression of ALP was higher on TiZr at all the time points tested (Fig. 5.8A). However, with regard to type I collagen expression, a variable behavior was seen on the materials at the 4 time points tested (Fig. 5.8B). At 1 day, the expression was higher on TiZr and at 4 days, the expression was higher on TiNb. At 10 and 15 days, the expression was higher on Ti compared to TiZr and TiNb.

Osteopontin, osteonectin, bone sialoprotein and osteocalcin:

The expression pattern of the above mentioned osteogenesis specific markers at different time points are shown in Fig. 5.8(C-F) respectively. As can be seen their expression levels were variable, osteopontin expression was higher on Ti compared to TiZr and TiNb (Fig. 5.8C) at all time points but osteonectin expression was higher on TiZr at day 1 and 4 and on TiNb at days 10 and 15 post induction (Fig. 5.8D). TiNb showed higher expression of osteocalcin on day 10 and 15 (Fig. 5.8F) and bone sialoprotein on day 1 in comparison to Ti and TiZr (Fig. 5.8E).

TGF- β 1 and bone morphogenetic protein (BMPs):

Fig. 5.9A shows the expression of TGF- β 1 on the materials. The expression was higher on TiNb compared to Ti and TiZr at the time points tested with significant levels at 10 and 15 days. The expression of BMP1 was significantly higher on Ti at day 1. However, no differences were seen at day 4 on the materials. A higher expression was seen on TiNb and TiZr at 10 and 15 days compared to Ti (Fig. 5.9B). No differences in the expression levels of BMP4 were seen on the materials at the time points tested (Fig. 5.9C).

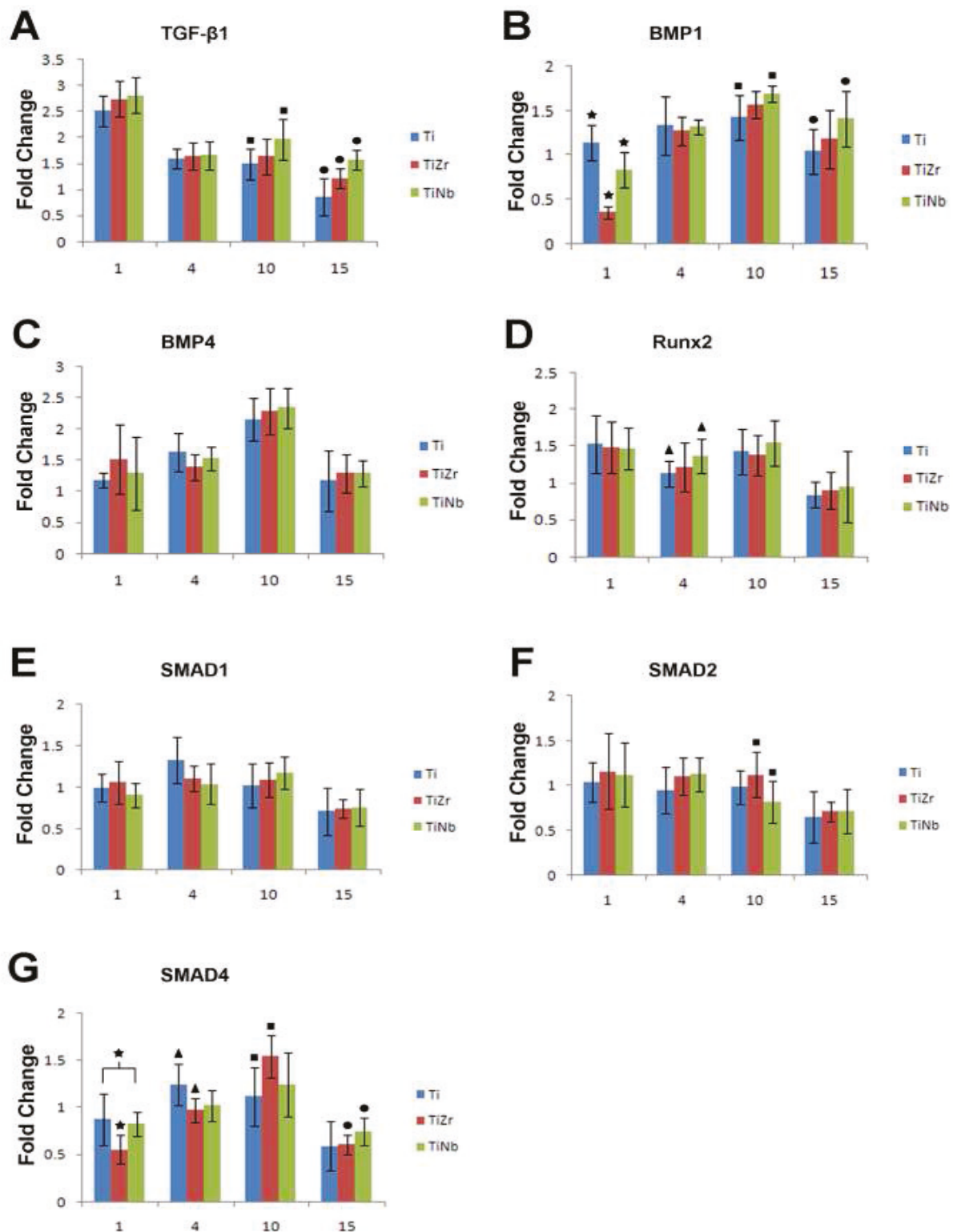


Figure 5.9. The fold expression of TGF-β1, BMPs, Runx2 and SMADs genes on the materials Ti, TiZr and TiNb at 1, 4, 10 and 15 days after differentiation. ★▲■● represents $p < 0.05$ between groups at 1, 4, 10 and 15 day time points respectively.

Runx2, SMAD's:

The activity of TGF β and BMP signaling is often manifested by the transcription factors Runx2 and Smads. Runx2 expression was similar between the materials at all the time points tested, except for day 4, where the expression was seen higher on TiNb and TiZr compared to Ti (Fig. 5.9D). As regards the expression of Smads (SMAD1, SMAD2 and SMAD4) no significant difference in the expression of SMAD1 was seen on the materials at the time points tested (Fig. 5.9E). SMAD2 also showed similar levels of expression except for day 4 where the expression levels were higher on TiZr, compared to Ti and TiNb (Fig. 5.9F). An inconsistent behavior in the expression of SMAD4 was seen on the materials with the level of expression higher on Ti at days 1 and 4 and higher on TiZr at day 10. However, at day 15, the expression was higher on TiNb (Fig. 5.9G).

Bone mineralizing markers: Dentin matrix protein (DMP1), Biglycan (Bgn):

Fig. 5.10(A-B) shows the gene expression behavior on the materials of the bone mineralizing markers. DMP1 shows no expression differences except at day 4 with a higher expression on TiZr and TiNb compared to Ti (Fig. 5.10A). Biglycan showed significant differences in the expression levels at days 4, 10 and 15. Higher expression was seen on TiZr at 4 days, with equal expression on the alloys compared to Ti at 10 days and higher expression on TiNb at 15 days compared to Ti and TiZr (Fig. 5.10B).

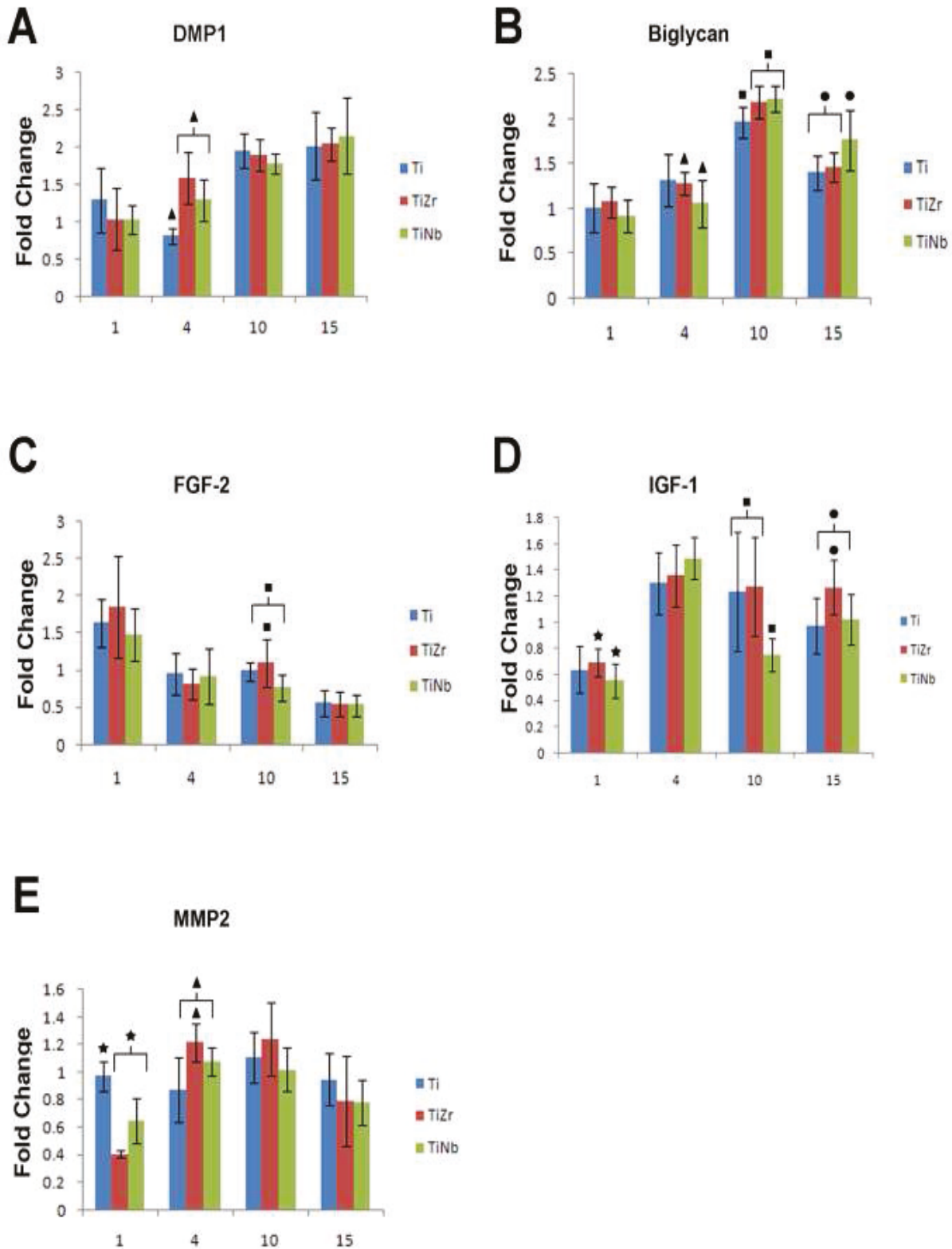


Figure 5.10. The fold expression of DMP1, Biglycan, FGF-2, IGF-1 and MMP2 genes on the three materials Ti, TiZr and TiNb at 1, 4, 10 and 15 days after differentiation. ★▲■● represents $p < 0.05$ between groups at 1, 4, 10 and 15 day time points respectively.

Fibroblast growth factor (FGF-2), Insulin growth factor (IGF-1), Matrix metalloproteinase (MMP2):

No significant difference in the expression of FGF-2 was seen between the materials at 1, 4 and 15 days but with higher expression on TiZr at 10 day interval (Fig. 5.10C). The expression level of IGF-1 was seen to be higher on TiZr at 1, 10 and 15 days with no difference seen at 4 day interval (Fig. 5.10D). The expression level of MMP2 was higher on Ti at day 1 and significantly higher on TiZr at 4 day interval (Fig. 5.10E). At 10 and 15 days, no significant differences were seen on the materials.

Agarose gel electrophoresis

The specificity of the PCR reaction for each gene was tested by loading the products after real time PCR reaction on a 2% agarose gel. We could clearly see a single product formed as observed by the presence of a single band upon ethidium bromide staining after loading the products. The products of each gene for all the three materials at the four time points namely 1, 4, 10 and 15 day intervals are shown in Fig. 5.11.

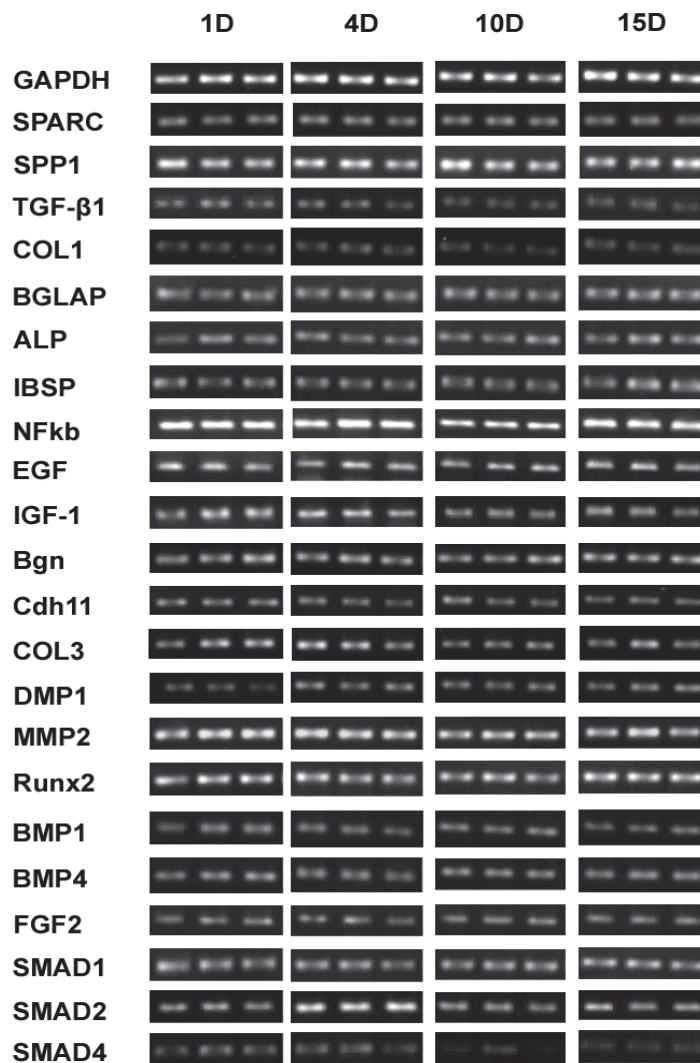


Figure 5.11. Real time PCR products of differentiation genes on the three materials Ti, TiZr and TiNb after 1, 4 10 and 15 days of differentiation.

5.4 Discussion

The initial interactions of osteoblasts with the material surface of an implant are important because they determine the functional outcome of the implant and its long term efficacy. Therefore the surface properties of an implant material play a pivotal role in regulating the behavior of osteoblast cells and it needs to be better understood in order to develop ideal biomaterials that would speed up the processes of osseointegration and osseointegration. With this view, we examined the expression patterns of the genes involved in adhesion and differentiation on the surfaces of Ti, TiZr and TiNb taking into consideration the differences in the surface properties of these materials.

5.4.1 Role of integrins and ECM molecules

Integrins are the α - β chain containing transmembrane receptors, of specific ECM components, and are known to transmit signals intracellularly to reorganize the cytoskeleton and other signaling machineries. Our results show that these integrins are differentially regulated during the initial interaction of osteoblasts with metal surfaces. As is shown in Fig. 5.4(A-C), $\alpha 2$, $\alpha 5$ and αV integrins were upregulated on the TiZr surface compared to Ti and TiNb at 4 and 24 h after plating the cells, suggesting that the higher surface energy of TiZr could induce the expression of the integrin genes in this regard. Furthermore, the corresponding increase in the expression of fibronectin and vitronectin genes ECM molecules to which $\alpha 5$ and αV integrins respectively bind) at the same time points on the same surface further strengthens our contention that integrins and their ECM ligands play a significant role in the adhesion of cells to Ti alloy surfaces. The general involvement of surface energy in the osteoblast cell adhesion was already shown by us and others earlier [53, 238, 246, 247, 249, 302]. Anselme et al. [177] had shown the involvement of various adhesion molecules in the process of osteoblast cell adhesion onto the surfaces; and Lai et al. [246] and Lim et al. [238] have demonstrated that cell adhesion on materials with high surface energy was better than the counterparts and our observations are in agreement with these studies.

5.4.2 Cytoskeletal organization

In our earlier study we have shown that MC3T3 cells not only attached better on TiZr surfaces but they also spread better on TiZr and demonstrated a more extensive network of actin stress fibers and presence of vinculin in focal adhesions [302]. Supporting these findings, in the present study we found significant differences in the expression of vinculin, FAK and paxillin genes that was seen on the TiZr and TiNb alloys as compared to Ti at 4 and 24 h time intervals. The higher expression of FAK on TiZr at 4 h time point compared to Ti and TiNb could be responsible for the better localization of vinculin in focal adhesions on TiZr. A similar increase in paxillin expression was seen at 24 h time point, although at 4 h interval no significant differences could be seen between the materials. Our results were well supported by Lai et al. [246] where the FAK expression was upregulated on the material with high surface energy.

Overall, it was seen that on the material with a higher surface energy, the genes involved in adhesion were highly expressed, which indicates that the initial adhesion is governed by the expression of these cell adhesion genes.. This further confirms the role of surface energy in accelerating the adhesion of cells onto material surfaces.

5.4.3 Cell differentiation genes

The second phase of cell-material interactions involves the process of proliferation and differentiation and the initial dynamics of cell adhesion induced signaling can significantly determine the initiation and progression of cell proliferation and differentiation in the cells. A number of surface properties of materials are known to influence the differentiation of cells and this includes the material surface roughness, topography and more significantly surface chemical composition. The involvement of surface roughness [39, 41, 46, 238, 246, 247] and surface topography [38, 48-51, 53, 272] in influencing the cell differentiation of osteoblasts has clearly been demonstrated and in addition to this, surface chemistry and wettability of the surface have also been shown to play a role in regulating the behavior of osteoblast cells [27, 52, 245, 247, 303].

The differentiation of osteoblast cells is further determined by ECM proteins and their mineralization. The major ECM proteins of osteoblasts include osteopontin, osteonectin, bone

sialoprotein and osteocalcin, which make up about 20% of its total content, the remaining 80% is made up of type I collagen. In the terminal steps of osteocyte differentiation a number of genes play a role in the mineralization of the ECM, these include biglycan and dentin matrix protein [124, 304-306]. The BMP pathway also plays a significant role in this process [307, 308]. In addition to these molecules, growth factors like TGF- β 1 and insulin like growth factor (IGF-1) in collaboration with integrins, control osteoblast growth and development as well as ECM remodeling and repair [309-311].

Keeping the above facts in consideration, we studied the expression of some of the genes in the above categories at 4 different time points after inducing MC3T3 cells into osteogenic differentiation as described in the results. In addition to these specific genes, expression of a general indicator of osteogenic differentiation alkaline phosphatase (ALP) gene was also examined. ALP expression was significantly higher on the TiZr surface followed by the TiNb surface compared to Ti at all the time intervals tested. Although the increase was not seen as a function of time, but the levels of ALP expression were higher on the TiZr and TiNb surfaces as compared to Ti, thereby indicating that the alloyed surfaces were superior to unalloyed Ti for osteogenesis.

Among the ECM genes studied, expression of type I collagen increased as a function of time on all material surfaces up to 10 days, but at day 15 it decreased (Although no significant difference was seen between the materials) (Fig. 5.8B). The expression of osteocalcin, osteopontin, bone sialoprotein and osteonectin was higher on both alloyed (TiNb and TiZr) surfaces as compared to pure Ti. Genes involved in matrix mineralization, i.e. DMP1 and Bgn were also comparatively higher on the alloys compared to pure Ti, although not much of difference could be noticed between the alloys. Although the expression of TGF- β 1 was higher on the alloys we did not observe any significant differences in the expression of SMADs genes (SMAD1 and SMAD2) although SMAD4 showed significant differences in the expression on the materials at the tested time points.

5.4.4 Suitable properties of Ti versus Ti alloys for orthopedic applications

Substrate composition, roughness and surface energy are some of the important properties of biocompatible materials that can, individually or synergistically, influence the response of cells

towards material surfaces. Substrate composition alone can also influence some of the cell behavior, e.g. differentiation of cells. In this study, we observed better expression of bone differentiation specific genes on the TiNb surface compared to Ti and TiZr. Although the differences in surface roughness between the materials were in the sub-micron range ($<0.5\ \mu\text{m}$) we could see significant differences in the gene expression profile of most genes at varied time intervals. Lincks et al. have [41] observed similar results with regard to the substrate composition difference where Ti-6Al-4V alloy scored better, compared to Ti even though the surface roughness were in the same range. Furthermore, another study by Shapira et al. [312] also showed similar results where replacement of one element of the alloy namely Nb with V in the alloy composition significantly effected the response of cells in directing differentiation. These results are in agreement with our results and the combined studies prove a point for the influence of the substrate composition in regulating the osteoblast differentiation. Furthermore, various studies show the effect of zirconia in promoting osteoblast cell response [49, 268, 313, 314]. Together, the addition of Zr and Nb to Ti has a profound influence on the response of osteoblast cells and effects the cell behavior towards the material surfaces.

In addition to the composition of the materials our study has shown that the total surface energy of implant materials is also a dominant factor in determining the initial interactions of cells with the materials thereby accelerating the attachment and adhesion of cells, although the possible role of substrate composition in determining the differentiation of cells on materials surfaces cannot be ignored as the expression of genes involved in osteogenesis were higher on the TiZr and TiNb compared to Ti. Addition of Zr and Nb as alloying elements to Ti highlights the role of surface composition and its influence on the behavior of osteoblast cells especially at the differentiation stage of cell- material interactions. The cells differentiate on all the materials, but the rate is slightly better on the TiNb and TiZr surfaces compared to Ti, which is significant in the early osseointegration of implant materials thereby speeding the bone tissue formation at the site of injury.

5.5 Conclusions

In this chapter, the molecular responses of osteoblast cells on the surfaces of the three materials Ti, TiZr and TiNb were evaluated. This was achieved by studying the gene expression profiles of candidate genes involved in adhesion and differentiation after various time periods of seeding the cells and during the process of differentiation. The results were interpreted with regard to the differences in the surface properties of the materials. The following conclusions can be drawn from this chapter:

- Gene profiles using PCR array showed the expression of only those genes specific to bone tissue on all the three material surfaces namely Ti, TiZr and TiNb, 1 and 4 days after inducing for differentiation.
- With regard to the gene expression on the three materials, the expression levels of the genes involved in differentiation (fold change) were higher on day 4 compared to the expression on day 1.
- Initially (day 1) the expression levels on TiNb were higher compared to Ti and TiZr however, after 4 days, the levels were elevated on TiZr.
- Integrin mediated cell signaling plays an important role during the initial interactions of osteoblast cell with the material surfaces. This was strengthened by the observations that the expressions of integrins $\alpha 2$, $\alpha 5$, αV were upregulated on the TiZr surface (with a higher surface energy) compared to Ti and TiNb during the initial time period of cell attachment on the surfaces at 4h and 24 h. The corresponding increase in the expression of fibronectin and vitronectin genes ECM molecules to which $\alpha 5$ and αV integrins respectively bind) at the same time points on the same surface supports the claim that integrins and their ECM ligands play a significant role in the adhesion of cells to Ti alloy surfaces.
- The higher level of gene expression during differentiation on TiZr and TiNb surfaces compared to those on Ti, at the different time periods tested, indicates the role of the substrate composition of materials on the osteoblast cell behavior.

- On the whole, the differentiation process was better on the alloys which supported the claim and further strengthened the effect of substrate composition on osteoblast cell behavior.

Having looked at the cellular and molecular responses of osteoblast cells on the material surfaces of Ti, TiZr and TiNb, we could conclude that, it is indeed the surface energy that has an edge and holds an upper hand over surface roughness in accelerating the attachment of cells thereby facilitating greater adhesion on to these surfaces. Moreover, in our study, since the roughness values of the materials were in the sub-micron range, the differences in surface energy become a crucial factor in effecting the cell behavior at early stages of cell-material interactions. Apart from surface roughness and surface energy, the other surface property that effects the cell response towards materials is the substrate composition. In our study, TiNb surface was better with regard to the molecular response of osteoblast cells in terms of differentiation processes when compared to TiZr and Ti suggesting that alloy material was superior than pure Ti for the differentiation process. Overall, the surface energy of the materials seems to play a crucial role in the initial response of adhesion and proliferation of the osteoblast cells while, the surface composition was important in determining the differentiation process. Since the initial adhesion and proliferation was more crucial, we chose TiZr over TiNb for further studies.

Also, in our study, though the percentage of cell adhesion on the materials especially on TiZr was minimum this was enough and adequate to accelerate the attachment of cells and trigger the processes of proliferation and differentiation. Hence, we wanted to explore the possibility of enhancing and improving the biological performance of the materials by changing the surface texture. To achieve this, the surface of TiZr was subjected to anodization and explored the response of osteoblast cells to these surfaces which form the basis for chapter 6.

6. Cell biological responses of osteoblasts on anodized nanotubular surface of a titanium-zirconium (TiZr) alloy

6.1 Introduction

Osseointegration of implant materials is necessary for their successful application in bone tissue engineering [175]. In the previous chapters, we have shown that Ti alloys were more suitable for adhesion, proliferation and differentiation of osteoblasts compared to Ti. Several reports on the comparative analysis of Ti and Ti based derivatives also suggest that TiZr alloys are strong candidates and suitable as bone implant materials [168, 169, 172, 302]. However, these require further improvements in the surface properties in order to enhance the formation of new bone tissue in the peri-implant region and to accelerate the process of osseointegration [18, 19, 25]. In our study, of the two Ti alloys namely TiZr and TiNb that were used though both supported differentiation, TiNb supported differentiation slightly better than TiZr. However, TiZr supported better adhesion and proliferation owing to its higher surface energy. Hence, we wanted to further improve upon the surface properties of this particular alloy since the initial stages of attachment are crucial for the longevity of an implant.

Many strategies for surface modification and rendering the alloy surfaces improved bioactive are being developed [88, 89, 315-318]. These approaches also give us the opportunity to better analyze the molecular responses of cells towards material surfaces and to do basic studies on how specific surface modifications of osteogenic biomaterials effect signaling pathways that regulate adhesion, proliferation and differentiation of osteoblasts [41-44, 48, 253].

Since surface properties of biomaterials are interdependent, it is difficult to pinpoint the role of one particular surface property that is responsible for a specific response of osteoblast cells. The comparative analysis of *in vitro* cellular responses towards micro-roughened and nano-structured surfaces is a useful experimental approach to identify factors that influence cell behavior during initial stages after cells make contact with the material surfaces. In the natural environment also, especially in the bone, the resident cells encounter and respond to a biochemical milieu that is generated by hydroxyapatite crystals embedded in the nanofibrillar assembly of type I collagen fibrils at the nanometric scale [93]. Nano-structured surfaces present a useful interface in understanding the biology of cells in comparison to the micro-rough surfaces [63-66, 69-72]. Several studies have shown the importance of nano-structured surfaces in improving the bioactivity and osteoconductivity of the material surfaces in general [30, 73-76] and response of osteoblast cells to nanofibres, nanorods, nanogrooves, nanopits and nanotubes has also been reported [71, 74, 77-84]. Therefore it becomes necessary to understand the osteoblasts response to nano-structured implant materials. Earlier studies have shown the improved response of osteoblasts to both topographically modified and rougher surfaces in comparison to only polished surface [64, 94, 95].

Anodization is a powerful technique that can produce surfaces with improved oxide layer thickness and form nanoscale structures such as nanoparticles and nanotubes [63, 64, 81, 85, 86, 88-90]. The cell biological consequences of these nanoscale features of titanium are well documented [63, 64, 71, 72, 79, 81, 82, 87, 91, 92]. Furthermore, osteoblast cell response to the changes in the surface features of Ti, at the sub-micron and micron scale, have been reported [54, 319-321] and one study by Zhao et al [27] reported the synergistic effect and requirement of both sub-micron and micron size features on the surfaces for better cell response. We wanted to explore the possibility of synergistic effect of various surface properties in achieving a better cell response on metallic implant surfaces and therefore chose two surfaces: one, acid etched surface and two, anodized surface which was electrochemically treated after undergoing acid etching to produce nanotubes with nanoscale surface roughness.

In this study, we successfully generated nanotubular features on the surface of a TiZr alloy using anodization under controlled conditions and studied the expression of genes related to adhesion and differentiation in cells plated on these surfaces. We also determined the cell morphology,

proliferation and differentiation in MC3T3 osteoblast cells that were kept in contact with these surfaces for various time periods. The results were compared with polished and acid etched surfaces to better understand the interactions at the cell-material interface.

6.2 Materials and methods

6.2.1 Substrate preparation

TiZr alloy discs of $\Phi 15 \times 1$ mm in dimensions were used in the study prepared as described in section 3.1 of chapter 3. Three sets of materials were prepared for the study. The as-prepared materials were polished using a 240 grit SiC paper (polished) so as to maintain uniformity. Second set consisted of an acid etched surface which was etched in a 2:3 (vol/vol) ratio of HF and HNO_3 for 5 min. The third set of materials was anodized in a 0.5 vol% HF at a constant voltage of 20V for 20 min. The cathode consisted of a Pt mesh and the substrate was used as the anode. The anode and cathode were suspended using a Pt wire connected to a 30V/3mA power supply. The materials were ultrasonically cleaned for 20 min in a series of distilled water, acetone, ethanol, distilled water and sterilized in an autoclave at 121 °C for 5 min for cell culture experiments.

6.2.2 Surface characterization

The surfaces of the materials were characterized for the morphology, roughness, topography, relative surface area and hydrophilicity using scanning electron microscope (SEM), atomic force microscope (AFM) and contact angle goniometer, respectively. The morphology of the material surfaces was observed using SEM at an accelerated voltage of 5 kV (3400N Hitachi, Japan). AFM was used to capture and calculate the topography, roughness and relative surface area of the materials respectively. The average of three roughness readings on three samples of each material type was measured and recorded. The contact angle measurements were performed using a contact angle goniometer (Kruss, GmbH, Germany). A water drop of 10 μl was added and the average of three readings on three samples of each material type was recorded.

6.2.3 Cell culture

Cells were maintained as described in section 3.3.1 of chapter 3 and used for the experiments.

6.2.4 Cell adhesion, morphology and spreading

Cell morphology and cell spreading after 24 h of seeding cells on the material surfaces were observed using SEM and actin immunofluorescence respectively and were performed following the protocol described in section 3.2.1 of chapter 3. The protocol for actin immunofluorescence is slightly modified and described below. Similarly, the quantitative assessment of cell adhesion was done using MTT assay after 4 h of cell seeding on the materials as described in section 3.3.2 of chapter 3 and average values of three separate experiments were recorded.

6.2.5 Cytoskeletal organization (actin immunofluorescence)

The spreading of the adherent cells after 24 h plating on the materials was assessed by the actin immunofluorescence. Cells at a density of 2.5×10^3 per disc were seeded on the three materials and allowed to attach and spread for 24 h. The cells were fixed in 3% formaldehyde for 30 min after which the cells were permeabilized for 5 min in 0.1% Triton-X-100 (Sigma Chemical, USA). Blocking was done with 1% BSA (Bovine Serum Albumin, Sigma, USA). Rhodamine phalloidin at 1:200 (Invitrogen, USA) was added and allowed to incubate in dark for 1 h for staining actin. The materials were inverted on vectashield mounting medium (Vector laboratories, CA) containing anti-fade and imaged using a confocal laser-scanning microscope (Zeiss, Germany).

6.2.6 Cell proliferation

Cells at a density of 2.5×10^3 per disc were seeded in triplicate and were cultured for different time periods of 1, 2, and 3 days, respectively. At the end of the specified time periods, MTT assay was done to calculate the number of viable cells on each material. The values were represented as the average of triplicate samples of each material from three separate experiments.

6.2.7 Cell differentiation

Cells at a density of 20×10^3 were seeded on the materials and were allowed to adhere and spread for 45 min after which complete medium was added till the substrates were immersed in the medium. After the cells reached confluency (typically as seen on TCP) cells were induced for differentiation as described in section 3.3.3 in chapter 3. After 1, 4 and 10 days post induction,

the differentiation of osteoblast cells on the three materials was evaluated using quantitative real-time PCR analysis of genes involved in osteogenesis. Furthermore, osteocalcin immunostaining was performed on the materials 2, 4, 7, 10, 15 and 21 days post induction to observe the deposition of osteocalcin in the cells and in the matrix. Also, ECM formation by the cells on the materials was observed using SEM at 2, 4, 7, 10, 15 and 21 days after differentiation.

6.2.7.1. Quantitative real time PCR

The gene expression profiles of cells on the materials was seen at 4 and 24 h after seeding the cells (adhesion) followed by 1, 4 and 10 days post induction for differentiation using quantitative real-time PCR approach. The protocols for isolation and purification of RNA, cDNA synthesis and RT-PCR were followed as described in section 3.4 of chapter 3. The primers sequences of the genes tested are given in table 6.1. Average C_T values were used obtained from triplicates of two separate experiments for calculating the fold change expression with respect to TCP (Tissue culture polystyrene) surface with endogenous control GAPDH using $2^{-\Delta\Delta C_T}$ method.

Table 6.1. Forward and reverse primers of genes used for RT-PCR experiments.

Gene	Primers (5'-3')		Product length (bp)
GAPDH	Fwd	AGCGAGACCCCACTAACATCA	118
Integrin $\alpha 2$	Rev	CTTTTGGCTCCACCCTTCAAGT	119
	Fwd	AAGTGCCCTGTGGACCTACCCA	
Integrin $\alpha 5$	Rev	TGGTGAGGGTCAATCCCAGGCT	111
	Fwd	ACCACCTGCAGAAACGAGAGGC	
Integrin αV	Rev	TGGCCCAAACTCACAGCGCA	121
	Fwd	TCCCACCGCAGGCTGACTTCAT	
Integrin $\beta 1$	Rev	TCGGGTTTCCAAGGTCGCACAC	122
	Fwd	TTCAGACTTCCGCATTGGCT	
Fibronectin	Rev	AATGGGCTGGTGCAGTTTTG	119
	Fwd	TGCAGTGGCTGAAGTCGCAAGG	
Vitronectin	Rev	GGGCTCCCCGTTTGAATTGCCA	114
	Fwd	TGTTGATGCAGCGTTCGCCCT	

FAK	Rev Fwd	TCCTGGCTGGGTTGCTGCTGAA AGCACCTGGCCACCTAAGCAAC	125
Vinculin	Rev Fwd	CATTGGACCGGTCAAGGTGGCA TCAAGCTGTTGGCAGTAGCCGC	120
Paxillin	Rev Fwd	TCTCTGCTGTGGCTCCAAGCCT AGGGCCTGGAACAGAGAGTGGA	129
Osteocalcin	Rev Fwd	AGCTGCTCCCAGTTTTCCCCTG AGCAGGAGGGCAATAAGGTAGT	118
Osteonectin	Rev Fwd	TCGTCACAAGCAGGGTTAAGC ATGTCCTGGTCACCTTGTACGA	103
Osteopontin	Rev Fwd	TCCAGGCGCTTCTCATTCTCAT TGATTCTGGCAGCTCAGAGGA	110
Type I collagen	Rev Fwd	CATTCTGTGGCGCAAGGAGATT CTCCTGACGCATGGCCAAGAA	100
TGF- β 1	Rev Fwd	TCAAGCATACTCGGGTTTCCA ACCCGCGTGCTAATGGTGGA	111
Type III collagen	Rev Fwd	GGGCACTGCTTCCCGAATGTCT CCCTGGCTCAAATGGCTCACCA	113
Alkaline phosphatase	Rev Fwd	CCTTTCCACCAGGACTGCCGTT ACCCGGCTGGAGATGGACAAAT	113
Bone sialoprotein	Rev Fwd	TTCACGCCACACAAGTAGGCA ACCGGCCACGCTACTTTCTTTA	113
BMP1	Rev Fwd	GGA ACTATCGCCGTCTCCATTT AGCCGCTGTGCTGGTATGA	106
BMP4	Rev Fwd	AGACGATGGGCTCGGGGAGTTT ATTCTGGTAACCGAATGCTG	89
Runx2	Rev Fwd	CCGGTCTCAGGTATCAAAGTAGC ATCACTGACGTGCCAGGCGTA	114
DMP1	Rev Fwd	AGGGCCCAGTTCTGAAGCACCT AGGACGGGTGATTTGGCTGGGT	113
Biglycan	Rev Fwd	TCACTGCTGTCCGTGTGGTCACT AACCGTATCCGCAAAGTGCCCAA	119

FGF-2	Rev	AGGCCATCAAAGGCTCCTGGTTCA	128
	Fwd	TTCTTCCTGCGCATCCATCCCG	
IGF-1	Rev	CGGTTGGCACACACTCCCTTGA	109
	Fwd	GTGTGTGGACCGAGGGGCTTTT	
	Rev	CACAGCTCCGGAAGCAACTCA	

6.2.7.2. Osteocalcin immunostaining

Osteocalcin immunostaining after the prescribed time periods was performed following the procedure described in section 3.3.3.2 of chapter 3.

6.2.7.3. Extracellular matrix analysis

The formation of ECM by the cells on the different substrates at the prescribed time periods was observed using a SEM (Jeol 3400 Japan) at 5kV and at different magnifications and the procedure described in section 3.2.1 of chapter 3 was followed.

6.2.8 Matrix mineralization

Alizarin red staining was done on the materials after 7, 15, 21 and 28 days following differentiation for staining calcium nodules to evaluate the mineralization of the extracellular matrix. The detailed protocol was followed as described in section 3.3.3.3 of chapter 3.

6.3 Results

6.3.1 Material surface characterization

Surface properties of the three types of modifications of TiZr used in our study, viz. polished, acid etched and anodized, were analyzed by three different methods and the same have been described below:

Morphologies observed using SEM

Fig. 6.1A shows the morphology of the polished surface with parallel grooves all over the surface due to grinding of the surface with no significant structural deviation. Fig. 6.1B and 6.1C show the morphology of the acid etched and anodized surfaces, respectively. The polished surface after acid etching resulted in a rough surface with uneven morphology exhibiting formation of numerous micro pits all over the surface. A similar morphology is seen on the anodized surface at a lower magnification where the micro pits are retained, but at higher magnification (representative image shown as inset in Fig. 6.1C) we could clearly distinguish the well structured nanotubes with diameters ranging from ~30-40 nm all over the anodized surface.

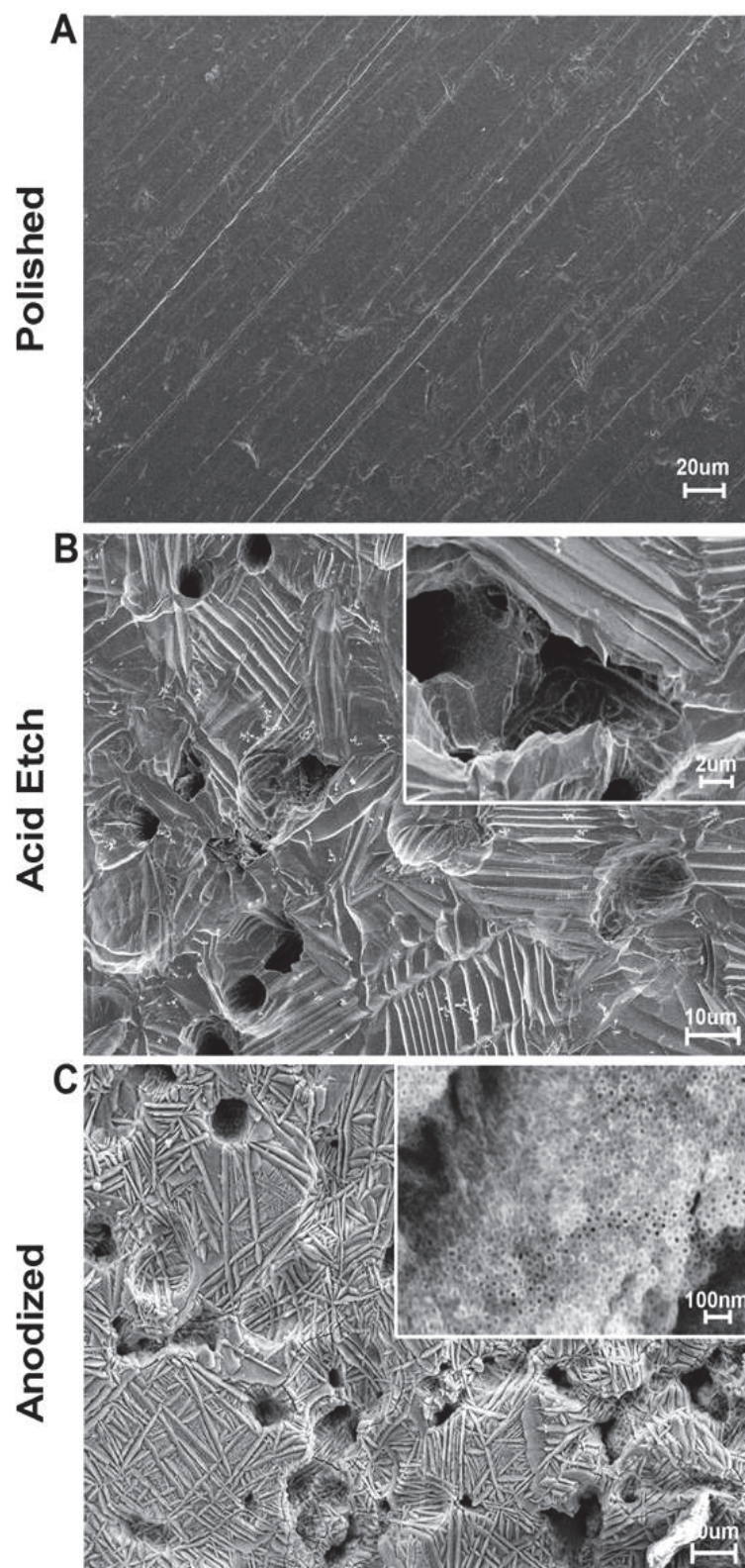


Figure 6.1. SEM image showing the morphology of cells on the three materials (A) polished, (B) acid etched (Inset shows high magnification image) and (C) anodized (Inset shows high magnification image with clear nanotubes of ~30-50 nm diameter).

Surface roughness and surface area evaluated using AFM

AFM was used to capture the topography, roughness and relative surface area of the three material surfaces as shown in Fig. 6.2. Based on the nano-scale roughness (RMS) and relative surface area (μm^2) of the surface we concluded that the roughness of the anodized surface was higher than acid etched and polished surfaces in the following order: anodized > acid etched > polished (see Table 6.2).

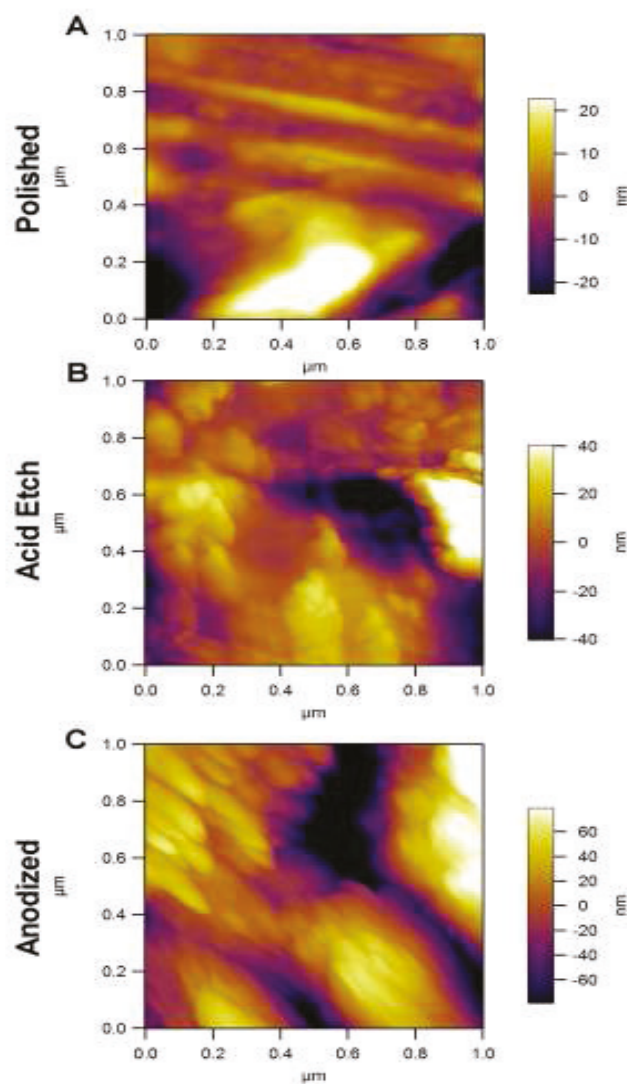


Figure 6.2. Surface topography image of the three material surfaces (A) polished, (B) acid etched and (C) anodized using AFM (scan area $1 \times 1 \mu\text{m}^2$).

Surface hydrophilicity

A similar hierarchy was seen with regard to the hydrophilicity of the material surfaces as measured by using water contact angle. Anodized surface was highly hydrophilic as is evident from its contact angle (6.50°) with water but the hydrophilicities of acid etched and polished surfaces were much lesser with the contact angle values of 67.58 and 63.85 respectively. Table 6.2 shows the values of surface roughness, relative surface area and water contact angles of the three material surfaces.

Table 6.2. Surface roughness, surface area and water contact angles of the three TiZr alloy surfaces.

Material (TiZr)	Surface roughness (RMS in nm)	Surface area (μm^2)	Area %	Water contact angle (θ)
Polished	10.24 ± 6.04	1.02 ± 0.04	3.17	63.85 ± 3.16
Acid etch	22.77 ± 10.84	1.13 ± 0.13	6.33	67.58 ± 1.37
Anodized	53.14 ± 5.33	1.30 ± 0.14	28.34	6.50 ± 1.38

6.3.2 Cell adhesion and spreading

The qualitative and quantitative assessment of cell adhesion and spreading was done on the three material surfaces as described. Percent adherent cells were assessed at 4 h after plating; cell spreading and cell adhesion related gene expression pattern were analyzed at 4 and 24 h after plating the cells.

6.3.2.1 Cell adhesion

Fig. 6.3 shows the percentage of cells that remained attached on the three material surfaces after 4 h of seeding the cells. As can be clearly seen the percentage of cells attached to the anodized surface (85%) was significantly higher when compared to acid etched (60%) and polished (40%) surfaces. This difference possibly reflects the most direct influence of material surface properties on the nature of their interaction with osteoblast cells.

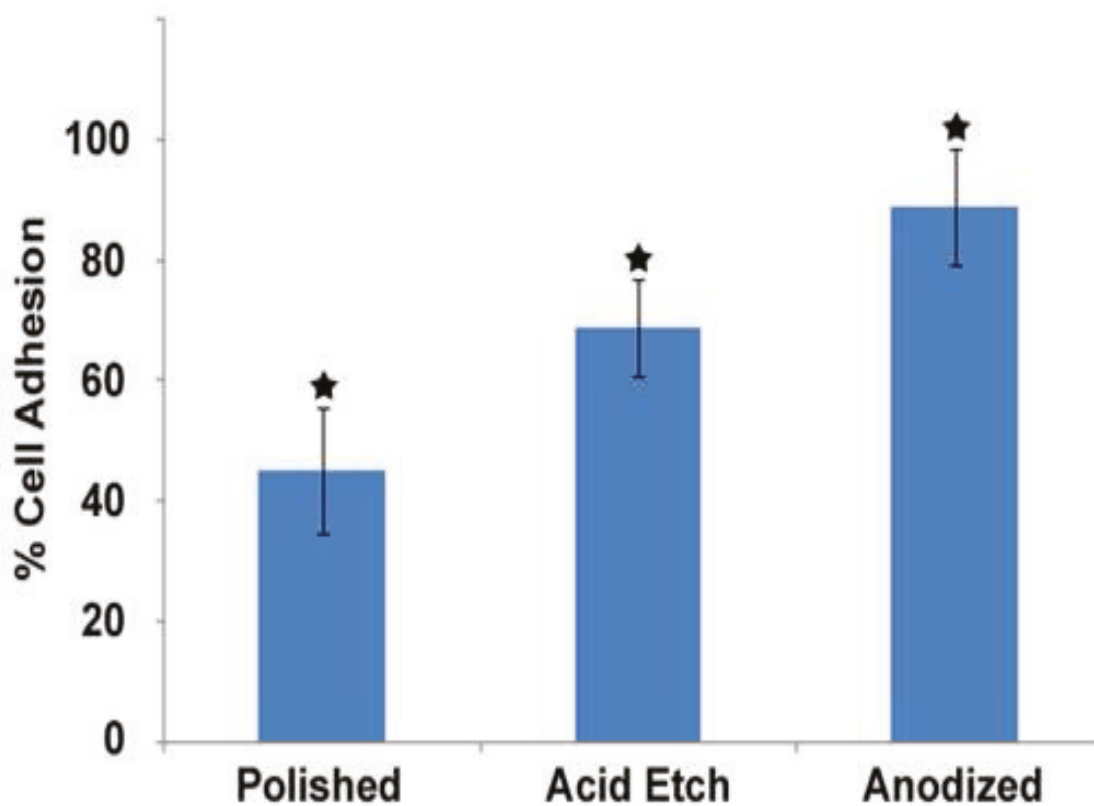


Figure 6.3. The percentage of cells attached to the three material surfaces after 4 h of cell seeding using MTT assay.★ represents $p < 0.05$ between materials.

6.3.2.2 Cell morphology and spreading

The morphology and spreading of cells on the material surfaces were observed using SEM (Fig. 6.4) and actin immunofluorescence (Fig. 6.5) after 24 h of seeding the cells. Cells on all the three material surfaces appear to be fully spread with spindle shaped morphology. On the polished surface, the cells were oriented in the direction of the grooves generated by the polishing of the surface with numerous filopodial extensions. Cells on the acid etched and anodized surfaces show an irregular morphology with long extensions and numerous filopodia formed on the surfaces indicating a strong attachment to the surfaces of these two materials.

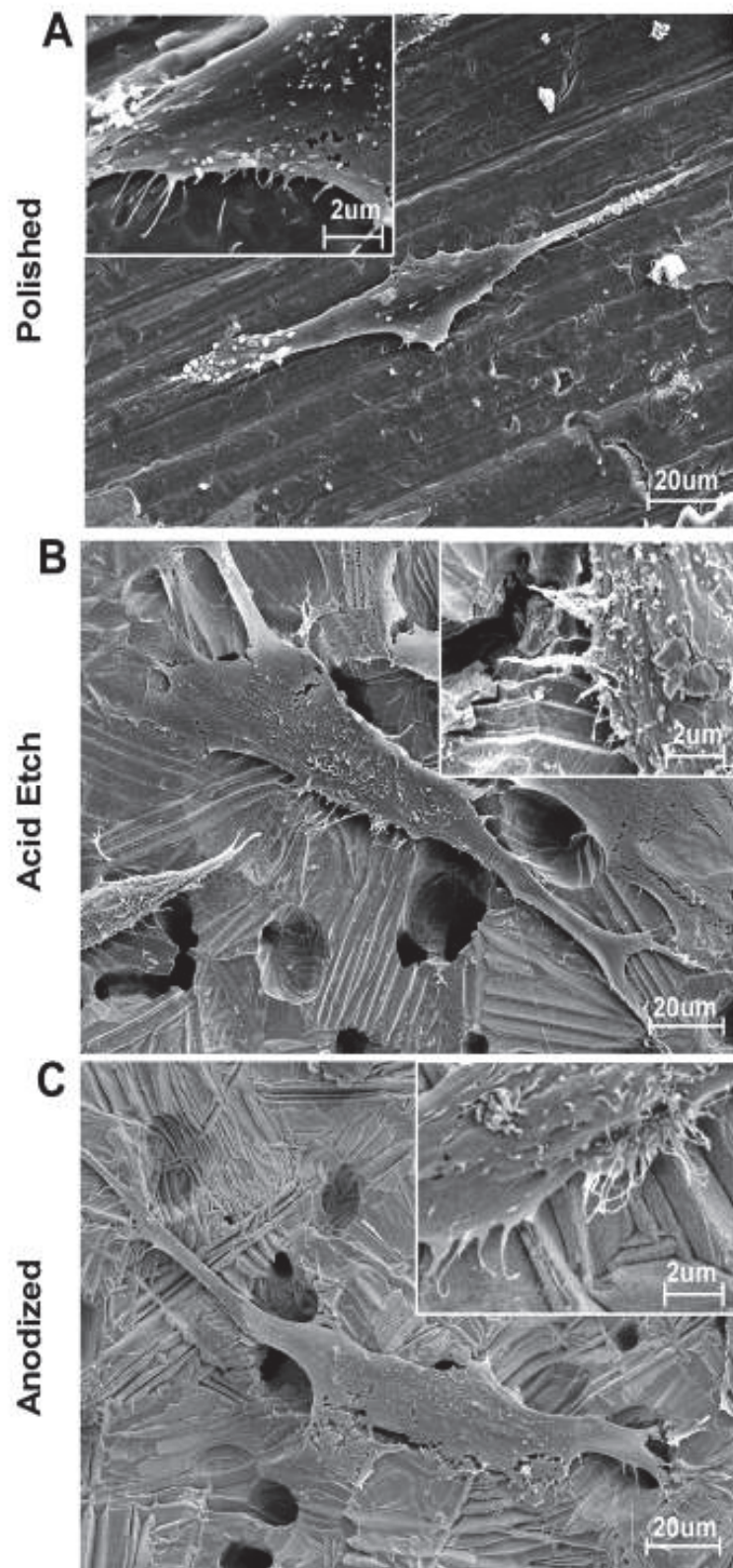


Figure 6.4. SEM image showing cell morphology on the three material surfaces (A) polished, (B) acid etched and (C) anodized (scale bar represents 20 μm). Inset shows high magnification image of the numerous filopodial extensions (scale bar represents 2 μm).

Spreading of the attached cells on the materials using actin immunofluorescence after 24 h of seeding (Fig. 6.5) indicated the stress fibers were seen oriented along the cortical regions of the cells on anodized and acid etched surfaces thereby suggesting a strong attachment to the surfaces. On the polished surface also the stress fibers were seen along the edges as well as distributed throughout the cells.

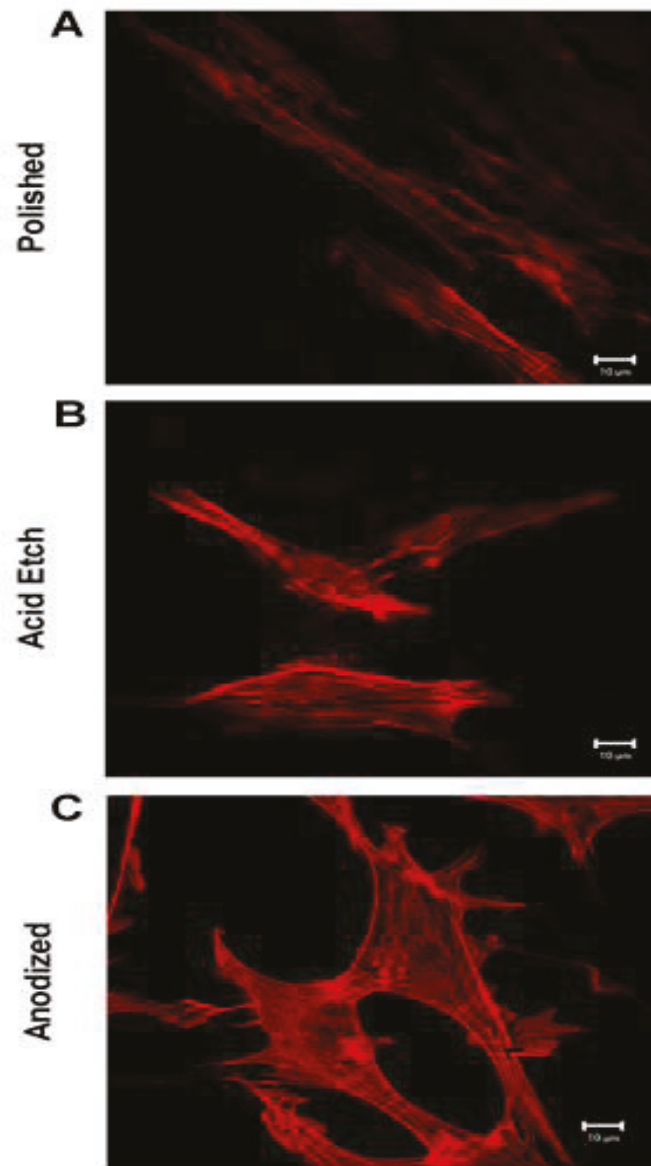


Figure 6.5. Actin immunostaining of cells on the three material surfaces (A) polished, (B) acid etched and (C) anodized (scale bar represents 10 µm).

6.3.2.3 Cell adhesion related gene expression

In order to understand the reasons behind the differences in the cell adhesion and cytoskeletal organization we analyzed the expression of several genes such as ECM components, integrins, focal adhesion proteins etc. that are known to regulate these processes. The gene expression levels were studied at 2 time points after cell seeding (4 h and 24 h) and the comparison of the data on the three material surfaces is shown in Fig. 6.6A and Fig. 6.6B.

Integrins

We evaluated the expression of three α integrins; $\alpha 2$ (collagen specific), $\alpha 5$ (fibronectin specific), αV (vitronectin specific) and one β integrin gene- $\beta 1$ chain (a common β chain for the collagen receptor with $\alpha 2$ and fibronectin receptor with $\alpha 5$). The expression of $\alpha 2$ was higher on the anodized surface and polished surface as compared to acid etched surface at 4 h, whereas at 24 h, the expression was higher only on the anodized surface. The expression of $\alpha 5$ was higher on the anodized than acid etched and polished surfaces at 4 h and 24 h time points. At 4 h, no significant difference in the expression of αV was seen on the materials whereas at 24 h, the expression was higher on the anodized surface compared to the other two surfaces. Similar expression was seen with regard to integrin $\beta 1$ expression with no significant difference at 4 h interval but a higher expression on the anodized surfaces at 24 h time point compared to the two surfaces. These data clearly show that expression of collagen and fibronectin binding integrins is strongly stimulated in osteoblasts that are plated on anodized surfaces.

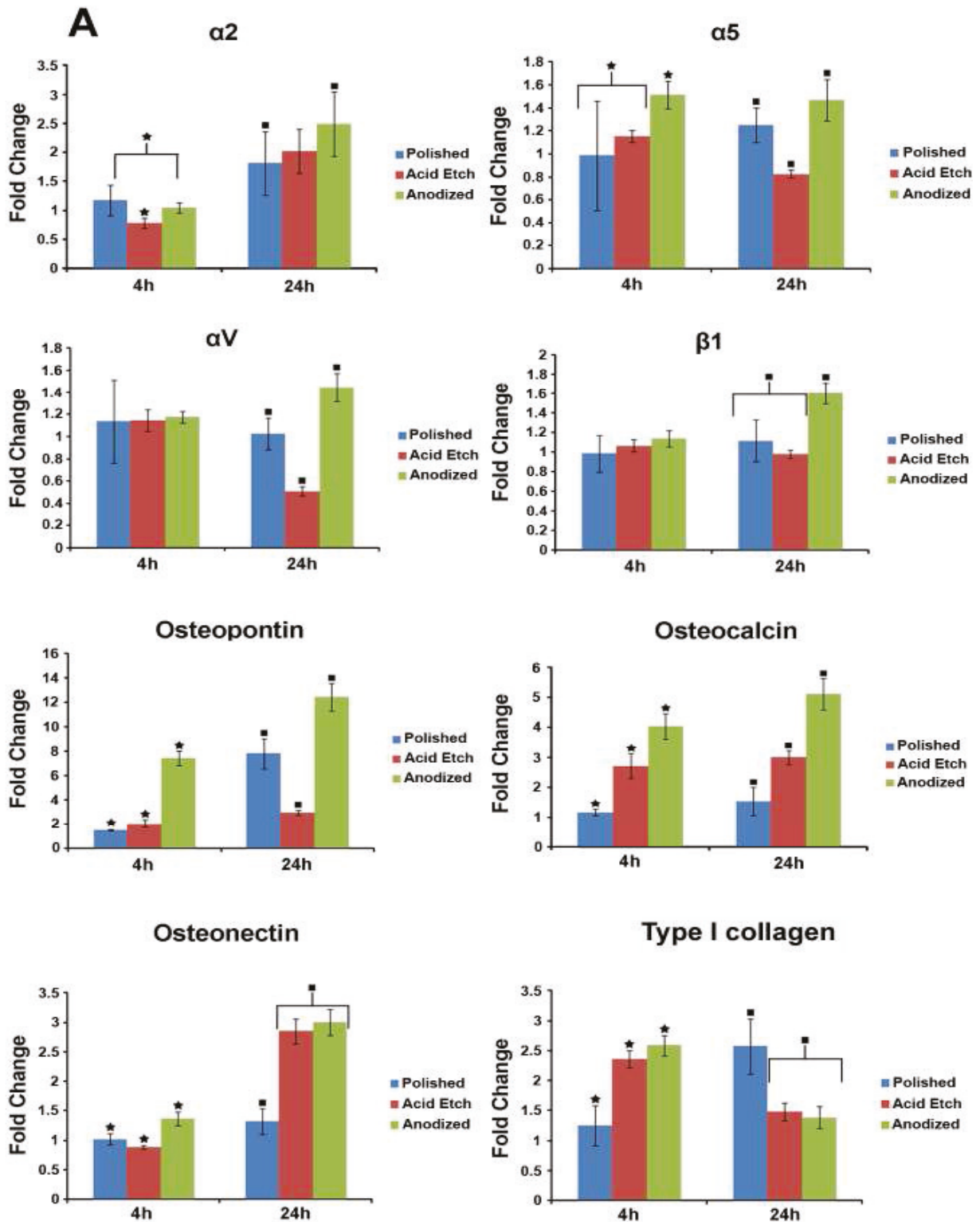


Figure 6.6A. The fold expression of integrins $\alpha 2$, $\alpha 5$, αV and $\beta 1$, osteopontin, osteocalcin, osteonectin and type I collagen genes on the three material surfaces after 4 and 24 h of adhesion. ★ ■ represents $p < 0.05$ between materials at 4 and 24 h respectively.

Extracellular matrix (ECM) components

Complementing the integrin gene expression pattern we found that expression of type I collagen genes was also higher on the anodized surface at 4 h interval whereas the expression was reduced on the acid etched and anodized surfaces at 24 h time point. The expression of both the markers fibronectin and vitronectin was significantly higher on the anodized surface at 4 h interval. However, at 24 h time point, no significant difference was seen between the anodized and the acid etched surfaces, but the expression was higher compared to the polished surface.

Focal adhesion markers

Focal Adhesion Kinase (FAK) a critical regulator of the formation of focal adhesion points between cells and the substratum and strengthening cell adhesion, was seen to be higher on the anodized surface compared to acid etched and polished surfaces at 4 h and 24 h time points, as shown in Fig. 6.6B. This correlated well to the higher percentage of cells we saw on anodized surfaces.

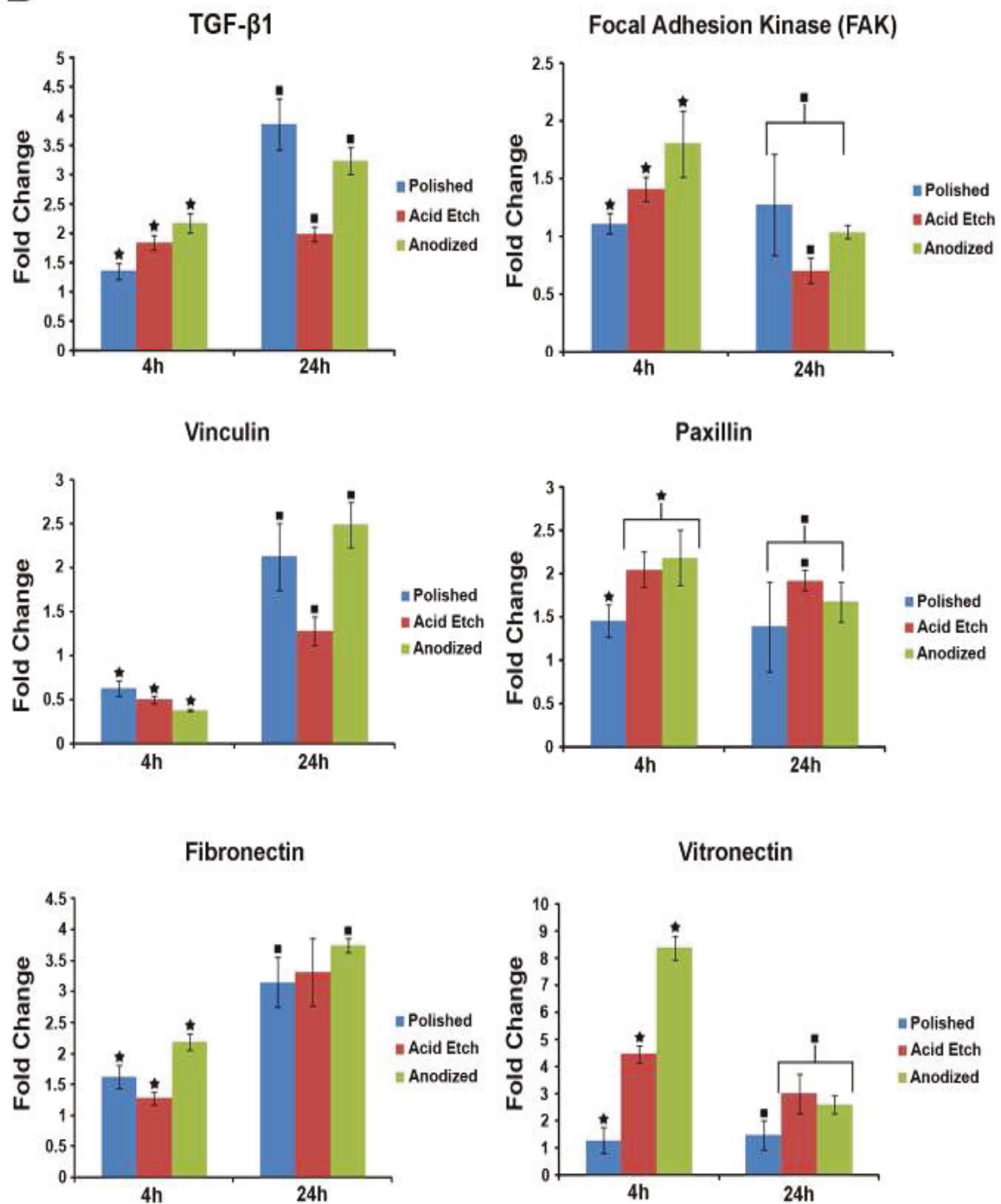
B

Figure 6.6B. The fold expression of TGF-β1, FAK, vinculin, paxillin, fibronectin and vitronectin genes on the three material surfaces after 4 and 24 h of adhesion. ★ ■ represents $p < 0.05$ between materials at 4 and 24 h respectively.

Further corroborating this observation was the higher expression of paxillin at the 4 h time point and vinculin at 24 h time point on the anodized surface as compared to the other two surfaces. It is well known that integrin mediated cell adhesion requires the cooperative action of these two molecules seen in focal adhesions and are required for the formation of the actin cytoskeleton. Good expression of only paxillin was seen on acid etched surface at 24 h and of only vinculin at 4 h time point.

Osteoblast specific markers

A significantly higher expression of osteopontin and osteocalcin genes was seen on the anodized surface compared to the acid etched and polished surfaces at 4 h and 24 h after adhesion on the materials respectively (as shown in Fig. 6.6A). A similar level of osteonectin gene expression was seen on the materials where the level of expression was higher on the anodized surface at 4 h and comparative expression on anodized and acid etched surface at 24 h time point compared to the polished surface. A similar level of TGF- β 1 expression was seen on the materials with higher expression on the anodized surface at 4 h interval followed by polished surface at 24 h time point.

Agarose gel electrophoresis

The specificity of the PCR reaction was tested by running the PCR products in a 2% agarose gel electrophoresis. We could clearly see the presence of only one band upon ethidium bromide staining of the gel after loading the products. We observed a single product (band) for all the adhesion genes of all the three material samples at both the time points. The PCR products of all the genes for the three samples at 4 and 24 h are shown in Figure 6.7.

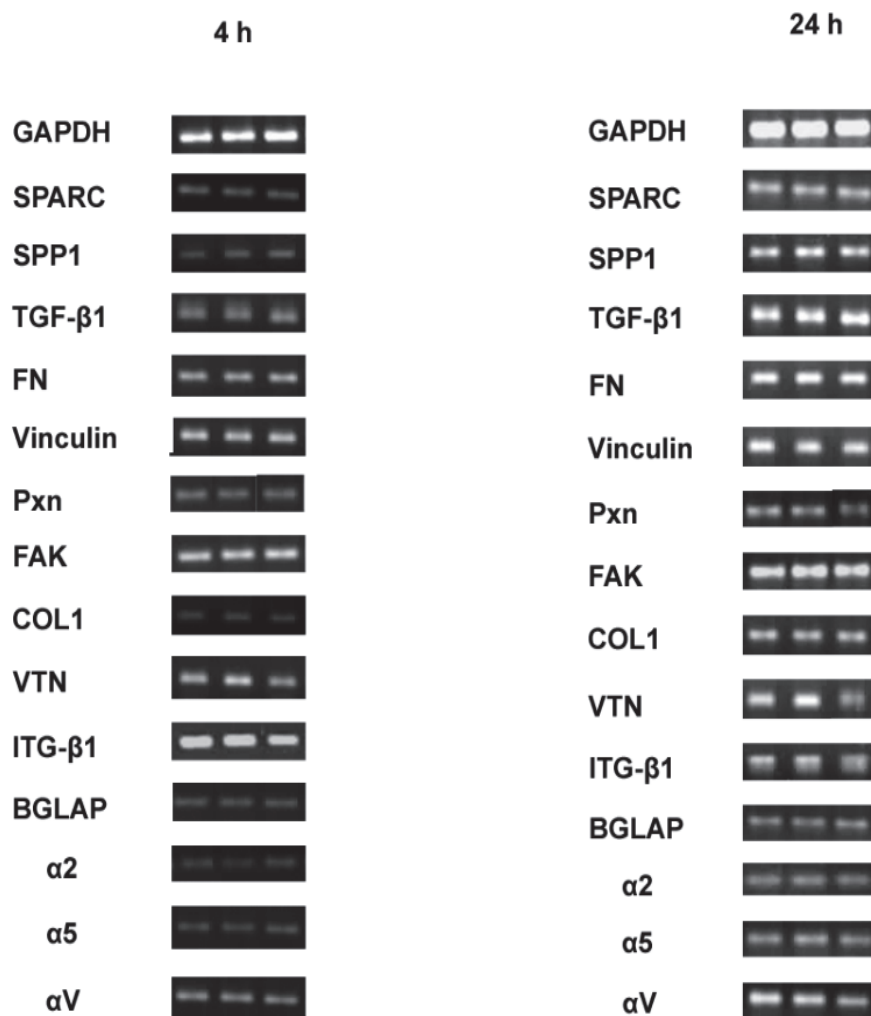


Figure 6.7. Real time PCR products of adhesion genes on the materials at 4 and 24h time intervals.

6.3.3 Cell proliferation

The number of viable cells present after 24, 48 and 72 h of seeding on the three material surfaces were evaluated using the MTT assay (Fig. 6.8) as described in materials and methods. We observed a steady increase in the cell number on all the three surfaces as a function of time; however the cell number was higher on the anodized surface at 24 and 48 h compared to acid etched and polished surfaces. No significant difference in the cell number was seen between the two surfaces at 72 h interval, but it was significantly higher as compared to the polished surface.

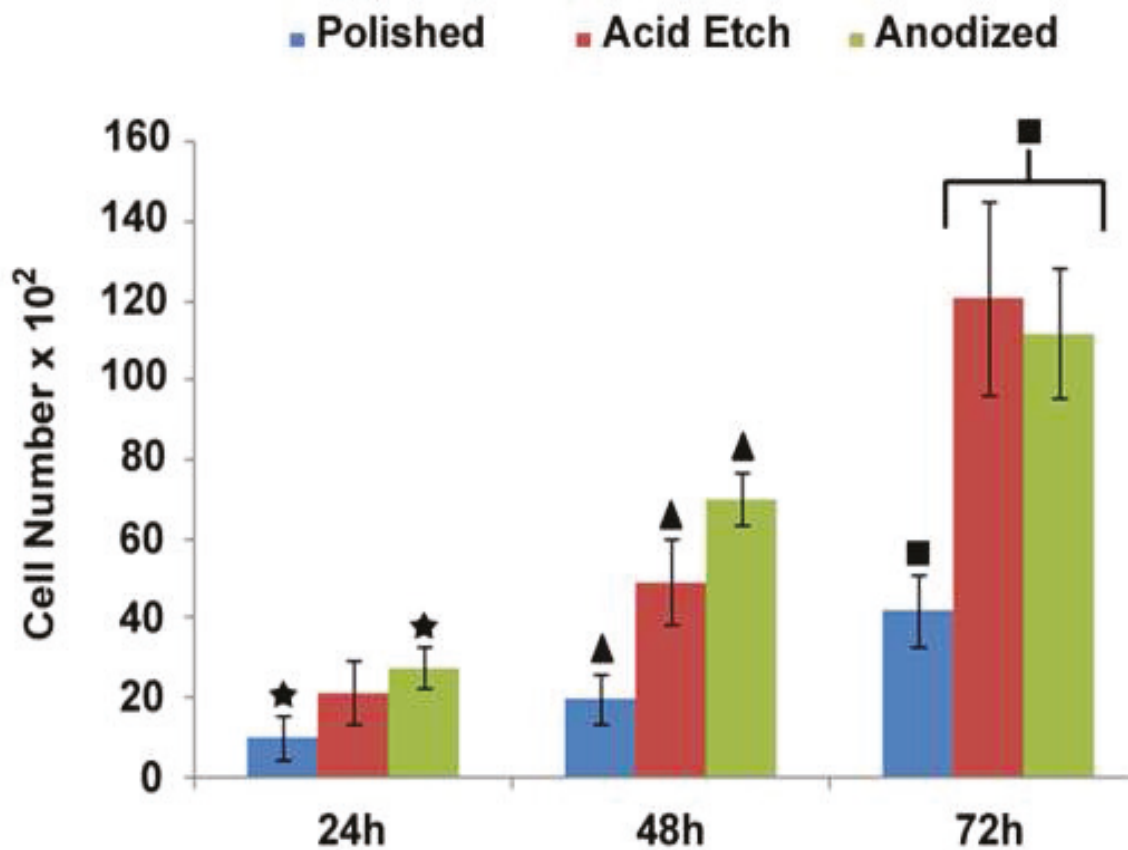


Figure 6.8. The proliferation of cells on the three material surfaces after 24, 48 and 72 h of cell seeding using MTT assay. ★ ▲ ■ represents $p < 0.05$ between materials at 24, 48 and 72 h respectively.

6.3.4 Cell differentiation

Cell differentiation on the three material surfaces was assessed using immunofluorescence of osteocalcin protein, extracellular matrix formation by SEM; and relative gene expression profiles of candidate genes involved in osteogenesis at specific time points namely after 1, 4 and 10 days.

6.3.4.1 Osteocalcin immunostaining

The extent of cell differentiation on the three material surfaces was seen using immunofluorescence of osteocalcin protein (Fig. 6.9). Osteocalcin protein expression is observed at final stages of osteoblast differentiation and is usually a marker for terminal differentiation. At various time points post induction namely 2, 4, 7, 10, 15 and 21 days, the intracellular and extracellular levels of osteocalcin deposition was observed on the three material surfaces. The left panel shows the staining for osteocalcin protein (Green) and the right panel shows the staining for nuclear stain DAPI (4',6-diamidino-2-phenylindole) (Blue). Although not much of a significant difference in the protein expression could be seen on the three material surfaces but intracellular expression was evident from day 2 through day 21 with signs of extracellular deposition starting from day 15 on all the material surfaces with greater expression of extracellular protein on day 21 on the anodized surface compared to acid etched and polished surfaces.

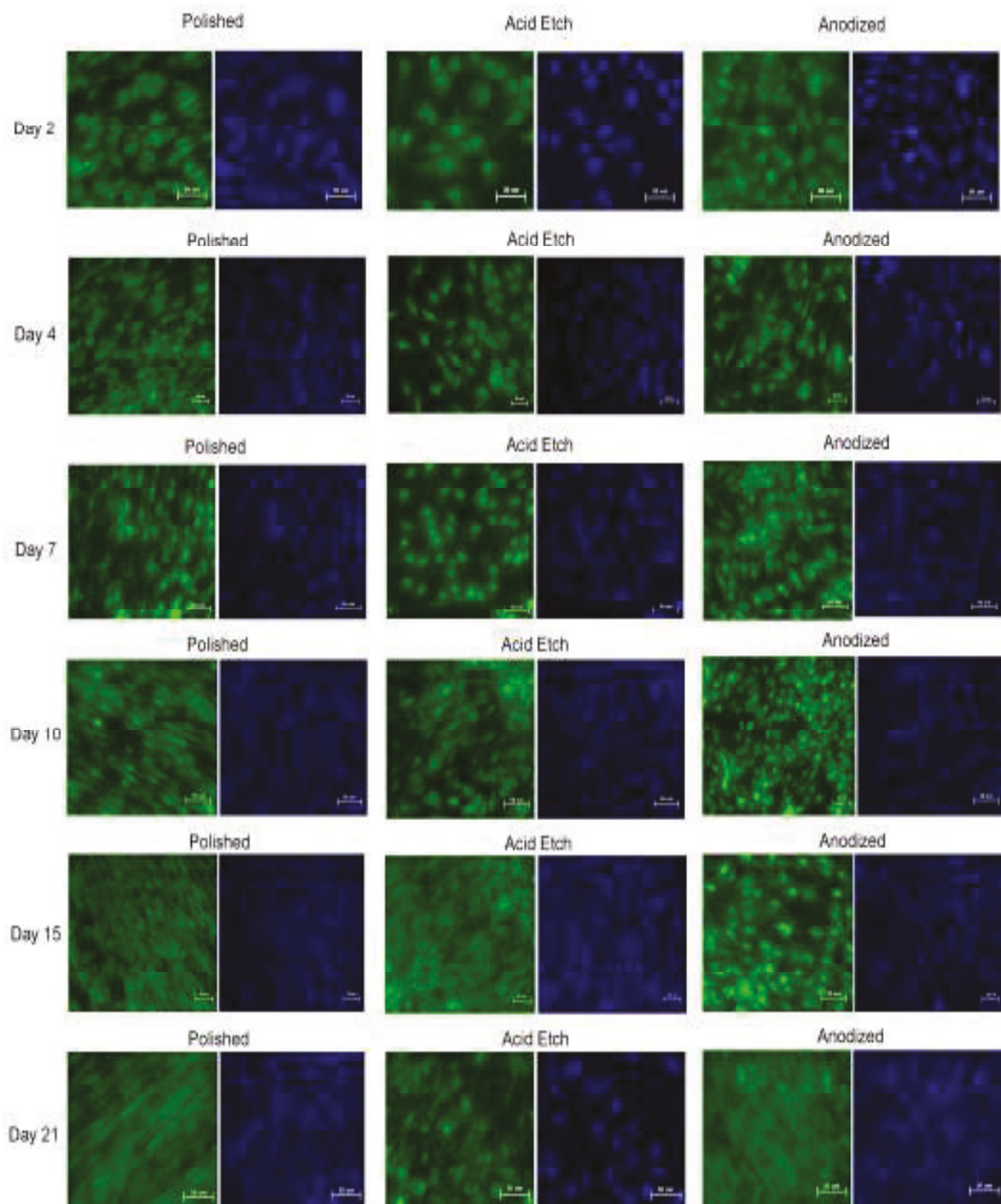
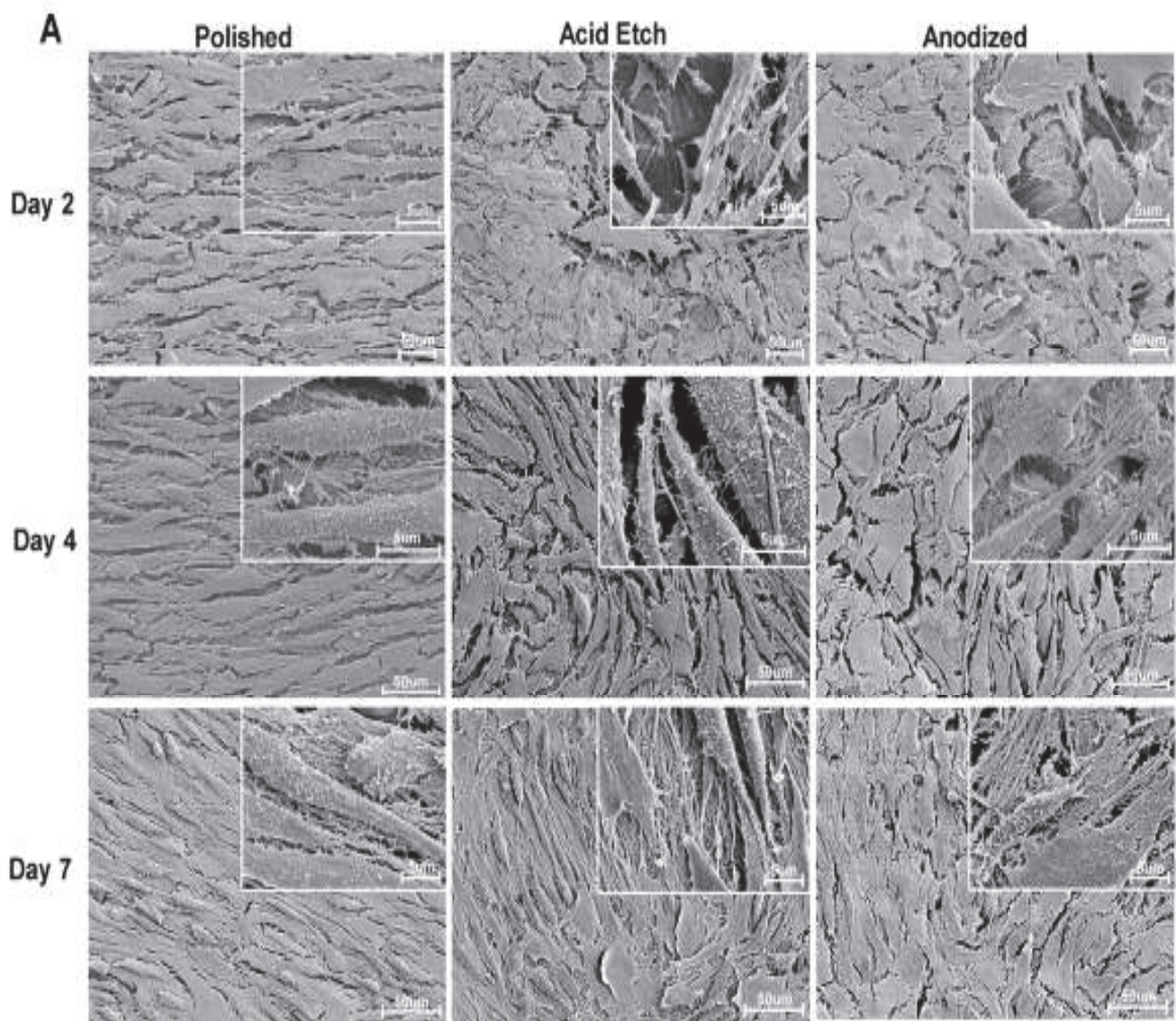


Figure 6.9. Immunostaining of osteocalcin protein at 2, 4, 7, 10, 15 and 21 days post induction on the three material surfaces. Intracellular and extracellular protein levels are stained green and the nucleus is stained blue using DAPI (scale bar represents 50 µm).

6.3.4.2 Extracellular matrix (ECM) analysis

Fig. 6.10 shows the formation of extracellular matrix deposition by the cells on the materials as seen using SEM at different time points namely 2, 4, 7, 10, 15 and 21 days post induction *in vitro*. We could observe that cells were more elongated on the polished surface as compared to the other two surfaces. ECM formation was seen as early as after 4 days on all surfaces and this became much thicker on anodized and thick ECM was seen as early as 7 days post induction with the process continuing till 21 days.



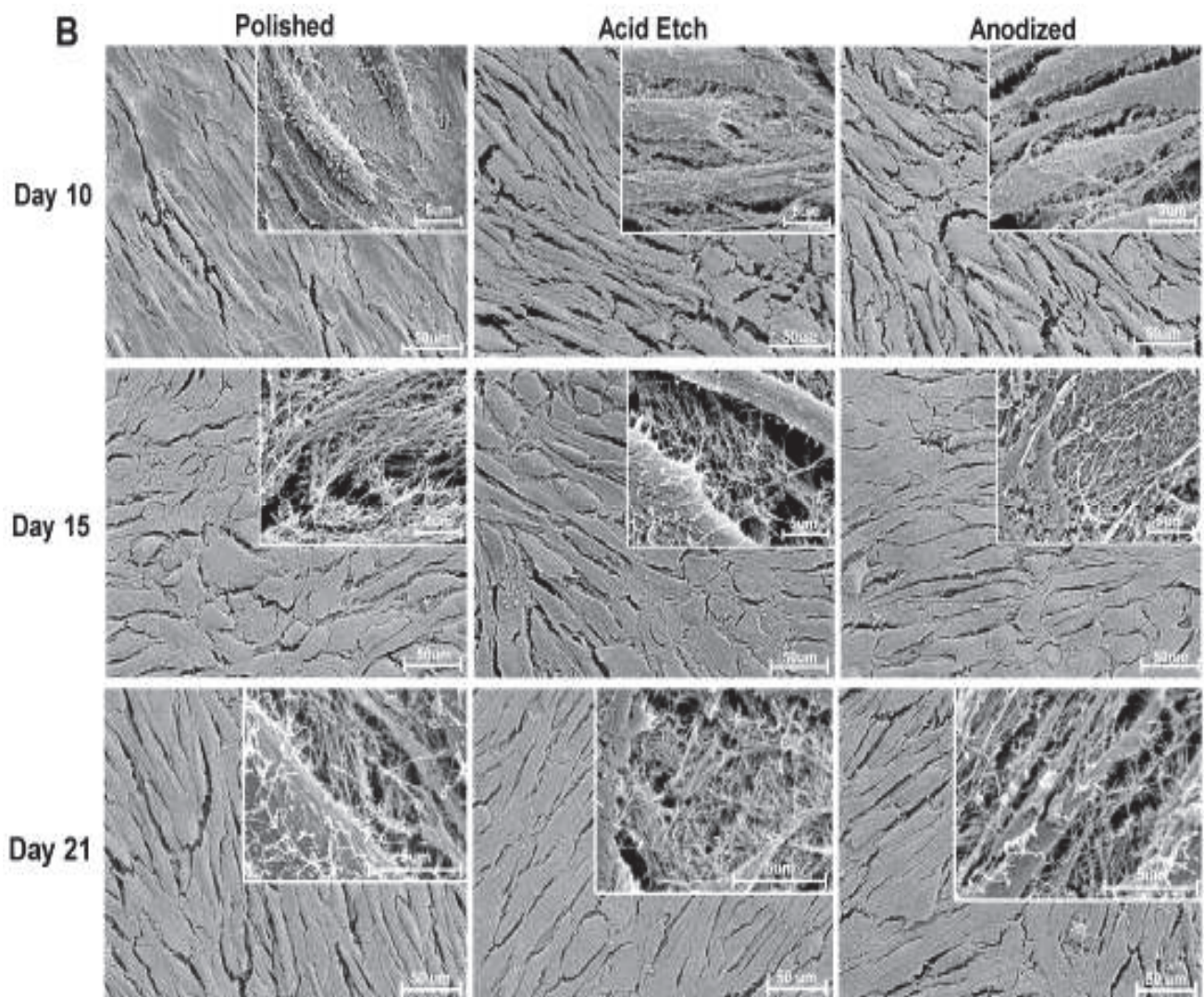


Figure 6.10. (A) SEM images showing extracellular matrix formation on the three material surfaces after 2, 4 and 7 days of differentiation. (B) Extracellular matrix formation on the three material surfaces after 10, 15 and 21 days of differentiation (scale bar represents 50 μm). Inset shows high resolution, high magnification image (scale bar represents 5 μm).

6.3.4.3 Expression of differentiation related genes

The gene expression pattern after 1, 4 and 10 days post induction on the three materials surfaces are shown in figures Fig. 6.11A and Fig. 6.11B.

Alkaline phosphatase (ALP), type I collagen, type III collagen

Although no significant difference in the expression of ALP gene was seen on any of the materials at day 1, a significant increase in ALP gene expression was seen at days 4 and 10 on the polished surface compared to the acid etched and anodized surfaces. Type I collagen expression was significantly higher on the anodized surface compared to the acid etched and polished surfaces at all the three time points tested whereas type III collagen expression was higher on the polished and acid etched surfaces at 4 day time point with no differences in the expression levels at 10 day time point. Anodized surface showed a higher expression only on the first day after inducing the cells to differentiate.

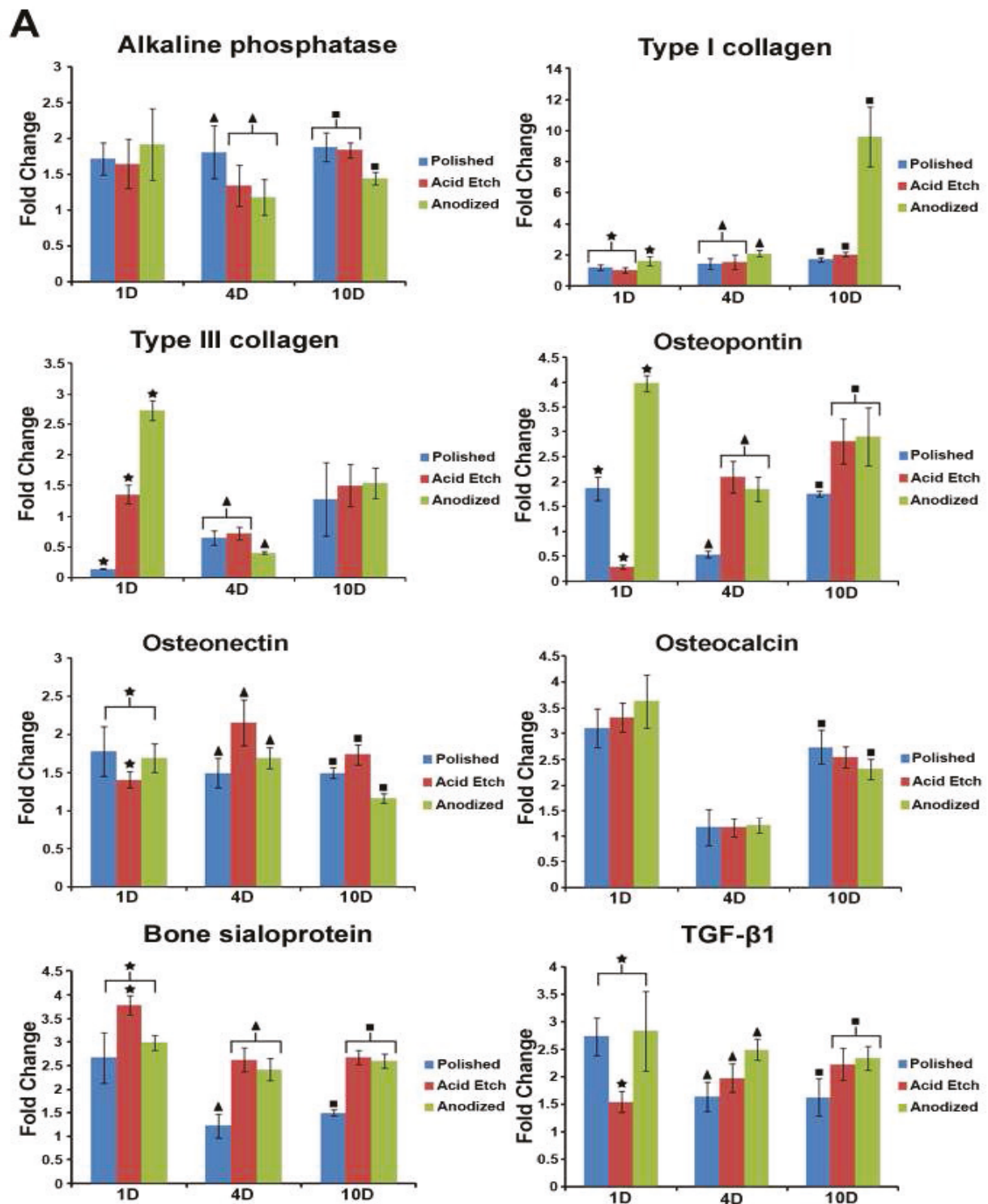


Figure 6.11A. The fold expression of alkaline phosphatase, type I collagen, type III collagen osteopontin, osteonectin, osteocalcin, bone sialoprotein and TGF- β 1 genes on the three material surfaces after 1, 4 and 10 days of differentiation. ★ ▲ ■ represents $p < 0.05$ between materials at 1, 4 and 10 days respectively.

Osteopontin, osteonectin, osteocalcin and bone sialoprotein

The expression of osteopontin was significantly higher on the anodized surface at 1 day interval than the other surfaces, with comparative expression on the acid etched and anodized surfaces and significantly higher expression compared to the polished surface at 4 day and 10 day time points. A similar kind of behavior was seen with regard to the expression of bone sialoprotein on the three surfaces. A higher expression was seen on the acid etched surface at 1 day interval with comparative and higher expression at 4 and 10 day intervals on the acid etched and anodized surfaces compared to the polished surfaces respectively. No significant difference in the expression levels of osteocalcin gene was seen on the materials at 1 and 4 day intervals but a higher expression on the acid etched and polished surfaces compared to the anodized surface at 10 day time point. A variation in the expression levels of osteonectin was seen on the materials at the three time points tested. At day 1, the expression was higher on the anodized and polished surfaces compared to the acid etched surface. However, at days 4 and 10, significantly higher expression was seen on the acid etched surface compared to the other surfaces.

TGF- β 1- Bone matrix proteins (BMP's) and Runx2

A significantly higher expression of TGF- β 1 was seen on the anodized surface compared to the other surfaces at the three time points tested. A variation in the expression of Runx2 was seen on the materials at the three time points. At day 1, the expression was comparative on the acid etched and anodized surface and significantly higher compared to the polished surface. At both 4 and 10 day intervals, the expression was higher on polished and anodized surfaces as compared to the acid etched surface. A similar trend in the expression patterns of BMP1 and BMP4 was seen at days 1 and 10, where the expression was higher on anodized and acid etched surfaces respectively. At day 4, BMP1 and BMP4 expression was higher on the acid etched surface compared to the other surfaces.

Bone mineralizing markers Dentin matrix protein (DMP1) and Biglycan (Bgn)

The expression of DMP1 was higher on the anodized surface at 1 day interval. However, at both 4 and 10 day intervals, the expression was higher on the acid etched surface compared to the other surfaces. A higher level of biglycan expression was seen on the anodized surface at 1 day

interval. However at day 4, its expression level decreased compared to acid etched and polished surfaces. No significant difference in the expression was seen at 10 day interval.

Insulin growth factor (IGF-1) and Fibroblast growth factor (FGF-2)

A variation in the expression patterns of IGF-1 and FGF-2 was seen on the materials at the three time points. FGF-2 expression was higher on the polished surface at 1 and 4 day intervals compared to the other two surfaces, however, at 10 day interval, the expression was higher on the anodized surface. IGF-1 expression was higher on the anodized surface at 1 day interval. At 4 and 10 day intervals, the expression was higher on the acid etched surface compared to the other surfaces.

B

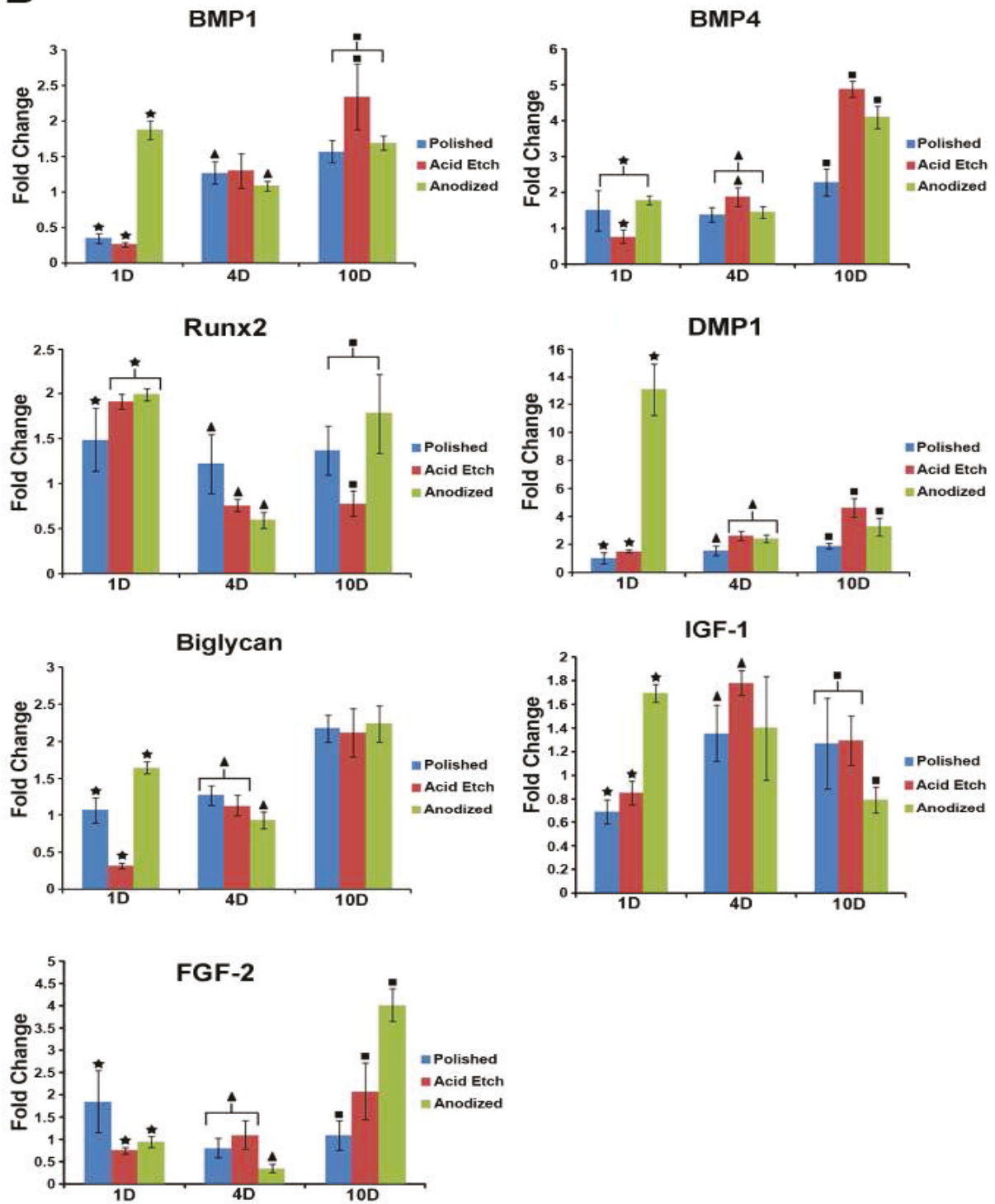


Figure 6.11B. The fold expression of BMP1, BMP4, Runx2, DMP1, Biglycan, IGF-1 and FGF-2 genes on the three material surfaces after 1, 4 and 10 days of differentiation. ★▲■ represents $p < 0.05$ between materials at 1, 4 and 10 days respectively.

Agarose gel electrophoresis

The specificity of the PCR reaction for each gene was tested by loading the products after real time PCR reaction on a 2% agarose gel. We could clearly see a single product formed as observed by the presence of a single band upon ethidium bromide staining after loading the products. The products of each gene for all the three materials at the three time points namely 1, 4 and 10 day intervals are shown in Figure 6.12.

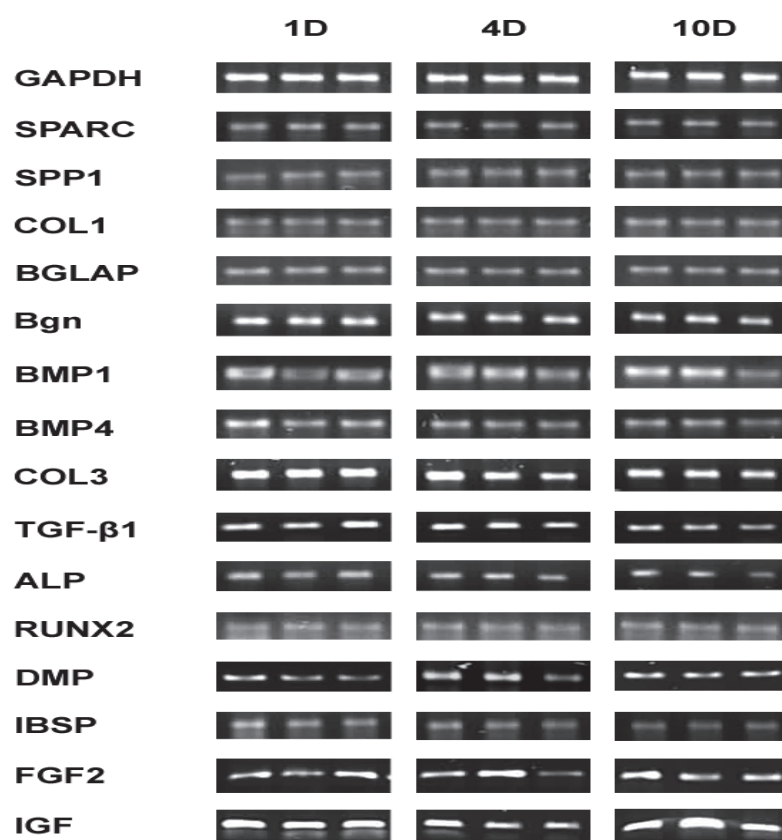


Figure 6.12. Real time PCR products of differentiation genes on the materials after 1, 4 and 10 days of differentiation.

6.3.5 Matrix mineralization

Figure 6.13 shows the alizarin red staining for matrix mineralization on the materials. As the days progressed, the intensity of the red color increased with time, indicating the deposition of calcium as stained with alizarin red dye. Qualitative analysis indicates that, the intensity increased on the materials, but this increase was found to be more on the polished and anodized but to a lesser extent on acid etched surface. The data further show the cells differentiated on all the three materials becoming mature osteoblasts and the materials supported the differentiation of osteoblasts.

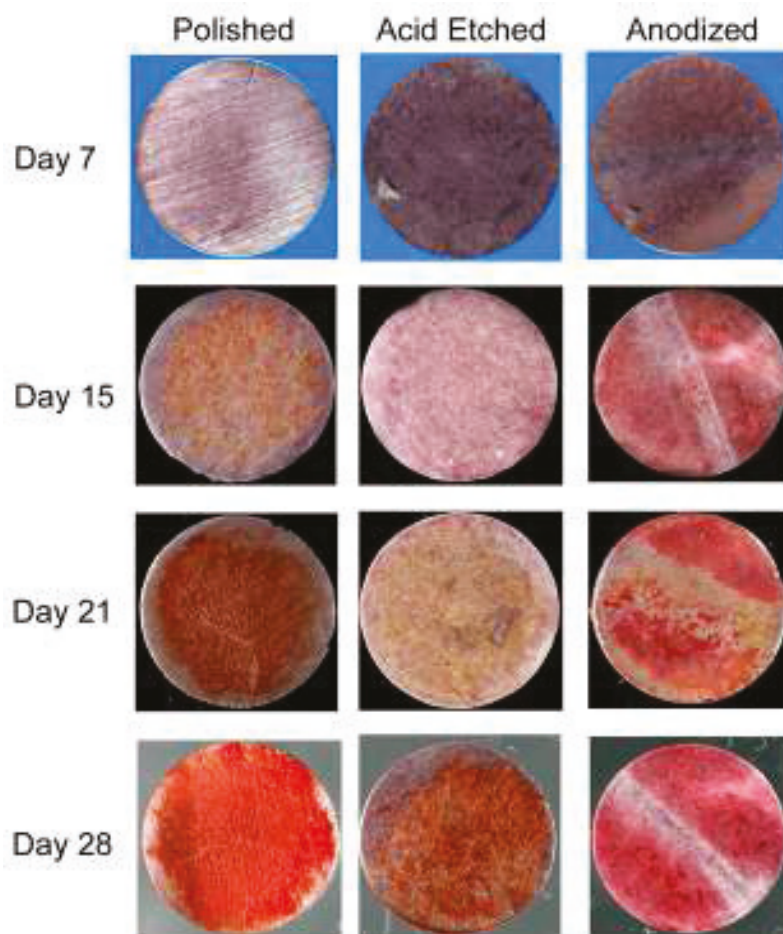


Figure 6.13. Alizarin red staining for calcium deposition on the materials after 7, 15, 21 and 28 days of differentiation on the materials.

6.4 Discussion

The results described above highlight three important issues in the emerging field of cell-material interactions. One is methodological where we have shown the conditions in which reproducible generation of nanotubular architecture with novel and defined physico-chemical properties on TiZr surface can be done. The other two points are related to how the electrochemical properties of the surfaces of tissue culture substrate materials can control the molecular and supra-molecular response of cells that come in its contact in the short and long term. These issues are discussed in detail below.

6.4.1 Nanotubular surfaces and anodization

In this study, we have successfully produced nanotubes on the surface of TiZr alloy using anodization technique with 0.5% HF as the electrolyte. The anodization technique has the advantage of producing surfaces with varied topographies at the nanometer scale and increases the oxide layer thickness on the surface and bioactivity of the metal surfaces as has been reported by others [82-84, 91] [76, 85, 88, 90]. Many different electrolytes and conditions have been reported using anodization of titanium. The use of HF has emerged to be very successful in this process as an etchant and a powerful electrolyte to produce nanotubes using the anodization technique [51, 63, 76, 94, 208]. Most of the earlier studies [63, 81, 82, 90] have produced nanotubes on the surfaces of pure Ti and Ti-6Al-4V alloy, ours is the first report for producing nanotubular surfaces on TiZr where tubular pattern and other surface properties are reported.

6.4.2 Cell adhesion and proliferation

It is assumed that many interactions of cells with the substratum occur at the nanometer scale and some others at the micrometer scale. Therefore, it would be interesting to compare the response of cells towards the surfaces with nanoscale patterns with those that have microscale patterns. With this aim we have looked at the behavior of osteoblast cells on the nanotubular surfaces produced by anodization and compared them to acid etched and polished surfaces which patterns at the micrometer or millimeter scale roughness respectively. Our analysis was done at various stages of cell- material interactions and more importantly the effect of various surface properties on the observed cell behavior.

The morphology of cells within 24 h after seeding them on the surfaces was observed using SEM for studying their shapes and fluorescence microscopy for cytoskeletal organization. We observed that the cells were fully spread and exhibited filopodial extensions from their surfaces on anodized and acid etched substrates (as shown in Fig. 6.4). In the immunofluorescence images we could also see actin stress fibers arranged along the cortical regions of the cells on the anodized and acid etched surface thereby illustrating a strong attachment on these surfaces (Fig. 6.5). Yu et al [226] observed similar kind of morphology of cells on TiO₂ nanotubes with fully spread behavior. Furthermore, we could also see a higher percentage of cells adhered onto the anodized surface compared to the acid etched and polished surfaces at 4 h seeding interval. A similar cell behavior was seen by Yao et al [63, 82] with regard to the cell adhesion. Both these observations could be due the higher surface wettability of the anodized surface which can play an important role in determining the total surface energy and thereby the strength of the interaction of cells with them.

In our study of cell proliferation, done by measuring viable cell number at 24, 48 and 72 h intervals after cell seeding, we found that initially cell proliferation was higher on the anodized surface as seen in Fig. 6.8. Although, the surface roughness and cell proliferation are inversely related, we noticed a greater proliferation on the nano-rough surface compared to the micro-rough surfaces. Studies done by Ercan et al [91] and Washburn et al [322] have also shown a similar behavior with regard to the proliferation on the anodized surface or on polymeric surfaces with nanometric roughness, without influencing the cell adhesion properties. Studies by Webster et al [70, 73] have shown greater osteoblast adhesion on surfaces with increased nano-roughness which offer a higher surface area and reactive sites for better protein adsorption as shown by Yao et al [82]. In agreement with these observations we also observed a higher surface area of the anodized surface compared to the acid etched and polished surfaces (as shown in Table 6.2).

The first phase of cell-material interactions during the adhesion of cells onto material surfaces is regulated by the physico-chemical surface properties. Further strengthening of cell adhesion is in the second phase and it is mediated by the adsorbed proteins that are deposited on the nano-roughened surfaces by the loosely attached cells. Fibronectin and collagen are two major proteins that mediate the adhesion of osteoblasts onto material surfaces. In our study, we observed high expression of fibronectin and collagen genes on the anodized surface compared to the other two

surfaces. These proteins mediate signal transduction processes by binding to integrin molecules on the cell surface and initiating a cascade of signaling pathways which support stronger cell adhesion to the underlying surface.

In our analysis we could clearly see higher expression of $\alpha 2$, $\alpha 5$ and $\beta 1$ integrin genes, which code for the collagen and fibronectin receptors, respectively, on the anodized nanotubular and acid etched surfaces compared to polished surfaces. These data strongly support our earlier observation that 80% of cells adhered to the anodized surface, 60% cells adhered on the acid etched surface and 40% cells on polished surface respectively. We could also observe a steady increase in the expression of most of the adhesion genes as a function of time from 4 h to 24 h intervals.

6.4.3 Cell differentiation

The differentiation of cells was assessed after plating the cells on the material surfaces and at different time points up to 10 days after inducing them for differentiation by three different methods: (a) osteocalcin activity (b) quantitative evaluation of ECM and (c) expression of candidate genes involved in osteogenesis. With regard to osteocalcin gene expression, we observed a higher expression on the polished surface compared to the other two surfaces at the 10 day interval, although the levels were higher on the anodized surface at 1 day interval. A study by Kotobuki et al [323] suggested that the expression of osteocalcin at the gene levels does not lead to matrix mineralization. Furthermore, the expression pattern of various other genes involved in osteogenesis was found to be comparatively expressed on the anodized and acid etched surfaces but with a lower expression on the polished surfaces. With regard to the expression of ALP, we found increased expression of the enzyme on polished surfaces after 10 days, though at day 1 the activity was similar on all surfaces. A similar behavior of ALP activity was seen by Mendonca et al [324] where the expression levels were higher on the machined surfaces compared to nanoscale coatings and the acid etched surfaces. Although we could not notice any specific trend in the expression pattern with regard to differentiation related genes as a function of time, we could notice higher expression for a majority of genes tested on the anodized surface, at multiple time points. Furthermore, we could also see the expression of certain differentiation genes to be higher on the acid etched surfaces as well. We could also see a

steady increase in the expression of osteocalcin protein using immunostaining (Fig. 6.9). Furthermore, the SEM images of the cells as a function of time show the extracellular matrix formation on the surfaces with marked differences seen at day 4 where, the onset of ECM was seen on the anodized and acid etched surfaces compared to the polished surface. A thick layer of ECM was seen on the surfaces as the number of days increased.

6.5 Conclusions

The surface properties of materials are important in determining the outcome of cell response and determine its effective functioning as an implant material. Therefore, it is absolutely necessary to have surfaces which can speed up the process of bone formation and better osseointegration. Moreover, the following conclusions could be drawn from this study:

- Nanotubes with diameters ranging from 30-40nm were successfully fabricated on the surface of TiZr alloy by anodization.
- TiZr alloy with nanotubular surface exhibited higher hydrophilicity, greater surface area and higher nano-roughness compare to acid etched and polished surfaces.
- Cell adhesion on the nanotubular surface as characterized by attached cell numbers and the gene expression profiles, was higher than that on the acid etched and polished surfaces.
- The proliferation of cells on the nanotubular surface was also higher than that on the acid etched and polished surfaces after 24, 48 and 72 h culture periods evaluated using MTT assay.
- The properties of nanotubular surface such as surface hydrophilicity, surface area and nano-roughness synergistically enhanced the biological outcome of bone cell-material interactions vis-à-vis osteoblast cell adhesion, proliferation and differentiation.

Our results show that the nanotubular surface produced by anodization technique is an efficient means to promote the accelerated attachment of osteoblasts and inducing rapid osseointegration at the bone-implant interface as evident by the enhanced behavior of cells on these surfaces at the cellular and molecular level.

7. Conclusions and Future directions

7.1 Conclusions

In this thesis, we have examined the behavior of osteoblast cells in response to material surfaces. Addressing this was important to understand the interactions that take place at the interface of cells and material surfaces, with a focus on identifying ideal surfaces for accelerating the osseointegration process. The surface properties play a critical role in determining these interactions as the bulk of these interactions occur at the surface of materials in *in vivo* environment. Evaluating the performance of materials *in vitro* gives an understanding of their performance *in vivo*.

In view of this, the cellular and molecular responses of osteoblast cells on two titanium alloys namely TiZr and TiNb were evaluated. The behavior of osteoblast cells at the cellular and molecular level, in response to the material surface properties at different stages of cell-material interactions namely the adhesion, proliferation and differentiation were studied. We could clearly establish the role of surface properties and their influence on osteoblast cell behavior. In our study, we found that a high surface energy was a dominant factor in accelerating the initial attachment of osteoblast cells on material surfaces. The role of substrate composition was speculated with regard to the differentiation process. An improved cellular response was observed on modified surfaces of TiZr using the anodization technique. The surface features namely higher nanoscale roughness and higher hydrophilicity contributed by the nanotubular morphology of the surface were important in enhancing the growth and differentiation of osteoblast cells when compared to unmodified surfaces.

In summary, the following conclusions can be drawn from the thesis

1. Influence of surface energy of titanium zirconium alloy on osteoblast cell functions *in vitro*

The two alloys of titanium namely TiZr and TiNb were biocompatible and were able to support the osteoblast cell growth. The morphology of cells also did not show any marked differences between the three material surfaces namely Ti, TiZr and TiNb on the surfaces studied and it can be concluded that it is a topography driven phenomenon where, the topography was similar on the three surfaces. Notable differences in the water contact angles and calculated surface energies were seen on the three material surfaces with the TiZr surface being more hydrophilic and having a higher surface energy. The roughness values of the materials were in the sub-micron range and therefore the differences in surface energy became a crucial factor in effecting the cell behavior at early stages of cell-material interactions. Increased adhesion and proliferation were seen on the TiZr surface with a higher surface energy compared to Ti and TiNb. The differentiation of cells was seen on all the three material surfaces but marked differences were seen with regard to ALP activity profiles. The activity was seen on the three material surfaces as a function of time, however, the process was accelerated on the TiZr surface compared to Ti and TiNb.

2. Role of surface properties of titanium alloys on the expression of adhesion and differentiation related genes

The molecular level responses of cells on the three material surfaces were evaluated by studying the expression profiles of genes involved in adhesion and differentiation. The expression of genes pertaining to adhesion were significantly higher on the TiZr surface with a higher surface energy compared to Ti and TiNb after 4h and 24h of cell seeding. Moreover, Integrin mediated cell signaling are differently regulated during the initial interactions of osteoblast cell with the material surfaces. This was strengthened by the observations that during the initial time period of cell attachment, the expression of integrins $\alpha 2$, $\alpha 5$, αV were upregulated on the TiZr compared to Ti and TiNb. The

corresponding increase in the expression of fibronectin and vitronectin genes (ECM molecules to which $\alpha 5$ and αV integrins respectively bind) at the same time points on the same surface supports the claim that integrins and their ECM ligands play a significant role in the adhesion of cells to Ti alloy surfaces. The expression of genes involved in differentiation was higher on the alloys surfaces compared to pure Ti. On the whole, the surface energy of materials plays a significant role in the adhesion and proliferation of osteoblasts and, the differentiation process was better on the alloys emphasizing the role of substrate composition of materials on osteoblast cell behavior.

3. Cell biological responses of osteoblasts on anodized nanotubular surface of a TiZr alloy

Of the three materials used in the study the TiZr alloy was selected for further improving the bioactive properties. In order to enhance the response of osteoblasts towards TiZr we have modified the surface using a technique called anodization and explored the response of osteoblast cells on these surfaces. Our results show that the nanotubular surface produced by anodization technique is an efficient means to promote accelerated attachment of osteoblasts and inducing rapid osseointegration at the bone-implant interface as evident by the enhanced behavior of cells on these surfaces at the cellular and molecular level. The nanotubular surface was more bioactive compared to the unmodified surface and acid etched surfaces. These results also indicate that optimized surface properties such as surface wettability, surface area and roughness at the nanoscale can synergistically improve biological outcome of cell-material interactions of osteoblasts vis-à-vis osteoblast cell adhesion, proliferation and differentiation.

7.2 Future directions

There are certain areas which could be explored from this study and the recommendations are formulated below:

- We have looked at the *in vitro* response of osteoblast cells towards the material surfaces. The ability of the materials to support bone growth and differentiation could be better understood by studying their properties *in vivo*. This could be attempted using animal model studies where animals such as rabbits could be used.
- The materials could be inserted in the region of tibia or femur bone for extended periods of time and carefully monitoring the progress of bone formation around the implant by histochemical studies. The *in vivo* cytotoxicity of the implant could also be evaluated by looking for the release of the metal into the blood stream and its possible effects if any.
- We have used MC3T3 cell line for this study where the cells might have lost some of their original osteoblast properties. Primary osteoblast cells or mesenchymal stem cells (MSCs) isolated from rat and mice models could be used for better evaluation of the performance of the materials and further understanding the role of surface properties in modulating the cell behavior. The use of these cells could give useful insights by mimicking the *in vivo* environment as encountered by the cells upon implantation of the materials.

Bibliography

- [1] Rupani A, Balint R, Cartmell S. Osteoblasts and their applications in bone tissue engineering. *Cell Health and Cytoskeleton* 2012;4:49-61.
- [2] Navarro M, Michiardi A, Castaño O, Planell J. Biomaterials in orthopaedics. *Journal of the Royal Society Interface* 2008;5:1137-58.
- [3] Nasab MB, Hassan MR. Metallic Biomaterials of Knee and Hip-A Review. *Trends in Biomaterials and Artificial Organs* 2010;24:69-82.
- [4] Internet]. nouhot. National Osteoporosis Society Figures; 2009. Available from: <http://www.nos.org.uk/NetCommunity/admin/DocumentDoc?id=47>.
- [5] Hoffman AS. Classes of Materials used in medicine: Introduction. In: Ratner BD, Hoffman AS, Schoen F, Lemons JE, editors. *Biomaterials Science: An Introduction to Materials in Medicine*: Elsevier Academic Press; 2004. p. 67.
- [6] Niinomi M. Mechanical biocompatibilities of titanium alloys for biomedical applications. *Journal of the mechanical behavior of biomedical materials* 2008;1:30-42.
- [7] Breme J, Biehl V. Metallic Biomaterials. In: Black J, Hastings G, editors. *Handbook of Biomaterial Properties*. London: Chapman and Hall 1998. p. 135-44.
- [8] Hallab NJ, Jacobs JJ, Katz JL. Application of Materials in Medicine, Biology, and Artificial Organs: Orthopedic applications. In: Ratner BD, Hoffman AS, Schoen FJ, Lemons JE, editors. *Biomaterials Science: An introduction to materials in medicine*: Elsevier Academic Press; 2004. p. 526-55.
- [9] Breme HJ, Helsen JA. Selection of Materials. In: Breme HJ, Helsen JA, editors. *Metals as Biomaterials*. Chichester: John Wiley & Sons; 1998. p. 1-35.
- [10] Ramsden J, Allen D, Stephenson D, Alcock J, Peggs G, Fuller G, et al. The design and manufacture of biomedical surfaces. *CIRP Annals-Manufacturing Technology* 2007;56:687-711.
- [11] Okazaki Y, Rao S, Tateishi T, Ito Y. Cytocompatibility of various metal and development of new titanium alloys for medical implants. *Materials Science and Engineering: A* 1998;243:250-6.
- [12] Okazaki Y, Gotoh E. Comparison of metal release from various metallic biomaterials in vitro. *Biomaterials* 2005;26:11-21.
- [13] Okazaki Y. Effect of friction on anodic polarization properties of metallic biomaterials. *Biomaterials* 2002;23:2071-7.
- [14] Geetha M, Singh A, Asokamani R, Gogia A. Ti based biomaterials, the ultimate choice for orthopaedic implants-A review. *Progress in Materials Science* 2009;54:397-425.
- [15] Niinomi M. Recent research and development in titanium alloys for biomedical applications and healthcare goods. *Science and Technology of Advanced Materials* 2003;4:445-54.
- [16] Niinomi M. Recent metallic materials for biomedical applications. *Metallurgical and materials transactions A* 2002;33:477-86.
- [17] Long M, Rack H. Titanium alloys in total joint replacement-a materials science perspective. *BIOMATERIALS-GUILDFORD*- 1998;19:1621-39.
- [18] Rolf S. The Corrosion Properties of Titanium and Titanium Alloys. In: Brunette D, Tengvall P, Textor M, Thomsen P, editors. *Titanium in medicine: material science, surface science, engineering, biological responses, and medical applications*: Berlin:Springer-Verlag; 2001. p. 145.
- [19] Hallab NJ, Urban RM, Jacobs JJ. Corrosion and biocompatibility of orthopaedic implants. In: Yaszemski M, Trantolo D, Lewandrowski K-U, Hasirci K-U, Wise D, Altobelli D, editors. *Biomaterials in Orthopedics UK*: Informa Health Care; 2003. p. 65.
- [20] Eisenbarth E, Meyle J, Nachtigall W, Breme J. Influence of the surface structure of titanium materials on the adhesion of fibroblasts. *Biomaterials* 1996;17:1399-403.

- [21] Thompson G, Puleo D. Ti-6Al-4V ion solution inhibition of osteogenic cell phenotype as a function of differentiation timecourse in vitro. *Biomaterials* 1996;17:1949-54.
- [22] Zaffe D, Bertoldi C, Consolo U. Accumulation of aluminium in lamellar bone after implantation of titanium plates, Ti-6Al-4V screws, hydroxyapatite granules. *Biomaterials* 2004;25:3837-44.
- [23] Li Y, Wong C, Xiong J, Hodgson P, Wen C. Cytotoxicity of titanium and titanium alloying elements. *Journal of dental research* 2010;89:493-7.
- [24] Black J. Biological performance of materials: Fundamentals of biocompatibility. Dekker (New York); 1992.
- [25] Hildebrand H, Hornez J. Biological response and biocompatibility. In: Helsen J, Breme H, editors. *Metals as Biomaterials*: Chichester, UK: Wiley; 1998. p. 265-90.
- [26] Kanazawa I, Yamaguchi T, Yano S, Yamauchi M, Yamamoto M, Sugimoto T. Adiponectin and AMP kinase activator stimulate proliferation, differentiation, and mineralization of osteoblastic MC3T3-E1 cells. *BMC cell biology* 2007;8:51.
- [27] Zhao G, Raines A, Wieland M, Schwartz Z, Boyan B. Requirement for both micron-and submicron scale structure for synergistic responses of osteoblasts to substrate surface energy and topography. *Biomaterials* 2007;28:2821-9.
- [28] Grausova L, Bacakova L, Kromka A, Vanecek M, Rezek B, Lisa V. Molecular markers of adhesion, maturation and immune activation of human osteoblast-like MG 63 cells on nanocrystalline diamond films. *Diamond and Related Materials* 2009;18:258-63.
- [29] Kalbacova M, Rezek B, Baresova V, Wolf-Brandstetter C, Kromka A. Nanoscale topography of nanocrystalline diamonds promotes differentiation of osteoblasts. *Acta biomaterialia* 2009;5:3076-85.
- [30] Webster TJ, Ergun C, Doremus RH, Siegel RW, Bizios R. Enhanced functions of osteoblasts on nanophase ceramics. *Biomaterials* 2000;21:1803-10.
- [31] Tambasco de Oliveira P, Nanci A. Nanotexturing of titanium-based surfaces upregulates expression of bone sialoprotein and osteopontin by cultured osteogenic cells. *Biomaterials* 2004;25:403-13.
- [32] de Oliveira PT, Zalzal SF, Beloti MM, Rosa AL, Nanci A. Enhancement of in vitro osteogenesis on titanium by chemically produced nanotopography. *Journal of Biomedical Materials Research Part A* 2007;80:554-64.
- [33] Anselme K, Biggerelle M. Topography effects of pure titanium substrates on human osteoblast long-term adhesion. *Acta biomaterialia* 2005;1:211-22.
- [34] Filová E, Bullett N, Bačáková L, Grausová L, Haycock J, Hlučilová J, et al. Regionally-selective Cell colonization Of micropatterned surfaces prepared plasma polymerization of acrylic acid and 1, 7-octadiene. *Physiological Research* 2009;58:669.
- [35] Bacakova L, Grausova L, Vacik J, Fraczek A, Blazewicz S, Kromka A, et al. Improved adhesion and growth of human osteoblast-like MG 63 cells on biomaterials modified with carbon nanoparticles. *Diamond and Related Materials* 2007;16:2133-40.
- [36] Schwartz Z, Boyan B. Underlying mechanisms at the bone-biomaterial interface. *Journal of cellular biochemistry* 1994;56:340-7.
- [37] Boyan BD, Hummert TW, Dean DD, Schwartz Z. Role of material surfaces in regulating bone and cartilage cell response. *Biomaterials* 1996;17:137-46.
- [38] Ong J, Prince C, Raikar G, Lucas L. Effect of surface topography of titanium on surface chemistry and cellular response. *Implant dentistry* 1996;5:83.
- [39] Martin J, Schwartz Z, Hummert T, Schraub D, Simpson J, Lankford Jr J, et al. Effect of titanium surface roughness on proliferation, differentiation, and protein synthesis of human osteoblast-like cells (MG63). *Journal of Biomedical Materials Research* 1995;29:389-401.

- [40] Sinha RK, Morris F, Shah SA, Tuan RS. Surface composition of orthopaedic implant metals regulates cell attachment, spreading, and cytoskeletal organization of primary human osteoblasts in vitro. *Clinical orthopaedics and related research* 1994;305:258.
- [41] Lincks J, Boyan B, Blanchard C, Lohmann C, Liu Y, Cochran D, et al. Response of MG63 osteoblast-like cells to titanium and titanium alloy is dependent on surface roughness and composition. *Biomaterials* 1998;19:2219-32.
- [42] Zreiqat H, Howlett CR. Titanium substrata composition influences osteoblastic phenotype: In vitro study. *Journal of Biomedical Materials Research* 1999;47:360-6.
- [43] Postiglione L, Di Domenico G, Ramaglia L, Montagnani S, Salzano S, Di Meglio F, et al. Behavior of SaOS-2 cells cultured on different titanium surfaces. *Journal of dental research* 2003;82:692-6.
- [44] Hallab NJ, Bundy KJ, O'Connor K, Moses RL, Jacobs JJ. Evaluation of metallic and polymeric biomaterial surface energy and surface roughness characteristics for directed cell adhesion. *Tissue engineering* 2001;7:55-71.
- [45] Anselme K, Bigerelle M, Noel B, Dufresne E, Judas D, Iost A, et al. Qualitative and quantitative study of human osteoblast adhesion on materials with various surface roughnesses. *Journal of Biomedical Materials Research* 2000;49:155-66.
- [46] Linez-Bataillon P, Monchau F, Bigerelle M, Hildebrand H. In vitro MC3T3 osteoblast adhesion with respect to surface roughness of Ti6Al4V substrates. *Biomolecular engineering* 2002;19:133-41.
- [47] Salido M, Vilches J, Gutierrez J, Vilches J. Actin cytoskeletal organization in human osteoblasts grown on different dental titanium implant surfaces. *Histology and histopathology* 2007;22:1355.
- [48] Jäger M, Urselmann F, Witte F, Zanger K, Li X, Ayers DC, et al. Osteoblast differentiation onto different biometals with an endoprosthetic surface topography in vitro. *Journal of Biomedical Materials Research Part A* 2008;86:61-75.
- [49] Hempel U, Hefti T, Kalbacova M, Wolf-Brandstetter C, Dieter P, Schlottig F. Response of osteoblast-like SAOS-2 cells to zirconia ceramics with different surface topographies. *Clinical Oral Implants Research* 2010;21:174-81.
- [50] Masaki C, Schneider GB, Zaharias R, Seabold D, Stanford C. Effects of implant surface microtopography on osteoblast gene expression. *Clinical Oral Implants Research* 2005;16:650-6.
- [51] Zhu X, Chen J, Scheideler L, Reichl R, Geis-Gerstorfer J. Effects of topography and composition of titanium surface oxides on osteoblast responses. *Biomaterials* 2004;25:4087-103.
- [52] Keselowsky BG, Collard DM, García AJ. Surface chemistry modulates focal adhesion composition and signaling through changes in integrin binding. *Biomaterials* 2004;25:5947-54.
- [53] Liu X, Lim JY, Donahue HJ, Dhurjati R, Mastro AM, Vogler EA. Influence of substratum surface chemistry/energy and topography on the human fetal osteoblastic cell line hFOB 1.19: phenotypic and genotypic responses observed in vitro. *Biomaterials* 2007;28:4535-50.
- [54] Zhu X, Chen J, Scheideler L, Altebaeumer T, Geis-Gerstorfer J, Kern D. Cellular reactions of osteoblasts to micron-and submicron-scale porous structures of titanium surfaces. *Cells Tissues Organs* 2004;178:13-22.
- [55] Allen LT, Tosetto M, Miller IS, O'Connor DP, Penney SC, Lynch I, et al. Surface-induced changes in protein adsorption and implications for cellular phenotypic responses to surface interaction. *Biomaterials* 2006;27:3096-108.
- [56] Dos Santos E, Farina M, Soares G, Anselme K. Surface energy of hydroxyapatite and β -tricalcium phosphate ceramics driving serum protein adsorption and osteoblast adhesion. *Journal of Materials Science: Materials in Medicine* 2008;19:2307-16.
- [57] Lord MS, Foss M, Besenbacher F. Influence of nanoscale surface topography on protein adsorption and cellular response. *Nano Today* 2010;5:66-78.
- [58] Wilson CJ, Clegg RE, Leavesley DI, Percy MJ. Mediation of biomaterial-cell interactions by adsorbed proteins: a review. *Tissue engineering* 2005;11:1-18.

- [59] Manivasagam G, Dhinasekaran D, Rajamanickam A. Biomedical Implants: Corrosion and its Prevention-A Review. *Recent Patents on Corrosion Science* 2010;2:40-54.
- [60] Le Guéhennec L, Soueidan A, Layrolle P, Amouriq Y. Surface treatments of titanium dental implants for rapid osseointegration. *Dental Materials* 2007;23:844-54.
- [61] Liu X, Chu PK, Ding C. Surface modification of titanium, titanium alloys, and related materials for biomedical applications. *Materials Science and Engineering: R: Reports* 2004;47:49-121.
- [62] Kurella A, Dahotre NB. Review paper: surface modification for bioimplants: the role of laser surface engineering. *Journal of biomaterials applications* 2005;20:5-50.
- [63] Yao C, Perla V, McKenzie JL, Slamovich EB, Webster TJ. Anodized Ti and Ti6Al4V possessing nanometer surface features enhances osteoblast adhesion. *Journal of Biomedical Nanotechnology* 2005;1:68-73.
- [64] Rodriguez R, Kim K, Ong JL. In vitro osteoblast response to anodized titanium and anodized titanium followed by hydrothermal treatment. *Journal of Biomedical Materials Research Part A* 2003;65:352-8.
- [65] Brammer KS, Oh S, Gallagher JO, Jin S. Enhanced cellular mobility guided by TiO₂ nanotube surfaces. *Nano letters* 2008;8:786-93.
- [66] Curtis ASG, Dalby M, Gadegaard N. Cell signaling arising from nanotopography: implications for nanomedical devices. *Nanomedicine* 2006;1:67-72.
- [67] Dalby M, Riehle M, Johnstone H, Affrossman S, Curtis A. In vitro reaction of endothelial cells to polymer demixed nanotopography. *Biomaterials* 2002;23:2945-54.
- [68] Gallagher J, McGhee K, Wilkinson C, Riehle M. Interaction of animal cells with ordered nanotopography. *NanoBioscience, IEEE Transactions on* 2002;1:24-8.
- [69] Park J, Bauer S, von der Mark K, Schmuki P. Nanosize and vitality: TiO₂ nanotube diameter directs cell fate. *Nano letters* 2007;7:1686-91.
- [70] Webster TJ, Eijffinger JU. Increased osteoblast adhesion on nanophase metals: Ti, Ti6Al4V, and CoCrMo. *Biomaterials* 2004;25:4731-9.
- [71] Decuzzi P, Ferrari M. Modulating cellular adhesion through nanotopography. *Biomaterials* 2010;31:173-9.
- [72] Lamers E, van Horssen R, te Riet J, van Delft F, Luttge R, Walboomers X, et al. The influence of nanoscale topographical cues on initial osteoblast morphology and migration. *European Cells and Materials* 2010;20:329-43.
- [73] Webster TJ, Schadler LS, Siegel RW, Bizios R. Mechanisms of enhanced osteoblast adhesion on nanophase alumina involve vitronectin. *Tissue engineering* 2001;7:291-301.
- [74] Dalby MJ, Gadegaard N, Tare R, Andar A, Riehle MO, Herzyk P, et al. The control of human mesenchymal cell differentiation using nanoscale symmetry and disorder. *Nature materials* 2007;6:997-1003.
- [75] Balasundaram G, Yao C, Webster TJ. TiO₂ nanotubes functionalized with regions of bone morphogenetic protein-2 increases osteoblast adhesion. *Journal of Biomedical Materials Research Part A* 2008;84:447-53.
- [76] Cui X, Kim HM, Kawashita M, Wang L, Xiong T, Kokubo T, et al. Preparation of bioactive titania films on titanium metal via anodic oxidation. *Dental Materials* 2009;25:80-6.
- [77] Biggs MJP, Richards R, Gadegaard N, Wilkinson CDW, Dalby M. The effects of nanoscale pits on primary human osteoblast adhesion formation and cellular spreading. *Journal of Materials Science: Materials in Medicine* 2007;18:399-404.
- [78] Biggs MJP, Richards RG, Gadegaard N, McMurray RJ, Affrossman S, Wilkinson CDW, et al. Interactions with nanoscale topography: adhesion quantification and signal transduction in cells of osteogenic and multipotent lineage. *Journal of Biomedical Materials Research Part A* 2009;91:195-208.

- [79] Lamers E, Frank Walboomers X, Domanski M, te Riet J, van Delft FC, Luttge R, et al. The influence of nanoscale grooved substrates on osteoblast behavior and extracellular matrix deposition. *Biomaterials* 2010;31:3307-16.
- [80] Tsai WB, Ting YC, Yang JY, Lai JY, Liu HL. Fibronectin modulates the morphology of osteoblast-like cells (MG-63) on nano-grooved substrates. *Journal of Materials Science: Materials in Medicine* 2009;20:1367-78.
- [81] Oh S, Daraio C, Chen LH, Pisanic TR, Finones RR, Jin S. Significantly accelerated osteoblast cell growth on aligned TiO₂ nanotubes. *Journal of Biomedical Materials Research Part A* 2006;78:97-103.
- [82] Yao C, Slamovich EB, Webster TJ. Enhanced osteoblast functions on anodized titanium with nanotube-like structures. *Journal of Biomedical Materials Research Part A* 2008;85:157-66.
- [83] Bjursten LM, Rasmusson L, Oh S, Smith GC, Brammer KS, Jin S. Titanium dioxide nanotubes enhance bone bonding in vivo. *Journal of Biomedical Materials Research Part A* 2010;92:1218-24.
- [84] Das K, Bose S, Bandyopadhyay A. TiO₂ nanotubes on Ti: Influence of nanoscale morphology on bone cell-materials interaction. *Journal of Biomedical Materials Research Part A* 2009;90:225-37.
- [85] Choi J, Wehrspohn RB, Lee J, Gösele U. Anodization of nanoimprinted titanium: a comparison with formation of porous alumina. *Electrochimica acta* 2004;49:2645-52.
- [86] Chiesa R, Sandrini E, Santin M, Rondelli G, Cigada A. Osteointegration of titanium and its alloys by anodic spark deposition and other electrochemical techniques: A review. *Journal of Applied Biomaterials and Biomechanics* 2003;1:91-107.
- [87] Suh JY, Jang BC, Zhu X, Ong JL, Kim K. Effect of hydrothermally treated anodic oxide films on osteoblast attachment and proliferation. *Biomaterials* 2003;24:347-55.
- [88] Yang B, Uchida M, Kim HM, Zhang X, Kokubo T. Preparation of bioactive titanium metal via anodic oxidation treatment. *Biomaterials* 2004;25:1003-10.
- [89] Sul YT, Johansson CB, Jeong Y, Albrektsson T. The electrochemical oxide growth behaviour on titanium in acid and alkaline electrolytes. *Medical engineering & physics* 2001;23:329-46.
- [90] Gong D, Grimes C, Varghese OK, Hu W, Singh R, Chen Z, et al. Titanium oxide nanotube arrays prepared by anodic oxidation. *Journal of Materials Research* 2001;16:3331-4.
- [91] Ercan B, Webster TJ. Greater osteoblast proliferation on anodized nanotubular titanium upon electrical stimulation. *International journal of nanomedicine* 2008;3:477.
- [92] Dalby MJ, McCloy D, Robertson M, Agheli H, Sutherland D, Affrossman S, et al. Osteoprogenitor response to semi-ordered and random nanotopographies. *Biomaterials* 2006;27:2980-7.
- [93] Weiner S, Wagner HD. The material bone: structure-mechanical function relations. *Annual Review of Materials Science* 1998;28:271-98.
- [94] Zhang Y, Bataillon-Linez P, Huang P, Zhao Y, Han Y, Traisnel M, et al. Surface analyses of micro-arc oxidized and hydrothermally treated titanium and effect on osteoblast behavior. *Journal of Biomedical Materials Research Part A* 2004;68:383-91.
- [95] Feng B, Weng J, Yang B, Qu S, Zhang X. Characterization of surface oxide films on titanium and adhesion of osteoblast. *Biomaterials* 2003;24:4663-70.
- [96] http://academic.kellogg.edu/herbrandsonc/bio201_mckinley/skeletal.htm.
- [97] Pande G, Sravanthi R, Kapoor R. Bioinspired and Biomimetic Functional Hybrids as Tools for Regeneration of Orthopedic Interfaces. In: George A, editor. *Advances in Biomimetics: In Tech*; 2011. p. 373-96.
- [98] Jayakumar P, Di Silvio L. Osteoblasts in bone tissue engineering. *Proceedings of the Institution of Mechanical Engineers, Part H: Journal of Engineering in Medicine* 2010;224:1415-40.
- [99] Lanza RP, Vacanti J. *Principles of tissue engineering*: Academic Press; 2007.
- [100] Yang X, Karsenty G. Transcription factors in bone: developmental and pathological aspects. *Trends in molecular medicine* 2002;8:340-5.

- [101] Kanczler J, Oreffo R. Osteogenesis and angiogenesis: the potential for engineering bone. *Eur Cell Mater* 2008;15:100-14.
- [102] Clines GA. Prospects for osteoprogenitor stem cells in fracture repair and osteoporosis. *Current opinion in organ transplantation* 2010;15:73.
- [103] Komori T. Regulation of bone development and maintenance by Runx2. *Frontiers in bioscience: a journal and virtual library* 2008;13:898.
- [104] Komori T. Regulation of bone development and extracellular matrix protein genes by RUNX2. *Cell and tissue research* 2010;339:189-95.
- [105] Hing KA. Bone repair in the twenty-first century: biology, chemistry or engineering? *Philosophical Transactions of the Royal Society of London Series A: Mathematical, Physical and Engineering Sciences* 2004;362:2821-50.
- [106] Cheng H, Jiang W, Phillips FM, Haydon RC, Peng Y, Zhou L, et al. Osteogenic activity of the fourteen types of human bone morphogenetic proteins (BMPs). *The Journal of Bone and Joint Surgery (American)* 2003;85:1544-52.
- [107] Fröhlich M, Grayson WL, Wan LQ, Marolt D, Drobic M, Vunjak-Novakovic G. Tissue engineered bone grafts: biological requirements, tissue culture and clinical relevance. *Current stem cell research & therapy* 2008;3:254.
- [108] Bilezikian JP, Raisz LG, Martin TJ. *Principles of bone biology*: Elsevier; 2008.
- [109] Young B, Wheeler PR. *Wheeler's functional histology: a text and colour atlas*: Churchill Livingstone; 2006.
- [110] Shirley D, Marsh D, Jordan G, McQuaid S, Li G. Systemic recruitment of osteoblastic cells in fracture healing. *Journal of orthopaedic research* 2005;23:1013-21.
- [111] Boyle WJ, Simonet WS, Lacey DL. Osteoclast differentiation and activation. *Nature* 2003;423:337-42.
- [112] Göthlin G, Ericsson J. The osteoclast: review of ultrastructure, origin, and structure-function relationship. *Clinical orthopaedics and related research* 1976:201.
- [113] Teitelbaum SL. Bone resorption by osteoclasts. *Science* 2000;289:1504-8.
- [114] Palumbo C, Palazzini S, Zaffe D, Marotti G. Osteocyte differentiation in the tibia of newborn rabbit: an ultrastructural study of the formation of cytoplasmic processes. *Cells Tissues Organs* 1990;137:350-8.
- [115] Ehrlich P, Lanyon L. Mechanical strain and bone cell function: a review. *Osteoporosis International* 2002;13:688-700.
- [116] Chen JH, Liu C, You L, Simmons CA. Boning up on Wolff's Law: Mechanical regulation of the cells that make and maintain bone. *Journal of biomechanics* 2010;43:108-18.
- [117] You L, Temiyasathit S, Lee P, Kim CH, Tummala P, Yao W, et al. Osteocytes as mechanosensors in the inhibition of bone resorption due to mechanical loading. *Bone* 2008;42:172-9.
- [118] Furlan F, Lecanda F, Screen J, Civitelli R. Proliferation, differentiation and apoptosis in connexin43-null osteoblasts. *Cell Communication and Adhesion* 2001;8:367-71.
- [119] Schiller PC, D'Ippolito G, Brambilla R, Roos BA, Howard GA. Inhibition of gap-junctional communication induces the trans-differentiation of osteoblasts to an adipocytic phenotype in vitro. *Journal of Biological Chemistry* 2001;276:14133-8.
- [120] Jørgensen NR, Henriksen Z, Sørensen OH, Eriksen EF, Civitelli R, Steinberg TH. Intercellular calcium signaling occurs between human osteoblasts and osteoclasts and requires activation of osteoclast P2X7 receptors. *Journal of Biological Chemistry* 2002;277:7574-80.
- [121] Knothe Tate ML. "Whither flows the fluid in bone?" An osteocyte's perspective. *Journal of biomechanics* 2003;36:1409-24.

- [122] Taylor AF, Saunders MM, Shingle DL, Cimbala JM, Zhou Z, Donahue HJ. Mechanically stimulated osteocytes regulate osteoblastic activity via gap junctions. *American Journal of Physiology-Cell Physiology* 2007;292:C545-C52.
- [123] Lane NE, Yao W, Balooch M, Nalla RK, Balooch G, Habelitz S, et al. Glucocorticoid-Treated Mice Have Localized Changes in Trabecular Bone Material Properties and Osteocyte Lacunar Size That Are Not Observed in Placebo-Treated or Estrogen-Deficient Mice. *Journal of Bone and Mineral Research* 2006;21:466-76.
- [124] Feng JQ, Ward LM, Liu S, Lu Y, Xie Y, Yuan B, et al. Loss of DMP1 causes rickets and osteomalacia and identifies a role for osteocytes in mineral metabolism. *Nature genetics* 2006;38:1310-5.
- [125] Toyosawa S, Shintani S, Fujiwara T, Ooshima T, Sato A, Ijuhin N, et al. Dentin matrix protein 1 is predominantly expressed in chicken and rat osteocytes but not in osteoblasts. *Journal of Bone and Mineral Research* 2001;16:2017-26.
- [126] Clarke B. Normal bone anatomy and physiology. *Clinical Journal of the American Society of Nephrology* 2008;3:S131-S9.
- [127] Kalfas IH. Principles of bone healing. *Neurosurgical focus* 2001;10:1-4.
- [128] Weiner S, Addadi L. Design strategies in mineralized biological materials. *Journal of Materials Chemistry* 1997;7:689-702.
- [129] Vincent JFV. Biomimetic modelling. *Philosophical Transactions of the Royal Society of London Series B: Biological Sciences* 2003;358:1597-603.
- [130] Ciancaglini P, Simão A, Camolezi F, Millan J, Pizauro J. Contribution of matrix vesicles and alkaline phosphatase to ectopic bone formation. *Brazilian journal of medical and biological research* 2006;39:603-10.
- [131] Shapiro F. Bone development and its relation to fracture repair. The role of mesenchymal osteoblasts and surface osteoblasts. *Eur Cell Mater* 2008;15:53-76.
- [132] Lemaire V, Tobin FL, Greller LD, Cho CR, Suva LJ. Modeling the interactions between osteoblast and osteoclast activities in bone remodeling. *Journal of theoretical biology* 2004;229:293-309.
- [133] Kobayashi Y, Udagawa N, Takahashi N. Action of RANKL and OPG for osteoclastogenesis. *Critical reviews in eukaryotic gene expression* 2009;19:61.
- [134] Martin T, Ng K. Mechanisms by which cells of the osteoblast lineage control osteoclast formation and activity. *Journal of cellular biochemistry* 1994;56:357-66.
- [135] Heinemann C, Heinemann S, Worch H, Hanke T. Development of an osteoblast/osteoclast co-culture derived by human bone marrow stromal cells and human monocytes for biomaterials testing. *European Cells and Materials* 2011;21:80-93.
- [136] Arkin AM, Katz JF. The Effects of Pressure on Epiphyseal Growth The Mechanism of Plasticity of Growing Bone. *The Journal of Bone and Joint Surgery (American)* 1956;38:1056-76.
- [137] Praemer A, Furner S, Rice DP, Surgeons AAoO. Musculoskeletal conditions in the United States: American Academy of Orthopaedic Surgeons Park Ridge, IL; 1992.
- [138] Lane NE. Epidemiology, etiology, and diagnosis of osteoporosis. *American Journal of Obstetrics and gynecology* 2006;194:S3-S11.
- [139] KHOSIA S, Riggs BL. Pathophysiology of age-related bone loss and osteoporosis. *Endocrinology and metabolism clinics of North America* 2005;34.
- [140] Jilka RL, Weinstein RS, Takahashi K, Parfitt AM, Manolagas SC. Linkage of decreased bone mass with impaired osteoblastogenesis in a murine model of accelerated senescence. *Journal of Clinical Investigation* 1996;97:1732.
- [141] Giannoudis PV, Dinopoulos H, Tsiridis E. Bone substitutes: An update. *Injury* 2005;36:S20-S7.
- [142] Laurencin C, Khan Y, El-Amin SF. Bone graft substitutes. Expert review of medical devices 2006;3:49-57.

- [143] Albert A, Leemrijse T, Druez V, Delloye C, Cornu O. Are bone autografts still necessary in 2006? A three-year retrospective study of bone grafting. *Acta orthopaedica belgica* 2006;72:734.
- [144] Bueno EM, Glowacki J. Cell-free and cell-based approaches for bone regeneration. *Nature Reviews Rheumatology* 2009;5:685-97.
- [145] Hernigou P, Poignard A, Beaujean F, Rouard H. Percutaneous Autologous Bone-Marrow Grafting for Nonunions Influence of the Number and Concentration of Progenitor Cells. *The Journal of Bone and Joint Surgery (American)* 2005;87:1430-7.
- [146] Kaigler D, Pagni G, Park CH, Tarle SA, Bartel RL, Giannobile WV. Angiogenic and osteogenic potential of bone repair cells for craniofacial regeneration. *Tissue Engineering Part A* 2010;16:2809-20.
- [147] Charnley J. Anchorage of the femoral head prosthesis to the shaft of the femur. *Journal of Bone and Joint Surgery-British Volume* 1960;42:28.
- [148] Sivakumar M, Kamachi Mudali U, Rajeswari S. Investigation of failures in stainless steel orthopaedic implant devices: fatigue failure due to improper fixation of a compression bone plate. *Journal of materials science letters* 1994;13:142-5.
- [149] Dong H, Nagamatsu Y, Chen KK, Tajima K, Kakigawa H, Shi S, et al. Corrosion behavior of dental alloys in various types of electrolyzed water. *Dental materials journal* 2003;22:482.
- [150] Vidal CV, Muñoz AI. Effect of thermal treatment and applied potential on the electrochemical behaviour of CoCrMo biomedical alloy. *Electrochimica acta* 2009;54:1798-809.
- [151] Brånemark P, Breine U, Johansson B, Roylance P, Röckert H, Yoffey J. Regeneration of bone marrow. *Cells Tissues Organs* 1964;59:1-46.
- [152] Niinomi M. Fatigue characteristics of metallic biomaterials. *International Journal of Fatigue* 2007;29:992-1000.
- [153] Pohler OEM. Unalloyed titanium for implants in bone surgery. *Injury* 2000;31:D7-D13.
- [154] Shabalovskaya SA. On the nature of the biocompatibility and on medical applications of NiTi shape memory and superelastic alloys. *Bio-medical materials and engineering* 1996;6:267-89.
- [155] Wang K. The use of titanium for medical applications in the USA. *Materials Science and Engineering: A* 1996;213:134-7.
- [156] Mjöberg B, Hellquist E, Mallmin H, Lindh U. Aluminum, Alzheimer's disease and bone fragility. *Acta Orthopaedica* 1997;68:511-4.
- [157] Okazaki Y, Rao S, Asao S, Tateishi T, KATSUDA SI, Furuki Y. Effects of Ti, Al and V concentrations on cell viability. *Materials transactions-JIM* 1998;39:1053-62.
- [158] Köster R, Vieluf D, Kiehn M, Sommerauer M, Kähler J, Baldus S, et al. Nickel and molybdenum contact allergies in patients with coronary in-stent restenosis. *The Lancet* 2000;356:1895-7.
- [159] Semlitsch MF, Weber H, Streicher RM, Schön R. Joint replacement components made of hot-forged and surface-treated Ti-6Al-7Nb alloy. *Biomaterials* 1992;13:781-8.
- [160] Niinomi M. Mechanical properties of biomedical titanium alloys. *Materials Science and Engineering: A* 1998;243:231-6.
- [161] Davidson J, Mishra A, Kovacs P, Poggie R. New surface-hardened, low-modulus, corrosion-resistant Ti-13Nb-13Zr alloy for total hip arthroplasty. *Bio-medical materials and engineering* 1994;4:231-43.
- [162] Okazaki Y, Ito Y, Kyo K, Tateishi T. Corrosion resistance and corrosion fatigue strength of new titanium alloys for medical implants without V and Al. *Materials Science and Engineering: A* 1996;213:138-47.
- [163] Ito A, Okazaki Y, Tateishi T, Ito Y. In vitro biocompatibility, mechanical properties, and corrosion resistance of Ti-Zr-Nb-Ta-Pd and Ti-Sn-Nb-Ta-Pd alloys. *Journal of Biomedical Materials Research* 1995;29:893-900.
- [164] Nouri A, Chen X, Hodgson PD, Wen CE. Preparation and characterisation of new titanium based alloys for orthopaedic and dental applications. *Advanced materials research* 2007;15:71-6.

- [165] Matsumoto H, Watanabe S, Hanada S. Strengthening of low Young's modulus beta Ti-Nb-Sn alloys by thermomechanical processing. *Proceeding of the Materials & Processes for Medical Devices Conference*. Boston, Massachusetts, USA: ASM International; 2006. p. 9-14.
- [166] Okazaki Y. A New Ti-15Zr-4Nb-4Ta alloy for medical applications. *Current Opinion in Solid State and Materials Science* 2001;5:45-53.
- [167] Niinomi M, Akahori T, Takeuchi T, Katsura S, Fukui H, Toda H. Mechanical properties and cytotoxicity of new beta type titanium alloy with low melting points for dental applications. *Materials Science and Engineering: C* 2005;25:417-25.
- [168] Kobayashi E, Matsumoto S, Doi H, Yoneyama T, Hamanaka H. Mechanical properties of the binary titanium-zirconium alloys and their potential for biomedical materials. *Journal of Biomedical Materials Research* 1995;29:943-50.
- [169] Ho WF, Chen WK, Wu SC, Hsu HC. Structure, mechanical properties, and grindability of dental Ti-Zr alloys. *Journal of Materials Science: Materials in Medicine* 2008;19:3179-86.
- [170] Kikuchi M, Takahashi M, Okuno O. Mechanical properties and grindability of dental cast Ti-Nb alloys. *Dental materials journal* 2003;22:328.
- [171] Trillo E, Ortiz C, Dickerson P, Villa R, Stafford S, Murr L. Evaluation of mechanical and corrosion biocompatibility of TiTa alloys. *Journal of Materials Science: Materials in Medicine* 2001;12:283-92.
- [172] Wen C, Yamada Y, Hodgson P. Fabrication of novel TiZr alloy foams for biomedical applications. *Materials Science and Engineering: C* 2006;26:1439-44.
- [173] Xiong J, Li Y, Wang X, Hodgson P, Wen C. Mechanical properties and bioactive surface modification via alkali-heat treatment of a porous Ti-18Nb-4Sn alloy for biomedical applications. *Acta biomaterialia* 2008;4:1963-8.
- [174] Chen X, Nouri A, Hodgson PD, Wen CE. Surface modification of TiZr alloy for biomedical application. *Advanced materials research* 2007;15:89-94.
- [175] Branemark PI. Osseointegration and its experimental background. *The Journal of Prosthetic Dentistry* 1983;50:399-410.
- [176] Puleo D, Nanci A. Understanding and controlling the bone-implant interface. *Biomaterials* 1999;20:2311-21.
- [177] Anselme K. Osteoblast adhesion on biomaterials. *Biomaterials* 2000;21:667-81.
- [178] Kokubo T. Design of bioactive bone substitutes based on biomineralization process. *Materials Science and Engineering: C* 2005;25:97-104.
- [179] Cho SA, Park KT. The removal torque of titanium screw inserted in rabbit tibia treated by dual acid etching. *Biomaterials* 2003;24:3611-7.
- [180] Takeuchi M, Abe Y, Yoshida Y, Nakayama Y, Okazaki M, Akagawa Y. Acid pretreatment of titanium implants. *Biomaterials* 2003;24:1821-7.
- [181] Wen H, Liu Q, De Wijn J, De Groot K, Cui F. Preparation of bioactive microporous titanium surface by a new two-step chemical treatment. *Journal of Materials Science: Materials in Medicine* 1998;9:121-8.
- [182] Takeuchi K, Saruwatari L, Nakamura HK, Yang JM, Ogawa T. Enhanced intrinsic biomechanical properties of osteoblastic mineralized tissue on roughened titanium surface. *Journal of Biomedical Materials Research Part A* 2005;72:296-305.
- [183] Wong M, Eulenberger J, Schenk R, Hunziker E. Effect of surface topology on the osseointegration of implant materials in trabecular bone. *Journal of Biomedical Materials Research* 1995;29:1567-75.
- [184] Klokkevold PR, Johnson P, Dadgostari S, Davies JE, Caputo A, Nishimura RD. Early endosseous integration enhanced by dual acid etching of titanium: a torque removal study in the rabbit. *Clinical Oral Implants Research* 2001;12:350-7.
- [185] Davies J. Mechanisms of endosseous integration. *The International journal of prosthodontics* 1998;11:391.

- [186] Trisi P, Lazzara R, Rebaudi A, Rao W, Testori T, Porter SS. Bone-implant contact on machined and dual acid-etched surfaces after 2 months of healing in the human maxilla. *Journal of periodontology* 2003;74:945-56.
- [187] Trisi P, Lazzara R, Rao W, Rebaudi A. Bone-implant contact and bone quality: evaluation of expected and actual bone contact on machined and Osseotite implant surfaces. *The International journal of periodontics & restorative dentistry* 2002;22:535.
- [188] Cochran D, Schenk R, Lussi A, Higginbottom F, Buser D. Bone response to unloaded and loaded titanium implants with a sandblasted and acid-etched surface: a histometric study in the canine mandible. *Journal of Biomedical Materials Research* 1998;40:1-11.
- [189] Cochran DL, Buser D, Ten Bruggenkate CM, Weingart D, Taylor TM, Bernard JP, et al. The use of reduced healing times on ITI® implants with a sandblasted and acid-etched (SLA) surface. *Clinical Oral Implants Research* 2002;13:144-53.
- [190] Buser D, Schenk R, Steinemann S, Fiorellini J, Fox C, Stich H. Influence of surface characteristics on bone integration of titanium implants. A histomorphometric study in miniature pigs. *Journal of Biomedical Materials Research* 1991;25:889-902.
- [191] Cochran D, Nummikoski P, Higginbottom F, Hermann J, Makins S, Buser D. Evaluation of an endosseous titanium implant with a sandblasted and acid-etched surface in the canine mandible: radiographic results. *Clinical Oral Implants Research* 1996;7:240-52.
- [192] Tengvall P, Elwing H, Lundström I. Titanium gel made from metallic titanium and hydrogen peroxide. *Journal of Colloid and Interface Science* 1989;130:405-13.
- [193] Tengvall P, Elwing H, Sjöqvist L, Lundström I, Bjursten LM. Interaction between hydrogen peroxide and titanium: a possible role in the biocompatibility of titanium. *Biomaterials* 1989;10:118-20.
- [194] Wang XX, Hayakawa S, Tsuru K, Osaka A. Bioactive titania gel layers formed by chemical treatment of Ti substrate with a H₂O₂/HCl solution. *Biomaterials* 2002;23:1353-7.
- [195] Pan J, Liao H, Leygraf C, Thierry D, Li J. Variation of oxide films on titanium induced by osteoblast-like cell culture and the influence of an H₂O₂ pretreatment. *Journal of Biomedical Materials Research* 1998;40:244-56.
- [196] Wang XX, Hayakawa S, Tsuru K, Osaka A. Improvement of bioactivity of H₂O₂/TaCl₅-treated titanium after subsequent heat treatments. *Journal of Biomedical Materials Research* 2000;52:171-6.
- [197] Sittig C, Textor M, Spencer N, Wieland M, Vallotton P. Surface characterization. *Journal of Materials Science: Materials in Medicine* 1999;10:35-46.
- [198] Wen H, Wolke J, De Wijn J, Liu Q, Cui F, De Groot K. Fast precipitation of calcium phosphate layers on titanium induced by simple chemical treatments. *Biomaterials* 1997;18:1471-8.
- [199] Kim HM, Miyaji F, Kokubo T, Nakamura T. Preparation of bioactive Ti and its alloys via simple chemical surface treatment. *Journal of Biomedical Materials Research* 1996;32:409-17.
- [200] Kokubo T, Miyaji F, Kim HM, Nakamura T. Spontaneous formation of bonelike apatite layer on chemically treated titanium metals. *Journal of the American Ceramic Society* 1996;79:1127-9.
- [201] Nishiguchi S, Fujibayashi S, Kim HM, Kokubo T, Nakamura T. Biology of alkali-and heat-treated titanium implants. *Journal of Biomedical Materials Research Part A* 2003;67:26-35.
- [202] Kokubo T, Kim HM, Kawashita M. Novel bioactive materials with different mechanical properties. *Biomaterials* 2003;24:2161-75.
- [203] Lee BH, Kim YD, Lee KH. XPS study of bioactive graded layer in Ti-In-Nb-Ta alloy prepared by alkali and heat treatments. *Biomaterials* 2003;24:2257-66.
- [204] Lee BH, Do Kim Y, Shin JH, Hwan Lee K. Surface modification by alkali and heat treatments in titanium alloys. *Journal of Biomedical Materials Research* 2002;61:466-73.
- [205] Bagno A, Di Bello C. Surface treatments and roughness properties of Ti-based biomaterials. *Journal of Materials Science: Materials in Medicine* 2004;15:935-49.

- [206] Lausmaa J. Mechanical, thermal, chemical and electrochemical surface treatment of titanium. Berlin: Springer-Verlag: Heidelberg and Berlin; 2001.
- [207] Kuromoto NK, Simão RA, Soares GA. Titanium oxide films produced on commercially pure titanium by anodic oxidation with different voltages. *Materials characterization* 2007;58:114-21.
- [208] Das K, Bose S, Bandyopadhyay A. Surface modifications and cell-materials interactions with anodized Ti. *Acta biomaterialia* 2007;3:573-85.
- [209] Sul YT, Johansson CB, Jeong Y, Röser K, Wennerberg A, Albrektsson T. Oxidized implants and their influence on the bone response. *Journal of Materials Science: Materials in Medicine* 2001;12:1025-31.
- [210] Sul YT, Johansson CB, Jeong Y, Wennerberg A, Albrektsson T. Resonance frequency and removal torque analysis of implants with turned and anodized surface oxides. *Clinical Oral Implants Research* 2002;13:252-9.
- [211] Rocci A, Martignoni M, Gottlow J. Immediate Loading of Brånemark System® TiUnite™ and Machined-Surface Implants in the Posterior Mandible: A Randomized Open-Ended Clinical Trial. *Clinical implant dentistry and related research* 2003;5:57-63.
- [212] Jungner M, Lundqvist P, Lundgren S. Oxidized titanium implants (Nobel Biocare® TiUnite™) compared with turned titanium implants (Nobel Biocare® mark III™) with respect to implant failure in a group of consecutive patients treated with early functional loading and two-stage protocol. *Clinical Oral Implants Research* 2005;16:308-12.
- [213] Park K, Heo S, Koak J, Kim S, Lee J, Kim S, et al. Osseointegration of anodized titanium implants under different current voltages: a rabbit study. *Journal of oral rehabilitation* 2007;34:517-27.
- [214] Sul YT, Johansson C, Wennerberg A, Cho LR, Chang BS, Albrektsson T. Optimum surface properties of oxidized implants for reinforcement of osseointegration: surface chemistry, oxide thickness, porosity, roughness, and crystal structure. *The International journal of oral & maxillofacial implants* 2005;20:349.
- [215] Schüpbach P, Glauser R, Rocci A, Martignoni M, Sennerby L, Lundgren AK, et al. The Human Bone–Oxidized Titanium Implant Interface: A Light Microscopic, Scanning Electron Microscopic, Back-Scatter Scanning Electron Microscopic, and Energy-Dispersive X-Ray Study of Clinically Retrieved Dental Implants. *Clinical implant dentistry and related research* 2005;7:s36-s43.
- [216] Zhu X, Kim KH, Jeong Y. Anodic oxide films containing Ca and P of titanium biomaterial. *Biomaterials* 2001;22:2199-206.
- [217] Zhao L, Wei Y, Li J, Han Y, Ye R, Zhang Y. Initial osteoblast functions on Ti-5Zr-3Sn-5Mo-15Nb titanium alloy surfaces modified by microarc oxidation. *Journal of Biomedical Materials Research Part A* 2010;92:432-40.
- [218] Wu J, Liu ZM, Zhao XH, Gao Y, Hu J, Gao B. Improved biological performance of microarc-oxidized low-modulus Ti-24Nb-4Zr-7.9 Sn alloy. *Journal of Biomedical Materials Research Part B: Applied Biomaterials* 2010;92:298-306.
- [219] Frauchiger V, Schlottig F, Gasser B, Textor M. Anodic plasma-chemical treatment of CP titanium surfaces for biomedical applications. *Biomaterials* 2004;25:593-606.
- [220] Shirkhanzadeh M, Azadegan M, Stack V, Schreyer S. Fabrication of pure hydroxyapatite and fluoridated-hydroxyapatite coatings by electrocrystallisation. *Materials Letters* 1994;18:211-4.
- [221] Ishizawa H, Ogino M. Characterization of thin hydroxyapatite layers formed on anodic titanium oxide films containing Ca and P by hydrothermal treatment. *Journal of Biomedical Materials Research* 1995;29:1071-9.
- [222] Born R, Scharnweber D, Rößler S, Stölzel M, Thieme M, Wolf C, et al. Surface analysis of titanium based biomaterials. *Fresenius' journal of analytical chemistry* 1998;361:697-700.
- [223] Zhao J, Wang X, Chen R, Li L. Fabrication of titanium oxide nanotube arrays by anodic oxidation. *Solid state communications* 2005;134:705-10.

- [224] Cai Q, Paulose M, Varghese OK, Grimes CA. The effect of electrolyte composition on the fabrication of self-organized titanium oxide nanotube arrays by anodic oxidation. *Journal of Materials Research* 2005;20:230-6.
- [225] Park J, Bauer S, Schlegel KA, Neukam FW, von der Mark K, Schmuki P. TiO₂ nanotube surfaces: 15 nm—An optimal length scale of surface topography for cell adhesion and differentiation. *Small* 2009;5:666-71.
- [226] Yu W, Jiang X, Zhang F, Xu L. The effect of anatase TiO₂ nanotube layers on MC3T3-E1 preosteoblast adhesion, proliferation, and differentiation. *Journal of Biomedical Materials Research Part A* 2010;94:1012-22.
- [227] Brunette DM. *Titanium in medicine: material science, surface science, engineering, biological responses, and medical applications*: Springer Verlag; 2001.
- [228] Griffith LG, Naughton G. Tissue engineering--current challenges and expanding opportunities. *Science* 2002;295:1009-14.
- [229] Sipe JD. Tissue engineering and reparative medicine. *Annals of the New York Academy of Sciences* 2002;961:1-9.
- [230] Le Guehennec L, Lopez-Heredia MA, Enkel B, Weiss P, Amouriq Y, Layrolle P. Osteoblastic cell behaviour on different titanium implant surfaces. *Acta biomaterialia* 2008;4:535-43.
- [231] Jayaraman M, Meyer U, Bühner M, Joos U, Wiesmann HP. Influence of titanium surfaces on attachment of osteoblast-like cells in vitro. *Biomaterials* 2004;25:625-31.
- [232] Eisenbarth E, Linez P, Biehl V, Velten D, Breme J, Hildebrand H. Cell orientation and cytoskeleton organisation on ground titanium surfaces. *Biomolecular engineering* 2002;19:233-7.
- [233] Khang D, Lu J, Yao C, Haberstroh KM, Webster TJ. The role of nanometer and sub-micron surface features on vascular and bone cell adhesion on titanium. *Biomaterials* 2008;29:970-83.
- [234] Mendonça G, Mendonça D, Aragao FJL, Cooper LF. Advancing dental implant surface technology—from micron-to nanotopography. *Biomaterials* 2008;29:3822-35.
- [235] Schneider GB, Zaharias R, Seabold D, Keller J, Stanford C. Differentiation of preosteoblasts is affected by implant surface microtopographies. *Journal of Biomedical Materials Research Part A* 2004;69:462-8.
- [236] Wennerberg A, Albrektsson T. Effects of titanium surface topography on bone integration: a systematic review. *Clinical Oral Implants Research* 2009;20:172-84.
- [237] Rosa AL, Beloti MM. Effect of cpTi surface roughness on human bone marrow cell attachment, proliferation, and differentiation. *Brazilian Dental Journal* 2003;14:16-21.
- [238] Lim JY, Liu X, Vogler EA, Donahue HJ. Systematic variation in osteoblast adhesion and phenotype with substratum surface characteristics. *Journal of Biomedical Materials Research Part A* 2004;68:504-12.
- [239] Ismail FSM, Rohanizadeh R, Atwa S, Mason R, Ruys A, Martin P, et al. The influence of surface chemistry and topography on the contact guidance of MG63 osteoblast cells. *Journal of Materials Science: Materials in Medicine* 2007;18:705-14.
- [240] Zreiqat H, Valenzuela SM, Nissan BB, Roest R, Knabe C, Radlanski RJ, et al. The effect of surface chemistry modification of titanium alloy on signalling pathways in human osteoblasts. *Biomaterials* 2005;26:7579-86.
- [241] Anselme K, Linez P, Bigerelle M, Le Maguer D, Le Maguer A, Hardouin P, et al. The relative influence of the topography and chemistry of TiAl6V4 surfaces on osteoblastic cell behaviour. *Biomaterials* 2000;21:1567-77.
- [242] Zorn G, Gotman I, Gutmanas E, Adadi R, Sukenik C. Surface modification of Ti45Nb alloy by immobilization of RGD peptide via self assembled monolayer. *Journal of Materials Science: Materials in Medicine* 2007;18:1309-15.

- [243] Rapuano B, Wu C, MacDonald D. Osteoblast-like cell adhesion to bone sialoprotein peptides. *Journal of orthopaedic research* 2004;22:353-61.
- [244] Rupp F, Scheideler L, Rehbein D, Axmann D, Geis-Gerstorfer J. Roughness induced dynamic changes of wettability of acid etched titanium implant modifications. *Biomaterials* 2004;25:1429-38.
- [245] Qu Z, Rausch-Fan X, Wieland M, Matejka M, Schedle A. The initial attachment and subsequent behavior regulation of osteoblasts by dental implant surface modification. *Journal of Biomedical Materials Research Part A* 2007;82:658-68.
- [246] Lai HC, Zhuang LF, Liu X, Wieland M, Zhang ZY. The influence of surface energy on early adherent events of osteoblast on titanium substrates. *Journal of Biomedical Materials Research Part A* 2010;93:289-96.
- [247] Zhao G, Schwartz Z, Wieland M, Rupp F, Geis-Gerstorfer J, Cochran D, et al. High surface energy enhances cell response to titanium substrate microstructure. *Journal of Biomedical Materials Research Part A* 2005;74:49-58.
- [248] Wang X, Li Y, Lin J, Hodgson P, Wen C. Apatite-inducing ability of titanium oxide layer on titanium surface: the effect of surface energy. *Journal of Materials Research* 2008;23:1682-8.
- [249] Lim JY, Shaughnessy MC, Zhou Z, Noh H, Vogler EA, Donahue HJ. Surface energy effects on osteoblast spatial growth and mineralization. *Biomaterials* 2008;29:1776-84.
- [250] Owens DK, Wendt RC. *Journal of applied polymer science* 1969;13:1741.
- [251] Allain C. Polar interactions at liquid/polymer interface. *Journal of Adhesion Science and Technology* 2007;21:961-81.
- [252] Lowry OH, Rosebrough NJ, Farr AL, Randall RJ. Protein measurement with the Folin phenol reagent. *J biol chem* 1951;193:265-75.
- [253] Shah A, Sinha R, Hickok N, Tuan R. High-resolution morphometric analysis of human osteoblastic cell adhesion on clinically relevant orthopedic alloys. *Bone* 1999;24:499-506.
- [254] Park JB, Lakes RS. *Biomaterials: an introduction*: Plenum Pub Corp; 1992.
- [255] Elagli K, Traisnel M, Hildebrand H. Electrochemical behaviour of titanium and dental alloys in artificial saliva. *Electrochimica acta* 1993;38:1769-74.
- [256] Oliveira NTC, Aleixo G, Caram R, Guastaldi AC. Development of Ti–Mo alloys for biomedical applications: microstructure and electrochemical characterization. *Materials Science and Engineering: A* 2007;452:727-31.
- [257] Wang Y, Zheng Y. The microstructure and shape memory effect of Ti-16 at.% Nb alloy. *Materials Letters* 2008;62:269-72.
- [258] Inoue A. Stabilization of metallic supercooled liquid and bulk amorphous alloys. *Acta materialia* 2000;48:279-306.
- [259] Steinemann S. Corrosion of surgical implants- in vivo and in vitro tests. In: Winter G, Leray J, Groot de K, editors. *Evaluation of Biomaterials*. New York: Wiley; 1980. p. 1-34.
- [260] Chen X, Nouri A, Li Y, Lin J, Hodgson PD, Wen C. Effect of surface roughness of Ti, Zr, and TiZr on apatite precipitation from simulated body fluid. *Biotechnology and bioengineering* 2008;101:378-87.
- [261] Hao L, Lawrence J. The adsorption of human serum albumin (HSA) on CO₂ laser modified magnesia partially stabilised zirconia (MgO-PSZ). *Colloids and Surfaces B: Biointerfaces* 2004;34:87-94.
- [262] Kennedy SB, Washburn NR, Simon CG, Amis EJ. Combinatorial screen of the effect of surface energy on fibronectin-mediated osteoblast adhesion, spreading and proliferation. *Biomaterials* 2006;27:3817-24.
- [263] Boyan B, Batzer R, Kieswetter K, Liu Y, Cochran D, Szmuckler-Moncler S, et al. Titanium surface roughness alters responsiveness of MG63 osteoblast-like cells to 1 α , 25-(OH) 2D3. *Journal of Biomedical Materials Research* 1998;39:77-85.

- [264] Castellani R, de Ruijter A, Renggli H, Jansen J. Response of rat bone marrow cells to differently roughened titanium discs. *Clinical Oral Implants Research* 1999;10:369-78.
- [265] Gerstenfeld LC, Chipman SD, Glowacki J, Lian JB. Expression of differentiated function by mineralizing cultures of chicken osteoblasts. *Developmental biology* 1987;122:49-60.
- [266] Stein GS, Lian JB, Owen TA. Relationship of cell growth to the regulation of tissue-specific gene expression during osteoblast differentiation. *The FASEB journal* 1990;4:3111-23.
- [267] Sader MS, Balduino A, de Almeida Soares G, Borojevic R. Effect of three distinct treatments of titanium surface on osteoblast attachment, proliferation, and differentiation. *Clinical Oral Implants Research* 2005;16:667-75.
- [268] Depprich R, Ommerborn M, Zipprich H, Naujoks C, Handschel J, Wiesmann HP, et al. Behavior of osteoblastic cells cultured on titanium and structured zirconia surfaces. *Head Face Med* 2008;4:29.
- [269] Wen C, Yamada Y, Hodgson P. Fabrication of novel alloy foams for biomedical applications. *Materials Forum* 2005;29:274-8.
- [270] Bowers KT, Keller JC, Randolph BA, Wick DG, Michaels CM. Optimization of surface micromorphology for enhanced osteoblast responses in vitro. *The International journal of oral & maxillofacial implants* 1992;7:302.
- [271] Galli C, Guizzardi S, Passeri G, Martini D, Tinti A, Mauro G, et al. Comparison of human mandibular osteoblasts grown on two commercially available titanium implant surfaces. *Journal of periodontology* 2005;76:364-72.
- [272] Brunette D. The effects of implant surface topography on the behavior of cells. *Int J Oral Maxillofac Implants* 1988;3:231-46.
- [273] Groessner-Schreiber B, Tuan RS. Enhanced extracellular matrix production and mineralization by osteoblasts cultured on titanium surfaces in vitro. *Journal of cell science* 1992;101:209-17.
- [274] Grinnell F. Cellular adhesiveness and extracellular substrata. *International review of cytology* 1978;53:65-144.
- [275] Altankov G, Grinnell F, Groth T. Studies on the biocompatibility of materials: Fibroblast reorganization of substratum-bound fibronectin on surfaces varying in wettability. *Journal of Biomedical Materials Research* 1996;30:385-91.
- [276] Brash JL. Protein adsorption at the solid-solution interface in relation to blood-material interactions. *Proteins at Interfaces* 1987:490-506.
- [277] Scotchford CA, Gilmore CP, Cooper E, Leggett GJ, Downes S. Protein adsorption and human osteoblast-like cell attachment and growth on alkylthiol on gold self-assembled monolayers. *Journal of Biomedical Materials Research* 2002;59:84-99.
- [278] Mrksich M, Whitesides GM. Using self-assembled monolayers to understand the interactions of man-made surfaces with proteins and cells. *Annual Review of Biophysics and Biomolecular Structure* 1996;25:55-78.
- [279] Tengvall P, Lundström I, Liedberg B. Protein adsorption studies on model organic surfaces: an ellipsometric and infrared spectroscopic approach. *Biomaterials* 1998;19:407-22.
- [280] Geiger B, Bershadsky A, Pankov R, Yamada KM. Extracellular matrix-cytoskeleton crosstalk. *Nat Rev Mol Cell Biol* 2001;2:793-805.
- [281] Sastry SK, Burridge K. Focal adhesions: a nexus for intracellular signaling and cytoskeletal dynamics. *Experimental cell research* 2000;261:25.
- [282] Ziegler WH, Gingras AR, Critchley DR, Emsley J. Integrin connections to the cytoskeleton through talin and vinculin. *Biochemical Society Transactions* 2008;36:235-40.
- [283] Zamir E, Geiger B. Molecular complexity and dynamics of cell-matrix adhesions. *Journal of cell science* 2001;114:3583-90.
- [284] Pande G. The role of membrane lipids in regulation of integrin functions. *Current opinion in cell biology* 2000;12:569-74.

- [285] Owen GR, Meredith D, Ap Gwynn I, Richards R. Focal adhesion quantification-a new assay of material biocompatibility? Review. *European cells & materials* 2005;9:85.
- [286] Bershadsky AD, Ballestrem C, Carramusa L, Zilberman Y, Gilquin B, Khochbin S, et al. Assembly and mechanosensory function of focal adhesions: experiments and models. *European journal of cell biology* 2006;85:165-73.
- [287] Hynes RO. Integrins: bidirectional, allosteric signaling machines. *Cell* 2002;110:673-87.
- [288] Gronowicz G, McCarthy M. Response of human osteoblasts to implant materials: Integrin-mediated adhesion. *Journal of orthopaedic research* 1996;14:878-87.
- [289] García AJ, Boettiger D. Integrin-fibronectin interactions at the cell-material interface: initial integrin binding and signaling. *Biomaterials* 1999;20:2427-33.
- [290] Jikko A, Harris SE, Chen D, Mendrick DL, Damsky CH. Collagen Integrin Receptors Regulate Early Osteoblast Differentiation Induced by BMP-2. *Journal of Bone and Mineral Research* 1999;14:1075-83.
- [291] Mizuno M, Fujisawa R, Kuboki Y. Type I collagen-induced osteoblastic differentiation of bone-marrow cells mediated by collagen- $\alpha 2\beta 1$ integrin interaction. *Journal of cellular physiology* 2000;184:207-13.
- [292] Mizuno M, Kuboki Y. Osteoblast-related gene expression of bone marrow cells during the osteoblastic differentiation induced by type I collagen. *Journal of biochemistry* 2001;129:133-8.
- [293] Suzawa M, Tamura Y, Fukumoto S, Miyazono K, Fujita T, Kato S, et al. Stimulation of Smad1 Transcriptional Activity by Ras-Extracellular Signal-Regulated Kinase Pathway: A Possible Mechanism for Collagen-Dependent Osteoblastic Differentiation. *Journal of Bone and Mineral Research* 2002;17:240-8.
- [294] Takeuchi Y, Suzawa M, Kikuchi T, Nishida E, Fujita T, Matsumoto T. Differentiation and transforming growth factor- β receptor down-regulation by collagen- $\alpha 2\beta 1$ integrin interaction is mediated by focal adhesion kinase and its downstream signals in murine osteoblastic cells. *Journal of Biological Chemistry* 1997;272:29309-16.
- [295] Xiao G, Wang D, Benson MD, Karsenty G, Franceschi RT. Role of the $\alpha 2$ -integrin in osteoblast-specific gene expression and activation of the Osf2 transcription factor. *Journal of Biological Chemistry* 1998;273:32988-94.
- [296] Tamura Y, Takeuchi Y, Suzawa M, Fukumoto S, Kato M, Miyazono K, et al. Focal Adhesion Kinase Activity Is Required for Bone Morphogenetic Protein—Smad1 Signaling and Osteoblastic Differentiation in Murine MC3T3-E1 Cells. *Journal of Bone and Mineral Research* 2001;16:1772-9.
- [297] Xiao G, Jiang D, Thomas P, Benson MD, Guan K, Karsenty G, et al. MAPK pathways activate and phosphorylate the osteoblast-specific transcription factor, Cbfa1. *Journal of Biological Chemistry* 2000;275:4453-9.
- [298] Liu YK, Uemura T, Nemoto A, Yabe T, Fujii N, Ushida T, et al. Osteopontin involvement in integrin-mediated cell signaling and regulation of expression of alkaline phosphatase during early differentiation of UMR cells. *FEBS letters* 1997;420:112-6.
- [299] Shimada K, Ikeda K, Ito K. Traf2 interacts with Smad4 and regulates BMP signaling pathway in MC3T3-E1 osteoblasts. *Biochemical and Biophysical Research Communications* 2009;390:775-9.
- [300] Setzer B, Bächle M, Metzger MC, Kohal RJ. The gene-expression and phenotypic response of hFOB 1.19 osteoblasts to surface-modified titanium and zirconia. *Biomaterials* 2009;30:979-90.
- [301] Zreiqat H, Markovic B, Walsh WR, Howlett CR. A novel technique for quantitative detection of mRNA expression in human bone derived cells cultured on biomaterials. *Journal of Biomedical Materials Research* 1996;33:217-23.
- [302] Sista S, Wen C, Hodgson PD, Pande G. The influence of surface energy of titanium-zirconium alloy on osteoblast cell functions in vitro. *Journal of Biomedical Materials Research Part A* 2011;97:27-36.

- [303] Ferguson S, Brogini N, Wieland M, De Wild M, Rupp F, Geis-Gerstorfer J, et al. Biomechanical evaluation of the interfacial strength of a chemically modified sandblasted and acid-etched titanium surface. *Journal of Biomedical Materials Research Part A* 2006;78:291-7.
- [304] Suzawa M, Takeuchi Y, Fukumoto S, Kato S, Ueno N, Miyazono K, et al. Extracellular matrix-associated bone morphogenetic proteins are essential for differentiation of murine osteoblastic cells in vitro. *Endocrinology* 1999;140:2125-33.
- [305] Ling Y, Rios HF, Myers ER, Lu Y, Feng JQ, Boskey AL. DMP1 depletion decreases bone mineralization in vivo: an FTIR imaging analysis. *Journal of Bone and Mineral Research* 2005;20:2169-77.
- [306] Chen XD, Fisher LW, Robey PG, Young MF. The small leucine-rich proteoglycan biglycan modulates BMP-4-induced osteoblast differentiation. *FASEB Journal* 2004;18:948-58.
- [307] Yamaguchi A, Komori T, Suda T. Regulation of osteoblast differentiation mediated by bone morphogenetic proteins, hedgehogs, and Cbfa1. *Endocrine reviews* 2000;21:393-411.
- [308] Nakayama K, Tamura Y, Suzawa M, Harada SI, Fukumoto S, Kato M, et al. Receptor Tyrosine Kinases Inhibit Bone Morphogenetic Protein-Smad Responsive Promoter Activity and Differentiation of Murine MC3T3-E1 Osteoblast-like Cells. *Journal of Bone and Mineral Research* 2003;18:827-35.
- [309] Kingsley DM. The TGF-beta superfamily: new members, new receptors, and new genetic tests of function in different organisms. *Genes & development* 1994;8:133-46.
- [310] Khan SN, Bostrom M, Lane JM. Bone growth factors. *The Orthopedic Clinics of North America* 2000;31:375.
- [311] Linkhart TA, Mohan S, Baylink DJ. Growth factors for bone growth and repair: IGF, TGF [beta] and BMP. *Bone* 1996;19:S1-S12.
- [312] Shapira L, Klinger A, Tadir A, Wilensky A, Halabi A. Effect of a niobium-containing titanium alloy on osteoblast behavior in culture. *Clinical Oral Implants Research* 2009;20:578-82.
- [313] Depprich R, Zipprich H, Ommerborn M, Naujoks C, Wiesmann HP, Kiattavorncharoen S, et al. Osseointegration of zirconia implants compared with titanium: an in vivo study. *Head & Face Medicine* 2008;4:186.
- [314] Saulacic N, Bosshardt D, Bornstein M, Berner S, Buser D. Bone apposition to a titanium-zirconium alloy implant, as compared to two other titanium-containing implants. *European Cells and Materials* 2012;23.
- [315] Jonášová L, Müller FA, Helebrant A, Strnad J, Greil P. Biomimetic apatite formation on chemically treated titanium. *Biomaterials* 2004;25:1187-94.
- [316] Xiao F, Tsuru K, Hayakawa S, Osaka A. In vitro apatite deposition on titania film derived from chemical treatment of Ti substrates with an oxysulfate solution containing hydrogen peroxide at low temperature. *Thin solid films* 2003;441:271-6.
- [317] Wu JM, Hayakawa S, Tsuru K, Osaka A. Porous titania films prepared from interactions of titanium with hydrogen peroxide solution. *Scripta materialia* 2002;46:101-6.
- [318] Fujibayashi S, Neo M, Kim HM, Kokubo T, Nakamura T. Osteoinduction of porous bioactive titanium metal. *Biomaterials* 2004;25:443-50.
- [319] Zhao G, Zinger O, Schwartz Z, Wieland M, Landolt D, Boyan BD. Osteoblast-like cells are sensitive to submicron-scale surface structure. *Clinical Oral Implants Research* 2006;17:258-64.
- [320] Zinger O, Zhao G, Schwartz Z, Simpson J, Wieland M, Landolt D, et al. Differential regulation of osteoblasts by substrate microstructural features. *Biomaterials* 2005;26:1837-47.
- [321] Klein MO, Bijelic A, Toyoshima T, Götz H, Von Koppenfels RL, Al-Nawas B, et al. Long-term response of osteogenic cells on micron and submicron-scale-structured hydrophilic titanium surfaces: sequence of cell proliferation and cell differentiation. *Clinical Oral Implants Research* 2010;21:642-9.

- [322] Washburn NR, Yamada KM, Simon CG, Kennedy SB, Amis EJ. High-throughput investigation of osteoblast response to polymer crystallinity: influence of nanometer-scale roughness on proliferation. *Biomaterials* 2004;25:1215-24.
- [323] Kotobuki N, Matsushima A, Kato Y, Kubo Y, Hirose M, Ohgushi H. Small interfering RNA of alkaline phosphatase inhibits matrix mineralization. *Cell and tissue research* 2008;332:279-88.
- [324] Mendonça G, Mendonça D, Simões LGP, Araújo AL, Leite ER, Duarte WR, et al. The effects of implant surface nanoscale features on osteoblast-specific gene expression. *Biomaterials* 2009;30:4053-62.